THESE DE DOCTORAT

Présentée par

Krishna Priya GANTI

En vue de l'obtention du grade de

Docteur en Sciences de l'Université de Strasbourg

Discipline : Sciences du vivant

Spécialité : Aspects Moléculaires et Cellulaires de la Biologie

Transcriptional control of expression of the Thymic Stromal Lymphopoietin (TSLP) gene

Soutenue publiquement le 27/09/2010 devant le jury:

Directeur de thèse :	Pr. Pierre Chambon
Directeur de thèse :	Dr. Daniel Metzger
Rapporteur externe :	Pr. Jean Francois Nicolas
Rapporteur externe :	Pr. Vincent Laudet
Examinateur :	Dr. Hinrich Gronemeyer
Examinateur :	Dr. Fillipo Rijli

Acknowledgements

I would like to express my sincere gratitude to ***Prof. Pierre Chambon*** *for accepting me as a graduate student in his laboratory. It was a great opportunity to work and learn under his supervision.*

I would like to thank ***Dr. Daniel Metzger*** *for his enduring support and encouragement. I thank* ***Dr. Mei Li*** *for her scientific and technical support. I thank* ***Dr. Andre Krust*** *for her support. Also, I would like to thank my jury members for giving their valuable time to assess my work.*

I gratefully thank all my colleagues: ***Pierre****,* ***Laetitia petit, Laetitia grand, Jean-Marc, Celine****,* ***Delphine, Zhang, Atish, Milan, Jacky, Hua****,* ***Manuel, Thanuja, Hakan, Fatima and Rocco*** *for the time we have been through in the lab.*

Thanks to the personnel of IGBMC-ICS core facilities especially animal facility, histopathology service, imaging service, cell culture, antibody service, and FACS analysis for their support.

I also would like to thank Colette, Valerie, Estelle, Benedicte and Armelle for their assistance.

Lastly, I would like thank all my mentors, friends and family for having supported me over the years and helped me reach where I am today.

TABLE OF CONTENTS

ABBREVIATIONS :

3C assay	*Chromosome conformation capture assay*
Ab	*Antibody*
ACTH	*Adrenocorticotropic hormone*
AD	*Atopic dermatitis*
ADAM33	*A disintegrin and metalloprotease 33 gene*
ADAMTS19	*ADAM metallopeptidase with thrombospondin type 1 motif, 19*
AF	*Activation function*
AIB1	*Amplified in breast 1*
AIP	*Aryl-hydrocarbon receptor interacting protein*
AMP	*Anti microbial peptide*
AP1	*Activator protein 1*
APC	*Antigen presenting cells*
ATF	*Activating transcription factor*
BAL	*Bronchoalveolar lavage*
BCR	*B cell receptor*
BCL2L1	*Bcl-2-like protein 1*
BTG2	*B-cell translocation gene FAMILY GENE 2*
CAR	*Constitutively activated receptor*
CBP	*CREB binding protein*
CCND1	*G1/S-specific cyclin-D1*
CCR10	*C-C chemokine receptor type 10*
CD	*Cluster of differentiation*
C-FOS	*V-fos FBJ murine osteosarcoma viral oncogene homolog*

ChIP	*Chromatin immunoprecipitation*
CITED1	*Cbp/p300-interacting transactivator 1*
C-JUN	*Jun oncogene*
COL	*Collagen*
COL4A3BP	*Collagen type IV alpha-3-binding protein*
CT	*Control*
CTNNA3	*A-T-catenin gene*
CYFIP2	*Cytoplasmic FMR1-interacting protein 2*
CYP24A1	*Cytochrome P450, family 24, subfamily A, polypeptide 1*
CYP26A1	*Cytochrome P450, family 26, subfamily A, polypeptide 1*
DBD	*DNA binding domain*
DC	*Dendritic cells*
DEX	*Dexamethasone*
DPAGT1	*Dolichyl-phosphate (UDP-N-acetylglucosamine) N-acetylglucosaminephosphotransferase 1*
DR	*Direct repeat*
EMSA	*Electrophoretic mobility shift assay*
ERK	*Extracellular-signal-regulated kinase*
FA	*Flucinolone acetonide*
FBXL18	*F-box and leucine-rich repeat protein 18*
FcεRI	*High-affinity Fc receptors for ige*
FKBP2	*FK506-binding protein 2*
FLG	*Filaggrin*
FOXJ1	*Forkhead box protein J1*
FXR	*Farnesoid x receptor*

GATA	*GATA DNA binding transcription factor*
GBA2	*Glucosidase, beta (bile acid) 2*
GCs	*Glucocortocoids*
GILZ	*Glucocorticoid induced leucine zipper*
GPR68	*G protein-coupled receptor 68*
GPX3	*Glutathione peroxidase 3*
GR	*Glucocorticoid receptor*
GRE	*Glucocorticoid response element*
GST	*Glutathione S-transferases*
HAT	*Histone acetyl transferase*
HDAC	*Histone deacetylase*
HLA-G	*Histocompatibility antigen, class I, G*
HSD11B2	*Corticosteroid 11-β-dehydrogenase isozyme 2*
IFN	*Interferon*
IgE	*Immunoglobulin E*
IgG	*Immunoglobulin G*
IKK	*Iκb kinase*
IL	*Interleukin*
IP	*Immunoprecipitaiton*
IR	*Inverted repeat*
IRAK	*Interleukin-1 receptor-associated kinase*
IκB	*Inhibitor of κb*
JAK	*Janus protein tyrosine kinase*
JDP	*Jun dimerization protein*
JNK	*C-Jun N-terminal kinase*

K	*Keratin*
KLF5	*Krueppel-like factor 5*
KO	*Knock-out*
KRT14	*Keratin 14*
LBD	*Ligand binding domain*
LC	*Langerhans cell*
LEKT1	*Lympho-epithelial kazal type inhibitor*
LXR	*Liver x receptor*
MAF	*V-maf musculoaponeurotic fibrosarcoma oncogene homolog*
MAPK	*Mitogen-activated protein kinase*
MC	*MC903, low calcemic analog of active Vitamin D3*
MCP	*Monocyte chemotactic protein*
MDC	*Macrophage derived chemokine*
MHC	*Major histocompatibility complex*
MIP	*Macrophage inflammatory protein*
MMP	*Matrix metalloproteinase*
MTG1	*Mitochondrial gtpase 1*
MUC20	*Mucin-20*
Mut	*Mutant*
NCoR	*Nuclear receptor corepressors*
NDUFA4L2	*NADH dehydrogenase (ubiquinone) 1 alpha subcomplex, 4-like 2*
NEU1	*Sialidase 1 (lysosomal neuraminidase)*
NF-κB	*Nuclear factor-kappa B*
nGRE	*Negative glucocorticoid response element*
NKT	*Natural killer T*

NKRF	*NF-kappab repressing factor*
NPSR	*Neuropeptide S receptor*
NR	*Nuclear receptor*
OPN3	*Opsin-3*
ORMDL3	*ORM1-like 3 (s. Cerevisiae)*
P65/RelA	*V-rel reticuloendotheliosis viral oncogene homolog A*
PCAF	*P300/CBP associated factor*
PCDH1	*Protocadherin 1 gene*
PDE	*Phosphodiesterase*
PDE4D	*Phosphodiesterase 4D gene*
PDGF	*Platelet-derived growth factor*
PHF	*PHD finger protein*
Pol II	*RNA polymerase II*
POMGNT1	*Protein O-linked-mannose beta-1,2-N-acetylglucosaminyltransferase 1*
PP	*Proximal promoter*
PPAR	*Peroxisome proliferator activated receptor*
PRKCB	*Protein kinase C beta*
PRKRA	*Protein kinase, interferon-inducible double stranded RNA dependent activator*
PTGER2	*Prostaglandin E2 receptor*
PXR	*Pregnane x receptor*
RA	*All-trans retinoid acid*
RAR	*Retinoic acid receptor*
RARE	*Retinoic acid response element*
RDH5	*Retinol dehydrogenase 5*
RDH11	*Retinol dehydrogenase 11*

RORA	*RAR-related orphan receptor alpha*
ROS	*Reactive oxygen species*
RU	*RU486, mifepristone*
RU24858	*Selective glucocorticoid receptor agonist RU 24858*
RXR	*Retinoid X receptor*
SGK3	*Serum/glucocorticoid regulated kinase family, member 3*
SLC2A8	*Solute carrier family 2, (facilitated glucose transporter) member 8*
SLC25A5	*Solute carrier family 25, member 5*
SLC25A34	*Solute carrier family 25, member 34*
Smad	*Similar to mothers against decapentaplegic*
SMRT	*Silencing mediator for retinoid and thyroid hormone receptor*
SNP	*Single nucleotide polymorphim*
SOCS	*Suppresors of cytokine signalling*
SP9	*Sp9 transcription factor homolog*
SPARC	*Secreted protein, acidic, cysteine-rich (osteonectin)*
SPINK	*Serine protease inhibitor, Kazal type 5*
SRC	*Steroid receptor coactivator*
STAT	*Signal Transducer and Activator of Transcription*
STRA13	*Stimulated by retinoic acid gene 13*
Tam	*Tamoxifen*
TARC	*Thymus and activation regulated chemokine*
TAT	*Tyrosine aminotransferase*
TBX	*T-box transcription factor*
TCF25	*Transcription factor 25 (basic helix-loop-helix)*
TEWL	*Trans epidermal water loss*

TF	*Transcription factor*
TGFβ	*Tumor growth factorβ*
TH1	*T helper cell type 1*
TH2	*T helper cell type 2*
TIF2	*Transcriptional mediators/intermediary factor 2*
TLR	*Toll-like receptor*
TNC	*Tenascin*
TNF	*Tumor necrosis factor*
TNFRSF19	*Tumor necrosis factor receptor superfamily, member 19*
TNFRSF25	*Tumor necrosis factor receptor superfamily, member 25*
TPA	*12-O-Tetradecanoylphorbol-13-acetate*
TRAM1	*Thyroid hormone receptor activator molecule 1*
Tregs	*Regulatory T cells*
TRPM7	*Transient receptor potential cation channel, subfamily M, member 7*
TSLP	*Thymic stromal lymphopoietin*
TSLPR	*Thymic stromal lymphopoietin receptor*
UPAR	*Urokinase receptor*
USF1	*Upstream stimulatory factor 1*
VD3	*1α 25 (OH)2 Vitamin D3*
VDR	*Vitamin d receptor*
VDRE	*Vitamin D response element*
WDR36	*WD repeat-containing protein 36*
Wt	*Wild type*

MOUSE LINES:

RXRα$^{ep-/-}$	Mice bearing an inducible ablation of RXRα in epidermal keratinocytes through an i.p. injection of Tam to K14-Cre-ERT2 (tg/0)/RXRαL2/L2 mice
RXRβ$^{ep-/-}$	Mice bearing an inducible ablation of RXRβ in epidermal keratinocytes through an i.p. injection of Tam to K14-Cre-ERT2 (tg/0)/ RXRβL2/L2 mice
RXRαβ$^{ep-/-}$	Mice bearing an inducible ablation of RXRα and RXRβ in epidermal keratinocytes through an i.p. injection of Tam to K14-Cre-ERT2 (tg/0)/RXRαL2/L2 RXRβL2/L2 mice
RARγ$^{-/-}$	Germline RARγ null mice
VDR$^{ep-/-}$	Mice bearing an inducible ablation of VDR in epidermal keratinocytes through an i.p. injection of Tam to K14-Cre-ERT2 (tg/0)/VDRL2/L2
RARαγ$^{ep-/-}$	Mice bearing an inducible ablation of RARα and RARγ in epidermal keratinocytes through an i.p. injection of Tam to K14-Cre-ERT2 (tg/0)/RARαL2/L2 RARγL2/L2 mice
RARγ/VDR$^{ep-/-}$	Mice bearing an inducible ablation of RARγ and VDR in epidermal keratinocytes through an i.p. injection of Tam to K14-Cre-ERT2 (tg/0)/ RARγL2/L2 VDRL2/L2mice
RARαγ/VDR$^{ep-/-}$	Mice bearing an inducible ablation of RARα, RARγ and VDR in epidermal keratinocytes through an i.p. injection of Tam to K14-Cre-ERT2 (tg/0)/RARαL2/L2 RARγL2/L2 VDRL2/L2mice
GR$^{ep-/-}$	Mice bearing an inducible ablation of GR in epidermal keratinocytes through an i.p. injection of Tam to K14-Cre-ERT2 (tg/0)/GRL2/L2

Résumé – Summary

Contrôle transcriptionnel de l'expression du gène de la « Thymic Stromal Lymphopoietin » (TSLP)

Transcriptional control of expression of the Thymic Stromal Lymphopoietin (TSLP)

La cytokine Thymic Stromal Lymphopoietin (TSLP) est exprimée d'une manière prédominante par les cellules épithéliales de la peau, des voies respiratoires et de l'intestin. L'expression constitutive de TSLP dans les cellules épithéliales du côlon participe au maintien de l'homéostasie immunitaire de l'intestin en le protégeant contre les infections pathogènes. Ainsi, TSLP est un facteur de survie pour l'intestin. Par ailleurs, il y a de nombreuses indications que TSLP peut jouer un rôle clé dans la genèse et l'évolution des maladies atopiques. Des études de patients ont montré que TSLP est fortement exprimé dans les kératinocytes de l'épiderme, dans les cellules épithéliales des voies aériennes, dans le liquide de lavage bronchoalvéolaire (BAL), ainsi que dans l'épithélium nasal au cours de la dermatite atopique (AD), de l'asthme et des rhinites allergiques. De plus, dans notre laboratoire, des études faites en utilisant un modèle « souris » de dermatite atopique, a montré que TSLP est nécessaire et suffisant pour induire une inflammation atopique. Moduler l'expression de TSLP, pouvant être une façon efficace de traiter l'inflammation atopique, nous avons orienté notre travail de thèse vers l'étude des mécanismes qui contrôlent l'expression du gène TSLP *in vivo.*

Des études antérieures réalisées dans le laboratoire d'accueil avaient révélé l'intervention possible de récepteurs nucléaires (NR) dans la régulation de l'expression de TSLP chez la souris. En effet, l'ablation sélective des récepteurs nucléaires RXRα et RXRβ dans les kératinocytes épidermiques de la souris (mutant RXRαβ$^{ep-/-}$) déclenche une augmentation de TSLP dans les kératinocytes. D'autres études, impliquant la suppression de la fonction d'activation ligand-dépendante (AF-2) de RXRα et RXRβ avaient suggéré que l'induction de TSLP dans l'épiderme des souris RXRαβ$^{ep-/-}$ n'était pas due à la perte des fonctions d'activation AF-2, mais à la suppression de la répression exercée par des hétérodimères associant RXRα et/ou RXRβ à d'autres récepteurs nucléaires non-ligandés.

L'analyse de ligands spécifiques pour différents NRs pour leur capacité à induire l'expression de TSLP révéla que la vitamine D3 active (VD3, l'agoniste du récepteur VDR) et l'acide all-trans rétinoïque (RA, agoniste des récepteurs RARα, β et γ) étaient capables d'induire l'expression de TSLP dans les kératinocytes épidermiques de la souris. Ces résultats indiquaient que RXRα, RXRβ, VDR et RARγ pourraient différemment contrôler l'expression de TSLP en fonction de la nature des ligands présents.

Mon travail de thèse a consisté à creuser les observations précédentes et à élucider les mécanismes qui régulent l'expression de TSLP *in vivo*. J'ai poursuivi trois objectifs principaux :

A. Comprendre les mécanismes par lesquels les NRs régulent l'expression de TSLP,
B. Identifier les facteurs de transcription additionnels qui pourraient participer à la régulation de l'expression de TSLP,
C. Déterminer si, et comment, les glucocorticoïdes (GCs), dont l'administration constitue l'une des thérapies les plus efficaces pour le traitement des maladies atopiques, modulent l'expression de TSLP.

A.) Comprendre les mécanismes par lesquels les NRs régulent l'expression de TSLP.

Pour démontrer que la synthèse de TSLP est contrôlée au niveau transcriptionnel par des NRs, des essais de « nuclear run-on » ont été effectués en utilisant des extraits épidermiques de la peau dorsale de mutants RXRαβ$^{ep-/-}$ ou de souris de type sauvage (comme contrôle), traitées par la vitamine D3 (VD3) ou l'acide rétinoïque (RA). Ils ont prouvé que la synthèse de TSLP est effectivement régulée au niveau transcriptionnel. Une analyse manuelle et bioinformatique de la région « en amont » du promoteur de TSLP a révélé la présence de plusieurs éléments (sites de l'ADN) de type DR1 (auxquels se fixent notamment les NRs RXR/PPAR/LXR/FXR), DR2 (RARE auxquels se fixent les RARs), et DR3 (VDRE) auxquels se fixe le VDR (Figure 1).

La capacité de ces éléments à s'associer aux NRs correspondants a été confirmée *in vitro* par des analyses de « décalage » (shift) de mobilité électrophorétique (EMSA). L'association de RXR/VDR et de RXR/RARγ avec les éléments DR3 et DR2 a été confirmée *in vivo* par des essais d'immunoprécipitation de la chromatine (ChIP). Des analyses « ChIP » plus poussées ont révélé que les fonctions de RXRα et RXRβ ne sont pas redondantes *in vivo*. En effet, dans les kératinocytes de l'épiderme suprabasal, et indépendamment de la présence du ligand, VDR est hétérodimérisé avec RXRα sur les éléments VDRE DR3-d, DR3-f et DR3-g du gène TSLP,

tandis que RARγ est hétérodimérisé avec RXRβ. Par ailleurs, RXRα est hétérodimérisé avec un (des) partenaire(s) NR non encore identifié(s) sur l'élément DR1-a du gène TSLP. La fonctionnalité des éléments DR3d et DR2b dans la régulation de l'activité de transcription de TSLP fut révélée par l'observation que l'activation médiée par les ligands VD3 et RA induit une interaction des régions englobant les sites DR3-d et DR2-b avec la région du promoteur proximal (comme on le constate par des essais de « chromosome Conformation Capture (3C)»), ce qui conduit également au recrutement par ces sites d'un complexe associant co-activateurs et l'ARN polymérase II. Au contraire, en l'absence de ligands, les hétérodimères VDR/RXRα et RARγ/RXRβ sont associés au co-répresseur SMRT.

Figure 1 : Représentation schématique de la position des sites régulateurs du promoteur TSLP sur lesquels différents facteurs de transcription peuvent se fixer.

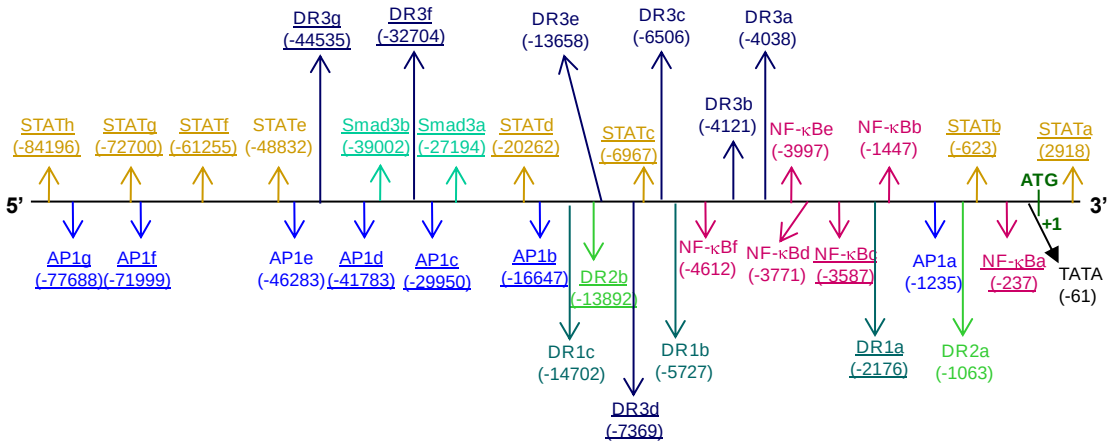

VDR et RARγ étant respectivement et spécifiquement hétérodimérisés avec RXRα et RXRβ, nous émirent l'hypothèse que la suppression par mutagénèse de VDR et de RARγ supprimerait la répression de l'expression de TSLP, comme l'avait fait la mutation RXRαβ$^{ep-/-}$. A notre étonnement, les kératinocytes des souris RARγ/VDR$^{ep-/-}$ n'exprimèrent pas TSLP à un niveau équivalent à celui observé dans les souris RXRαβ$^{ep-/-}$, ce qui nous suggéra que RARα pourrait éventuellement remplacer et compenser la perte de RARγ. De fait, la suppression des trois récepteurs, RARα, RARγ et VDR (souris RARα/RARγ/VDR$^{ep-/-}$) se traduisit par une augmentation de la production de TSLP équivalente à celle des animaux RXRαβ$^{ep-/-}$.

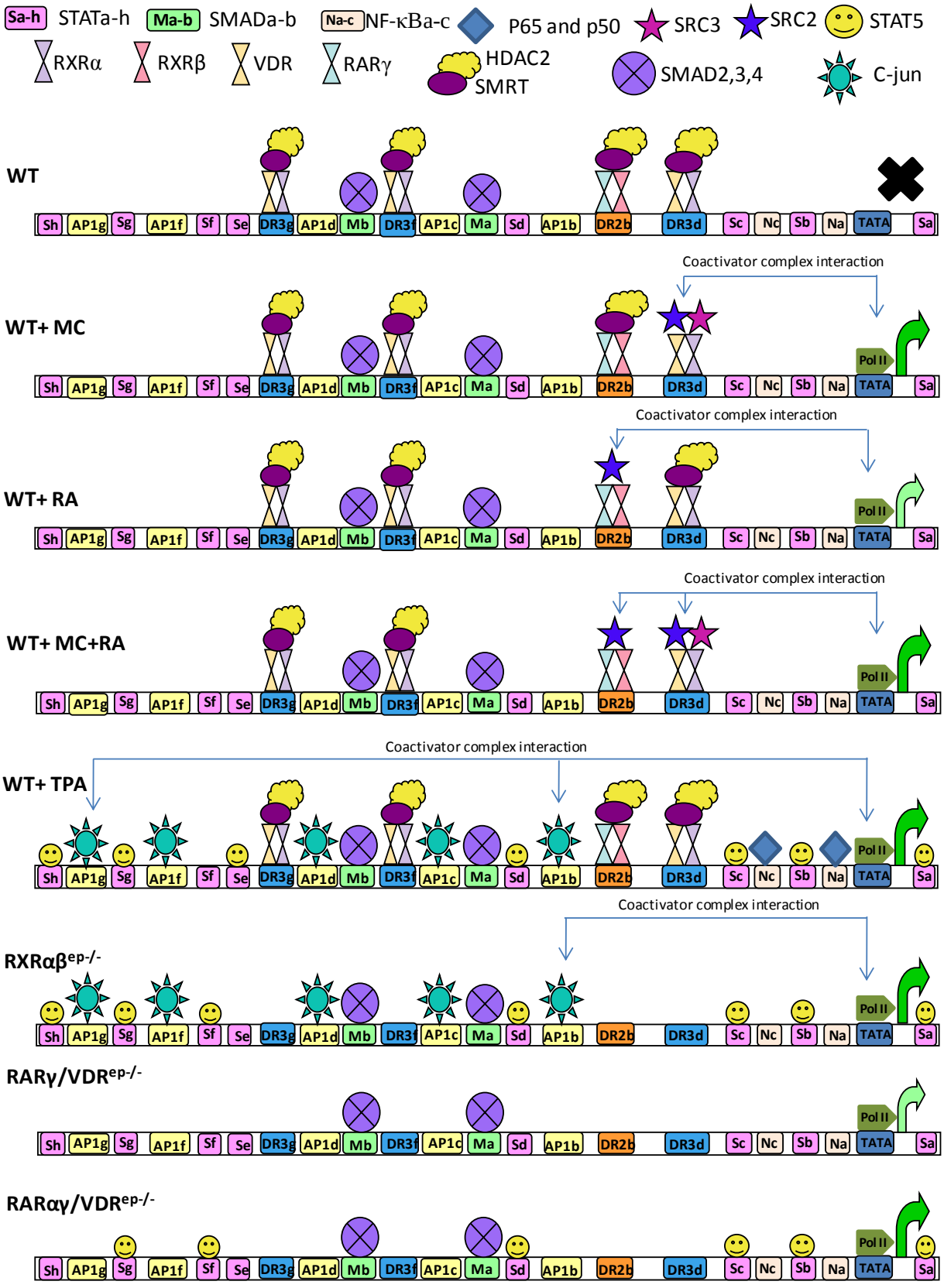

Figure 2: Représentation schématique de la distribution des facteurs régulation de la

transcription du gène TSLP chez la souris, dans les keratinocytes de la peau, « sauvage » (WT), traitée par MC, RA, MC + RA, TPA ou portant des mutations RXRαβ$^{ep-/-}$, RARγ/VDR$^{ep-/-}$ et RARγα/VDR$^{ep-/-}$.

B.) Identifier les facteurs de transcription additionnels qui pourraient participer à la régulation de l'expression de TSLP.

Une analyse poussée *in silico* de la région promotrice du gène TSLP révéla la présence de sites de liaison pour plusieurs autres facteurs de transcription, tels que NFκB (a et c), AP1 (a-g), STAT (a-h) et Smad (a, b) (Fig.1). Dans des conditions physiologiques, dans les kératinocytes de l'épiderme, seul les sites Smad3 a et b apparaissaient occupés par les facteurs Smad 2, 3 ou 4, alors que la liaison des sites NFκB (p65/p50) (NFκB a and c), AP1 (Jun/Fos), et de sites STATa, b, c, d, e, g et h par le facteur STAT5 à leurs éléments régulateurs (sites spécifiques de fixation) sur le DNA, nécessitait une stimulation topique par le phorbol ester TPA. En outre, un traitement par MC903 (analogue de la vitamine D3 active) provoquait la fixation du facteur STAT5 sur les sites STATa, b, c ,d, f, h, et chez les mutants RXRαβ$^{ep-/-}$ AP1 était lié à un site spécifique (AP1b), tandis que chez les mutants RARα/RARγ/VDR$^{ep-/-}$, la liaison de Smad3 à son site spécifique était augmentée (Figure 2).

Pris dans leur ensemble, ces résultats nous ont suggéré que, selon les stimuli, la transcription de TSLP est régie par un équilibre délicat entre la dissociation de complexes de répression et l'assemblage de complexes activateurs sur les multiples éléments de régulation. Il sera intéressant d'étudier les mécanismes moléculaires intervenant dans l'activation de ces différentes voies de régulation de la transcription de TSLP en procédant chez la souris à des ablations conditionnelles ciblées des gènes impliqués dans ces complexes, ainsi qu'en invalidant par mutation les divers éléments (sites) de régulation..

C). Déterminer si, et comment, les glucocorticoïdes (GCs), dont l'administration constitue l'une des thérapies les plus efficaces pour le traitement des maladies atopiques, modulent l'expression de TSLP.

Les glucocorticoïdes (GCs) qui sont couramment utilisés comme agents thérapeutiques dans les maladies atopiques emploient différentes stratégies pour réprimer l'expression des gènes

« inflammatoires ». Leur effet sur l'expression de TSLP demeurait inexploré. Nous avons d'abord vérifié s'ils pouvaient agir efficacement dans notre modèle « souris » de dermatite atopique (AD) (induction d'un phénotype AD sur l'oreille et la peau dorsale de souris Balb/c de type sauvage par traitements « MC903 » répétés, provoquant la synthèse de TSLP). Un traitement par les GCs se révéla efficace dans la prévention de la génération du phénotype AD et l'analyse par QPCR d'échantillons de tissus démontra que le traitement par les GCs supprimait l'expression basale, ainsi que l'expression MC903-induite de TSLP. De plus, l'utilisation de mutants « souris » dépourvus du récepteur des GCs (le GR), nous permit de démontrer que la répression par les GCs était médiée par le GR. Des tests de « nuclear run-on » sur les mêmes échantillons révéla que cette répression par le GR s'exerçait au niveau de la transcription.

Une analyse bioinformatique de 20 kilobases de séquences d'ADN en amont et en aval du site d'initiation de la traduction de TSLP ne révèla pas d'éléments d'activation (+)GRE classiques ou « composites » connus, ni de sites de répression nGRE, mais dévoila la présence d'une nouvelle séquence composée de deux motifs « inversés répétés » (IR) séparés par un 1 bp (appelée ci-après élément IR1 nGRE), localisées dans la région promotrice « en amont » des gènes TSLP de la souris (m) et de l'homme (h). L'utilisation d'une protéine GR recombinante humaine, et des techniques « EMSA » et de supershift à l'aide d'anticorps, permit de montrer que l'élément putatif (m)TSLP IR1nGRE, et son homologue putatif humain (h)TSLP IR1 nGRE, ainsi que l'élément activateur TAT (+)GRE, se lient de façon semblable à la protéine GR. Ces liaisons étaient spécifiques, et nécessitaient l'intégrité de l'élément consensus activateur (+)GRE et du (m)TSLP IR1nGRE putatif, comme le montrait l'absence de liaison entre le GR et des mutants (+)GRE et IR1 nGRE. Des essais ChIP pratiqués sur de l'épiderme de souris traité à la Dexaméthasone (DEX, un agoniste de GR) et au RU486 (un antagoniste de GR), ont montré que cet IR1nGRE pouvait recruter le co-répresseur SMRT associé au GR après traitement DEX, et que ce recrutement pouvait être réversé par co-traitement avec l'antagoniste des glucocorticoïdes RU486. En outre, bien que le IR1nGRE lui-même ne s'associait pas à la région du promoteur proximal, il empêchait l'interaction qui pouvait être induite par MC903 avec la région du promoteur proximal, bloquant ainsi la transcription de TSLP induite par MC903.

Afin de déterminer si l'élément nGRE à lui seul était suffisant pour générer la répression, nous avons inséré les éléments VDRE et TSLP IR1 nGRE (séparés l'un de l'autre par une région d'ADN dépourvue de tout site transrégulateur) en amont d'un promoteur « SV40 enhancerless », lui-même localisé en 5' de la séquence codante pour la luciférase, présente dans le vecteur pGL3. Utilisant ce plasmide dans des essais de transfection *in vitro*, nous avons montré que les GCs réprimaient effectivement les activités basales et VD3-induite de la luciférase. De plus, des essais ChIP ont confirmé le recrutement du complexe répresseur sur l'élément IR1nGRE, démontrant clairement que l'élément IR nGRE est capable à lui seul de médier la transrépression. Afin de déterminer si l'espacement de 1 bp des motifs inversés répétés de l'IR1 nGRE est un facteur déterminant dans la répression, nous avons généré des éléments IR nGREs ayant des espacements de 0 à 5 bp. Bien que IR0, IR1 et IR2 aient une activité de répression (quoique dans une moindre mesure, pour IR0), IR3, IR4 et IR5 nGREs n'eurent aucun effet sur l'activité luciférase. Une analyse de mutations portant alternativement chacune des bases de l'élément IR nGRE permit d'évaluer la contribution relative des bases individuelles de IR1 et IR2 nGREs dans l'activité de répression. A l'exception d'une base, toutes les autres transitions de base furent bien tolérées, suggérant que le GR lié à des éléments IR1 et IR2 « dégénérés » pourrait également intervenir dans la transrepression induite par les GCs *in vivo*.

Afin de déterminer si des éléments IR nGREs pourraient réguler l'expression d'autres gènes que TSLP, une analyse bioinformatique des génomes de la souris et de l'homme à été réalisée pour rechercher la présence d'éléments IRO, IR1 et IR2 nGRE. 996 gènes orthologues ont été trouvés contenant des éléments nGRE consensus (51 IR0, 379 IR1, 566 IR2). Au sein de chaque famille, nous avons choisi au hasard, chez la souris, 15 gènes pour vérifier s'ils étaient exprimées dans l'épiderme, et si leur expression pouvait être réprimée par l'administration topique de GCs. Une analyse par RT-PCR quantitative des RNA épidermiques démontra que la plupart des gènes exprimés pouvaient être réprimés par un tel traitement. Des essais ChIP ont en outre confirmé que la répression de ces gènes était toujours associée à la liaison du GR et des corépresseurs au IR nGRE. Ainsi, l'ensemble des résultats que nous avons obtenus indiquent que les éléments du type IR nGRE régulent l'expression d'une grande population de gènes, dont la répression peut jouer un rôle dans la médiation des effets bénéfiques, mais aussi éventuellement nuisibles, lors d'une corticothérapie.

Bien que les GCs soient efficaces dans le traitement de l'inflammation, leur effets secondaires à long terme peuvent être débilitants. L'effet anti-inflammatoire des GCs a été le plus souvent attribué à la « transrépression indirecte » médiée par l'action du GR sur des facteurs de transcription liés à l'ADN tels que NFκB, AP1 etc…, alors que leur effets secondaires seraient plutôt le fait de la transactivation médiée par des éléments activateurs (+)GRE. Cela a conduit à la recherche et au développement de ligands du GR, dits « dissociés », tel que le composé RU24858, qui sont censés agir par le mécanisme de « transrépression indirecte » et avoir perdu leur « fonction activatrice de la transcription ». Cependant, bien que le composé RU24858 ait effectivement perdu sa fonction d'activation, ses effets secondaires débilitants subsistaient *in vivo*. Cette observation nous conduisit à émettre l'hypothèse que l'effet secondaire provoqué par les GC « dissociés » pourrait être attribué à leur capacité à toujours induire notre nouvelle « transrépression directe » médiée par les IR nGREs. De fait, lorsque nous avons testé le RU24858 sur des cellules ou des animaux, il s'est comporté comme un faible transactivateur sur des éléments (+)GRE, et a réprimé efficacement l'expression des gènes pro-inflammatoires, mais s'est aussi montré très efficace pour induire la « transrépression directe » médiée par les éléments IR nGRE. Comme un certain nombre de gènes impliqués dans divers processus physiologiques contiennent des séquences de type IR nGRE, nous concluons que les effets secondaires des GCs peuvent être, au moins partiellement, causés par leur action répressive médiée par les IR nGREs.

Conclusion :

Ainsi, notre travail donne un aperçu intéressant sur les mécanismes contrôlant l'expression du gène TSLP dans les kératinocytes épidermiques. Dans des conditions physiologiques, la transcription de TSLP est réprimée par les hétérodimères VDR/RXRα et/ou RARγ/(RARα)/RXRβ. Cette répression peut être levée, soit par la libération des complexes NR non-ligandés, ou par l'activation avec des ligands agonistes de VDR et/ou de RARγ ou encore par l'activation de transactivateurs NFκB, AP1, STAT ou Smad. Nous avons également découvert des éléments cis-régulateurs négatifs (IR nGRE) qui, en liant le GR associé à des ligands agonistes, médient la « transrepression directe » d'un sous-ensemble de gènes cibles dont

la répression pourrait être à l'origine d'une fraction importante des effets secondaires indésirables de la thérapie par les glucocorticoïdes.

Il est évident que la synthèse de glucocorticoïdes qui conserveraient leur effets anti-inflammatoires, mais seraient dépourvus d'activité de « transrepression directe », et aussi de « transactivation » médiée par des (+)GRE, et en conséquence débarrassés d'une partie au moins des effets indésirables des glucocorticoïdes actuellement utilisés en thérapeutique, serait un grand progrès dans le traitement des affections inflammatoires par les glucocorticoïdes.

INTRODUCTION

1. Biology of the skin

Skin, the largest organ of the body, is an indispensible barrier forming an interface between the organism and its environment. It consists of lower dermis and upper multi-layered epidermis abundant with keratinocytes (consists of about 94% keratinocytes and the rest include melanocytes, langerhan cells, and resident lymphocytes). Epidermis forms the physical barrier protecting the organism from biological, chemical, and physical assaults. Though semi-permeable, epidermis prevents the exit of moisture from and the entry of microbes into the organism, thus forming an effective barrier.

1.1 Epidermal barrier formation

Epidermis is a self-regenerating tissue under both, normal and in injury conditions. It maintains a population of mitotically active cells in the basal layer of epidermis *(Ito et al., 2005; Fuchs & Raghavan, 2002; Niemann & Watt, 2002)*. The basal keratinocytes undergo a linear program of differentiation to form transcriptionally active spinous cells to enucleated granular cells, resulting finally in differentiated squames in the stratum corneum.

The stratum corneum once formed becomes analogous to bricks and mortar i.e, protein enriched corneocytes connected by corneodesmosomes (forming the bricks), which are embedded in a matrix of lipid bilayer (mortar), forming a protective barrier *(Elias, 1983; Kalinin et al., 2002; Nemes & Steinert, 1999)*. Tight junctions forming cell-cell junctions connecting neighbouring cells, located in the granular layer also play an essential role in retaining the water content of the body. For instance, mice lacking claudin show defective barrier formation and die within one day of birth *(Furuse et al., 2002.)*, whereas E-cadherin null mice die prenatally due to excess water loss *(Tunggal et al., 2005)*. This process of differentiation from a mitotically active basal cell to the terminally differentiated squamous cell is maintained throughout life as part of epidermal regeneration *(Steinert, 2000; Segre, 2003)*. Changes in this process of barrier formation leads to low to severe abnormalities, ultimately leading to several skin disorders.

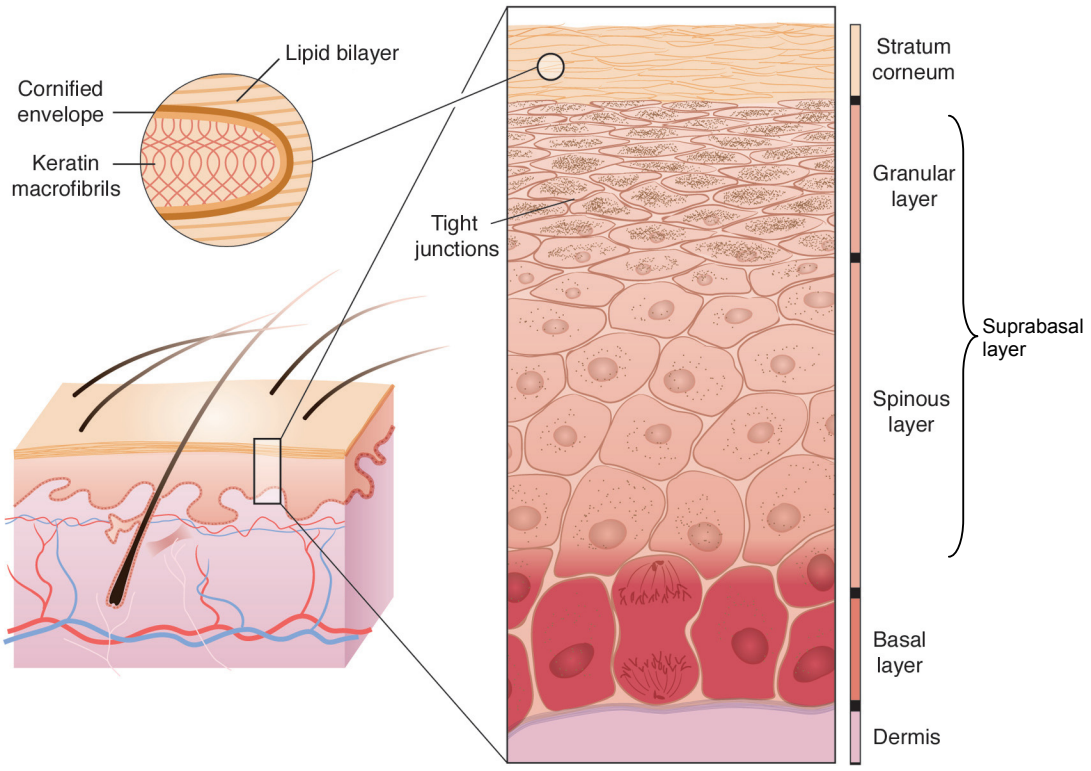

Figure 1: Schematic diagram of the stages of epidermal differentiation, resulting in a permeability barrier

[Adapted from J.Clin.Invest. 116:1150-1158, 2006]

1.1.1 Epidermal protein component

Keratins are the major structural proteins of the epidermis. Based on biochemical properties keratins can be divided into two subgroups, type 1 and type 2 keratins. In vitro and in vivo, type 1 and type 2 keratins polymerize to form hetero-polymeric keratin intermediate filaments (KIF). The major keratins expressed in basal layer are K5 and K14, whereas K1 and K10 are the major keratins expressed in the suprabasal layer. The significance of keratins in barrier formation is known by the fact that mutations in keratins lead to serious complications involving the skin. Both in humans and in mouse models of human disease, mutations in K5/K14 lead to epidermal bullosa simplex and mutations in K1/K10 lead to epidermolysis hyperkeratosis *(Roland et al., 2008)*.

The other major protein present in the epidermis is filaggrin (FLG), which is stored in keratohyalin granules as latent pro-filaggrin and proteolytically processed by caspase 14 to

the active filaggrin *(O'Regan et al., 2008)*. Mice having mutations in filaggrin *(Presland et al., 2000)* or caspase 14 null mice *(Denecker et al., 2007)* develop barrier abnormalities showing the importance of this protein in barrier formation. Filaggrin aggregates KIFs into tight bundles, ultimately leading to a flattened corneocytes *(Palmer et al., 2006)*. Together they form 80-90% of the protein mass of mammalian epidermis *(Roop, 1995; Nemes et al., 1999)*. Filaggrin is further processed to yield hydrophilic amino acids which retain the moisture content of the epidermis, thus forming the natural moisturizing factor of the skin. These amino acids also help in maintaining the pH of the skin at 4.5 to 5, wherein antimicrobial peptides (AMPs) and proteases are active, whereas pathogens cannot survive in this acidic pH condition *(O'Regan et al., 2008)*. Use of harsh alkaline soaps on low skin abnormalities like dry skin, alters the pH of the skin, creating a favourable environment for microbes to thrive and deteriorate infection.

In addition, there are several other structural proteins like involucrin, loricrin, trichohyalin and small proline rich protein (SPRs), which are cross-linked by transglutaminases to form a reinforced cornified envelope. Transglutaminases (TGM) are calcium dependent enzymes which form N-ε-γ-glutamyl lysine isopeptides between proteins. There are 10 classes of transglutaminases and 1, 2, 3, and 5 are expressed in the skin *(Candi et al., 2005)*. Transglutaminase 1 present in suprabasal layer plays an important role in barrier formation. TGM1-null mice die before birth due to excessive water loss *(Matsuki et al., 1998)*. Mutations in TGM1 in humans lead to lamellar ichthyosis *(Raghunath et al., 2003)*.

Processing of cornified envelope proteins, loss of nuclei and mitochondria, and desquamation, all require proteolytic cleavage by proteases. There are several serine and cysteine proteases present in the cornified envelope. The activity of these proteases is kept under control by protease inhibitors *(Brattsand et al., 2005; Stefansson et al., 2008)*. Loss of function of any of these proteins also leads to defective barrier formation.

1.1.2 Epidermal lipid component

Cornified envelope proteins are embedded in lipid envelope, consisting mostly of ceramides, free fatty acids, cholesterol and cholesterol esters *(Downing et al., 1987)*. Skin lipids form a hydrophobic layer in the epidermis and avoid transepidermal water loss (TEWL) and thus

maintain an effective barrier. TEWL is a measure of barrier integrity. Lipids are synthesized and stored in lamellar granules, which are extruded into extracellular space during cornification. Sphingolipids and phospholipids form the major lipids in the epidermis. Hydrolysis of sphingolipids generates ceramides, while phospholipids generate free fatty acids *(Downing et al., 1987)*. Saturated and monounsaturated fatty acids are synthesized in the epidermis while others must be obtained from food and blood flow. Essential fatty acid deficiency in humans and mice causes profound changes in the epidermis *(Proksch et al., 1992)* Disruption of the fatty acid transport protein 4 encoding gene leads to disturbed epidermal barrier and lethality of mice immediately after birth *(Herrmann et al., 2003)*.

Cholesterol can be absorbed from circulation by basal cells, but it is also synthesized de novo from acetate. Cholesterol synthesis is increased during epidermal barrier repair. Hydroxy Methyl Glutaryl CoA (HMG CoA) reductase is the rate limiting enzyme in cholesterol biosynthesis. Inhibition of HMG CoA reductase by topical application of lovastatin results in disturbed barrier function and epidermal hyperproliferation *(Proksch et al., 1992)*.

1.2 Skin immune system

In addition to the epidermis providing a physical barrier, skin also provides an immune barrier to the organism. The resident skin cells include epidermal keratinocytes, langerhan cells and T cells, and dermal dendritic cells, mast cells, macrophages, T cells and NKT cells. Collectively, they form the innate immune component acting as first line of defence towards infections and help to recruit the adaptive arm of immunity.

Keratinocytes

Keratinocytes secrete a variety of anti-microbial peptides (AMPs) as a defence mechanism in response to infection *(Schauber & Gallo, 2009)*. They also express receptors which specifically recognise the bacterial and viral components, and upon stimulation, secrete the AMPs like LL-37, defensins and other pro-inflammatory cytokines and chemokines, which recruit other immune cells in response to infection *(Kobayashi et al., 2009; Metz et al., 2006)*. Recently, keratinocytes have been shown to express MHC class II molecules, and act as antigen–presenting cells in the skin *(Kim et al., 2009)*.

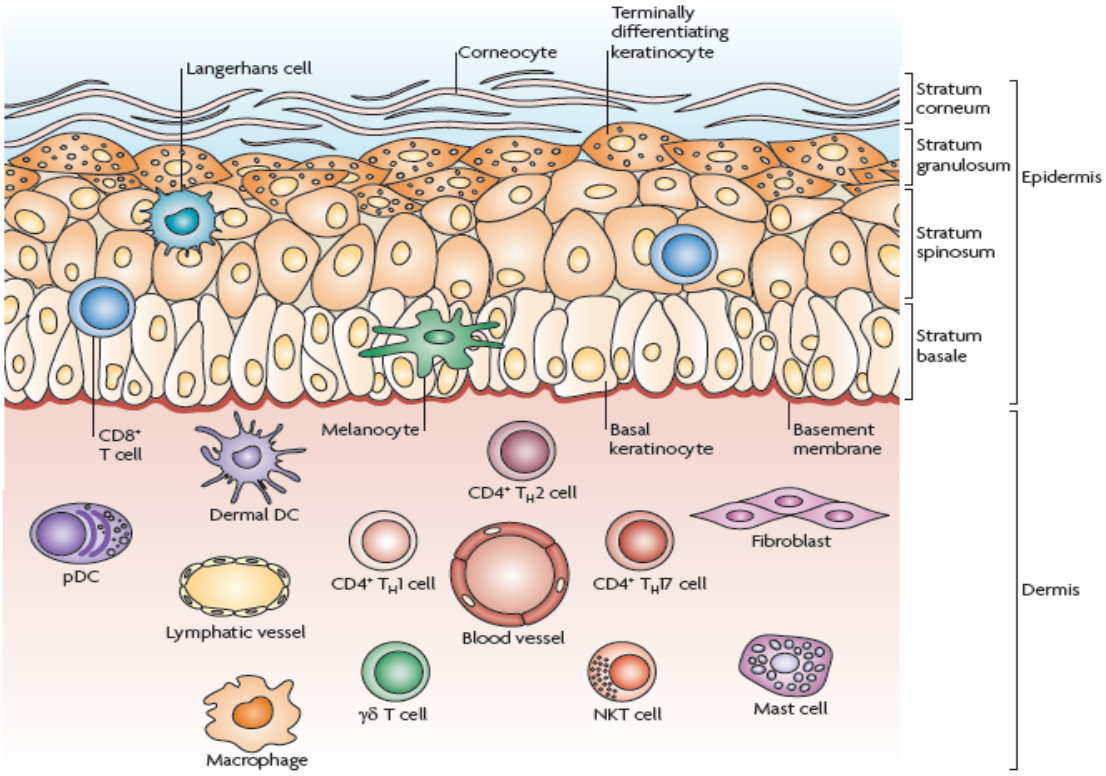

Figure 2: Skin anatomy and cellular effectors.

[Adapted from Nat. Rev.Immunology vol 9, 679-691(2009)]

Dendritic cells (DCs)

DCs are professional antigen presenting cells, which detect the invading pathogen and process and present them to T-cells. In the skin, specialized DCs called Langerhan cells (LCs) are present in the epidermis. Both LCs and dermal DCs take up antigens and present to T-cells in the skin draining lymph nodes and modulate T-cell differentiation and recruitment of the adaptive immune cells to the site of infection *(Villadangos & Young, 2008)*. The involvement of DCs in innate immune response is less well understood and largely unknown for skin DCs. In staphylococcal aureus infection of the skin, DCs recruit neutrophils through IL1R/MyD88 signalling *(Miller et al., 2006)*. Autocrine / paracrine activation of DCs or LCs by IL1β is one of the proposed mechanisms leading to the control of bacterial skin infection *(Miller et al., 2006)*. Additionally DC derived IL1 and IL23 are also involved in the promotion of IL17 production in memory T-cells, offering protection against certain bacteria *(van Beelen et al., 2007)*.

Mast cells

Mast cells (MCs) or allergy cells are the masters of innate immunity in the skin. They play a pivotal role in allergic inflammation. They release inflammatory mediators like histamine, leukotrines and prostaglandins, upon binding of IgE to the FcεRI receptor exposed on their cell surface *(Kraft & Kinet, 2007; Hakim-Rad et al., 2009)*. It has been reported that degranulation of MCs in the presence of an antigen facilitates the sensitization to this antigen *(McLachlan et al., 2008)*. They also play a crucial role in innate host defense, offering protection against bacteria, viruses and fungi. Experiments using MC knock-in mouse model have shown that activation of skin MCs is crucial for protection against infection with Pseudomonas aeruginosa *(Siebenhaar et al., 2007)*. Another study using similar mouse model has shown that MCs offer protection against group A Streptococcus infection. This study demonstrated that MC-derived cathelicidin is one of the essential mediators leading to bacterial killing and possibly also to enhanced recruitment of neutrophils to the site of infection *(Di Nardo et al., 2008)*. MCs also limit allergic inflammation by producing the anti-inflammatory cytokine IL10 and AMPs *(Grimbaldeston et al., 2007)*.

Macrophages

Skin macrophages are predominantly sessile, but under inflammatory conditions, they migrate to lymph node. They enable differential immune responses and also have a role in wound healing *(Zaba et al., 2007)*.

T Cells

Though there are three main types of cells (Th1, Th2 and Th17) found in skin during various inflammatory diseases, studies have suggested that the resident γδT cells and NKT cells have a major role in skin immune homeostasis and pathology *(Boyman et al., 2007)*. Studies in mice have shown that γδT cells negatively regulate inflammation as well as carcinogenesis *(Girardi et al., 2001 & 2002),* whereas in humans they play an important role in wound healing by producing growth factors *(Toulon et al., 2009)*. NKT cells possess the ability to recognise bacterial glycolipids *(Kronenberg, 2005)* and they were also shown to be the source of IFNγ and IL4 in allergic contact dermatitis *(Gober et al., 2008).*

2. Atopic Diseases

Atopic diseases include atopic dermatitis (AD), asthma, allergic rhinitis, allergic conjunctivitis and food allergy, which share related clinical features and similar pathogenic mechanisms *(Kay, 2001; Lack, 2008; Ciprandi & Passalacqua, 2008; Passalacqua & Ciprandi, 2008; Incorvaia et al., 2008; Leonardi et al., 2008)*. The prevalence of these diseases have dramatically increased worldwide in the last decade, affecting approximately 10-20% of children and 2-3% of adults for atopic dermatitis *(Leung et al., 2004)*, and 10% of children and 3% of adults for asthma *(Tattersfield et al., 2002)*. The expanding population of affected patients adds an important burden to health care costs. The term "atopy" *(Kay, 2001)* is borrowed from Greek, meaning "out of place"; it usually refers to immunoglobulin E (IgE)-mediated responses to common allergens. The allergen can be pollen, house-dust mites, cat dander, food, latex and some medicines. Persons with "atopy" are easily sensitive to allergens and exhibit exaggerated responses characterized by the production of allergen specific IgE antibodies and positive reactions in skin prick test *(Galli et al., 2008)*. However, a small percentage of patients have no IgE involvement. Atopic diseases are notably associated with T helper cell type 2 (TH2) inflammation by amplification and persistence of TH2 cells secreting TH2 cytokines such as interleukin-4 (IL-4), IL-5, IL-9 and IL-13 *(Pucci & Incorvaia, 2008)*. Atopic diseases are also associated with eosinophilia and mast cell degranulation *(Galli et al., 2007)*.

Clinicians have long recognized that the various manifestations of atopic diseases are often present in a characteristic sequence, referred to as the "atopic march" *(Hahn & Bacharier, 2005; Spergel, 2005; Spergel & Paller, 2003)*. Affected infants with atopic dermatitis have a higher risk to develop asthma during the childhood or later in adulthood. A number of epidemiologic and birth-cohort studies have shown that approximately half of AD patients develop symptoms of asthma, particularly with severe atopic dermatitis. However, the immunological and molecular mechanisms of this progression are still unclear. Understanding the pathogenesis and underlying link between atopic diseases will be beneficial for early and accurate prevention or novel therapies of these allergic diseases.

2.1 Atopic dermatitis (AD) and related atopic diseases

Atopic dermatitis (AD) is a chronic, relapsing skin inflammatory disease that is characterized by pruritic, eczematoid skin lesions *(Leung et al., 2003)*. It frequently starts in early infancy: a total of 45% of all cases of AD begin within the first 6 months of life, 60% begin during the first year, and 85% begin before 5 years of age *(Bieber, 2008)*. Up to 70% of these children have a spontaneous remission before adolescence. AD can also start in adults. AD is usually manifested as itchy, eczematous lesions on cheeks or scalps, later with crusted erosions in infants (Figure 2). In childhood or adolescence, dry, scaly lesions and lichenification involve in more regions including flexures, dorsal parts of limbs and neck (Figure 2).

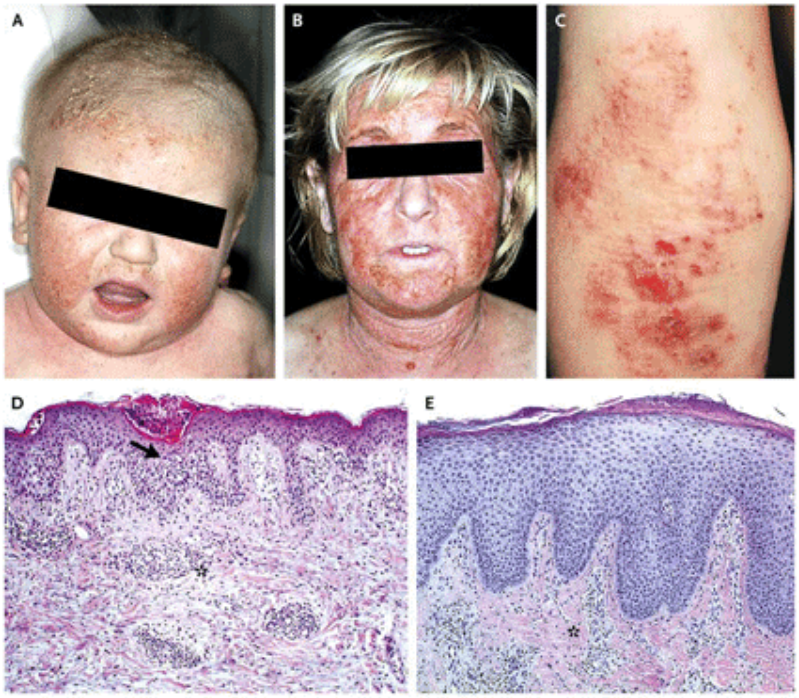

Figure 2: Clinical and histological aspects of atopic dermatitis.

Panel A shows initial lesions of early-onset atopic dermatitis involving the cheek and scalp in an infant at 4 months of age. Panel B shows classic head and neck manifestations of atopic dermatitis in an adult. Panel C shows typical chronic, lichenified flexural lesions in an adult. Panel D shows the typical histologic aspects of acute lesions (hematoxylin and eosin). The arrow indicates a spongiotic area within the epidermis. Panel E shows a chronic lesion with thickening of the epidermis (hematoxylin and eosin). The asterisks indicate the prominent perivascular infiltrate.

[Cited from Bieber T New England Journal of Medicine 2008 Apr 3;358(14):1483-94.]

2.1.1 AD Pathogenesis

AD shares common immunological features with other atopic diseases, including TH2 inflammation with the production of TH2 cytokines, peripheral and lesional eosinophilia, and elevated IgE. Skin lesions evolve as the results of complex interactions between IgE bearing antigen presenting cells, T-cell activation, mast cell degranulation, eosinophils, as well as keratinocytes *(Leung & Bieber, 2003)* (Figure 3).

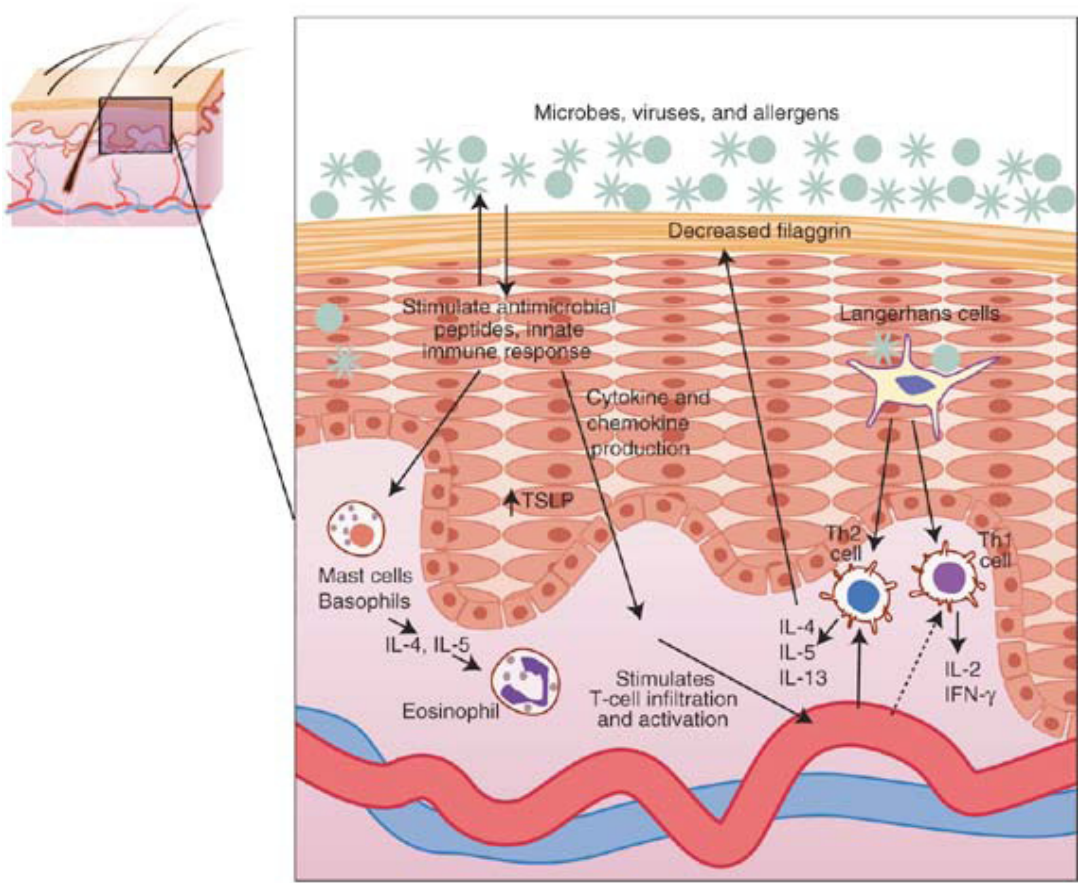

Figure 3: Immune response in barrier impaired-skin in atopic dermatitis.

[Cited from Scharschmidt TC et al. J invest Dermatol 2008 May;128(5):1061-4]

Disruption of the barrier function of the skin is an important and well-recognized etiologic factor in the pathogenesis of AD, which leads to higher TEWL and increased permeability to environmental irritants and allergen *(Leung et al., 2003)* (Figure 3). A reduced content of ceramides has been reported in the cornified envelope of both lesional and nonlesional skin in AD patients *(Leung et al., 2004)*. Alterations in the expression of enzymes involved in the subtle balance of epidermal adhesion structures are also likely to contribute to the

breakdown of the epidermal barrier in patients with AD *(Bieber, 2008)*. Whether the epidermal alterations are primary or are secondary to the underlying inflammation remains still unclear. It has been found that antimicrobial peptides are downregulated in the skin of AD and it is difficult to limit microbial infections of the AD skin. Lesional and normal looking skin of AD patients is often colonized by bacteria such as *Staphylococcus aureus* or fungi such as malassezia *(Lin et al., 2007; Roll et al., 2004)*.

Table 1. Pathogen related receptors (PRRs) that may be defective in subjects with AD

PRRs	Defects in AD	Cell	Ligands	Major function
TLRs	TLR2	KC, DC, LC, PMN, Monocyte, Mast cell, NK	Bacterial components (LPS, PGN, LTA) or yeast (Zymosan)	Production of AMPs, chemokines, and cytokines.
	TLR9	B cell, pDC, NK, KC	Viral and bacterial CpG	
NLRs	NOD1–2	KC, DC, LC, phagocytes,	PGN (Gram-positive and -negative bacteria)	Production of cytokines, chemokines, and AMPs.
CD14	?	DC, KC, macrophages	LPS and other bacterial components	Production of cytokines and chemokines
Soluble PRRs	MBL (?)		Surface of microbes	Opsonization or lysis of microbes. Leukocyte chemotaxis

AMP, antimicrobial peptide; DC, dendritic cell; KC, keratinocyte; LPS, lipopolysaccharide; LTA, lipoteichoic acid; MBL, mannose-binding lectin; NK, natural killer; NLR, NOD leucine rich containing protein; NOD, nucleotide-binding oligomerization domain; pDC, plasmacytoid DC; PGN, peptidoglycan; PMN, neutrophil; TLR, Toll-like receptor.
?, contradictory evidence.

Table 2. Skin innate immunity and related defects observed in AD patients

Skin innate system	Major components	AD defects
Anatomical/ physical barrier	Cornified envelope	Reduced FLG, LOR, and INV expression; SPINK5 deficit; cystatin M/E deficit; enhanced SCCE expression; reduced lipids (ceramides, sphingosine); trauma from itch-scratch cycle
	Tight junctions	Reduced claudin-1
Cellular elements	PMN, NK, DC, LC, Mast cell, KC	Reduced function or migration into the skin of effector cells (PMN, NK, pDC); PRRs dysfunction (TLR2, TLR9, NOD1/2)
Secretory elements	AMP	Decreased AMPs (HBD2, HBD3, LL37, DCD, sphingosine)
	Cytokines/ chemokines	Reduction in MIP3α /CCL20, IL-8/CXCL8

AD, atopic dermatitis;AMP, antimicrobial peptide; DC, dendritic cell; DCD, dermcidin; HBD, human β-defensin; KC, keratinocyte; LL-37, cathelicidin; MIP-3α, macrophage inflammatory protein-3α; NK, natural killer; NOD, nucleotide-binding oligomerization domain; pDC, plasmacytoid DC; PMN, neutrophil; PRR, pattern-recognition receptor; SCCE, stratum corneum chymotryptic enzyme; SPINK5, serine protease inhibitor, Kazal-type; TLR, Toll-like receptor.

[Cited from Journal of Investigative Dermatology (2009) 129, 14–30]

2.1.2 Genetics of AD

AD has a high familial occurrence, with a 2-fold increased risk for a child to develop AD when one of the parents is affected and a 3-fold increase in cases in which both of the parents are affected. Using genome wide linkage analysis and the studies of candidate genes several genes involved in atopy were identified. Interestingly, null mutations in one gene crucial for the integrity of the epithelial barrier, filaggrin (*FLG)*, a member of the epidermal differentiation complex on chromosome 1q21, were recently reported to be strongly associated with AD, and to influence asthma *(Vercelli, 2008; Palmer et al., 2006; Sandilands et al., 2007; O'Regan et al., 2008; Weidinger et al., 2008; McLean et al., 2008; Brown et al., 2008)*. According to a recent meta-analysis, the effect of *FLG* variants on the risk of AD exceeds that of any other candidate gene investigated so far *(Baurecht et al., 2007)*. Netherton syndrome, an autosomal recessive disorder caused by mutations in SPINK5, gene encoding a serine protease inhibitor LEKT1 (lympho epithelial kazal type inhibitor) leads to impaired barrier formation with increased production of thymic stromal lymphopoietin (TSLP, discussed in chapter 4) and AD-like phenotype *(Chavanas et al. 2000)*. Recent evidence has shown that polymorphisms in TSLP and TSLPR (TSLP receptor) genes are associated with atopic eczema, asthma, airway hyper-responsiveness, IgE concentrations and eosinophilia *(Yu et al., 2010; Harada et al., 2010; Gao et al., 2010)*. Several genes associated with atopic diseases are mentioned below (figure 4), classified according to their function.

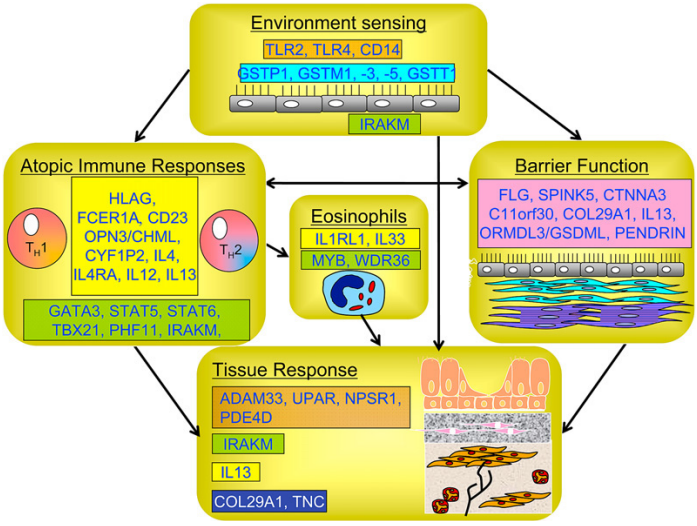

Figure 4: Susceptibility genes for allergic disease.

Group 1: sensing the environment. This group of genes encodes molecules that directly modulate the effect of environmental risk factors for allergic disease. For example, genes such as TLR2, TLR4, and CD14, encoding components of the innate immune system, interact with microbes to alter the risk of allergic immune responses *(Yang et al., 2007)*. Polymorphisms of glutathione-S-transferase genes (GSTM1, GSTM2, GSTM3, GSTM5, GSTT1, and GSTP1 *(London & Romieu, 2009; Breton et al., 2009)* have been shown to modulate the effect of exposures involving oxidant stress, such as tobacco smoke and air pollution on asthma susceptibility.

Group 2: barrier function. A high proportion of the novel genes identified for susceptibility to allergic disease through genome-wide linkage and association approaches have been shown to be expressed in the epithelium. This includes genes such as FLG *(Palmer et al., 2006)*, which directly affects epidermal barrier function and is associated not only with increased risk of atopic dermatitis but also with increased atopic sensitization. Other susceptibility genes, such as ORMDL3/GSDML *(Moffatt et al., 2007)*, PCDH1 *(Koppelman, 2009)*, and C11orf30 *(Esparza-Gordillo, 2009)*, are also expressed in the epithelium and might have a role in possibly regulating epithelial barrier function.

Group 3: regulation of (atopic) inflammation. This group includes genes that regulate TH1/TH2 differentiation and effector function (eg, IL13, IL4RA, and STAT6 *(Kabesch et al., 2006)*; TBX21 [encoding T-box transcription factor] *(Suttner K et al., 2009)*; and GATA3 *(Pykalainen et al., 2005)*, as well as genes such as IRAKM *(Balaci et al., 2007)*, PHF11 *(Zhang et al., 2003)*, and UPAR *(Barton et al., 2009)* that potentially regulate both atopic sensitization and the level of inflammation that occurs at the end-organ location for allergic disease. This also includes the genes shown to regulate the level of blood eosinophilia (IL1RL1, IL33, MYB, and WDR36) *(Gudbjartsson et al., 2009)*.

Group 4: tissue response genes. This group includes genes that modulate the consequences of chronic inflammation (eg, airway remodeling), such as ADAM33 *(Van Eerdewegh et al., 2002)* and PDE4D *(Himes et al., 2009)*, which are expressed in fibroblasts and smooth muscle, and COL29A1 *(Soderhall et al., 2007)*, encoding a novel collagen expressed in the skin linked to atopic dermatitis. Some genes can affect more than 1 disease component. For example, IL13 regulates both atopic sensitization through IgE isotype switching but also has

direct effects on the airway epithelium and mesenchyme, promoting goblet cell metaplasia and fibroblast proliferation *(Holloway et al., 2007)*.

[*Adapted from J Allergy Clin Immunol 2010;125:S81-94.]*

2.2 Atopic march: from AD to allergic rhinitis/asthma

In the typical sequence of progression of clinical signs of atopic diseases, clinical signs of AD frequently precede the development of asthma and allergic rhinitis, suggesting that AD is a starting point in the atopic march (Figure 5). More than 50% of AD patients with moderate to severe AD develop asthma and/or allergic rhinitis later in life *(Spergel & Paller, 2003)*. There are a number of studies indicating that the severity of AD can influence the course of respiratory allergy *(Rhodes et al., 2001; Rhodes et al., 2002; Gustafsson et al., 2000)*. It has been reported that 70% of the patients with severe AD developed asthma compared with 30% of the patients with mild AD, and approximately 8% in the general population. Similarly, the severity of AD correlated with elevated levels of total and specific serum IgE *(Oettgen & Geha, 2001)*, and elevation of IgE levels has also been correlated with the risk of developing asthma *(Burrows et al., 1989)*. In contrast, the absence of AD was associated with a lesser asthma severity.

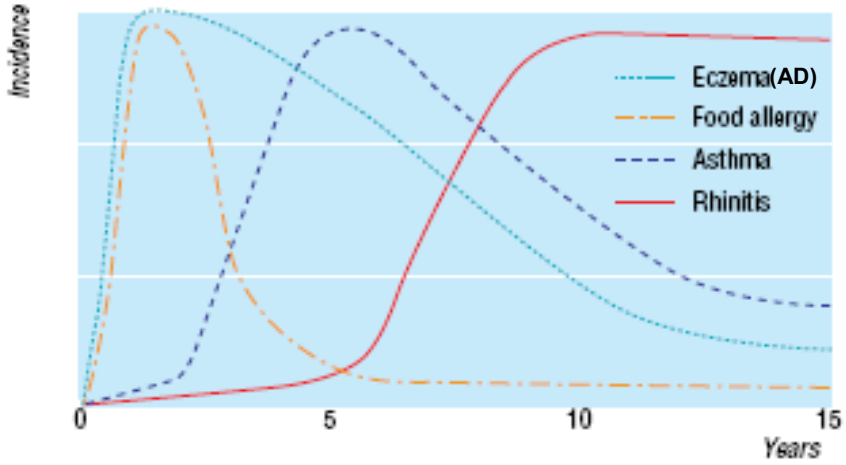

Figure 5 Incidence of different atopic diseases. AD peaks in the first years of life and declines later. Asthma and allergic rhinitis increase over time as sensitization develops.

[Cited from Barnetson & Rogers Childhood atopic eczema. BMJ. 2002 Jun 8;324(7350):1376-9.]

Skin has been recognized as one of the initiation sites for allergen sensitization *(Bieber, 2008)*, and skin sensitization may precede airway sensitization. Epicutaneous allergen sensitization might evoke a systemic allergic response, including of the upper and lower airways. Studies have also indicated that patients with skin sensitization to dust mites develop airway sensitization to the same allergen. Atopic children exposed to topical emollients with detectable peanut protein had an increased risk of developing peanut sensitization *(Lack et al.,2003)*. In an experimental model of AD, *Spergel et al, 1998*, epicutaneously applied ovalbumin (OVA) with occlusive patch to tape-stripped skin to induce dermatitis in mice, showing epidermal thickening and spongiotic changes with epidermal infiltration of CD4+ T cells and eosinophils, and increases in the expression of both TH2 and TH1 cytokines (IL-4, IL-5, and IFN-γ). Epicutaneously sensitized mice, subsequently challenged with a single exposure to inhaled OVA, showed a significant increase in the number of eosinophils in the bronchoalveolar lavage (BAL) fluid, and airway hyperresponsivenes. This study provides a strong support to a role of epicutaneous sensitization in the atopic march. In addition, other investigators *(Kondo et al., 1998; Wang et al., 1996; Bellinghausen et al., 1999)* have demonstrated that epicutaneous sensitization with allergens elicits a TH2-dominant systemic immune response. In these studies, increased serum IgE and local production of IL-4 and IL-5 were observed in the skin and draining lymph nodes after epicutaneous allergen sensitization. Moreover, skin barrier disruption further enhances the TH2 response *(Kondo et al., 1998)*. This may be relevant to the clinical observation that higher epidermal barrier impairment in AD infants is associated with higher prevalence of sensitization to aeroallergens *(Boralevi et al., 2008)*.

2.3 AD management

Patients with AD should avoid contact with irritants, as they have a lower threshold of irritant responsiveness *(Nassif et al., 1994)*. Food allergens have been shown to play a role in a subset of patients with AD, with milk, egg, peanut, soy, wheat and fish accounting for approximately 90% of the foods found to exacerbate AD *(Sicherer et al., 1999)*. Removal of proven food allergens from the patient's diet can lead to significant clinical improvement. Omalizumab, a humanized IgG1 monoclonal antibody (mAb) against IgE that recognizes and masks an epitope in the CH3 region of IgE responsible for binding to the high-affinity Fc epsilon (FCεRI) receptor on mast cells and basophils, has been shown to be an effective treatment of allergic asthma and allergic rhinitis *(Corren et al., 2003; Kopp et al., 2002)*.

Studies using probiotics have shown that perinatal administration of the *Lactobacillus rhamnosus* strain GG reduces the incidence of AD in at-risk children during the first 2 years of life *(Kalliomäki et al., 2002)*. A follow-up study from the same group assessed the persistence of potential to prevent AD at 4 years *(Kalliomäki et al., 2003)*, thus emphasising the need to activate Th1 response early in life to avoid proallergic Th2 pathway later in life.

Several topical barrier creams have become available for use in the management of AD. These physiologic moisturizers contain either ceramide or fatty acid palmitamide or the anti-inflammatory molecule glycyrrhetinic acid, telmesteine, shea butter, caprylol glycine, and hyaluronic acid in a hydrolipidic base. Ceramide dominant cream TriCeramTM has been shown to result in significant improvement in childhood AD, both in clinical score as well as improved barrier function *(Chamlin et al., 2002)*. These studies reveal the importance of effective barrier maintenance to avoid immunological complications.

2.3.1 Corticosteroids

Topical corticosteroid application has been the mainstay of treatment for AD, showing efficacy in both acute and chronic disease. By acting on multiple resident and infiltrating cells, primarily through suppression of the expression of inflammatory genes, they are effective in reducing inflammation and pruritus *(Barnes, 2002)*. In addition, topical corticosteroids might have an effect on bacterial colonization in AD, reducing the density of *S aureus (Nilsson et al., 1992; Stalder et al., 1994)*. Topical corticosteroids are available in extremely high (class 1) to low (class 7) potencies. Choice of which topical corticosteroid preparation to prescribe will depend in large part on the severity and distribution of eczematous lesions. Though effective, their use is limited by side effects which can include inhibition of barrier function, thinning of skin and resultant striae, as well as acneiform eruptions *(Lutgemeier et al., 1987; Oikarinen & Autio, 1991; Hardie et al., 1977)*. Systemic glucocorticoids such as oral prednisone are highly immunosuppressive but generally avoided in the treatment of chronic AD because of systemic toxicities *(Ellison et al., 2000)*. Rarely, short courses of oral glucocorticoids might be initiated for acute exacerbations of AD while other treatment measures are being introduced. If used, intensive topical therapy should be initiated during systemic treatment to prevent rebound flaring of AD.

2.3.2 Calcineurin inhibitors

Tacrolimus (FK 506) and Pimecrolimus are potent calcineurin inhibitors, which are active topically and have been shown to be effective for treatment of AD *(Bekersky et al., 2001; Boguniewicz et al., 1998; Paller et al., 2001; Meingassner et al., 1997; Eichenfield & Beck, 2003)*. Both tacrolimus and pimecrolimus work through inhibition of phosphorylase activity of the calcium-dependent serine/threonine phosphatase calcineurin and the dephosphorylation of the nuclear factor of activated T-cell protein (NF-ATp), a transcription factor necessary for the expression of inflammatory cytokines including IL-2, IL-4, and IL-5 *(Tocci et al., 1989; Stuetz et al., 2001)*. They might also inhibit the transcription and release of other T-cell derived cytokines including IL-3, IFN-γ, TNF-α and GM-CSF, which can contribute to allergic inflammation *(Hultsch et al., 1998)*. Long-term open-label studies with tacrolimus ointment applied on up to 100% of the body surface area have been performed for up to 12 months in adults and children, with demonstrated sustained efficacy and no significant side effects

The majority of the studies of topical pimecrolimus and tacrolimus discussed above assessed efficacy of these medications as primary monotherapy of AD, with topical or systemic steroids used as "rescue" for disease flares. Clearly, new steroid-free topical agents might offer improved long-term management options for patients with AD. Evolution of topical therapy will likely include combinations of topical anti-inflammatory agents including calcineurin inhibitors and topical corticosteroids. The combination of topical calcineurin inhibitors and topical steroids becomes an appealing choice, with calcineurin inhibitors as first-line pharmacologic therapy to treat AD and steroids to be administered for short courses as rescue therapy. The advantage of this strategy is 2-fold; first, the exposure to topical steroids is limited, markedly reducing the risk of side effects, and second, when topical steroids are used, they are applied on steroid naive skin, maximizing their efficacy and avoiding tachyphylaxis *(du Vivier, 1976; Queille-Roussel et al., 2001)*.

3. Transcriptional regulation of gene expression

A basic aspect of cellular response to environmental stimulus is modulation of gene expression. Eukaryotic chromosomes are organized into a regularly repeating protein DNA unit termed the nucleosome. The basic protein unit of the nucleosome is the histone core, a small, highly basic, globular moiety, which forms a histone octamer, around which is wrapped DNA superhelix to form a compact chromatin structure. The net effect of this arrangement is to create a thermodynamic barrier against the access of transcription factors to their DNA substrate. Modulation of gene expression involves changes in the organization of genomic DNA in chromatin: DNA and histone modifications and chromatin remodelling. Besides the general transcription machinery, several factors act in a cooperative manner to regulate this process of gene expression. These include transcription factors (TFs) – sequence specific DNA binding proteins, and coregulators – proteins which do not bind to the DNA directly, but modulate gene expression by binding to the other transcription factors and chromatin remodelling enzymes. In general, active chromatin is associated with TFs which recruit coactivators along with histone acetyl transferases (HATs) which add acetyl group to the histone tails, thus unwinding the chromatin for TFs to bind (Figure 6), whereas corepressors and histone deacetylases (HDACs) are marks of repressed chromatin (Figure 7).

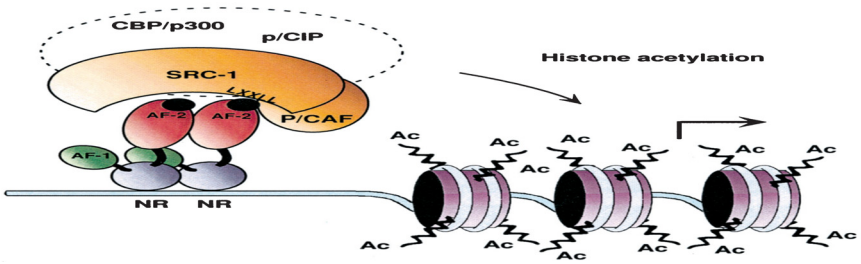

Figure 6: Schematic of a transcriptionally active chromatin

Nuclear receptors (NRs) recruit coactivators like SRC-1, P/CAF, p300/CBP, p/CIP, which possess histone acetyl transferase activity, leading to chromatin decompaction and transcriptional activation.

[Modified from Robyr et al., 2000]

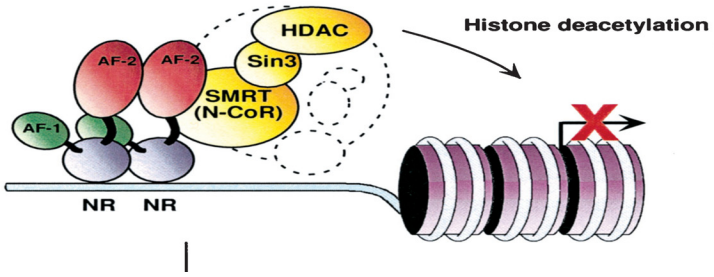

Figure 7: Schematic of a transcriptionally inactive chromatin

NRs assemble corepressors SMRT or NCoR, which in turn recruit histone deacetylases (HDACs), leading to transcriptional repression.

[Modified from Robyr et al., 2000]

Transcription factors:

3.1 Nuclear Receptors (NRs)

Nuclear receptors comprise a family of ligand-dependent and orphan transcription factors that mediate a complex array of extracellular signals into transcriptional responses, many of which specifically regulate the expression of target genes involved in metabolism, development and reproduction. Their primary function is to mediate the transcriptional response in target cells to hormones such as the sex steroids (progestins, estrogens, and androgens), adrenal steroids (glucocorticoids and mineralocorticoids), vitamin D3, thyroid and retinoid (all-trans) hormones, in addition to a variety of other metabolic ligands. There are 49 and 48 nuclear receptors known to exist in mouse and humans, respectively, and these proteins comprise the single largest family of metazoan transcription factors, the nuclear receptor superfamily.

The nuclear receptors are characterized by an N-terminal A/B region which contains a transcriptional activation function, referred to as activation function 1(AF1). This region is weakly conserved and can act independently of ligand binding. It is known to interact with cofactors and other transcription factors. There is a central DNA-binding domain (DBD) which targets the receptor to specific DNA sequences known as hormone response elements (HREs). The DBD is composed of two highly conserved zinc fingers that set the nuclear receptors apart from other DNA-binding proteins *(Berg, 1989; Klug & Schwabe, 1995).* The C-terminal half of the receptor encompasses the ligand-binding domain (LBD), which

possesses the essential property of hormone recognition and ensures both specificity and selectivity of the physiologic response. It comprises of a ligand dependent transactivation function domain, AF-2 in the C-terminal region, which is indispensable for ligand-dependent activation by nuclear receptors *(Bourguet et al., 2000; Li et al., 2003)*. The D region acts as a hinge between DBD and LBD, allowing rotation of DBD. It is weakly conserved and harbours nuclear localization signal (NLS) (Figure 8).

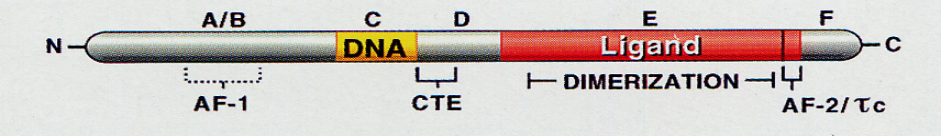

Figure 8: Schematic of a Nuclear Receptor structure

[Adapted from Mangelsdorf & Evans, 1995]

Based on sequence alignment and phylogenetic tree construction, NR superfamily is broadly classified into six evolutionary groups of unequal size *(Germain P. et al., 2006)*:

- *Group 1*: Retinoid Acid Receptor (RAR), Vitamin D Receptor (VDR), Thyroid Receptor (TR), Peroxisome Proliferator-Activated Receptor (PPAR), Constitutively Activated Receptor (CAR), Pregnane X Receptor (PXR), Liver X Receptor (LXR), Farnesoid X Receptor and orphan receptors, Retinoid-related Orphan Receptor (ROR), Rev-erbs.
- *Group 2*: Retinoid X receptor (RXR), Chicken Ovalbumin Upstream Promoter Transcription Factor (COUP-TF) and Hepatocyte Nuclear Factor (HNF-4).
- *Group 3*: Estrogen Receptor (ER), Glucocorticoid Receptor (GR), Mineralocorticoid Receptor (MR), Progesterone Receptor (PR), Androgen Receptor (AR) and Estrogen receptor-related (ERRs).
- *Group 4*: nerve growth factor induced clone B group of receptors, NGFI-B, NURR1, and NOR1.
- *Group 5*: orphan receptors, steroidogenic factor 1 (SF1) and the receptors related to the *Drosophila* FTZ-F1.
- Group 6: Germ cell nuclear factor (GCNF1) receptor

Nuclear receptors primarily act through direct association with specific DNA sequences known as hormone response elements (HREs) *(Mangelsdorf & Evans, 1995; Chambon, 1996; Laudet & Gronemeyer, 2002)*. For the nonsteroid members of the receptor

superfamily, the HREs consist of a minimal core hexad consensus sequence, AGGTCA, which can be configured into a variety of structured motifs. These HREs directly reflect the mode of receptor binding, which can be as heterodimers, homodimers, or monomers. In contrast, the steroid hormone receptors bind exclusively as homodimers to palindromes separated by three nucleotides. Based on their dimerization and DNA binding properties, the nuclear receptor superfamily can be broadly divided into four classes as mentioned in the table below *(Stunnenberg, 1993)*.

Class	Hormone receptor	HRE	Dimerization
I	Steroid receptors	Inverted repeat (IR)	Homodimers
II	RXR partners, Ligand dependent receptors	Direct repeat (DR)	Heterodimers
III	Orphan receptors	Direct repeat (DR)	Homodimers
IV	Orphan receptors	Direct repeat (DR)	Monomers

3.1.1 Retinoid X Receptor (RXR)

A search for proteins that could enhance RAR binding to retinoic acid response element (RARE), led to the discovery of Retinoid X Receptors (RXRs) by Yu et al., 1991 and Leid et al., 1992. Additionally, RXRs were shown to form stable heterodimers with TR and VDR, increasing their DNA binding efficiency and transcriptional function on their respective response elements. Subsequently, RXRs were found to be heterodimerization partners for DNA binding of several other receptors. There are three isotypes of RXR; RXRα, RXRβ, and RXRγ which have 2 isoforms each *(Fleischhauer et al., 1992; Liu & Linney, 1993; Nagata et al., 1994; Brocard et al., 1996)*. The functional relevance of these isoforms is yet to be characterized. RXRα is predominantly expressed in liver, kidney, epidermis and intestine. RXRβ is ubiquitously expressed, whereas RXRγ expression is restricted to muscle, brain and pituitary. RXRα is the major RXR expressed in skin.

RXRs heterodimerize with RARs, VDR, PPARs, LXRs, TR, FXR, PXR and CARs. Being obligate heterodimerization partners for most of the non-steroid members of NR family, RXRs regulate a number of genes. In vitro studies demonstrated that these heterodimers act as ligand-dependent transcriptional regulators by binding to specific DNA-response

elements found into the promoter region of target genes and the interaction of RXR increases the DNA-binding efficiency of its partner. Moreover, both in vitro and in vivo approaches have revealed that all these nuclear receptors require RXR as a heterodimerization partner for their function *(Laudet & Gronemeyer, 2002)*. In addition, RXRs form heterodimers with two members of the small nerve growth factor-induced clone B (NGFIB) subfamily, namely NGFIB and NURR1, which can also interact with DNA as monomers and homodimers *(Forman et al., 1995; Perlmann & Jansson, 1995)*. RXR heterodimers recognize distinct types of response elements. For instance, RXR-RAR heterodimers bind to a direct repeat of the AGGTCA core motif with a 5-base pair spacing (DR-5) and DR-2, whereas RXR-TR and RXR-LXR bind to DR-4, RXR-VDR and RXR-PXR to DR-3, and RXR-PPAR to DR-1 *(Glass, 1994)*. The spacing is critical and determines the specificity of the binding. However, the sequence of the core motif itself, the sequence of the spacer, or that of the flanking nucleotides may also play a role in this interaction In vitro, RXRs can also form homodimers that can bind to DNA through DR-1 elements, suggesting the existence of a RXR-specific signaling *(Mangelsdorf et al., 1991; Mader et al., 1993).*

The in vivo functional significance of RXRs was determined by studies involving genetic ablation of the isotypes in mice. RXRα null are embryonic lethal due to hypoplasia of the myocardium, resulting in cardiac failure *(Kastner et al., 1994; Sucov et al., 1994)*. They also show ocular malformation. Some of the RXRβ null mice are lethal, but among the surviving mice, males are sterile *(Kastner et al., 1996)*, whereas RXRγ null mice are normal except for higher serum thyroid and thyroid stimulating hormone levels and increased metabolic rates *(Krezel et al., 1996)*. These studies show that though there is a redundancy of different isotypes in certain aspects, other functions do need the selective RXRs for heterodimerization.

3.1.2 Retinoic Acid Receptor (RAR)

The family of NRs which mediate the physiological effects of retinoids (all-trans retinoic acid and its analogs) are known as Retinoic Acid Receptors (RARs). RARs play an essential role during development, like in morphogenesis, organogenesis, and differentiation (*Chambon, 2005)*. Like RXRs, there are three isotypes of RARs; RARα, RARβ, and RARγ

and there are several isoforms for each isotype *(Giguere et al., 1987; Petkovich et al., 1987; Chambon, 1996)*. There are 2 isoforms each for RARα and RARγ, whereas RARβ has 4 isoforms. RARα is expressed in almost all of the tissues, whereas RARβ and RARγ are more selective *(Dolle et al., 1990)*. RARγ is the major RAR expressed in skin. Owing to the redundancy of the receptor, all RAR single-null mutant mice are viable. RARα null males are sterile, RARβ null mice show abnormalities in the vitreous body in eyes, and impaired locomotion and motor coordination abilities and RARγ nulls show skeletal and epithelial defects.

RARs execute their functions in vitro by heterodimerizing with the RXRs, with no specificity for a particular isotype. The RXR-RAR heterodimers act as ligand-dependent transcriptional regulators by binding to the specific retinoic acid response element (RARE) DNA sequences found in the promoter region of retinoid target genes. RAREs correspond to direct repeats of polymorphic arrangements of the canonical motif 5'-PuG (G/T) TCA separated by five (generally referred to as DR5) or one (DR1) or two (DR2) nucleotides (Pu-purine) *(Leid et al., 1992; Mangelsdorf & Evans, 1995)*. In the absence of RAR agonist, the RAR-RXR heterodimer regulates gene expression by recruiting corepressor complex comprising of NCoR or SMRT and HDAC or DNA methyl transferase, which leads to an inactive, condensed chromatin, thus preventing transcription, whereas binding of agonist results in release of corepressor complex and recruitment of a coactivator complex along with HAT or Histone arginine methyl transferase to activate transcription *(Glass & Rosenfeld, 2000)*.

3.1.3 Vitamin D Receptor (VDR)

The biologic effects of 1α, 25(OH) 2D3 (active vitamin D3, VD3) are mediated through the Vitamin D Receptor (VDR). VDR is expressed mainly in intestine, thyroid and kidney and has a major role in calcium homeostasis. The VDR was the first NR gene for which human mutations were identified *(Hughes et al., 1988)* and disruption of VDR function due to VDR gene mutation or the absence of the 1, 25(OH) 2D3 ligand leads to rickets *(Kato et al., 2002)*. The VDR knockouts fail to thrive, generally die before 4 months of age and show alopecia, infertility, hypocalcemia, and severely impaired bone formation. Female mice have uterine hypoplasia and impaired folliculogenesis *(Li et al., 1997; Yoshizawa et al., 1997;*

Van Cromphaut et al., 2001; Zeitz et al., 2003). VDR polymorphism is known to be associated with asthma *(Raby et al., 2004),* and VDR null mice fail to develop experimental asthma phenotype *(Wittke et al., 2004)*.

Similar to RARs, the VDR functions as a ligand-activated transcription factor that binds to specific DNA sequence elements (VDREs) in vitamin D responsive genes and ultimately influences the rate of transcription *(Haussler et al., 1997)*. In general, VDREs are imperfect direct repeats of the sequence GGGTGA separated by a three nucleotide spacer (DR3) *(Morrison et al., 1989)*. Binding of the VD3 to VDR hormone binding domain (HBD) induces heterodimerization of VDR with RXR and high affinity binding of the VDR-RXR heterodimer to the VDRE promoter sequences, recruiting coactivator complex for enhancing transcription.

3.1.4 Glucocorticoid Receptor (GR)

Glucocorticoids (GCs) are steroid hormones essential for maintaining normal physiological homeostasis. The functions of GCs are mediated by GR, which is ubiquitously expressed. There are two isoforms of GR, GRα and GRβ, which are encoded by the human GR gene. GRα is the predominant isoform. Alternate splicing and translation initiation sites yield several other isoforms of GR, whose physiological role is not completely understood (Figure 9). GRα alone binds to endogenous GCs. Expression of GRβ is low and its physiological relevance is less well understood *(Oakley et al., 1995 & 1997)*. It is known to act as a dominant negative repressor of GRα. GRβ is the major isoform expressed in glucocorticoid resistant asthma *(Gross et al., 2009; Kino et al., 2009)*.

GC bound GR mediates vast array of signalling mechanisms. Endogenous GCs are produced in response to environmental or stress signals through the Hypothalamus-Pituitary-Adrenal (HPA) axis *(Chrousos, 1995)*. The critical role of GR during development is revealed by the fact that GR knockout mice die a few hours after birth due to lung abnormalities *(Cole et al., 1995)*. In addition, study of the skin from the GR knockout foetuses has shown that GR is essential for effective barrier formation during development *(Bayo et al., 2008)*.

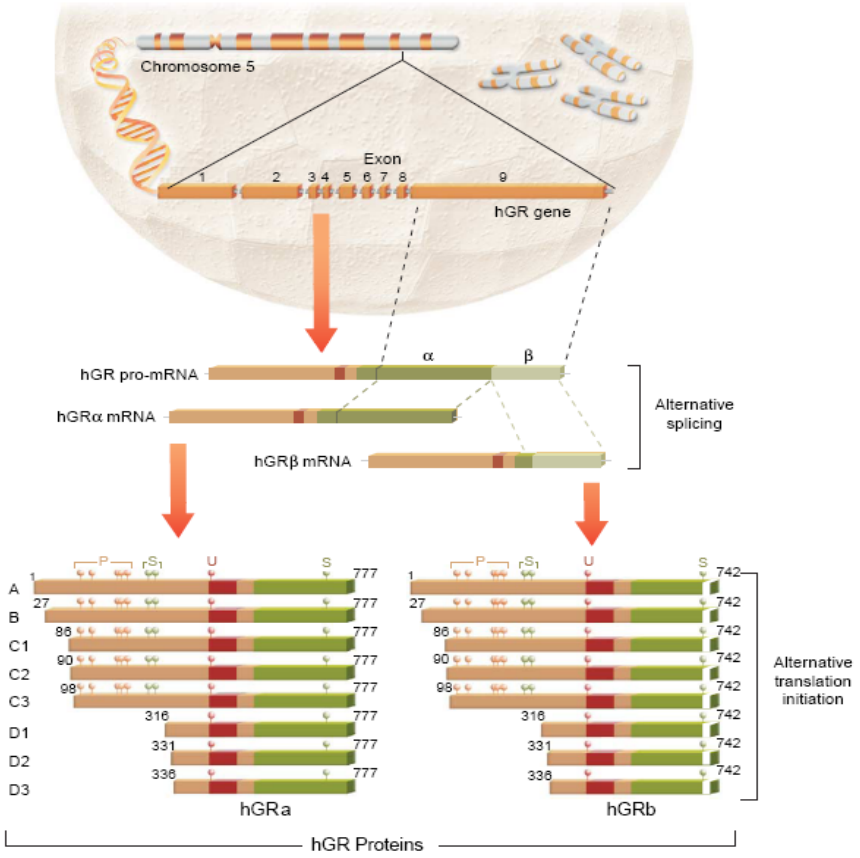

Figure 9: Multiple isoforms of human GR

One GR gene generates multiple GR isoforms. Alternative splicing of exon 9 generates GRa (dark green) and GRb (light green). Each GRa or GRb mRNA produces additional isoforms by alternative translation initiation. Numbers denote the first and last residues for each human GR isoform. Each GR protein is covalently modified by phosphorylation (P) at residues S113, S141, S203, S211 and S226, ubiquitination (U) at K417 (equivalent of K426 in mouse GR) and sumolyation (S) at residues K277, K293 and K703.

[Adapted from TRENDS in Cell Biology Vol.16 No.6 June 2006]

In absence of ligand, GR is inactive in the cytoplasm bound to a chaperone complex composed of heat shock proteins (hsp90, hsp56, hsp40), immunophilins (FKBP51, FKBP52, cyp44, pp5), p23, Src and others, which conceal the nuclear localization signal (NLS) (Figure 10) *(Dittmar et al., 1997)*. Ligand binding induces a conformational change in GR that leads to its dissociation from the multimeric complex and its translocation into the nucleus. In the nucleus, ligand-bound GR dimerizes and binds to the DNA sequence called glucocorticoid response elements (GREs), which are characterized by an inverted

palindrome separated by a 3 nucleotide spacer sequence 5'- AGAACAnnnTGTTCT-3' *(Schoneveld et al., 2004)*. GRE half-sites are sufficient to elicit GR-mediated transcriptional changes. DNA binding by GR induces a conformational change in the receptor that results in the physical association with a variety of coregulatory factors and their recruitment to the chromatin.

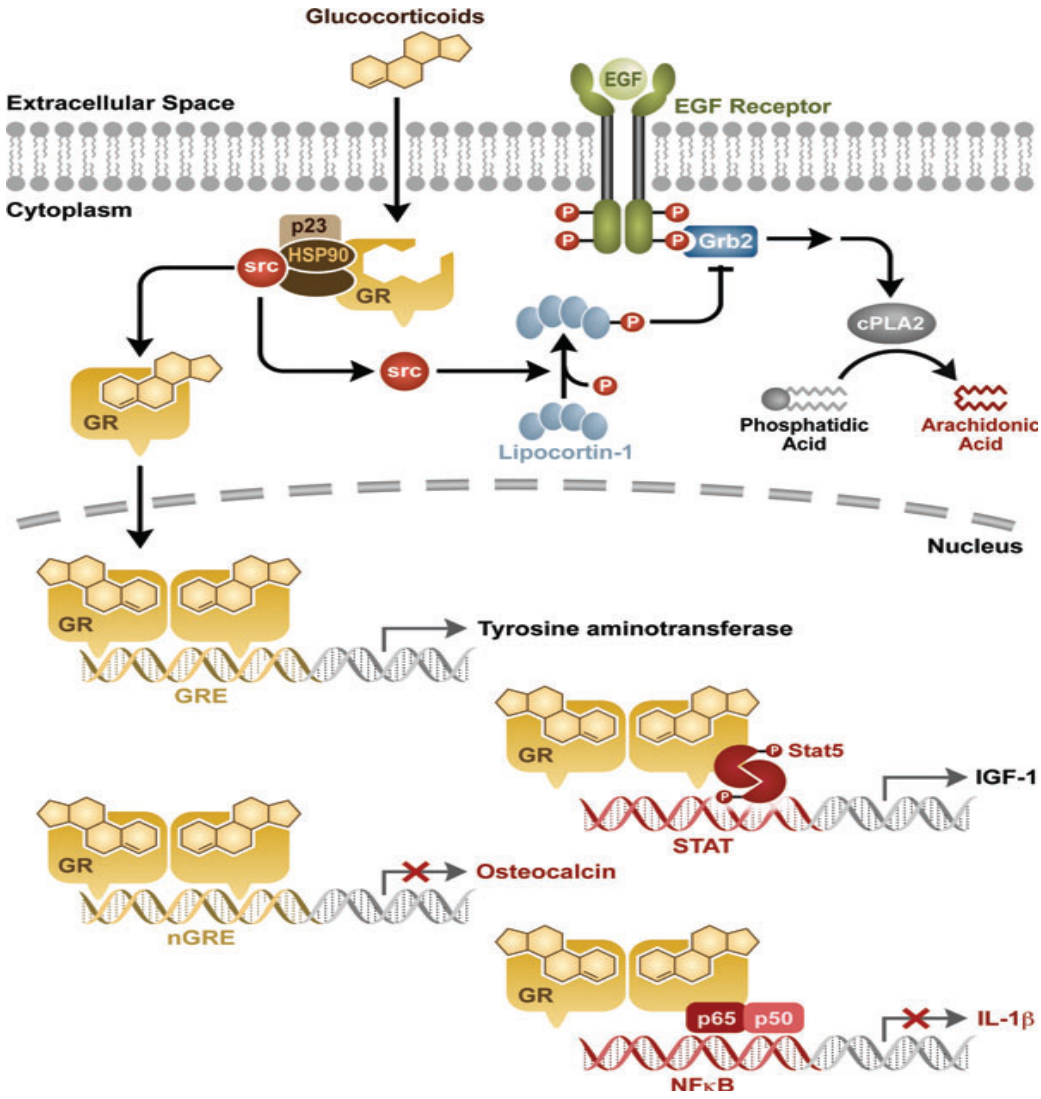

Figure 10: Schematic representation of GR signaling pathway.

[Cited from Ann. N.Y. Acad. Sci. 1179: 167–178 2009]

GR promotes gene induction by several mechanisms, it can both activate and repress target genes by both DNA-dependent and -independent functions (Figure 10). In DNA dependent

gene activation mechanism, GR binding to GREs (Glucocorticoid response elements) recruits coactivators that in turn promote the recruitment of the basal transcriptional machinery. Further, GR recruits chromatin-remodeling coactivators that alter the nucleosomal structure of the DNA and create a more favorable environment for gene expression *(Glass & Rosenfeld. 2000; Rosenfeld & Glass. 2001; Wallberg et al., 1999; Nagaich et al., 2004)*. GR can also regulate gene activity independent of DNA binding via protein–protein interactions with other transcription factors (Figure 10). GR-dependent gene activation by this mechanism is best illustrated by STATs. It has been shown that GR physically interacts with STAT-5, which is directly associated with the DNA. GR is recruited to the STAT5-DNA complex without it directly interacting with the DNA. The GR–STAT-5 association leads to activation of several target genes. GR is also capable of interacting with STAT-3 and -6 to promote gene activation *(Schindler, 1999; Zhang et al., 1997; Biola et al., 2000).*

GR also plays a role in repression of transcription by interacting with negative GREs (nGREs), located on DNA (Figure 10). There is no definitive sequence yet characterized for an nGRE. The interaction of GR–nGRE leads to gene silencing by competing with, and displacing, other transcription factors from the DNA *(Meyer et al., 1997; Novac et al., 2006)*. But nGRE mediated gene silencing has been reported only for a few genes. Most of the genes are repressed by a mechanism of "tethered transrepression", wherein GR interacts with other proteins independent of DNA binding (Figure 10). This mechanism of signalling has been best characterized for the transcription factors NF-κB, AP1 and SMAD3, and to a lesser extent for NF-AT and IRFs, all of which are involved in inflammatory signalling cascades. GR can physically bind to p65 and repress the NF-κB -mediated transcription in several ways. GR interacts with p65 and sequesters the NF-κB complex, thereby preventing NF-κB from reaching its DNA-binding site *(McKay & Cidlowski, 1998; Almawi & Melemedjian, 2002)*. GR can also interact with DNA-bound NF-κB to inhibit the recruitment of the transcriptional machinery. Similar to NF-κB, GR can bind and repress the transcriptional activity of other transcription factors *(Schule et al., 1990; Song et al., 1999).*

The transactivation function of GR can be dissociated from "tethered transrepression" by introducing point mutation, Alanine to Threonine (A458T) in the D-loop of the DNA binding domain *(Heck et al., 1994)*. Initial studies using this mutant GR in cell transfection

assays have shown that though GR cannot bind to DNA, it was efficient in repressing AP1 mediated collagenase gene expression like the wild type reporter. Mice harboring the A458T mutation (GRdim), defective in dimerization and hence DNA binding, have shown similar results *(Reichardt et al., 1998)*. In addition, unlike the GR null, the GRdim mutants are viable, indicating the importance of DNA binding independent functions of GR in vivo.

3.2 NF-κB signaling complex

In mammals the Nuclear Factor κB (NF-κB) family of transcription factors contains five members: NF-κB1 (p105/p50), NF-κB2 (p100/p52), RelA (p65), RelB, and c-Rel. NF-κB1 and NF-κB2 are synthesized as large polypeptides that are post translationally cleaved to generate the DNA binding subunits p50 and p52, respectively. Members of the NF-κB family are characterized by the presence of a Rel homology domain, which contains a nuclear localization sequence and is involved in sequence-specific DNA binding, dimerization, and interaction with the inhibitory IκB proteins *(Gewirtz et al., 2001)*. The NF-κB members dimerize to form homo- or heterodimers, which are associated with specific responses to different stimuli and differential effects on transcription. NF-κB dimers bind promoter and enhancer regions containing κB consensus sequences 5′ GGGRNWYYCC 3′ (N-anybase; R-purine; W-adenine or thymine; and Y-pyrimidine). NF-κB1 (p50) and NF-κB2 (p52) lack transcriptional activation domains, and their homo dimers are thought to act as repressors. In contrast, Rel-A, Rel-B, and c-Rel carry transcriptional activation domains, and with the exception of Rel-B, they are able to form homo- and heterodimers with the other members of this family of proteins. The balance between different NF-κB homo- and heterodimers will determine which dimers are bound to specific κB sites, and thereby regulate the level of transcriptional activity. These proteins are expressed in a cell- and tissue-specific pattern that provides an additional level of regulation. For example, NF-κB1 (p50) and RelA are ubiquitously expressed, and the p50/RelA heterodimers constitute the most common inducible NF-κB binding activity. In contrast, NF-κB2, Rel-B, and c-Rel are expressed specifically in lymphoid cells and tissues. In unstimulated cells, NF-κB dimers are retained in the cytoplasm in an inactive form as a consequence of their association with members of another family of proteins called IκB (inhibitors of κB). IκB family of proteins includes IκB α, IκB β, IκBγ, Bcl-3, and the

carboxyl-terminal regions of NF-κB1 (p105) and NF-κB2 (p100). Recent studies have also identified a novel family member, IκB ε that is thought to act in the nucleus *(Yamazaki et al., 2001)*. IκB proteins bind with different affinities and specificities to NF-κB dimers. Thus, not only are there different NF-κB dimers in a specific cell type, but the large number of combinations between IκB and NF-κB dimers illustrates the sophistication of the system.

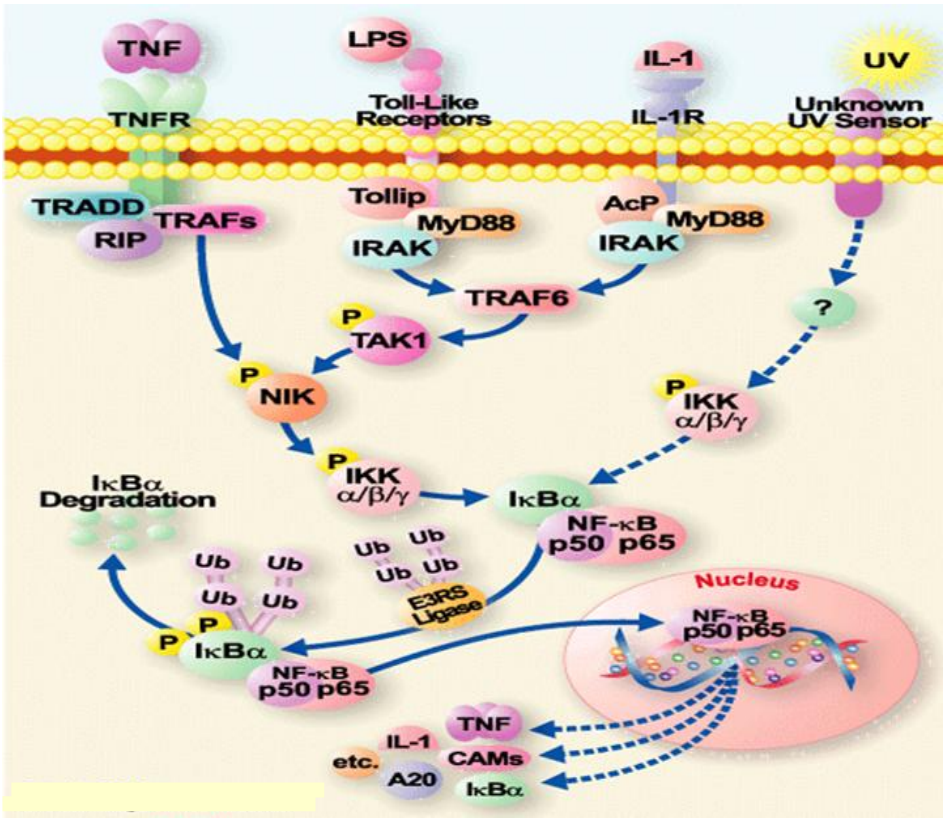

Figure 11: Schematic representation of NF-κB signaling pathway.

Although several non-receptor-mediated pathways (such as oxidative stress or UV irradiation) lead to activation of NF-κB, it is the receptor-mediated events which result in activation of these transcription factors that have been best characterized (Figure 11). The binding of a ligand (e.g., tumor necrosis factor alpha [TNF-α], interleukin 1 [IL-1], CD40L, lipopolysaccharide [LPS]) to its receptor triggers a series of events involving protein kinases that result in the recruitment and activation of IκB kinases (IKKs) that phosphorylate IκB. There are at least three components of this signal; some complex—IKKα, IKKβ, and NEMO/IKKγ—which together provide an additional level of regulation that controls gene transcription. The phosphorylation of two serine residues at the NH2 terminus of IκB

molecules (e.g. Ser32 and Ser36 in IκBα), leads to the polyubiquitination on Lys21 and Lys22 of IκBα and subsequent degradation of the tagged molecule by the 26S proteasome *(Karin and Ben-Neriah, 2000)*. The degradation of IκB exposes the nuclear localization sequence and allows NF-κB dimers to translocate to the nucleus, bind to κB motifs present in the promoters of many genes, and regulate transcription. As part of an autocrine loop, binding of NF-κB will induce the transcription of IκB genes and so provide a mechanism for limiting the activation of NF-κB activity *(Brown et al., 1993)*. In this system, the activation of NF-κB is independent of de novo protein synthesis and so allows a rapid response to appropriate stimuli.

3.3 AP1 family of transcription factors

The transcription factor Activator Protein 1 (AP1) is encoded by proto-oncogenes and regulates various aspects of cell proliferation and differentiation. Many of the properties and regulatory functions of eukaryotic transcriptional regulators were initially discovered and described in studies on these proteins *(Angel & Karin, 1991; Curran & Franza, 1988)*. The AP1 family consists of several groups of basic region leucine zipper (bZIP-domain) proteins: the Jun, the Fos, ATF-2 and the MAF subfamilies *(Angel & Karin, 1991)*. Mammalian Jun proteins include c-Jun, JunB, and JunD. Fos proteins are c-Fos, FosB, Fra-1 and Fra-2. Maf proteins are c-Maf, MafB, MafA, MafG/F/K and Nrl. ATF proteins are ATF2, LRF1/ATF3, B-ATF, JDP1, and JDP2. AP-1 proteins dimerize and bind to their DNA target sites identified by either 12-*O*-tetradecanoylphorbol-13-acetate (TPA) response elements (5′-TGAG/CTCA-3′) or cAMP response elements (CRE, 5′-TGACGTCA-3′) *(Chimenov & Kerppola, 2001)*. Dozens of different homo- and heterodimeric combinations with different regulatory properties, as determined by the characteristics of the subunits, can form. The activity of individual AP1 components can be regulated at different levels. One level is transcriptional. Some AP1-encoding genes are tightly regulated: c-jun and c-fos are the best-characterized examples of this group. Their expression is subject to regulation by a large number of stimuli and signaling pathways *(Whitmarsh & Davis, 1996)*. Though jun proteins can form both either homo- or heterodimers with fos members, fos can only form heterodimers with jun as they cannot form stable homodimers *(Angel & Karin, 1991)*.

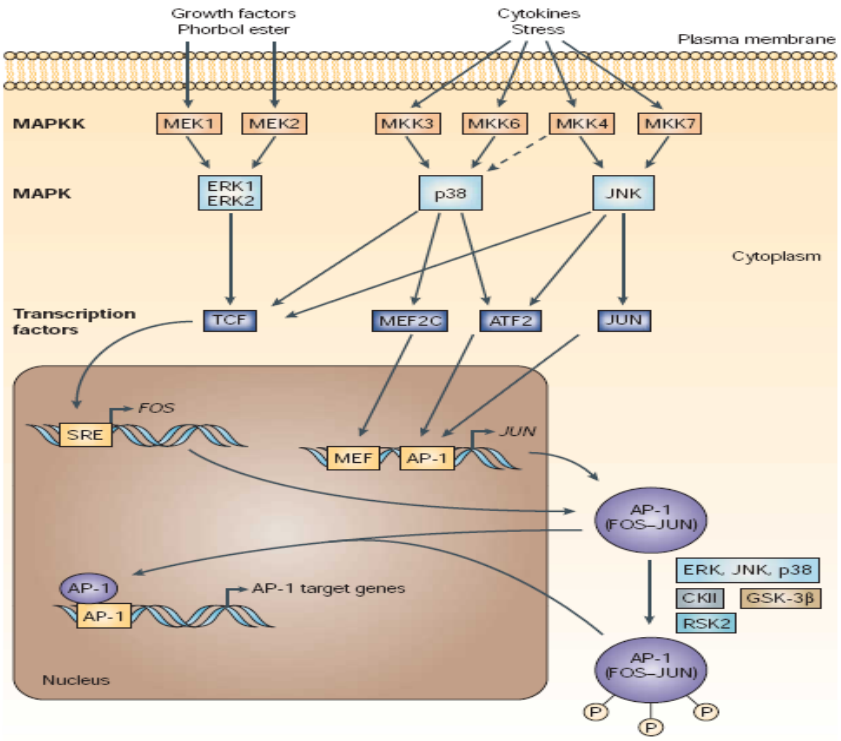

Figure 12: Schematic representation of AP1 signaling pathway.

[Adapted from nature reviews cancer vol.3 nov 2003 859]

Other AP1 coding genes, such as junD and ATF-2, are expressed at fairly constant levels *(de Groot et al., 1991; Van Dam et al., 1995)*. In addition to the intracellular concentrations of these proteins, the specifc activity of AP-1 factors is subject to regulation at the protein level, by post- translational modifcations and interactions with other proteins. The mitogen-activated protein kinase (MAPK) signaling pathways play a predominant role in this regard *(Ip & Davis, 1998; Karin et al., 1997; Whitmarsh & Davis, 1996)*. These pathways are characterized by modules composed of three protein kinases: MAPKKKs phosphorylate and thereby activate MAPKKs, which in turn phosphorylate MAPKs. The three best-characterized subfamilies of MAPKs are named ERK, JNK and p38. In general, different MAPKs are members of separate modules, and are regulated by distinct extracellular stimuli. For example, ERKs are activated by receptor tyrosine kinases and relay proliferation or differentiation signals. JNK and p38-type MAPKs are activated predominantly by stress stimuli and pathogenic insults, and also by mitogens in some cell types. Interestingly, all three classes of MAPKs are involved in the regulation of distinct AP1 components. c-Jun is regulated by JNK phosphorylation and in some cell types also by ERK-mediated mechanisms. c-Fos is a substrate for regulatory phosphorylations by ERK, and ATF-2 is

regulated by JNK and p38 kinases *(Karin, 1995; Whitmarsh & Davis, 1996)*. Phosphorylated and hence activated c-fos and c-jun form dimers and bind to the response element on AP1 target genes. Unlike its other family members, JunB and FosB negatively regulate gene transcription *(Robert Chiu et al., 1989)*. Signalling by AP1 transcription factors has been shown to be involved in, or at least correlated with, phenomena as diverse as cell proliferation, transformation, cell differentiation, cell migration and apoptosis.

3.4 JAK- STAT signalling pathway

Signal Transducers and Activators of Transcription (STATs), as the name suggests, have a dual role. They act signal transducers in the cytoplasm and as transcription factors when in the nucleus. They respond rapidly to extracellular signals, and reprogram gene expression. In mammals, there are seven STAT genes, STAT1, STAT2, STAT3, STAT4, STAT5A, STAT5B, and STAT6 *(Takeda & Akira, 2000)*. STAT proteins are characterised by the presence of a Src homology domain. There is sufficient diversity in the STAT amino acid sequences and their tissue-specific distributions to account for their diverse roles in responses to extracellular signaling proteins. In the absence of specific receptor stimulation, STAT proteins are inactive as transcription factors and are localized in the cytoplasm. They are activated rapidly in response to receptor-ligand coupling and are recruited to the intracellular domain of the receptor through specific binding between STAT Src-homology 2 (SH2) domains and receptor phosphotyrosine residues. These SH2-phosphotyrosine interactions are highly specific and are a critical step in determining the specificity of receptor-mediated STAT activation. Many growth factor receptors have intrinsic tyrosine kinase activity, but most STAT-activating cytokine receptors do not. Instead, the required tyrosine kinase activity is provided by receptor-associated cytoplasmic proteins from the Janus kinase (JAK) family *(Leonard, 2001)*. JAKs are also evolutionarily conserved, and there are four JAK proteins in mammalian cells, JAK1, JAK2, JAK3, and TYK2. JAKs bind specifically to intracellular domains of cytokine receptor signaling chains and catalyze ligand-induced phosphorylation of themselves and of intracellular tyrosine residues on the receptor, creating STAT docking sites. Phosphorylation of STATs on activating tyrosine residues leads to STAT homo- and heterodimerization and their transport from the cytoplasm to the nucleus for DNA binding. Most STAT dimers recognize an 8– to 10–base pair inverted repeat DNA element with a consensus sequence of 5'-TT(N4–6)AA-3'.

Differential binding affinity of a particular activated STAT dimer for a single target DNA sequence is determined by variations in the exact nucleotide sequence *(Ehret et al., 2001)*. The affinity of a STAT-DNA complex for a natural target gene promoter is also determined by cooperative dimer-dimer interactions mediated by NH2-terminal amino acids *(Xu et al., 1996; Vinkemeier et al., 1996)*. STAT dimers have the intrinsic ability to recruit nuclear co-activators that mediate chromatin modifications and communication with the core promoters, and thus induce transcription of target genes *(Chin et al., 1996; Ouchi et al., 2000)*.

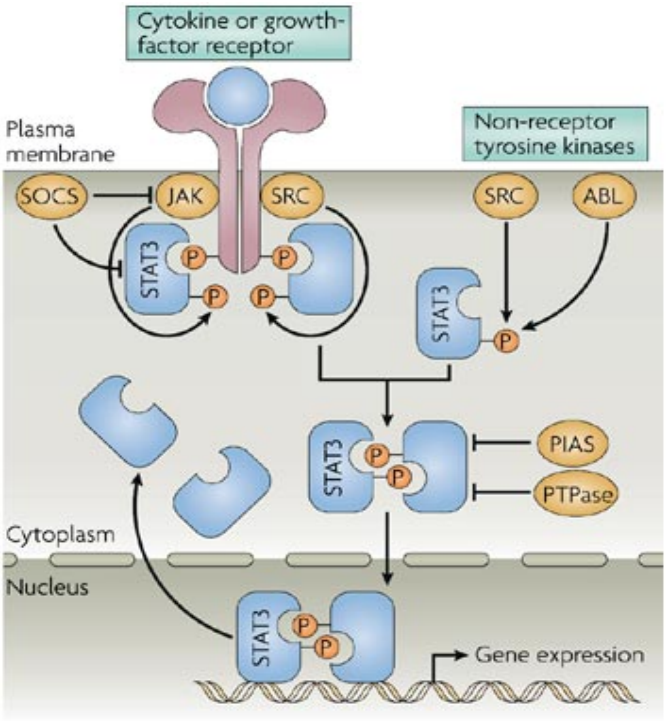

Figure 13: Schematic representation of JAK-STAT signaling pathway.

The JAK-STAT signaling pathways do not usually function autonomously; rather, they are regulated by a vast array of intrinsic and environmental stimuli. Diverse protein kinases, including several mitogen-activated protein kinases (MAPKs), phosphorylate STATs on serine residues, allowing additional cellular signaling pathways to potentiate the primary STAT-activating stimulus *(Decker & Kovarik, 2000)*. Similarly, it is possible that additional sites of regulated serine phosphorylation or other posttranslational modifications may regulate attenuation of STAT activity *(Mowen et al., 2001; Ahmed et.al., 2000)*. Negative regulation of the JAK-STAT pathway is accomplished by common mechanisms as receptor internalization to endocytic vesicles and subsequent receptor degradation. Protein Tyrosine

Phosphatases (PTPase) specifically inhibit STATs. They dephosphorylate STATs either at the level of the membrane-associated receptor-kinase complex *(David et al., 1995; Myers et al., 2001; Irie-Sasaki et al., 2001)* or, in the nucleus. Dephosphorylated STAT dimers are recycled back to the cytoplasm as latent STAT monomers *(Haspel et al., 1996; David et al., 1993)*. Suppressor of Cytokine Signaling (SOCS) proteins directly bind to and inactivate the JAK kinases *(Krebs & Hilton, 2001)*. Expression of SOCS genes can be stimulated by the same cytokines that enhance STAT activation, so the SOCS proteins can act in classic feedback inhibition loops. Protein inhibitors of activated STATs (PIAS) bind to phosphorylated STAT dimers, preventing DNA recognition *(Shuai, 2000)*. The steady-state and signal-inducible concentrations of all the positive and negative regulators determine the intensity and duration of the signal response in a particular cell type.

3.5 TGFβ Superfamily

The Transforming Growth Family β (TGFβ) superfamily is a multifunctional cytokine family that regulates cell growth, tissue remodelling and angiogenesis. In mammals the TGFβ superfamily of growth factors consists of about 30 genes: 3 TGFβ isoforms, 4 activin β-chains, the protein nodal, 10 bone morphogenetic proteins (BMPs) and 11 growth and differentiation factors (GDFs). All these ligands are synthesized as dimeric pre-proproteins, which are then processed and secreted as dimeric growth factors *(Gray & Mason, 1990)*. A hallmark of TGFβ superfamily ligands is the so called 'cysteine knot' *(Shi & Massagué, 2003)*, a structural motif in the mature protein that is formed by three intramolecular disulphide bonds between six strictly conserved Cys residues. With the exceptions of GDF3, GDF9 and BMP15, all ligands use an additional conserved Cys residue to form an intermolecular disulphide bond for stabilization of the dimer. Although homodimers seem to be the prevalent form, additional combinatorial variety occurs through heterodimerization, which is exemplified by activin βA–βB heterodimers, nodal–BMP4 and nodal–BMP7 *(Yeo & Whitman, 2001)*. Receptors for the TGFβ superfamily ligands consist of a cysteine rich extracellular domain, a single-pass transmembrane domain and a significantly conserved intracellular Ser–Thr kinase domain *(Shi & Massagué, 2003)*.

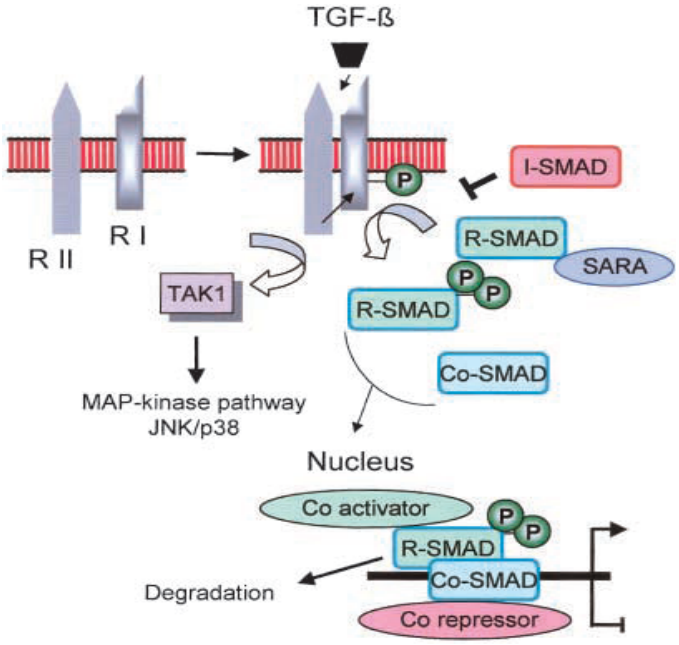

Figure 14: Schematic representation of the TGFβ signal transduction pathway.

[Adapted from Cell Tissue Res (2002) 307:1–14]

Two functional classes of receptors can be distinguished: type II and type I; binding of the ligand causes bridging of the pre-formed dimers of type II receptors and dimers of type I receptors to form heterotetrameric, active receptor complexes *(Feng & Derynck, 2005)*. The type II receptor kinase is thought to be constitutively active and, within an established receptor complex, phosphorylates the type I receptor. Phosphorylation of the receptor leads to the recruitment of regulated SMADs (R- SMADs): SMAD1, SMAD2, SMAD3, SMAD5 and SMAD8, which are sequestered in a complex with SMAD anchor for receptor activation (SARA) in the cytoplasm *(Tsukazaki et al., 1998)*. The type I receptor then phosphorylates the R- SMADs on two Ser residues at their extreme C termini, which allows them to form complexes with the common mediator (Co-SMAD) SMAD4 *(Shi & Massagué, 2003)*, and also to form homomeric complexes. SMAD complexes accumulate in the nucleus, where SMAD4-containing complexes are directly involved in regulating the transcription of target genes, both positively and negatively (Figure 14). SMADs bind to the SMAD binding element (SBE) characterised by C-G containing sequences, CAGAC *(Shi et al., 1998)*. R-SMADs and SMAD4 share two highly conserved domains, termed MH1 and MH2, which are separated by a less conserved Pro-rich linker region. Except for SMAD2, which cannot bind DNA directly owing to a small insert encoded by an extra exon15, the MH1 domains of

the R- SMADs and SMAD4 are responsible for DNA binding. The linker region is phosphorylated by kinases such as mitogen-activated protein kinases (MAPKs), glycogen synthase kinase-3β (GSK-3β) *(Sapkota et al., 2007)* and cyclin-dependent kinases (CDKs) *(Liu, 2006)*, and is thus thought to integrate inputs from other signalling pathways. The MH2 domain mediates SMAD–receptor interactions, SMAD–SMAD interactions and SMAD interactions with transcription factors, co-activators and co-repressors. SMADs seem to be unable to directly recruit the basal transcription machinery to responsive promoters and instead regulate transcription through chromatin remodelling. SMAD-dependent chromatin remodelling and histone modifications are thought to facilitate the subsequent recruitment of the general transcription machinery to target gene promoters *(Ross et al., 2006)*.

Negative feedback in the TGFβ superfamily signalling pathways is mediated by induction of the inhibitory SMADs (I-SMADs) SMAD6 and SMAD7, and is thought to function in signal termination *(Itoh & ten Dijke, 2007)*. I-SMADs are transcriptionally induced in response to TGFβ and BMPs in a SMAD-dependent manner and can inhibit signalling by distinct and diverse mechanisms. I-SMADs either interact with type I receptors, leading to a competitive inhibition of R- SMAD binding or inactivate receptors by interacting with ubiquitin ligases *(Kavsak et al, 2000; Ebisawa et al., 2001; Ogunjimi et al., 2005)* and protein phosphatase (PP1) *(Shi et al., 2004)* and targeting them to active receptors thereby leading to their degradation or inactivation by dephosphorylation of receptors, respectively.

3.6 Coregulators

Coactivators

Transcriptional regulation is dependent not only on transcription factor activation and chromatin remodeling, but also on a host of regulatory proteins referred to as coactivators and corepressors *(Glass et al., 1997*; *McKenna et al., 1999)*. Coactivators usually do not bind to DNA, but are recruited to the target gene promoters through protein-protein interactions with the targeted transcription factors, and function as linker molecules between DNA binding proteins and protein modifying enzymes, which facilitate local structural alterations. Some coactivators have intrinsic chromatin modifying enzymatic activity. The p160/steroid receptor coactivator (SRC) family is a well-studied family of transcriptional

coregulatory proteins that function through histone tail modifications, altering chromatin structure, and facilitating transcription initiation. Its members are SRC1, glucocorticoid receptor interacting protein (GRIP1; also known as SRC2, TIF2), and P/CIP (also known as SRC3, AIB1, TRAM1, and RAC3) *(Torchia et al., 1998)*. The P160/SRC family members share a common structure frame that includes an N-terminal basic helix-loop- helix domain, a PAS (PER, aryl hydrocarbon receptor nuclear translocator (ARNT), and SIM homology domain, a C-terminal transcriptional activation domain, and a central region containing three NR interacting LXXLL (where L is leucine and X is any amino acid) motifs *(McKenna et al., 1999)*. SRC1 and SRC3 have been shown to have histone acetyltransferase (HAT) activity, which is necessary for the formation of an open chromatin structure *(Spencer et al., 1997)*.

Corepressors

As is indicated by the name, corepressor proteins in general coordinate the inactivation of transcriptionally active complexes through the direct interaction with DNA-binding transcription factors and the coordinate recruitment of chromatin modifying enzymes, which may condense the chromatin to an inactive state. The first corepressors to be identified were for NRs, the silencing mediator of retinoid and thyroid hormone receptors (SMRT) and the nuclear hormone receptor corepressor (NCoR) *(Davie & Dent, 2004)*. These two proteins share similar domain architecture and function in a similar fashion. Both proteins interact with various transcription factors (often dimers, with one corepressor per dimer) through a C-terminal region, and nucleate the assembly of multiprotein repressor complexes through N-terminal repression domains, which interact with chromatin remodelling enzymes such as histone deacetylases (HDACs).

Reports also suggest that there are role reversals for coregulators. For instance, HDAC1 which normally recruits SMRT and NCoR, acts as coactivator of GR mediated transcription *(Qiu et al., 2006)*. Allosteric influences in the DNA-binding hormone response element can regulate the ability of SRC2 to bind distinct parts of GR and control its coactivator/corepressor function *(Rogatsky et al., 2002)*. In another example, SRC3 functions as a growth repressor in the lymphocytes; it sequesters IKK, allowing IκB levels to rise, thereby inhibiting NFκB activity *(Coste et al., 2006)*.

3.7 Chromatin remodelling enzymes

Addition of acetyl groups to histone tails alters the histone-DNA and histone-protien interactions, making the chromatin more accessible for transcription. This process of gene regulation is mediated by enzymes called Histone Acetyl Transferases (HATs). The most extensively studied are four families of HATs, the GNAT family, the p300/CBP family, the MYST family, and the RH109 family *(Marmorstein & Trievel, 2009)*. HATs also interact with other co-activators like SRCs to recruit general transcription machinery.

Histone deacetylation is one of the most important processes that mediate transcriptional repression. A large family of proteins called HDACs mediates this process. In vertebrates the family of HDACs consists of 11 members, which are divided into 3 sub classes; class I – HDAC1 – HDAC3, class II HDAC4- HDAC7, HDAC9, and HDAC10, class III NAD+ dependent sirtuins and class IV – HDAC11 *(de Ruijter et al., 2003; Thiagalingam et al., 2003)*. In general, removal of acetyl groups from histone tails induces condensation in chromatin structure that prevents gene transcription. However, deacetylation does not occur independently, HDACs are recruited to the chromatin in co-ordination with the co-repressor complexes.

4. Thymic stromal lymphopoietin (TSLP)

4.1 TSLP and its receptor

Thymic stromal lymphopoietin (TSLP) was originally identified as a growth factor in the supernatant of Z210R.1 thymic stromal cells that support proliferation and survival of the NAG8/7 pre-B cell line *(Friend et al, 1994)*. Subsequent characterization and cloning showed that TSLP is a short-chain four α-helical bundle type I cytokine that is closely related to IL-7 *(Sims et al, 2000)*. A cDNA clone encoding human TSLP has been isolated by database search methods. Sequence prediction shows a rather poor homology between mouse and human TSLP, which share only 43% amino acid identity. However, it has been found that human and mouse TSLP exert similar biological functions *(Ziegler & Liu, 2006)*.

The TSLP receptor complex consists of a TSLP-binding chain (TSLPR) and the IL7 receptor-α (IL-7Rα) chain *(Ziegler & Liu, 2006; Park et al., 2000)* Human and mouse TSLPR share 39% amino acid identity. Although TSLPR is a type 1 cytokine receptor, several type 1 cytokine receptor 'hallmark' motifs are altered in TSLPR *(Ziegler & Liu, 2006)*. For example, TSLPR lacks the second of four conserved extracellular domain cysteine residues, suggesting that TSLPR might have a unique folding pattern. TSLPR contains the conserved 'box1' sequence found in type I cytokine receptors, but lacks the conserved 'box2'. Those motifs regulate the binding of Janus protein tyrosine kinase (Jak). Furthermore, unlike other cytokine receptors, TSLPR contains a single tyrosine residue four amino acids away from its C terminus. TSLP may activate STAT5 *(Isaksen et al., 1999)* and this activation requires the Box1 region of both TSLPR and IL-7Rα. In addition to activation of STAT5, TSLP may activate other pathways, including those often activated by other cytokines, such as PI3-K/Akt, MAPK (mitogen activated protein kinase), and/or Src family kinase pathways *(Liu et al., 2007)*.

4.2 TSLP expression

Both mouse and human TSLP are expressed predominantly by epithelial cells, with the highest expression in lung, skin and gut *(Reche et al., 2001)*. TSLP is constitutively

expressed by intestinal epithelial cells, and is known to play an important role in maintaining gut immune homeostasis. In a mouse model of Inflammatory Bowel Disease (IBD), TSLPR deficient mice show rapid onset and severity of disease to commensals *(Taylor et al., 2009)*. Further evidence for the involvement of TSLP in maintaining gut homeostasis is the finding that colonic epithelial cells from patients with Crohn's disease have lower expression of the TSLP gene *(Rimoldi et al., 2005)*.

Several in vitro studies have demonstrated that expression of TSLP can be induced by a wide variety of stimuli like TLR ligands, bacterial and viral products, pro-inflammatory (IL1β and TNFα) and Th2 cytokines *(Bogiatzi et al., 2007; Kato et al., 2007; Lee & Ziegler, 2007)*. In vivo studies using mouse as a model organism have revealed that TSLP could be induced by the protein antigen ovalbumin (i) in nasal epithelium in a mouse model of allergic rhinitis, and (ii) in lung, BAL fluid, and mast cells in an asthma model *(Hyde et al., 2007; Miyata et al., 2008; Mou et al., 2009)*. Topical application of haptens like FITC, oxazolone and TPA (our unpublished observation) are also known to induce TSLP in keratinocytes of mouse skin. Si-RNA mediated silencing of E-cadherin in airway epithelial cells leads to increased TSLP expression *(Heijink et al., 2007)*.

In addition, overexpression of IL13 in mouse skin induces TSLP *(Zheng et al., 2009)*. SPINK5 *(Chavanas et al, 2000)* and notch signalling deficient mice *(Demehri et al., 2008)* show increased TSLP production in skin. SOCS7 null mice show cutaneous abnormalities and increased infiltration of TSLP producing mast cells *(Knisz et al., 2009)*. Tissue damage, for instance, inciting physical injury by tape-stripping of both mouse and human skin also increases TSLP *(our unpublished observation & Angelova-Fischer et al., 2010)*, thus making TSLP a sensor for epidermal integrity.

4.3 TSLP and Nuclear Receptors

Earlier studies in our laboratory have shown that, keratinocyte selective ablation of the nuclear receptors RXRα and RXRβ (RXRαβ ep-/- mutants) leads to an increased expression of TSLP in the keratinocytes and towards development of skin and systemic abnormalities similar to human AD in mice *(Li et al., 2005)*. Moreover, topical application of vitamin D3 or its low calcemic analogue MC903, an agonist for VDR, induces TSLP production by the

keratinocytes, and repeated application leads to the development of AD-like phenotype in a TSLP dependent manner. All-trans retinoic acid (RA), RAR agonist is also known to induce TSLP in the keratinocytes *(Li et al., 2006)*. Together these ligands synerzise and enhance the production of TSLP. All these studies demonstrate that NRs do play an important role in the regulation of TSLP.

4.4 TSLP effects on immune cells

TSLP can act on immune cells of multiple lineages (Figure 15), including dendritic cells, T cells, NKT cells, mast cells and B cells. Based on TSLP receptor expression and potential function in model system, eosinophils and macrophages may also respond to TSLP, but further studies are required.

Dendritic cells (DC)

DCs, as described in chapter 1.2.2, are APCs that bridge between innate and adaptive immunity. DCs can be activated directly by pathogens via TLRs or by mediators produced by epithelial cells. Activated DCs upregulate costimulatory molecules including MHC class II antigens, and release cytokines and chemokines that together induce recruitment, activation, and differentiation of T cells. Human DCs express TSLP receptors and rapidly respond to TSLP, as evaluated by the upregulation of MHC class II, CD40, CD80, CD86, OX40L, and TH2 chemokines including TARC and MDC *(Soumelis et al., 2002)*. Following TSLP stimulation, DCs control homeostasis and differentiation of human CD4+ T cells to inflammatory TH2 cells, and CD8+ T cells to proallergic cytotoxic cells with IL-13 production *(Gilliet et al., 2003)*. In mice, TSLP induces the maturation of DCs, and TSLP-activated DCs regulate the differentiation of naive CD4+ T cells to TH2 cells *(Zhou et al., 2005; Al-Shami et al., 2005)*. These results suggest that in both humans and mice, TSLP-activated DCs promote the differentiation of T cells to proallergic cells. TSLP activated DCs are also able to support the maintenance and polarization of CRTH2+ Th2 effector memory cells *(Wang et al., 2006)*. TSLP has the ability to suppress Th1 differentiation by inhibiting the expression of p40 subunit of IL12 both in human and mouse DCs *(Rimoldi et al., 2005; Zaph et al., 2007; Taylor et al., 2009)*.

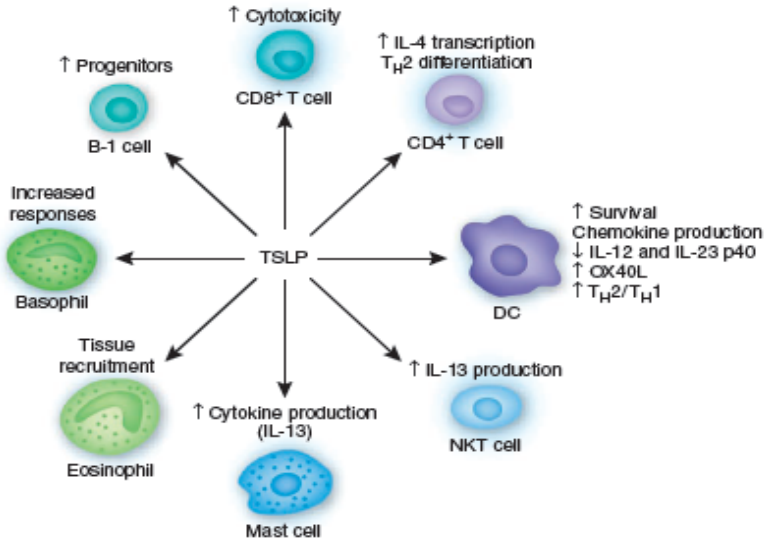

Figure 15: TSLP produced by epithelial cells can act on immune cells of multiple lineages.

[Adapted from Ziegler & Artis, 2010]

T cells

In mice, disruption of IL-7Rα signaling leads to T-cell and B-cell lymphopenia, and an absence of γδ T cells *(Puel & Leonard, 2000)*. In humans, mutation of the IL-7R gene results in a form of severe combined immunodeficiency in which T cells are profoundly diminished in number while other lineages are intact *(Giliani et al., 2005)*. It is reasonable to predict that TSLP might partially replace the role of IL-7 in T-cell development, because IL-7Rα is also shared by TSLP. Indeed, although the lack of TSLPR (TSLPR-/- mice) does not affect hematopoiesis, TSLPR/γc double knockout mice have more impaired T-cell development than do γc-deficient mice, and recovery of T cells is defective in sublethally irradiated TSLPR knockout mice *(Al-Shami et al., 2004)*. Similarly, transgenic overexpression of TSLP in IL7(-/-) lymphopenic mice promotes the generation of functional B cell and T cell, consistent with the ability of TSLP to compensate for IL-7 deficiency *(Chappaz et al., 2007)*. Thus, TSLP-TSLPR interactions may be involved in, but are not necessary for normal T-cell lymphopoiesis.

TSLPR deficiency in mice has been associated with defective development of an inflammatory allergic response to OVA in the lung *(Zhou et al., 2005; Al-Shami et al., 2005)* but this can be reversed by the addition of wild-type (WT) CD4+ T cells *(Al-Shami, A., 2005)*. Interestingly, a comparison of the four possible combinations of DCs and CD4+ T cells from WT versus TSLPR KO mice in a proliferative assay revealed that the absence of TSLPR on CD4+ T cells appeared to be even more deleterious than the loss of TSLPR on

DCs *(Al-Shami, A., 2005)*. Moreover, it was shown that TSLP can regulate differentiation of preactivated mouse CD4+ T cells toward the TH2 phenotype in a DC-independent fashion *(Omori et al., 2007)*. Together these data demonstrate a unique role of TSLP in the regulation of CD4+ T cell action.

It has been proposed a species difference between human and mouse TSLP, as human TSLP seemed to act on DCs, with only an indirect effect on T cells, whereas the mouse TSLP seemed to act directly on both DCs and T cells *(Ziegler & Liu, 2006)*. However, others reported that CD4+ T cells in both human and mouse can directly respond to TSLP *(Al-Shami et al., 2004 & Rochman et al., 2007)*. Analysis of human CD4+ T cells showed that preactivated, but not naive CD4+ T cells express TSLPR, and also that TSLP can rapidly activate STAT5 and induce the expression of STAT5 target genes, indicating the presence of functional TSLP receptors on activated human T cells. Consistent with this, TSLP augments the proliferation rate of T cell receptor (TCR)-activated human CD4+ T cells *(Al-Shami et al., 2004)*, analogous to the effect previously observed in mice *(Rochman et al., 2007)*.

NKT cells

NKT cells represent a subpopulation of T cells that have properties of both conventional T cells and NK cells. A recent study *(Nagata et al., 2007)* has proposed a role of TSLP on NKT cells. The authors found that NKT cells express TSLP receptor, as well as IL-7 receptor α -chain. TSLP acts on NKT cells to preferentially increase their IL-13 production, but not IFN-γ and IL-4. By using lung-specific TSLP transgenic mice and NKT knockout mice, they showed that in allergen induced asthma, TSLP acts on NKT cells to enhance AHR by upregulating their IL-13 production, whereas eosinophilia and IgE production are not influenced.

Mast cells

It also has been established that mast cells not only express high levels of TSLP mRNA, but also can respond to TSLP. Immunostaining of a bronchial biopsy of an asthmatic patient has revealed TSLP receptor expression on infiltrating mast cells *(Allakhverdi et al., 2007)*. Furthermore, stimulation of human mast cells in vitro with IL-1β and TNF-α in the presence of TSLP strongly augments the production of proinflammatory TH2 cytokines, including IL-5, IL-6, IL-10 and IL-13, as well as chemokines that are involved in allergic diseases *(Allakhverdi et al., 2007)*. Consistent with this, blocking endogenous TSLP, which is released by activated human epithelial cells, completely inhibited the production of IL-13 by

mast cells. This suggests that TSLP may facilitate crosstalk between epithelial cells and mast cells.

B cells

TSLP has effects in B-cell lymphopoiesis *(Ziegler & Liu, 2006)*. *In vitro* studies have indicated that TSLP is capable of supporting the growth of fetal liver and adult B cell progenitors, as well as their differentiation to the immunoglobulin M–positive (IgM+) stage of B cell development *(Levin et al., 1999)*. Subsequent studies have shown that TSLP influences distinct B cell progenitors in fetal liver and adult bone marrow *(Vosshenrich et al., 2003 & 2004)*. Fetal liver pro–B cells respond to both TSLP and IL-7, but only bone marrow pre–BCR (B cell receptor)+ pre–B cells respond to TSLP. Those findings are consistent with the observation that although both have equal expression of high-affinity TSLP receptors and both respond to IL-7, the fetal liver–derived NAG8/7 cell line but not the bone marrow–derived IxN2b cell line, responds to TSLP *(Isaksen et al., 2002)*. It has been recently reported that local increase in TSLP in a keratin 5–driven TSLP transgenic mice induces systemic alterations in B cell development, and promote humoral autoimmunity *(Astrakhan et al., 2007)*. In another study, TSLP has been found to be involved in epithelial cell triggered frontline immunoglobulin class switching *(Xu et al., 2007)*.

In helminth- or allergen- induced inflammatory responses, TSLP promotes basophils to drive Th2 differentiation. TSLP can recruit eosinophils to the site of Th2 inflammation. Collectively, these data suggest a model in which TSLP, acting through DCs, granulocytes, natural killer T cells or directly on CD4+ T cells, can promote TH2 cell differentiation and TH2 cytokine–associated inflammation.

4.5 TSLP in atopic diseases

In addition to being produced by the epithelial cells, recently, it was demonstrated that allergen activated basophils also produce TSLP, and thus may also be important in the initiation of TH2 responses *(Sokol et al., 2008)*. More and more studies have suggested that TSLP is a master regulator in atopic diseases, including AD and asthma *(Liu, 2006)*.

TSLP and AD

TSLP protein is highly expressed in acute and chronic atopic dermatitis lesions from atopic dermatitis patients, but not in normal skin or nonlesional skin in patients with atopic dermatitis. TSLP is expressed mainly in keratinocytes of the apical layers of the epidermis, suggesting that TSLP production is a feature of fully differentiated keratinocytes. TSLP was not found in skin lesions from patients with nickel induced contact dermatitis or disseminated lupus erythematosus. Interestingly, TSLP expression in patients with AD was associated with Langerhans cell migration and activation in situ, suggesting that TSLP may contribute directly to the activation of these cells, which could then migrate into the draining lymph nodes and prime allergen-specific TH2 responses *(Soumelis et al., 2002; Soumelis & Liu 2004)*. Recent evidence also indicates the presence of TSLP in serum samples of AD infected children *(Lee et al., 2010).*

Mice studies on TSLP provide strong evidences to support TSLP function in atopic dermatitis. Studies from *Yoo et al. 2005*, as well as from our laboratory *(Li et al., 2005)* have demonstrated that mice overexpressing TSLP in keratinocytes developed a similar AD-like dermatitis. Mutations affecting the expression of TSLP in mouse skin; like ablation of NRs, Notch deficiency, or SPINK deficiency, all of which lead to induction of TSLP in the skin as well as in the serum, show AD-like phenotype indicating a potential link between TSLP and the development of Th2 inflammation. TSLP knockout mice (TSLP -/-) or mice lacking TSLP specifically in the epidermal keratinocytes (TSLP ep-/-) do not develop inflammation in a MC903 induced model of AD *(Li et al., 2009).*

TSLP and asthma

It has been shown by in situ hybridization that TSLP RNA levels are increased in asthmatic airways (bronchial epithelium and submucosa) from asthma patients, and was correlated with both the expression of TH2-attracting chemokines and with disease severity *(Ying et al., 2005)*. This suggests that production of TSLP in the lung could be important for the development or/and maintenance of asthma. Mice lacking the TSLPR (TSLPR-/- null mice) fail to develop experimental asthma in response to OVA sensitization and challenge *(Zhou et al., 2005 & Al-Shami et al., 2005)*, suggesting that TSLP signaling is playing an important role in allergic lung inflammation. In addition, transgenic mice overexpressing TSLP under the lung-specific SPC (surfactant protein C) promoter *(Zhou et al., 2005)* develop a spontaneous lung inflammation characterized by a massive infiltration of leukocytes

(including TH2 cells), goblet cell hyperplasia, and subepithelial fibrosis, as well as increased serum IgE levels.

TSLP and allergic rhinitis

Recently, TSLP was found to be involved in the development of allergic rhinitis. TSLP detected by RT-PCR and immunohistochemistry is significantly increased in nasal mucosa from allergic rhinitis patients compared with normal control individuals, and TSLP production is tightly correlated with that of IL-4 and severity of allergic rhinitis *(Mou et al., 2008)*. TSLP expression was also found to be up-regulated predominantly in the nasal epithelium in an OVA sensitized and challenged mouse model of allergic rhinitis *(Miyata et al., 2008)*, which was abolished in mast cell-deficient mice. Furthermore, the administration of neutralizing TSLP antibody during the challenge phase of the OVA protocol inhibited the development of allergic rhinitis. These results suggest that nasal epithelial TSLP expression plays an important role in the development of allergic rhinitis.

TSLP and atopic march

TSLP is also known to play a role in atopic march. Studies in mice have shown that higher expression of TSLP in the skin, leads to an increased response to allergen challenge in the lung *(Zhang et al., 2009)* Mice lacking TSLP or one of its signalling receptor IL7Rα, do not show this phenotype upon antigen challenge *(Demehri et al., 2009)*.

These studies show that TSLP is both necessary and sufficient for the development of Th2 inflammation, thus becoming a potential therapeutic target in the treatment of allergic diseases.

References

Ahmed ST, Ivashkiv LB. (2000) Inhibition of IL-6 and IL-10 signaling and Stat activation by inflammatory and stress pathways. *J Immunol. 165(9):5227-37.*

Allakhverdi, Z. et al. (2007) Thymic stromal lymphopoietin is released by human epithelial cells in response to microbes, trauma, or inflammation and potently activates mast cells. *J Exp Med 204, 253-8.*

Almawi, W.Y. & Melemedjian, O.K. (2002) Negative regulation of nuclear factor-κB activation and function by glucocorticoids. *J. Mol. Endocrinol*. *28: 69–78.*

Al-Shami, A. et al. (2004) A role for thymic stromal lymphopoietin in CD4(+) T cell development. *J Exp Med 200, 159-68.*

Al-Shami, A., Spolski, R., Kelly, J., Keane-Myers, A. & Leonard, W. J. (2005) A role for TSLP in the development of inflammation in an asthma model. *J Exp Med 202, 829-39.*

Angel, P. & Karin M. (1991) The role of Jun, Fos and the AP-1 complex in cell-proliferation and transformation. *Biochim Biophys Acta. 1072(2-3):129-57.*

Angelova-Fischer I, Fernandez IM, Donnadieu MH, Bulfone-Paus S, Zillikens D, Fischer TW, Soumelis V. (2010) Injury to the Stratum Corneum Induces In Vivo Expression of Human Thymic Stromal Lymphopoietin in the Epidermis. *J Invest Dermatol*. *Jun 17.*

Astrakhan, A. et al. (2007) Local increase in thymic stromal lymphopoietin induces systemic alterations in B cell development. *Nat Immunol 8, 522-31.*

Balaci L, Spada MC, Olla N, Sole G, Loddo L, Anedda F, et al. (2007) IRAK-M is involved in the pathogenesis of early-onset persistent asthma. *Am J Hum Genet;80:1103-14*

Barnes PJ. (2000) New directions in allergic diseases: mechanism-based anti-inflammatory therapies. *J Allergy Clin Immunol 106:5-16.*

Barnetson RS, Rogers M. (2002) Childhood atopic eczema. *BMJ. 324(7350):1376-9.*

Barton SJ, Koppelman GH, Vonk JM, Browning CA, Nolte IM, Stewart CE, et al. (2009) PLAUR polymorphisms are associated with asthma, PLAUR levels, and lung function decline. *J allergy Clin Immunol;123:1391-400, e17.*

Baurecht H. et al. (2007) Toward a major risk factor for atopic eczema: meta-analysis of filaggrinpolymorphism data. *J Allergy Clin Immunol 120, 1406-12*.

Bayo P, Sanchis A, Bravo A, Cascallana JL, Buder K, Tuckermann J, Schütz G, Pérez P. (2008) Glucocorticoid Receptor Is Required for Skin Barrier competence. *Endocrinology 149(3):1377–1388.*

Bekersky I, Fitzsimmons W, Tanase A, Maher RM, Hodosh E, Lawrence I. (2001) Nonclinical and early clinical development of tacrolimus ointment for the treatment of atopic dermatitis. *J Am Acad Dermatol 44:S17-27.*

Bellinghausen, I., Brand, U., Enk, A. H., Knop, J. & Saloga, J. (1999) Signals involved in the early TH1/TH2 polarization of an immune response depending on the type of antigen. *J Allergy Clin Immunol 103,298-306.*

Berg, J.M. (1989). DNA binding specificity of steroid receptors. *Cell 57, 1065-l 068.*

Bieber, T. Atopic dermatitis. *N Engl J Med 358, 1483-94 (2008).*

Biola, A., K. Andreau, M. David, et al. (2000). The glucocorticoid receptor and STAT6 physically and functionally interact in T-lymphocytes. *FEBS Lett.**487:** 229–233*.

Bogiatzi SI, Fernandez I, Bichet JC, Marloie-Provost MA, Volpe E, Sastre X, Soumelis V. (2007) Cutting Edge: Proinflammatory and Th2 cytokines synergize to induce thymic stromal lymphopoietin production by human skin keratinocytes. *J Immunol 178:3373–7.*

Boguniewicz M, Fiedler VC, Raimer S, Lawrence ID, Leung DY, Hanifin JM. (1998) A randomized, vehicle-controlled trial of tacrolimus ointment for treatment of atopic dermatitis in children: Pediatric Tacrolimus Study Group. *J Allergy Clin Immunol 102:637-44.*

Boralevi, F. et al. (2008) Epicutaneous aeroallergen sensitization in atopic dermatitis infants - determining the role of epidermal barrier impairment. *Allergy 63, 205-10.*

Bourguet W, Germain P, and Gronemeyer H (2000) Nuclear receptor ligand-binding domains: three-dimensional structures, molecular interactions and pharmacological implications. *Trends Pharmacol Sci 21:381–388*.

Boyman, O., Conrad, C., Tonel, G., Gilliet, M. & Nestle, F. O. (2007) The pathogenic role of tissue-resident immune cells in psoriasis. *Trends Immunol. 28, 51–57.*

Brattsand M, Stefansson K, Lundh C, Haasum Y, Egelrud T (2005) A proteolytic cascade of kallikreins in the stratum corneum. *J Invest Dermatol 124:198–203.*

Breton CV, Vora H, Salam MT, Islam T, Wenten M, Gauderman WJ, et al. (2009) Variation in the GST mu locus and tobacco smoke exposure as determinants of childhood lung function. *Am J Respir Crit Care Med;179:601-7.*

Brocard J, Kastner P, and Chambon P (1996). Two novel RXRα isoforms from mouse testis. *Biochem Biophys Res Commun 229:211–218.*

Brown, K., S. Park, T. Kanno, G. Franzoso, and U. Siebenlist. (1993) Mutual regulation of the transcriptional activator NF-κB and its inhibitor, IκB-α. *Proc. Natl. Acad. Sci. USA 90:2532–2536.*

Brown, S. J. et al. (2008) Filaggrin null mutations and childhood atopic eczema: a population-based case control study. *J Allergy Clin Immunol 121, 940-46 e3.*

Burrows, B., Martinez, F. D., Halonen, M., Barbee, R. A. & Cline, M. G. (1989) Association of asthma with serum IgE levels and skin-test reactivity to allergens. *N Engl J Med 320, 271-7.*

Candi E, Schmidt R, Melino G. (2005) The cornified envelope: a model of cell death in the skin. *Nat Rev Mol Cell Biol 6: 328–340.*

Chambon P (1996) A decade of molecular biology of retinoic acid receptors. *FASEBJ 10:940–954.*

Chambon P (2005) The nuclear receptor superfamily: a personal retrospect on the first two decades. *Mol Endocrinol 19:1418–1428.*

Chamlin SL, Kao J, Frieden IJ, Sheu MY, Fowler AJ, Fluhr JW, et al. (2002) Ceramide dominant barrier repair lipids alleviate childhood atopic dermatitis: changes in barrier function provide a sensitive indicator of disease activity. *J Am Acad Dermatol 47:198-208.*

Chappaz, S., Flueck, L., Farr, A. G., Rolink, A. G. & Finke, D. (2007) Increased TSLP availability restores T and B-cell compartments in adult IL-7 deficient mice. *Blood 110, 3862-70.*

Chavanas, S. et al. (2000) Mutations in SPINK5, encodes a serine protease inhibitor, cause Netherton syndrome. *Nat. Genet. 25, 141–142.*

Chimenov, Y. & Kerppola, T. K. (2001) Close encounters of many kinds: Fos–Jun interactions that mediate transcription regulatory specificity. *Oncogene 6, 533–542*.

Chin YE, Kitagawa M, Su WC, You ZH, Iwamoto Y, Fu XY. (1996) Cell growth arrest and induction of cyclin-dependent kinase inhibitor p21 WAF1/CIP1 mediated by STAT1. *Science. 272(5262):719-22.*

Chrousos, G.P. (1995) The hypothalamic-pituitaryadrenal axis and immune-mediated inflammation. *N. Engl. J. Med. 332: 1351–1362*.

Ciprandi, G. & Passalacqua, G. (2008) Allergy and the nose. *Clin Exp Immunol 153 Suppl 1, 22-6*.

Cole TJ, Blendy AP, Monaghan K, Schmid W, Aguzzi A, Fantuzzi G, Hummler E, Unsicker K, Schutz G (1995) Targeted disruption of the glucocorticoid receptor gene blocks adrenergic chromaffin cell development and severely retards lung maturation. *Genes Dev 9:1608–1621*

Corren J, Casale T, Deniz Y, Ashby M. (2003) Omalizumab, a recombinant humanized anti-IgE antibody, reduces asthma-related emergency room visits and hospitalizations in patients with allergic asthma. *J Allergy Clin Immunol 111:87-90*.

Coste, A., Antal, M.C., Chan, S., Kastner, P., Mark, M., O'Malley, B.W., and Auwerx, J. (2006). Absence of the steroid receptor coactivator-3 induces B-cell lymphoma. *EMBO J. 25, 2453–2464.*

Curran T, Franza BR Jr. (1988) Fos and Jun: the AP-1 connection. *Cell. Nov 4;55(3):395-7*

David M, Grimley PM, Finbloom DS, Larner AC. (1993) A nuclear tyrosine phosphatase downregulates interferon-induced gene expression. *Mol. Cell. Biol*. 13, 7515.

David, M., Chen, H. E., Goelz, S., Larner, A. C., Neel, B. G. (1995) Differential regulation of the alpha/beta interferon-stimulated Jak/Stat pathway by the SH2 domain-containing tyrosine phosphatase SHPTP1. *Mol. Cell. Biol. 15, 7050.*

Davie JK, Dent SY. (2004) Histone modifications in corepressor functions. *Curr Topics Dev Biol 59:145–163.*

de Groot RP, Rijken PJ, den Hertog J, Boonstra J, Verkleij AJ, de Laat SW, Kruijer W. (1991) Nuclear responses to protein kinase C signal transduction are sensitive to gravity changes. *Exp Cell Res. 197(1):87-90.*

de Ruijter AJ, van Gennip AH, Caron HN, Kemp S, van Kuilenburg AB. (2003) Histone deacetylases (HDACs): characterization of the classical HDAC family. *Biochem J 370: 737–749.*

Decker T, Kovarik P. (2000) Serine phosphorylation of STATs.*Oncogene 19, 2628-37.*

Demehri, S. et al. (2008) Notch-deficient skin induces a lethal systemic B-lymphoproliferative disorder by secreting TSLP, a sentinel for epidermal integrity. *PLoS Biol. 6, e123.*

Demehri, S., Morimoto, M., Holtzman, M.J. & Kopan, R. (2009) Skin-derived TSLP triggers progression from epidermal-barrier defects to asthma. *PLoS Biol.* **7**, *e1000067.*

Denecker G et al. (2007) Caspase-14 protects against epidermal UVB photodamage and water loss. *Nature Cell Biology* ***9****, 666 – 674*

Di Nardo A, Yamasaki K, Dorschner RA, Lai Y, Gallo RL (2008) Mast cell cathelicidin antimicrobial peptide prevents invasive group A Streptococcus infection of the skin. *J Immunol, 180:7565-7573.*

Dittmar, K.D., D.R. Demady, L.F. Stancato, et al. (1997). Folding of the glucocorticoid receptor by the heat shock protein (hsp) 90-based chaperone machinery. The role of p23 is to stabilize receptor.hsp90 heterocomplexes formed by hsp90.p60.hsp70. *J. Biol.Chem. 272: 21213–21220.*

Dolle P, Ruberte E, Leroy P, Morriss-Kay G, and Chambon P (1990) Retinoic acid receptors and cellular retinoid binding proteins. I. A systematic study of their differential pattern of transcription during mouse organogenesis. *Development 110:1133–1151*.

Downing D T, Stewart M E, Wertz P W, Colton S W, Abraham W, Strauss J S. (1987) Skin lipids: an update. *J Invest Dermatol 88: 2s–6s.*

du Vivier A. (1976) Tachyphylaxis to topically applied steroids. *Arch Dermatol 112:1245-8.*

Ebisawa, T. et al. (2001) Smurf1 interacts with transforming growth factor-β type I receptor through SMAD7 and induces receptor degradation. *J. Biol. Chem. 276, 12477–12480.*

Ehret, G. B. *et al.*, (2001) DNA binding specificity of different STAT proteins. Comparison of in vitro specificity with natural target sites. *J. Biol. Chem. 276, 6675.*

Eichenfield LF, Beck L. (2003) Elidel (pimecrolimus) cream 1%: a nonsteroidal topical agent for the treatment of atopic dermatitis. *J Allergy Clin Immunol 111:1153-68.*

Elias, P.M. (1983) Epidermal lipids, barrier function, and desquamation. *J. Invest. Dermatol. 80:44s–49s.*

Ellison JA, Patel L, Ray DW, David TJ, Clayton PE. (2000) Hypothalamic-pituitary-adrenal function and glucocorticoid sensitivity in atopic dermatitis. *Pediatrics 105:794-9.*

Esparza-Gordillo J, Weidinger S, Folster-Holst R, Bauerfeind A, Ruschendorf F, Patone G, et al. (2009) A common variant on chromosome 11q13 is associated with atopic dermatitis. *Nat Genet 41:596-601.*

Feng, X. H. & Derynck, R. (2005) Specificity and versatility in TGFβ signaling through SMADs. *Annu. Rev. Cell Dev.Biol. 21, 659–693*.

Fleischhauer K, Park JH, DiSanto JP, Marks M, Ozato K, and Yang SY (1992) Isolation of a full-length cDNA clone encoding a N-terminally variant form of the human retinoid X receptor β. *Nucleic Acids Res 20:1801*.

Forman BM, Umesono K, Chen J, and Evans RM (1995) Unique response pathways are established by allosteric interactions among nuclear hormone receptors. *Cell 81:541–550.*

Friend, S. L. et al. (1994) A thymic stromal cell line supports in vitro development of surface IgM+ B cells and produces a novel growth factor affecting B and T lineage cells. *Exp Hematol 22, 321-8.*

Fuchs, E., and Raghavan, S. (2002) Getting under the skin of epidermal morphogenesis. *Nat. Rev.Genet. 3:199–209*.

Furuse, M., et al. (2002) Claudin-based tight junctions are crucial for the mammalian epidermal barrier: a lesson from claudin-1-deficient mice. *J. CellBiol. 156:1099–1111.*

Galli, E. et al. (2007) Atopic dermatitis and asthma. *Allergy Asthma Proc 28, 540-3.*

Galli, S. J., Tsai, M. & Piliponsky, A. M. (2008) The development of allergic inflammation. *Nature 454, 445-54.*

Gao PS, Rafaels NM, Mu D, Hand T, Murray T, Boguniewicz M, Hata T, Schneider L, Hanifin JM, Gallo RL, Gao L, Beaty TH, Beck LA, Leung DY, Barnes KC. (2010) Genetic variants in thymic stromal lymphopoietin are associated with atopic dermatitis and eczema herpeticum. *J Allergy Clin Immunol. (6):1403-1407*.

Germain P. et al. (2006) Overview of nomenclature of nuclear receptors. *Pharmacol Rev 58:685–704.*

Gewirtz, A. T., T. A. Navas, S. Lyons, P. J. Godowski, and J. L. Madara. (2001) Bacterial flagellin activates basolaterally expressed TLR5 to induce epithelial proinflammatory gene expression. *J. Immunol. 167:1882–1885.*

Giguere V, Ong ES, Segui P, and Evans RM (1987) Identification of a receptor for the morphogen retinoic acid. *Nature (Lond) 330:624–629.*

Giliani, S. et al. (2005) Interleukin-7 receptor alpha (IL-7Ralpha) deficiency: cellular and molecular bases. Analysis of clinical, immunological, and molecular features in 16 novel patients. *Immunol Rev 203, 110-26.*

Gilliet, M. et al. (2003) Human dendritic cells activated by TSLP and CD40L induce proallergic cytotoxic T cells. *J Exp Med 197, 1059-63.*

Girardi, M. et al. (2001) Regulation of cutaneous malignancy by γδ T cells. *Science 294, 605–609*.

Girardi, M. et al. (2002) Resident skin-specific γδ T cells provide local, nonredundant regulation of cutaneous inflammation. *J. Exp. Med. 195, 855–867.*

Glass CK (1994) Differential recognition of target genes by nuclear receptor monomers, dimers, and heterodimers. *Endocr Rev 15:391–407.*

Glass CK and Rosenfeld MG (2000) The coregulator exchange in transcriptional functions of nuclear receptors. *Genes Dev 14:121–141*

Glass CK, Rose DW, Rosenfeld MG. (1997) Nuclear receptor coactivators. *Curr Opin Cell Biol 9:222–232.*

Gober, M. D., Fishelevich, R., Zhao, Y., Unutmaz, D. & Gaspari, A. A. (2008) Human natural killer T cells infiltrate into the skin at elicitation sites of allergic contact dermatitis. *J. Invest. Dermatol. 128, 1460–1469.*

Gray, A. M. & Mason, A. J. (1990) Requirement for activin A and transforming growth factor-β1 pro-regions in homodimer assembly. *Science 247, 1328–1330.*

Grimbaldeston MA, Nakae S, Kalesnikoff J, Tsai M, Galli SJ (2007) Mast cell-derived interleukin 10 limits skin pathology in contact dermatitis and chronic irradiation with ultraviolet B. *Nat Immunol 8:1095-1104.*

Gross KL, Lu NZ, Cidlowski JA. (2009) Molecular mechanisms regulating glucocorticoid sensitivity and resistance. *Mol Cell Endocrinol 300:7-16.*

Gudbjartsson DF, Bjornsdottir US, Halapi E, Helgadottir A, Sulem P, Jonsdottir GM, et al. (2009) Sequence variants affecting eosinophil numbers associate with asthma and myocardial infarction. *Nat Genet 41:342-7.*

Gustafsson, D., Sjoberg, O. & Foucard, T. (2000). Development of allergies and asthma in infants and young children with atopic dermatitis--a prospective follow-up to 7 years of age. *Allergy 55, 240-5*

Hahn, E. L. & Bacharier, L. B. (2005) The atopic march: the pattern of allergic disease development in childhood. *Immunol Allergy Clin North Am 25, 231-46.*

Hakim-Rad K, Metz M, Maurer M (2009) Mast cells: makers and breakers of allergic inflammation. *Curr Opin Allergy Clin Immunol 9:427-430.*

Harada M, Hirota T, Jodo AI, Hitomi Y, Sakashita M, Tsunoda T, Miyagawa T, Doi S, Kameda M, Fujita K, Miyatake A, Enomoto T, Noguchi E, Masuko H, Sakamoto T, Hizawa N, Suzuki Y, Yoshihara S, Adachi M, Ebisawa M, Saito H, Matsumoto K, Nakajima T, Mathias RA, Rafaels N, Barnes KC, Himes BE, Duan QL, Tantisira KG, Weiss ST, Nakamura Y, Ziegler SF, Tamari M. (2010) TSLP Promoter Polymorphisms are Associated with Susceptibility to Bronchial Asthma. *Am J Respir Cell Mol Biol. Jul 23.*

Hardie RA,Waring AJ, Barnetson RS. (1977) Atrophic skin striae following the use of clobetasol propionate ointment. *Practitioner 219:376-8.*

Haspel RL, Salditt-Georgieff M, Darnell JE Jr. (1996) The rapid inactivation of nuclear tyrosine phosphorylated Stat1 depends upon a protein tyrosine phosphatase. *EMBO J. 15, 6262-8.*

Haussler MR, Haussler CA, Jurutka PW, Thompson PD, Hsieh JC, Remus LS, Selznick SH, Whitfield GK. (1997) The vitamin D hormone and its nuclear receptor: molecular actions and disease states. *J Endocrinol 154(Suppl):S57–S73.*

Hayashi, H. et al. (1997) The MAD-related protein SMAD7 associates with the TGFβ receptor and functions as an antagonist of TGFβ signaling. *Cell 89, 1165–1173.*

Heck, S., Kullmann, M., Gast, A., Ponta, H., Rahmsdorf, H.J., Herrlich, P.,and Cato, A.C. (1994). A distinct modulating domain in glucocorticoid receptor monomers in the repression of activity of the transcription factor AP-1. *EMBO J. 13, 4087–4095.*

Heijink IH, Kies PM, Kauffman HF, Postma DS, van Oosterhout AJ, Vellenga E. (2007) Down-regulation of E-cadherin in human bronchial epithelial cells leads to epidermal growth factor receptor-dependent Th2 cell-promoting activity. *J Immunol. 178(12):7678-85.*

Herrmann T, van der Hoeven F, Grone H J et al. (2003) Mice with targeted disruption of the fatty acid transport protein 4 (Fatp 4, Slc27a4) gene show features of lethal restrictive dermopathy. *J Cell Biol 161: 1105–1115.*

Himes BE, Hunninghake GM, Baurley JW, Rafaels NM, Sleiman P, Strachan DP, et al. (2009) Genome-wide association analysis identifies PDE4D as an asthma-susceptibility gene. *Am J Hum Genet 84:581-93.*

Holloway JW, Koppelman GH. (2007) Identifying novel genes contributing to asthma pathogenesis. *Curr Opin Allergy Clin Immunol 7:69-74.*

Hughes MR, Malloy PJ, Kieback DG, Kesterson RA, Pike JW, Feldman D, and O'Malley BW (1988) Point mutations in the human vitamin D receptor gene associated with hypocalcemic rickets. *Science (Wash DC) 242:1702–1705.*

Hultsch T, Muller KD, Meingassner JG, Grassberger M, Schopf RE, Knop J. (1998) Ascomycin macrolactam derivative SDZ ASM 981 inhibits the release of granule-associated mediators and of newly synthesized cytokines in RBL 2H3 mast cells in an immunophilin-dependent manner. *Arch Dermatol Res 290:501-7.*

Incorvaia, C. et al. (2008) Allergy and the skin. *Clin Exp Immunol 153 Suppl 1, 27-9.*

Ip YT, Davis RJ. (1998) Signal transduction by the c-Jun N-terminal kinase (JNK)--from inflammation to development. *Curr Opin Cell Biol. 10(2):205-19.*

Irie-Sasaki, J. *et al.* (2001) CD45 is a JAK phosphatase and negatively regulates cytokine receptor signalling. *Nature 409, 349-354.*

Irvine A D, McLean W H. (2006) Breaking the (un)sound barrier: filaggrin is a major gene for atopic dermatitis. *J Invest Dermatol 126: 1200–1202.*

Isaksen, D. E. et al. (1999) Requirement for stat5 in thymic stromal lymphopoietin-mediated signal transduction. *J Immunol 163, 5971-7.*

Isaksen, D. E. et al. (2002) Uncoupling of proliferation and Stat5 activation in thymic stromal lymphopoietinmediated signal transduction. *J Immunol 168, 3288-94.*

Ito, M., et al. (2005) Stem cells in the hair follicle bulge contribute to wound repair but not to homeostasis of the epidermis. *Nat. Med. 11:1351–1354*.

Itoh, S. & ten Dijke, P. (2007) Negative regulation of TGF-β receptor/SMAD signal transduction. *Curr. Opin. Cell Biol. 19, 176–184.*

Kabesch M, Schedel M, Carr D, Woitsch B, Fritzsch C, Weiland SK, et al. (2006) IL-4/IL-13 pathway genetics strongly influence serum IgE levels and childhood asthma. *J Allergy Clin Immunol 117:269-74.*

Kalinin, A.E., Kajava, A.V., and Steinert, P.M. (2002) Epithelial barrier function: assembly and structural features of the cornified cell envelope. *Bioessays.24:789–800.*

Kalliomäki M, Salminen S, Arvilommi H, Kero P, Koskinen P, Isolauri E. (2001) Probiotics in primary prevention of atopic disease: a randomised placebo-controlled trial. *Lancet 357:1076-9.*

Kalliomaki M, Salminen S, Poussa T, Arvilommi H, Isolauri E. (2003) Probiotics and prevention of atopic disease: 4-year follow-up of a randomised placebo-controlled trial. *Lancet 361:1869-71.*

Karin M, Liu Z, Zandi E. (1997) AP-1 function and regulation. Curr Opin Cell Biol. 9(2):240-6.

Karin, M., and Y. Ben-Neriah. (2000) Phosphorylation meets ubiquination: the control of NF-κB activity. *Annu. Rev. Immunol. 18:621–663.*

Kastner P, Grondona JM, Mark M, Gansmuller A, LeMeur M, Decimo D, Vonesch JL, Dolle P, and Chambon P (1994) Genetic analysis of RXR α developmental function: convergence of RXR and RAR signaling pathways in heart and eye morphogenesis. *Cell 78:987–1003.*

Kastner P, Mark M, Leid M, Gansmuller A, Chin W, Grondona JM, Decimo D, Krezel W, Dierich A, and Chambon P (1996) Abnormal spermatogenesis in RXRβ mutant mice. *Genes Dev 10:80–92.*

Kato A, Favoreto S Jr, Avila PC, Schleimer RP. (2007) TLR3- and Th2 cytokine-dependent production of thymic stromal lymphopoietin in human airway epithelial cells. *J Immunol 179:1080–*7.

Kato S, Yoshizazawa T, Kitanaka S, Murayama A, and Takeyama K (2002) Molecular genetics of vitamin D- dependent hereditary rickets. *Horm Res 57:73–78.*

Kavsak, P. et al. (2000) SMAD7 binds to Smurf2 to form an E3 ubiquitin ligase that targets the TGF-β receptor for degradation. *Mol. Cell 6, 1365–1375.*

Kay, A. B. (2001) Allergy and allergic diseases. First of two parts. *N Engl J Med 344, 30-7.*

Kay, A. B. (2001) Allergy and allergic diseases. Second of two parts. *N Engl J Med 344, 109-13.*

Kim BS, Miyagawa F, Cho YH, Bennett CL, Clausen BE, Katz SI. (2009) Keratinocytes function as accessory cells for presentation of endogenous antigen expressed in the epidermis. *J Invest Dermatol. 129(12):2805-17.*

Kino T, Su YA, Chrousos GP. (2009) Human glucocorticoid receptor isoform beta: recent understanding of its potential implications in physiology and pathophysiology. *Cell Mol Life Sci 66:3435-3448.*

Klug, A., and Schwabe, J.W.R. (1995). Zinc fingers. *FASEB J. 9,597-604.*

Knisz J, Banks A, McKeag L, Metcalfe DD, Rothman PB, Brown JM. (2009) Loss of SOCS7 in mice results in severe cutaneous disease and increased mast cell activation. *Clin Immunol. 132(2):277-84.*

Kobayashi M, Yoshiki R, Sakabe J, Kabashima K, Nakamura M, Tokura Y (2009) Expression of toll-like receptor 2, NOD2 and dectin-1 and stimulatory effects of their ligands and histamine in normal human keratinocytes. *Br J Dermatol 160:297-304.*

Kondo, H., Ichikawa, Y. & Imokawa, G. (1998) Percutaneous sensitization with allergens through barrier disrupted skin elicits a Th2-dominant cytokine response. *Eur J Immunol 28, 769-79.*

Kopp MV, Brauburger J, Riedinger F, Beischer DI, horst GK, amin W, et al. (2002) The effect of anti-IgE treatment on in vitro leukotriene release in children with seasonal allergic rhinitis. *J Allergy Clin Immunol 110:728-35.*

Koppelman GH, Meyers DA, Howard TD, Zheng SL, Hawkins GA, Ampleford EJ, et al. (2009) Identification of PCDH1 as a novel susceptibility gene for bronchial hyperresponsiveness. *Am J Respir Crit Care Med 180:929-35.*

Kraft S, Kinet JP (2007) New developments in FcepsilonRI regulation, function and inhibition. *Nat Rev Immunol 7:365-378.*

Krebs, D. L. & D. J. Hilton (2001) SOCS proteins: negative regulators of cytokine signaling. *Stem Cells 19, 378.*

Krezel W, Dupe V, Mark M, Dierich A, Kastner P, and Chambon P (1996) RXRγ null mice are apparently normal and compound RXRα$^{+/-}$/RXRβ$^{-/-}$/RXRγ$^{-/-}$ mutant mice are viable. *Proc Natl Acad Sci USA 93:9010–9014.*

Kronenberg, M. Toward an understanding of NKT cell biology: progress and paradoxes. *Annu. Rev. Immunol. 23, 877–900 (2005).*

Lack, G. (2008) Clinical practice. Food allergy. *N Engl J Med 359, 1252-60.*

Lack, G., Fox, D., Northstone, K. & Golding, J. (2003) Factors associated with the development of peanut allergy in childhood. *N Engl J Med 348, 977-85.*

Laudet V and Gronemeyer H (2002) *The Nuclear Receptor Facts Book*, Academic Press, San Diego.

Lee EB, Kim KW, Hong JY, Jee HM, Sohn MH, Kim KE. (2010) Increased serum thymic stromal lymphopoietin in children with atopic dermatitis. *Pediatr Allergy Immunol. 21(2 Pt 2):e457-60.*

Lee HC, Ziegler SF. (2007) Inducible expression of the proallergic cytokine thymic stromal lymphopoietin in airway epithelial cells is controlled by NFkappaB. *Proc Natl Acad Sci USA 104:914–9.*

Leid M, Kastner P, and Chambon P (1992) Multiplicity generates diversity in the retinoic acid signalling pathways. *Trends Biochem Sci 17:427–433.*

Leonard, W. J. (2001) Role of Jak kinases and STATs in cytokine signal transduction. *Int. J. Hematol. 73, 271-7.*

Leonardi, A., Motterle, L. & Bortolotti, M. (2008) Allergy and the eye. *Clin Exp Immunol 153 Suppl 1, 17-21.*

Leung, D. Y. & Bieber, T. (2003) Atopic dermatitis. *Lancet 361, 151-60.*

Leung, D. Y., Boguniewicz, M., Howell, M. D., Nomura, I. & Hamid, Q. A. (2004) New insights into atopic dermatitis. *J Clin Invest 113, 651-7.*

Leung, D. Y., Jain, N. & Leo, H. L. (2003) New concepts in the pathogenesis of atopic dermatitis. *Curr Opin Immunol 15, 634-8.*

Levin, S. D. et al. (1999) Thymic stromal lymphopoietin: a cytokine that promotes the development of IgM+ B cells in vitro and signals via a novel mechanism. *J Immunol 162, 677-83.*

Li Y, Lambert MH, and Xu HE (2003) Activation of nuclear receptors: a perspective from structural genomics. *Structure 11:741–746.*

Li YC, Pirro AE, Amling M, Delling G, Baron R, Bronson R, and Demay MB (1997) Targeted ablation of the vitamin D receptor: an animal model of vitamin D dependent rickets type II with alopecia. *Proc Natl Acad Sci USA 94:9831–9835*.

Li, M. et al. (2005) Retinoid X receptor ablation in adult mouse keratinocytes generates an atopic dermatitis triggered by thymic stromal lymphopoietin. *Proc Natl Acad Sci U S A 102, 14795-800.*

Li, M. et al. (2006) Topical vitamin D3 and low-calcemic analogs induce thymic stromal lymphopoietin in mouse keratinocytes and trigger an atopic dermatitis. *Proc Natl Acad Sci U S A 103, 11736-41.*

Li, M. et al. (2009) Induction of Thymic Stromal Lymphopoietin Expression in Keratinocytes Is Necessary for Generating an Atopic Dermatitis upon Application of the Active Vitamin D3 Analogue MC903 on Mouse Skin. *J Invest Dermatol. 129(2):498-502.*

Leid, M., Kastner. P.. Lyons, R.. Nakshatri, H., Saunders, M., Zacharewski, **T.,** Chen, J. Y., Staub, **A.,** Gamier, J. M., Mader, S., et al. (1992) Purification, cloning, and RXR identity of the HeLa cell factor with which RAR or TRheterodimerizes to bind target sequences efficiently. *Cell 68, 377-395*

Lin, Y. T., Wang, C. T. & Chiang, B. L. (2007) Role of bacterial pathogens in atopic dermatitis. *Clin Rev Allergy Immunol 33, 167-77.*

Liu Q and Linney E (1993) The mouse retinoid-X receptor-γ gene: genomic organization and evidence for functional isoforms. *Mol Endocrinol 7:651–658*.

Liu, F. (2006) SMAD3 phosphorylation by cyclin-dependent kinases. *Cytokine Growth Factor Rev. 17, 9–17.*

Liu, Y. J. et al. (2007) TSLP: an epithelial cell cytokine that regulates T cell differentiation by conditioning dendritic cell maturation. *Annu Rev Immunol 25, 193-219.*

Liu, Y. J. (2006) Thymic stromal lymphopoietin: master switch for allergic inflammation. *J Exp Med 203, 269-73.*

London SJ, Romieu I. (2009) Gene by environment interaction in asthma. *Annu Rev Public health 30:55-80.*

Lutgemeier MD, Lubach D. (1987) Development and regression of dermal corticosteroid atrophy. 4. Concentration dependence of the skin thinning effect of triamcinolone acetonide. *Derm Beruf Umwelt 35:55-7.*

Mader S, Chen JY, Chen Z, White J, Chambon P, and Gronemeyer H (1993) The patterns of binding of RAR, RXR and TR homo- and heterodimers to direct repeats are dictated by the binding specificities of the DNA binding domains. *EMBO J 12:5029–5041.*

Mangelsdorf DJ, Umesono K, Kliewer SA, Borgmeyer U, Ong ES, and Evans RM (1991) A direct repeat in the cellular retinol-binding protein type II gene confers differential regulation by RXR and RAR. *Cell 66:555–561.*

Mangelsdorf DJ and Evans RM (1995) The RXR heterodimers and orphan receptors. *Cell 83:841–850.*

Marmorstein, R. and Trievel, R.C. (2009) Histone modifying enzymes:structures, mechanisms, and specificities. *Biochim. Biophys. Acta 1789, 58–68*

Matsuki, M., et al. (1998) Defective stratum corneum and early neonatal death in mice lacking the gene for transglutaminase 1 (keratinocyte transglutaminase). *Proc. Natl. Acad. Sci. U. S. A. 95:1044–1049.*

McKay, L.I. & J.A. Cidlowski. (1998) Cross-talk between nuclear factor-ê B and the steroid hormone receptors: mechanisms of mutual antagonism. *Mol.Endocrinol. 12: 45–56.*

McKenna NJ, Lanz RB, O'Malley BW. (1999) Nuclear receptor coregulators: Cellular and molecular biology. *Endocr Rev 20:321–344*.

McLachlan JB, Shelburne CP, Hart JP, Pizzo SV, Goyal R, Brooking-Dixon R, Staats HF, Abraham SN (2008) Mast cell activators: a new class of highly effective vaccine adjuvants. *Nat Med 14:536-541.*

McLean, W. H. et al. (2008) Filaggrin variants confer susceptibility to asthma. *J Allergy Clin Immunol 121,1294-5; author reply 1295-6.*

Meingassner JG, Grassberger M, Fahrngruber H, Moore HD, Schuurman H, Stutz A. (1997) A novel anti-inflammatory drug, SDZ ASM 981, for the topical and oral treatment of skin diseases: in vivo pharmacology. *Br J Dermatol 137:568-76.*

Metz M, Lammel V, Gibbs BF, Maurer M (2006) Inflammatory murine skin responses to UV-B light are partially dependent on endothelin-1 and mast cells. *Am J Pathol 169:815-822.*

Meyer, T., J. Carlstedt-Duke & D.B. Starr. (1997) A weak TATA box is a prerequisite for glucocorticoid dependent repression of the osteocalcin gene. *J. Biol.Chem*. *272: 30709–30714.*

Miller LS, O'Connell RM, Gutierrez MA, Pietras EM, Shahangian A, Gross CE, Thirumala A, Cheung AL, Cheng G, Modlin RL (2006) MyD88 mediates neutrophil recruitment initiated by IL-1R but not TLR2 activation in immunity against Staphylococcus aureus. *Immunity 24:79-91.*

Miyata M, Hatsushika K, Ando T, Shimokawa N, Ohnuma Y, Katoh R, Suto H, Ogawa H, Masuyama K, Nakao A. (2008) Mast cell regulation of epithelial TSLP expression plays an important role in the development of allergic rhinitis. *Eur J Immunol. 38(6):1487-92.*

Moffatt MF, Kabesch M, Liang L, Dixon AL, Strachan D, Heath S, et al. (2007) Genetic variants regulating ORMDL3 expression contribute to the risk of childhood asthma. *Nature 448:470-3.*

Morrison NA, Shine J, Fragonas J-C, Verkest V, McMenemy L, Eisman JA. (1989) 1,25-dihydroxyvitamin D-responsive element and glucocorticoid repression in the osteocalcin gene. *Science 246: 1158–61.*

Mou Z, Xia J, Tan Y, Wang X, Zhang Y, Zhou B, Li H, Han D. (2009) Overexpression of thymic stromal lymphopoietin in allergic rhinitis. *Acta Otolaryngol. 129(3):297-301.*

Mowen, K. A. et al. (2001) Arginine methylation of STAT1 modulates IFNalpha/beta-induced transcription. *Cell 104, 731-741.*

Myers MP, Andersen JN, Cheng A, Tremblay ML, Horvath CM, Parisien JP, Salmeen A, Barford D, Tonks NK. (2001) TYK2 and JAK2 are substrates of protein-tyrosine phosphatase 1B. *J. Biol. Chem. 276, 47771-4.*

Nagaich, A.K., D.A.Walker, R.Wolford, et al. (2004) Rapid periodic binding and displacement of the glucocorticoid receptor during chromatin remodeling. *Mol Cell. 14: 163–174.*

Nagata T, Kanno Y, Ozato K, and Taketo M (1994) The mouse Rxrb gene encoding RXRβ: genomic organization and two mRNA isoforms generated by alternative splicing of transcripts initiated from CpG island promoters. *Gene 142:183–189.*

Nagata, Y., Kamijuku, H., Taniguchi, M., Ziegler, S. & Seino, K. I. (2007) Differential Role of Thymic Stromal Lymphopoietin in the Induction of Airway Hyperreactivity and Th2 Immune Response in Antigen-Induced Asthma with Respect to Natural Killer T Cell Function. *Int Arch Allergy Immunol 144, 305-314.*

Nassif A, Chan SC, Storrs FJ, Hanifin JM. (1994) Abnormal skin irritancy in atopic dermatitis and in atopy without dermatitis. *Arch Dermatol 130:1402-7.*

Nemes, Z., and Steinert, P.M. (1999) Bricks and mortar of the epidermal barrier. *Exp. Mol. Med. 31:5–19.*

Nestle, O F., et al. (2009) Skin immune sentinels in health and disease *Nat. Rev.Immunol 9: 679-691*

Nick Z. Lu and John A. Cidlowski. (2006) Glucocorticoid receptor isoforms generate transcription specificity. *Trends Cell Biol.16(6):301-7.*

Niemann, C., and Watt, F.M. (2002) Designer skin: lineage commitment in postnatal epidermis. *Trends Cell Biol. 12:185–192*.
Nilsson EJ, Henning CG, Magnusson J. (1992) Topical corticosteroids and *Staphylococcus aureus* in atopic dermatitis. *J Am Acad Dermatol 27:29-34.*

Novac, N., D. Baus, A. Dostert, et al. (2006) Competition between glucocorticoid receptor and NFκB for control of the human FasL promoter. *Faseb J. 20: 1074–1081*.

Oakley, R.H., J.C. Webster, M. Sar, et al. (1997) Expression and subcellular distribution of the betaisoform of the human glucocorticoid receptor. *Endocrinology 138: 5028–5038.*

Oakley, R.H., C.M. Jewell, M.R. Yudt, et al. (1999) The dominant negative activity of the human glucocorticoid receptor beta isoform. Specificity and mechanisms of action. *J. Biol. Chem. 274: 27857–27866.*

Oettgen, H. C. & Geha, R. S. (2001) IgE regulation and roles in asthma pathogenesis. *J Allergy Clin Immunol 107, 429-40.*

Ogunjimi, A. A. et al. (2005) Regulation of Smurf2 ubiquitin ligase activity by anchoring the E2 to the HECT domain. *Mol. Cell 19, 297–308*.

Oikarinen A, Autio P. (1991) New aspects of the mechanism of corticosteroid induced dermal atrophy. *Clin Exp Dermatol 16:416-9.*

Omori, M. & Ziegler, S. (2007) Induction of IL-4 expression in CD4(+) T cells by thymic stromal lymphopoietin. *J Immunol 178, 1396-404.*

O'Regan, G. M., Sandilands, A., McLean, W. H. & Irvine, A. D. (2008) Filaggrin in atopic dermatitis. *J Allergy Clin Immunol. 122(4):689-93.*

Ouchi T, Lee SW, Ouchi M, Aaronson SA, Horvath CM. (2000) Collaboration of signal transducer and activator of transcription 1 (STAT1) and BRCA1 in differential regulation of IFN-gamma target genes. *Proc Natl Acad Sci U S A. 97(10):5208-13.*

Paller AE, ichenfield LF, Leung DY, Stewart D, Appell M. (2001) A 12-week study of tacrolimus ointment for the treatment of atopic dermatitis in pediatric patients. *J Am Acad Dermatol 44:S47-57.*

Palmer CN, Irvine AD, Terron-Kwiatkowski A, Zhao Y, Liao H, Lee SP, et al. (2006) Common loss-of-function variants of the epidermal barrier protein filaggrin are a major predisposing factor for atopic dermatitis. *Nat Genet 38:441-6.*

Park, L. S. et al. (2000) Cloning of the murine thymic stromal lymphopoietin (TSLP) receptor: Formation of a functional heteromeric complex requires interleukin 7 receptor. *J Exp Med 192, 659-70.*

Passalacqua, G. & Ciprandi, G. (2008) Allergy and the lung. *Clin Exp Immunol 153 Suppl 1, 12-6.*

Perlmann T and Jansson L (1995) A novel pathway for vitamin A signaling mediated by RXR heterodimerization with NGFI-B and NURR1. *Genes Dev 9:769–782.*

Petkovich M, Brand NJ, Krust A, and Chambon P (1987) A human retinoic acid receptor which belongs to the family of nuclear receptors. *Nature (Lond) 330:444–450.*

Presland R B, Boggess D, Lewis S P, Hull C, Fleckman P, Sundberg J P. (2000) Loss of normal profilaggrin and filaggrin in flaky tail (ft / ft) mice: an animal model for the filaggrin-deficient skin disease ichthyosis vulgaris. *J Invest Dermatol 115: 1072–1081.*

Proksch E, Feingold K R, Elias P M. (1992) Epidermal HMG CoA reductase activity in essential fatty acid deficiency: barrier requirements rather than eicosanoid generation regulate cholesterol synthesis. *J Invest Dermatol 99:216–220.*

Pucci, S. & Incorvaia, C. (2008) Allergy as an organ and a systemic disease. *Clin Exp Immunol 153 Suppl 1, 1-2.*

Puel, A. & Leonard, W. J. (2000) Mutations in the gene for the IL-7 receptor result in T(-)B(+)NK(+) severe combined immunodeficiency disease. *Curr Opin Immunol 12, 468-73.*

Pykalainen M, Kinos R, Valkonen S, Rydman P, Kilpelainen M, Laitinen LA, et al. (2005) Association analysis of common variants of STAT6, GATA3, and STAT4 to asthma and high serum IgE phenotypes. *J Allergy Clin Immunol 115:80-7.*

Qiu, Y., Zhao, Y., Becker, M., John, S., Parekh, B.S., Huang, S., Hendarwanto, A., Martinez, E.D., Chen, Y., Lu, H., et al. (2006) HDAC1 acetylation is linked to progressive modulation of steroid receptor induced gene transcription. *Mol. Cell 22, 669–679.*

Queille-Roussel C, Paul C, Duteil L, Lefebvre MC, Rapatz G, Zagula M, et al. (2001) The new topical ascomycin derivative SDZ ASM 981 does not induce skin atrophy when applied to normal skin for 4 weeks: a randomized, double-blind controlled study. *Br J Dermatol 144:507-13.*

Raby, B. A. et al. (2004) Association of vitamin D receptor gene polymorphisms with childhood and adult asthma. *Am J Respir Crit Care Med 170, 1057-65.*

Raghunath, M., et al. (2003) Self-healing collodion baby: a dynamic phenotype explained by a particular transglutaminase-1 mutation. *J. Invest. Dermatol.120:224–228.*

Reche, P. A. et al. (2001) Human thymic stromal lymphopoietin preferentially stimulates myeloid cells. *J Immunol 167, 336-43.*

Reichardt HM, Kaestner KH, Tuckermann J, Kretz O, Wessely O, Bock R, Gass P, Schmid W, Herrlich P, Angel P, Schutz, G (1998) DNA binding of the glucocorticoid receptor is not essential for survival. *Cell 93:531–541*

Rhodes, H. L., Sporik, R., Thomas, P., Holgate, S. T. & Cogswell, J. J. (2001) Early life risk factors for adult asthma: a birth cohort study of subjects at risk. *J Allergy Clin Immunol 108, 720-5.*

Rhodes, H. L., Thomas, P., Sporik, R., Holgate, S. T. & Cogswell, J. J. (2002) A birth cohort study of subjects at risk of atopy: twenty-two-year follow-up of wheeze and atopic status. *Am J Respir Crit Care Med 165, 176-80.*

Rimoldi, M. et al. (2005) Intestinal immune homeostasis is regulated by the corsstalk between epithelial cells and dendritic cells. *Nat. Immunol. 6, 507–514.*

Rimoldi, M. et al. (2005) Monocyte-derived dendritic cells activated by bacteria or by bacteria-stimulated epithelial cells are functionally different. *Blood 106, 2818–2826.*

Robert Chiu, Peter Angel, and Michael Karin. (1989) Jun-B Differs in Its Biological Properties from, and Is a Negative Regulator of, c-Jun. *Cell 59, 979-966.*

Robyr D, Wolffe AP, Wahli W. (2000) Nuclear Hormone Receptor Coregulators In Action: Diversity For Shared Tasks. *Mol Endo 14(3):329-47.*

Rochman, I., Watanabe, N., Arima, K., Liu, Y. J. & Leonard, W. J. (2007) Cutting edge: direct action of thymic stromal lymphopoietin on activated human CD4+ T cells. *J Immunol 178, 6720-4.*

Rochman, Y. & Leonard, W. J. (2008) Thymic stromal lymphopoietin: a new cytokine in asthma. *Curr Opin Pharmacol 8, 249-54.*

Rogatsky, I., Luecke, H.F., Leitman, D.C., and Yamamoto, K.R. (2002). Alternate surfaces of transcriptional coregulator GRIP1 function in different glucocorticoid receptor activation and repression contexts. *Proc. Natl. Acad. Sci. USA 99, 16701–16706.*

Roland Moll, Markus Divo, Lutz Langbein. (2008) The human keratins: biology and pathology. *Histochem Cell Biol 129:705–733*

Roll, A., Cozzio, A., Fischer, B. & Schmid-Grendelmeier, P. (2004) Microbial colonization and atopic dermatitis. *Curr Opin Allergy Clin Immunol 4, 373-8.*

Roop D. (1995) Defects in the barrier. *Science 267: 474–475.*

Rosenfeld, M.G. & C.K. Glass. (2001) Coregulator codes of transcriptional regulation by nuclear receptors. *J. Biol. Chem. 276: 36865–36868.*

Ross, S. et al. (2006) SMADs orchestrate specific histone modifications and chromatin remodeling to activate transcription. *EMBO J. 25, 4490–4502.*

Sandilands, A. et al. (2007) Comprehensive analysis of the gene encoding filaggrin uncovers prevalent and rare mutations in ichthyosis vulgaris and atopic eczema. *Nat Genet 39, 650-4.*

Sapkota G, Alarcón C, Spagnoli FM, Brivanlou AH Massagué, J. (2007) Balancing BMP signalling through integrated inputs into the SMAD1 linker. *Mol. Cell 25, 441–454.*

Schauber J, Gallo RL (2008) Antimicrobial peptides and the skin immune defense system. *J Allergy Clin Immunol 122:261-266.*

Schindler, C. (1999). Cytokines and JAK-STAT signaling. *Exp. Cell Res. 253: 7–14.*

Schoneveld, O.J., I.C. Gaemers & W.H. Lamers. (2004) Mechanisms of glucocorticoid signalling. *Biochim. Biophys. Acta 1680: 114–128.*

Schule, R., P. Rangarajan, S. Kliewer, *et al*. (1990) Functional antagonism between oncoprotein c-Jun and the glucocorticoid receptor. *Cell 62: 1217–1226.*

Segre, J. (2003) Complex redundancy to build a simple epidermal permeability barrier. *Curr. Opin.Cell Biol. 15:776–782.*

Seshasayee D, Lee WP, Zhou M, Shu J, Suto E, Zhang J, Diehl L, Austin CD, Meng YG, Tan M, Bullens SL, Seeber S, Fuentes ME, Labrijn AF, Graus YM, Miller LA, Schelegle ES, Hyde DM, Wu LC, Hymowitz SG, Martin F. (2007) In vivo blockade of OX40 ligand inhibits thymic stromal lymphopoietin driven atopic inflammation. *J Clin Invest. 117(12):3868-78.*

Shi, W. et al. (2004) GADD34–PP1c recruited by SMAD7 dephosphorylates TGFβ type I receptor. *J. Cell Biol.164, 291–300.*

Shi, Y. & Massagué, J. (2003) Mechanisms of TGF-β signalling from cell membrane to the nucleus. *Cell 113, 685–700.*

Shi, Y. et al. (1998) Crystal structure of a SMAD MH1 domain bound to DNA: Insights on DNA-binding in TGF-β signaling. *Cell 94, 585–594.*

Sicherer SH, Sampson HA. (1999) Food hypersensitivity and atopic dermatitis: pathophysiology, epidemiology, diagnosis, and management. *J Allergy Clin Immunol 104:S114-22.*

Shuai, K. (2000) Modulation of STAT signaling by STAT-interacting proteins. *Oncogene 19, 2638-44.*

Siebenhaar F, Syska W, Weller K, Magerl M, Zuberbier T, Metz M, Maurer M (2007) Control of Pseudomonas aeruginosa skin infections in mice is mast cell-dependent. *Am J Pathol, 170:1910-1916.*

Sims, J. E. et al. (2000) Molecular cloning and biological characterization of a novel murine lymphoid growth factor. *J Exp Med 192, 671-80.*

Smith, F.J., et al. (2006) Loss-of-function mutations in the gene encoding filaggrin cause ichthyosis vulgaris. *Nat. Genet*. *38:337–342.*

Soderhall C, Marenholz I, Kerscher T, Ruschendorf F, Esparza-Gordillo J, Worm M, et al. (2007) Variants in a novel epidermal collagen gene (COL29A1) are associated with atopic dermatitis. *PLoS Biol 5:e242.*

Sokol, C. L., Barton, G. M., Farr, A. G. & Medzhitov, R. (2008) A mechanism for the initiation of allergen induced T helper type 2 responses. *Nat Immunol 9, 310-8.*

Song, C.Z., X. Tian & T.D. Gelehrter. (1999) Glucocorticoid receptor inhibits transforming growth factor-â signaling by directly targeting the transcriptional activation function of Smad3. *Proc. Natl. Acad.Sci. USA 96: 11776–11781*.

Soumelis, V. & Liu, Y. J. (2004) Human thymic stromal lymphopoietin: a novel epithelial cell-derived cytokine and a potential key player in the induction of allergic inflammation. *Springer Semin Immunopathol 25,325-33.*

Soumelis, V. et al. (2002) Human epithelial cells trigger dendritic cell mediated allergic inflammation by producing TSLP. *Nat Immunol 3, 673-80.*

Spencer TE, Jenster G, Burcin MM, et al. (1997) Steroid receptor coactivator-1 is a histone acetyltransferase. *Nature 389:194–198.*

Spergel, J. M. & Paller, A. S. (2003) Atopic dermatitis and the atopic march. *J Allergy Clin Immunol 112, S118-27.*

Spergel, J. M. (2005) Atopic march: link to upper airways. *Curr Opin Allergy Clin Immunol 5, 17-21.*

Spergel, J. M. et al. (1998) Epicutaneous sensitization with protein antigen induces localized allergic dermatitis and hyperresponsiveness to methacholine after single exposure to aerosolized antigen in mice. *J Clin Invest 101, 1614-22.*

Stalder JF, Fleury M, Sourisse M, Rostin M, Pheline F, Litoux P. (1994) Local steroid therapy and bacterial skin flora in atopic dermatitis. *Br J Dermatol 131:536-40.*

Stefansson K, Brattsand M, Roosterman D, Kempkes C, Bocheva G, Steinhoff M et al.(2008) Activation of proteinase-activated receptor-2 by human kallikrein-related peptidases. *J Invest Dermatol 128:18–25*

Steinert, P.M. (2000) The complexity and redundancy of epithelial barrier function. *J. Cell Biol. 151:F5–F8.*

Stuetz A, Grassberger M, Meingassner JG. (2001) Pimecrolimus (Elidel, SDZ ASM 981): preclinical pharmacologic profile and skin selectivity. *Semin Cutan Med Surg 20:233-41.*

Stunnenberg, H.G. (1993). Mechanisms of transactivation by retinoic acid receptors. *Bioessays 75, 309-315.*

Suttner K, Rosenstiel P, Depner M, Schedel M, Pinto LA, Ruether A, et al. (2009) TBX21 gene variants increase childhood asthma risk in combination with HLX1 variants. *J Allergy Clin Immunol 123:1062-8, e1-8.*

Takeda, K. & Akira, S. (2000) STAT family of transcription factors in cytokine-mediated biological responses. *Cytokine Growth Factor Rev. 11, 199–207.*

Tattersfield, A. E., Knox, A. J., Britton, J. R. & Hall, I. P. (2002) Asthma. *Lancet 360, 1313-22.*

Taylor, B.C. *et al.* (2009) TSLP regulates intestinal immunity and inflammation in mouse models of helminth infection and colitis. *J. Exp. Med. 206, 655–667.*

Thiagalingam S, Cheng KH, Lee HJ, Mineva N, Thiagalingam A, Ponte JF. (2003) Histone deacetylases: unique players in shaping the epigenetic histone code. *Ann N Y Acad Sci 983: 84–100.*

Tocci MJ, Matkovich DA, Collier KA, Kwok P, Dumont F, Lin S, et al. (1989) The immunosuppressant FK506 selectively inhibits expression of early T cell activation genes. *J Immunol 143:718-26.*

Torchia J, Glass C, Rosenfeld MG. (1998) Co-activators and corepressors in the integration of transcriptional responses. *Curr Opin Cell Biol 10:373–383.*

Toulon, A. et al. (2009) A role for human skin-resident T cells in wound healing. *J. Exp. Med. 206, 743–750.*

Tsukazaki, T., Chiang, T. A., Davison, A. F., Attisano, L. & Wrana, J. L. (1998) SARA, a FYVE domain protein that recruits SMAD2 to the TGFβ receptor. *Cell 95, 779–791.*

Tunggal, J.A., et al. (2005) E-cadherin is essential for in vivo epidermal barrier function by regulating tight junctions. *EMBO J. 24:1146–1156.*

van Beelen AJ, Zelinkova Z, Taanman-Kueter EW, Muller FJ, Hommes DW, Zaat SA, Kapsenberg ML, de Jong EC (2007) Stimulation of the intracellular bacterial sensor NOD2 programs dendritic cells to promote interleukin-17 production in human memory T cells. *Immunity 27:660-669.*

Van Cromphaut SJ, Dewerchin M, Hoenderop JG, Stockmans I, Van Herck E, Kato S, Bindels RJ, Collen D, Carmeliet P, Bouillon R, et al. (2001) Duodenal calcium absorption in vitamin D receptor-knockout mice: functional and molecular aspects. *Proc Natl Acad Sci USA 98:13324–3329.*

van Dam H, Wilhelm D, Herr I, Steffen A, Herrlich P, Angel P. (1995) ATF-2 is preferentially activated by stress-activated protein kinases to mediate c-jun induction in response to genotoxic agents. *EMBO J. Apr 18;14(8):1798-811.*

Van Eerdewegh P, Little RD, Dupuis J, Del Mastro RG, Falls K, Simon J, et al. (2002) Association of the ADAM33 gene with asthma and bronchial hyperresponsiveness. *Nature. 418:426-30.*

Vercelli, D. (2008) Discovering susceptibility genes for asthma and allergy. *Nat Rev Immunol 8, 169-82.*

Villadangos JA, Young L (2008) Antigen-presentation properties of plasmacytoid dendritic cells. *Immunity 29:352-361.*

Vinkemeier U, Cohen SL, Moarefi I, Chait BT, Kuriyan J, Darnell JE Jr. (1996) DNA binding of in vitro activated Stat1 alpha, Stat1 beta and truncated Stat1: interaction between NH2-terminal domains stabilizes binding of two dimers to tandem DNA sites. *EMBO J. 15(20):5616-26.*

Vosshenrich, C. A., Cumano, A., Muller, W., Di Santo, J. P. & Vieira, P. (2003) Thymic stromal-derived lymphopoietin distinguishes fetal from adult B cell development. *Nat Immunol 4, 773-9.*

Vosshenrich, C. A., Cumano, A., Muller, W., Di Santo, J. P. & Vieira, P. (2004) Pre-B cell receptor expression is necessary for thymic stromal lymphopoietin responsiveness in the bone marrow but not in the liver environment. *Proc Natl Acad Sci U S A 101, 11070-5.*

Wallberg, A.E., K.E. Neely, J.A. Gustafsson, et al. (1999) Histone acetyltransferase complexes can mediate transcriptional activation by the major glucocorticoid receptor activation domain. *Mol. Cell Biol. 19: 5952–5959.*

Wang, L. F., Lin, J. Y., Hsieh, K. H. & Lin, R. H. (1996) Epicutaneous exposure of protein antigen induces a predominant Th2-like response with high IgE production in mice. *J Immunol 156, 4077-82.*

Wang, Y.H. et al. (2006) Maintenance and polarization of human TH2 central memory T cells by thymic stromal lymphopoietin-activated dendritic cells. *Immunity 24, 827–838.*

Weidinger, S. et al. (2008) Filaggrin mutations, atopic eczema, hay fever, and asthma in children. *J Allergy Clin Immunol 121(5) 1203-1209.*

Whitmarsh AJ, Davis RJ. (1996) Transcription factor AP-1 regulation by mitogen-activated protein kinase signal transduction pathways. *J Mol Med. 74(10):589-607.*

Wittke, A., Weaver, V., Mahon, B. D., August, A. & Cantorna, M. T. (2004) Vitamin D receptor-deficient mice fail to develop experimental allergic asthma. *J Immunol 173, 3432-6.*

Xu X, Sun YL, Hoey T. (1996) Cooperative DNA binding and sequence-selective recognition conferred by the STAT amino-terminal domain. *Science. 273(5276):794-7.*

Xu, W. et al. (2007) Epithelial cells trigger frontline immunoglobulin class switching through a pathway regulated by the inhibitor SLPI. *Nat Immunol 8, 294-303.*

Yamazaki, S., T. Muta, and K. Takeshige. (2001) A novel IκB protein, IκB-α, induced by proinflammatory stimuli, negatively regulates nuclear factor-κB in the nuclei. *J. Biol. Chem. 276: 27657–27662.*

Yang IA, Savarimuthu S, Kim ST, Holloway JW, Bell SC, Fong KM. (2007) Gene environmental interaction in asthma. *Curr Opin Allergy Clin Immunol 7: 75-82.*

Yeo, C. & Whitman, M. (2001) Nodal signals to SMADs through Cripto-dependent and Cripto-independent mechanisms. *Mol. Cell 7, 949–957.*

Ying, S. et al. (2005) Thymic stromal lymphopoietin expression is increased in asthmatic airways and correlates with expression of Th2-attracting chemokines and disease severity. *J Immunol 174, 8183-90.*

Yoo, J. et al. (2005) Spontaneous atopic dermatitis in mice expressing an inducible thymic stromal lymphopoietin transgene specifically in the skin. *J Exp Med 202, 541-9.*

Yoshizawa T, Handa Y, Uematsu Y, Takeda S, Sekine K, Yoshihara Y, Kawakami T, Arioka K, Sato H, Uchiyama Y, et al. (1997) Mice lacking the vitamin D receptor exhibit impaired bone formation, uterine hypoplasia and growth retardation after weaning. *Nat Genet 16:391–396.*

Yu JI, Kang IH, Chun SW, Yun KJ, Moon HB, Chae SC. (2010) Identifying the polymorphisms in the thymic stromal lymphopoietin receptor (TSLPR) and their association with asthma. *BMB Rep. 43(7):499-505.*

Yu, V. C., Delsert. C., Andersen, B., Holloway, J. M., Devary, 0. V., Naar, **A.** M., Kim, S. Y., Boutin, J. M., Class, C. K., and Rosenfeld, M. C. (1991) RXR beta: a coregulator that

enhances binding of retinoic acid, thyroid hormone, and vitamin D receptors to their cognate response elements. *Cell 67, 1251-1266*

Zaba, L. C., Fuentes-Duculan, J., Steinman, R. M.,Krueger, J. G. & Lowes, M. A. (2007) Normal human dermis contains distinct populations of CD11c+BDCA-1+ dendritic cells and CD163+FXIIIA+ macrophages. *J. Clin. Invest. 117, 2517–2525.*

Zaph, C. et al. (2007) Epithelial-cell-intrinsic IKK-β expression regulates intestinal immune homeostasis. *Nature 446, 552–556.*

Zeitz U, Weber K, Soegiarto DW, Wolf E, Balling R, and Erben RG (2003) Impaired insulin secretory capacity in mice lacking a functional vitamin D receptor. *FASEB J 17:509–511.*

Zhang Y, Leaves NI, Anderson GG, Ponting CP, Broxholme J, Holt R, et al. (2003) Positional cloning of a quantitative trait locus on chromosome 13q14 that influences immunoglobulin E levels and asthma. *Nat Genet 34:181-6.*

Zhang, Z. et al. (2009) Thymic stromal lymphopoietin overproduced by keratinocytes in mouse skin aggravates experimental asthma. *Proc. Natl. Acad. Sci. USA 106, 1536–1541.*

Zhang, Z., S. Jones, J.S. Hagood, et al. (1997) STAT3 acts as a co-activator of glucocorticoid receptor signaling. *J. Biol. Chem. 272: 30607–30610.*

Zheng T, Oh MH, Oh SY, Schroeder JT, Glick AB, Zhu Z. (2009) Transgenic expression of interleukin-13 in the skin induces a pruritic dermatitis and skin remodeling. *J Invest Dermatol. 129(3):742-51.*

Zhou, B. et al. (2005) Thymic stromal lymphopoietin as a key initiator of allergic airway inflammation in mice. *Nat Immunol 6, 1047-53.*

Ziegler, S. F. & Liu, Y. J. (2006) Thymic stromal lymphopoietin in normal and pathogenic T cell development and function. *Nat Immunol 7, 709-14.*

Ziegler SF & Artis D. **(**2010) Sensing the outside world: TSLP regulates barrier immunity. *Nat. Immunol. 11(4):289-93.*

OBJECTIVE

Earlier studies done in our laboratory have revealed crucial insight into the possible role of nuclear receptors (NRs) in regulating the expression of TSLP in mice. Indeed, selective ablation of RXRα and RXRβ in epidermal keratinocytes of mice ($RXR\alpha\beta^{ep-/-}$ mutant) led to an increased expression of TSLP in the keratinocytes. Further studies involving deletion of the ligand dependent activation function (AF-2) domain in RXRα and RXRβ mutants suggested that the induction of TSLP is not due to the loss of transactivation, but due to the relief of an NR mediated repression. As RXRs heterodimerize with other NRs for binding to cognate response elements on the DNA, it appeared that there could be NR partners involved in this process of repression, and that their agonistic ligands could possibly activate TSLP transcription. Analysis of various NR ligands for their ability to induce TSLP expression revealed that active vitamin D3 (VD3, agonist for VDR) and all-trans-retinoic acid (RA, agonist for RARs) were able to induce the expression of TSLP in mouse epidermal keratinocytes. Taken together, these results suggested that RXRα, RXRβ, VDR and RAR may be differentially regulating the expression of TSLP depending on the stimulus.

My thesis research was aimed at further exploring the above observations and elucidating the mechanisms that regulate TSLP expression *in vivo*.

My thesis work was focussed on three broad objectives:

1. To understand the mechanism by which NRs regulate the expression of TSLP
2. To identify other additional transcription factors that may regulate TSLP expression
3. To investigate whether glucocorticoids, one of the most effective therapeutics used for the treatment of atopic diseases, modulate the expression of TSLP.

The results of the above studies are described and discussed in the following sections:

(I) Novel widespread response elements mediates direct transrepression by agonist liganded glucocorticoid receptor. *(Manuscript submitted)*

(II) Functional dissection of the Thymic Stromal Lymphopoietin (TSLP) promoter. *(Manuscript in preparation)*

(III) Induction of Thymic Stromal Lymphopoietin Expression in Keratinocytes Is Necessary for generating an Atopic Dermatitis upon Application of the Active Vitamin D3 Analogue MC903 on Mouse Skin. *(Published)*

RESULTS AND DISCUSSSION

RESULT I

Novel widespread response elements mediates direct transrepression by agonist-liganded glucocorticoid receptor

(Manuscript submitted)

Novel widespread response elements mediate direct transrepression by agonist-liganded glucocorticoid receptor

Milan Surjit, Krishna Priya Ganti[1], Atish Mukherji[1], Tao Ye, Guoqiang Hua, Daniel Metzger, Mei Li, and Pierre Chambon*.

Institut de Génétique et de Biologie Moléculaire et Cellulaire (CNRS UMR7104, Inserm U964, Université de Strasbourg, Collège de France), Illkirch, 67404, France.

***Correspondence:** chambon@igbmc.fr (P.C.)

[1] These authors contributed equally to this work

Summary

The GR nuclear receptor (NR) is known to directly transactivate glucocorticoid (GC)-induced transcription through binding to simple (+)GRE DNA binding sequences (DBS). GC-induced transcriptional transrepression through GR binding to more complex “negative” GREs (nGREs) has been documented in few instances. Instead, repression by GCs has been essentially ascribed to “tethered” indirect transrepression. We report the discovery of a mechanism of GC-induced direct transrepression through which members of a novel large family of GR DBS (IR nGREs), unrelated to (+)GRE, act as conformational effectors of bound agonist-liganded GR to generate cis-acting GR-SMRT/NCoR repressing complexes. Conserved IR nGREs are present in >1000 mouse/human orthologue genes, which are GC-repressible *in vivo*. Thus, our study introduces a new regulatory paradigm for NR action through which variations in a single ligand can coordinately turn on or off two sets of genes differing in their response element DBS, a possibility that particularly suits GR signaling, as GCs are secreted by adrenals in a circadian and stress-related fashion.

Highlights

Introduction

Glucocorticoids (GCs) are peripheral effectors of circadian and stress-related homeostatic systems fundamental for survival throughout the life span of vertebrates (Chrousos, 2009; Nader et al., 2010). They are widely used to combat inflammatory and allergic disorders and their therapeutic effects have been mainly ascribed to their capacity to suppress the production of proinflammatory cytokines (Rhen and Cidlowski 2005). GCs act by diffusing through the cell membrane and binding to the glucocorticoid receptor (GR), that belongs to the nuclear receptor (NR) superfamily. In absence

of GCs, GR is maintained in the cytoplasm by molecular chaperones. Binding of GCs generates a conformational switch in the GR ligand binding domain (LBD) which affects GR interactions with chaperones and facilitates nuclear translocation (Pratt et al., 2006, Ricketson et al., 2007). Once in the nucleus, GR binds to glucocorticoid response elements (GREs) and regulates transcription of target genes. Classical "simple" GREs belong to a family of imperfect palindromes consisting of two inverted hexameric half-site motifs separated by three base pairs (bp), which display striking variability with only five invariant positions across the 15 bp recognition sequence (Meijsing et al., 2009). Such "simple" GREs [(+)GRE] confer transcriptional transactivation to agonist-liganded GR through association with co-activators, of which SRC1, TIF2/SRC2 and SRC3 are critically important (Lonard and O'Malley, 2007). "Composite" GREs consist of DNA binding sites (DBS) for GR which, in association with binding sites for other transcription factors, can act synergistically to mediate transactivation or transrepression of transcription. Only in a few of cases, binding of GR to rather wide promoter regions has been implicated in GC-induced transrepression, and no simple consensus sequence for "repressing" negative GREs (nGREs) has emerged (Dostert and Heinzel, 2004 and Refs therein). Remarkably, "tethering" GREs do not contain DBS for GR per se, but instead contain binding sites for other DNA-bound regulators, such as NF-κB and AP1, that recruits GR (Karin, 1998; Kassel and Herrlich, 1997; and Refs therein). In contrast with (+)GREs, "tethering" GREs are commonly associated with "indirect" transrepression of transcription.

Atopic dermatitis (AD) is an inflammatory skin disease that exhibits a high prevalence (Bieber, 2008). We recently developed mouse models which closely mimic human AD (Li et al., 2005, 2006 and 2009), and revealed that induction of the Thymic Stromal Lymphopoietin (TSLP) cytokine in epidermal keratinocytes is necessary and sufficient to trigger a human AD-like syndrome. As topical GCs are important tools for AD treatment, we wondered whether their therapeutic effect could

result from repression of TSLP expression. We report here that GCs transcriptionally repress TSLP expression in AD mouse models, and demonstrate that this GC-induced transrepression is mediated through the direct binding of GR to a "simple" nGRE belonging to a family of evolutionary-conserved cis-acting negative response element (IR nGRE) found in numerous genes, the expression of which is repressed by GCs.

Results

A) Glucocorticoid-induced GR-mediated transcriptional repression of TSLP expression.

The GC agonist, fluocinolone acetamide (FA), was applied for 6 hours to ears of mice concomitantly treated with the "low-calcemic" Vitamin D3 (VitD3) analog MC903 (Calcipotriol; hereafter called MC) to trigger TSLP expression (Li et al., 2006). In wild type (WT) mice, FA application resulted in ~50% inhibition of basal TSLP RNA level, which could be relieved by co-application of the GC antagonist RU486 (mifepristone, hereafter named RU), while MC-induced increase of TSLP RNA, which was fully blocked by FA, was also restored by RU co-treatment (Figure 1A). Similarly, the retinoic acid (RA)-induced increase of TSLP transcripts (Li et al., 2006) was efficiently blocked by FA and restored by RU (Figure S1A). As expected, the expression of the GC-inducible GPX3 (glutathione peroxidase) gene which harbours a (+)GRE (Tuckermann et al., 1999) was enhanced by FA (Figure 1A), and inhibited by RU co-treatment. In contrast, FA or RU had no effect on the MC-dependent expression of the CYP24A1 gene (a VitD3 target) (Figure 1A).To further investigate whether inhibition of TSLP synthesis by FA was dependent on its induction by MC or RA, FA was applied to ears of RXRαβ$^{ep-/-}$ or VDR/RARαγ$^{ep-/-}$ mice (selectively lacking in epidermal keratinocytes both RXRα and β, or VDR and

both RARα and RARγ, respectively) which express high levels of TSLP in epidermal keratinocytes (Li et al., 2005, and our unpublished data). In both cases a 3-day FA treatment of their ears reduced TSLP RNA levels by ~70% (Figure 1B, left panel; and data not shown).

The involvement of GR in FA-induced inhibition of MC-induced TSLP expression in keratinocytes was demonstrated using adult conditional mutant mice in which GR was selectively ablated in keratinocytes ($GR^{ep-/-}$ mice). Although the basal TSLP level was similar in vehicle-treated WT and $GR^{ep-/-}$ mice, topical treatments with MC and FA had dramatically different effects in WT and $GR^{ep-/-}$ mice, as FA blocked MC-induced increase of TSLP expression in WT, but not in $GR^{ep-/-}$ mice (Figure 1B, right panel). In addition, MC treatment was more efficient in $GR^{ep-/-}$ than in WT mice, indicating that endogenous GCs may partially inhibit MC-induced expression of TSLP in WT epidermis. The expression of TSLP was similarly repressed by FA and restored by RU in mouse intestinal epithelium (Figure S1B) and in human lung epithelial cells A549 (Figure S1C), whereas expression of the (+)GRE-containing mouse GPX3 and human GILZ (GC-Induced Leucine Zipper, Wang et al., 2004) GC-induced genes was enhanced by FA and RU inhibited upon further addition of RU.

Nuclear run-on assays demonstrated that GR-mediated FA inhibition of TSLP expression was transcriptional. Using dorsal epidermis from WT mice, no *in vitro* [32P]-labelled run-on TSLP transcripts could be revealed upon topical treatment (6 hours) with vehicle, whereas they were detected upon MC topical treatment (Figure 1C). In contrast, these transcripts were not detected upon MC and FA co-treatment, whereas addition of RU to MC and FA co-treatment restored the nuclear run-on transcription signal (Figure 1C).

B) A putative negative GRE is located in the TSLP promoter region.

As neither NF-κB nor AP1 are involved in TSLP expression induced by MC903 in mouse epidermis (our unpublished data), its repression was unlikely to be mediated by a "tethering" GRE. A bioinformatics analysis of 20 kilobases of DNA sequences located upstream and downstream from the mouse and human TSLP translation startsite (referred as position +1) did not reveal any classical (+)GRE or known "composite" activating or repressing GRE, but unveiled the presence of a palindromic sequence consisting of two inverted repeated (IR) motifs separated by one bp (called hereafter IR1 nGRE), in the upstream promoter region of both mouse (m) and human (h) TSLP genes (Figure 1E). Using a recombinant human GR protein in electrophoretic mobility shift assays (EMSA) and supershift assays with GR antibody, we showed that this putative mTSLP IR1 nGRE and its human counterpart, as well as the TAT (+)GRE (Meijsing et al., 2009), all bound similarly to the GR protein (Figure 1D, left panel). These bindings were specific, as they required the integrity of the consensus (+)GRE and of the mTSLP IR1 nGRE, as shown by the lack of GR binding to a mutant (+)GRE and to three mutants (Mut1, 2, and 3) of the putative mTSLP IR1 nGRE (Figures 1E and 1D, middle panel). Importantly, all complexes formed between the recombinant GR protein and either the putative IR1 nGREs or the (+)GRE similarly migrated. As GR binds (+)GREs as a dimer (Wrange et al., 1989), these similar migrations indicate that two GR monomers may bind these putative nGREs. Finally, competition bindings between [32P]-labelled mTSLP IR1 nGRE probe and excess cold (+)GRE probe, and between [32P]-labelled (+)GRE and excess cold mTSLP IR1 nGRE, indicated that GR has a higher affinity for (+)GRE than for the putative IR1 nGRE (Figure 2D, right panel).

C) Binding of GC agonist-liganded GR to the putative TSLP IR1 nGRE enables the formation of a repressing complex.

The GC-induced binding of GR to the putative TSLP IR1 nGRE, the generation of a repressing complex, and its effect on the organization of the TSLP promoter regions, were investigated *in vivo* by chromatin immunoprecipitation (ChIP) assays with WT dorsal epidermis and intestinal epithelium, as well as *in vitro* with cultured A549 human lung epithelial cells. Four regions of the TSLP promoter were analyzed: the proximal promoter (PP) region, the region that contains the IR1 nGRE, and the two regions that contain the DR3d VitD3 response element (VDRE) and the DR2b Retinoic Acid response element(RARE) (our unpublished data) (see Figures 1F, and S1D). ChIP assays of dorsal epidermis with a GR antibody revealed a weak binding of GR, as well as SMRT and NCoR corepressors to the nGRE region (Figure 1G). These bindings were strongly increased upon a 6hr topical FA treatment. Importantly, the concomitant disappearance of both GR and SMRT/NCoR bindings to the nGRE region in $GR^{ep-/-}$ mutant mice (Figure 1G), indicated that corepressor bindings were associated with that of GR, which was confirmed by coimmunoprecipitation of GR and corepressors, when shorter segments of the nGRE region were explored (Figure 1H).

As a control aimed at showing that, in the same cells, FA treatment was effective at inducing GR and NR coactivator recruitment to (+)GREs, aliquots of ChIP DNA were used to show that GR, as well as SRC2 and SRC3, were recruited to the (+)GRE region of the GPX3 gene, which is located 1.65 kb from the transcription startisite (Figure 1I). Interestingly, Pol II was also associated with this FA-induced activating complex, the formation of which, as well as the binding of GR to (+)GRE, was antagonized by RU (Figure 1I). Importantly, on its own, a topical treatment with RU did not allow the binding of GR to the GPX3 (+)GRE (Figure 1I).

As both SMRT and NCoR are known to recruit histone deacetylase (HDACs) to repressing complexes, we looked for their recruitment to mTSLP nGRE. As for GR and corepressors, HDAC2 and HDAC3 were weakly bound to the nGRE in vehicle-treated epidermis, and FA strongly enhanced this

recruitment (Figure 1J), thus further supporting the conclusion that GC-induced binding of GR to TSLP IR1 nGRE results in the generation of a repressing complex. It is noteworthy that a topical treatment with RU precluded FA-induced generation of this repressing complex on nGRE, whereas application of MC903 had no effect (Figures 1G and 1J). Similarly, application of retinoic acid (RA) had no effect on FA-induced generation of a repressing complex on nGRE (Figure S1E, upper panels).

To confirm whether a similar mechanism holds true in another setting, we used mouse intestinal epithelium, which revealed, upon a FA intraperitoneal treatment, a strong binding of GR together with SMRT and NCoR corepressors to the IR1 nGRE region. Addition of RU also precluded the generation of this FA-induced repressing complex, whereas VitD3 addition had no effect (Figure S1F, upper panel). Similarly, addition of FA to A549 human cells resulted in a stronger binding of GR together with SMRT and NCoR to the nGRE region, which was suppressed in the presence of RU (Figure S1G). Note that in the same A549 cells, FA addition induced binding of an activating complex to the GILZ gene (+)GRE (Figure S1H).

D) Generation of a repressing complex on the IR1 nGRE precludes the formation of an activating complex on TSLP VDRE, RARE, and proximal promoter region (PP).

In the absence of an agonist ligand, a repressing complex containing VDR and NR corepressor SMRT was associated in epidermal keratinocytes with TSLP DR3d VDRE (Figure 1G), whereas it was replaced by a VDR-SRC2/SRC3-Pol II activating complex upon MC topical treatment (Figure 1G, and our unpublished results). As a FA topical treatment resulted in inhibition of MC-induced TSLP transcription (Figure 1A), we investigated the effect of binding the FA-induced repressing complex to IR1 nGRE on generation of the MC-induced activating complex on DR3d VDRE. Upon MC903 and FA

co-treatment, VDR binding to VDRE was not inhibited, whereas those of SRC2, SRC3 and Pol II were drastically reduced, and a weak association of SMRT co-repressor could be noticed (Figure 1G). No association of GR to DR3d VDRE was detected, but these latter changes clearly resulted from binding of FA to GR, as RU co-treatment (MC+FA+RU) restored the activation binding pattern observed upon treatment with MC alone (Figure 1G). No GR binding to the proximal promoter region could be detected upon FA treatment. However, this FA treatment precluded VDR, SRC2, SRC3 and Pol II bindings observed upon MC treatment, and a RU co-treatment (MC+FA+RU) reversed the effect of FA, indicating the involvement of FA-liganded GR in preventing the association of VDR, SRC2/SRC3 and Pol II with the PP region (Figure 1G, lower panels). Similarly, the generation of a repressing complex on IR1 nGRE precluded the formation of an activating complex on DR2b RARE and on the proximal promoter (Figure S1E). Note that, in contrast to the DR3d complex, the DR2b RARE complex contains SRC2 only.

In keeping with the above data, in intestinal epithelium, the generation of a repressing complex on TSLP IR1 nGRE also precluded formation of a VitD3-induced activating complex on DR3d VDRE and the proximal promoter region (PP) (see Figure S1F, middle panels).

E) GC-induced formation of a repressing complex on IR1 nGRE precludes interaction between VDRE and the PP regions.

That, in presence of MC903, the same activating complexes (VDR, SRC2/SRC3 and Pol II) were associated with DR3d VDRE and PP regions indicated that these two regions could be in close apposition, in keeping with our previous Chromosome Conformation Capture (3C) assays showing association of these two regions through chromatin looping (our unpublished data, and Figure 1K).

We therefore performed 3C assays on epidermal chromatin of mice topically treated with vehicle, FA, MC, MC+FA, RU and MC+FA+RU. Cross-linked chromatin was digested with NLA III restriction enzyme to separate DR3d, nGRE and PP regions (see Figure 1F), which were then ligated to reveal possible interactions between PP region and DR3d VDRE or nGRE regions, respectively (see Figure 1K). No interaction between nGRE and PP region could be detected upon FA or RU treatment, whereas an interaction was observed upon MC treatment between DR3d VDRE and PP regions, which was precluded upon FA co-treatment (MC+FA), and restored upon RU addition (MC+FA+RU) (Figure 1K). Interactions between DR3d VDRE and PP regions were similarly revealed upon digestion with Alu I restriction enzyme (see Figures S1 I and J).

F) The activity of the TSLP nGRE which functions on its own is affected by changes in spacing and/or sequence of its inverted repeated motifs.

To investigate whether, in addition to nGRE, other DNA elements may be required to generate a repressing activity, we inserted the TSLP IR1 nGRE upstream of an enhancerless SV40 promoter located 5' to the luciferase coding sequence of pGL3 vector (Figure 2A). A VDRE separated from the IR1 nGRE by a 314bp-long DNA segment devoid of any known transregulator binding site (not shown) was inserted into this vector to generate a luciferase-expressing reporter plasmid. This plasmid was transfected into A549 cells, followed by addition of active vitamin D3 and /or FA. FA addition did not affect luciferase expression in absence of nGRE, whereas its presence resulted in decreased luciferase expression (which could be prevented by concomitant RU addition -not shown-) of both basal and VDRE-mediated VitD3-induced transcription. As expected, FA-induced increase in luciferase expression was observed when IR1 nGRE was replaced by a (+)GRE (Figures 2A and B). Thus, on its own, TSLP IR1 nGRE is sufficient to mediate a FA-inducible repressing activity, which

resulted from the generation of a repressing complex containing the SMRT corepressor and GR, as shown by ChIP assay (Figures 2C). Importantly replacing, in the luciferase plasmid, IR1 nGRE by a mutant to which the recombinant GR does not bind (IR1 nGRE mut1, see Figures 1D and E) resulted in no GR binding (Figure 2D) and no FA-inducible repressing activity (Figure 2E), thus supporting the conclusion that GR bind directly to TSLP nGRE in cultured cells. Note that, in keeping with our above data *in vivo*, the addition of RU to FA prevented the formation of the repressing complex (Figure 2C), and also that RU on its own was unable to induce GR binding to TSLP IR1 nGRE inserted in the pGL3 vector (Figures 2C and D).

We next investigated whether the 1 base spacing between the inverted repeated motifs of TSLP IR1 nGRE was critical for its repressing function. pGL3-based luciferase plasmids containing the VDRE and TSLP nGRE motifs spaced by 0 to 5 bases (IR0 to IR5 nGREs) were constructed and transfected into A549 cells (Figures 2D and E, and data not shown). ChIP assays showed that, upon FA addition, GR similarly bound IR1 and IR2 nGREs, whereas its binding was less efficient on IR0 nGRE, and not detectable on IR3, IR4 and IR5 nGREs (Figure 2D). Accordingly, upon FA addition, the decrease in basal and VitD3-induced luciferase activity was stronger for IR1 and IR2 than for IR0 nGRE, whereas no significant change in luciferase activity could be detected for IR3, IR4 and IR5 nGREs (Figure 2E, and data not shown).

pGL3-based luciferase plasmids containing VDRE and TSLP IR1 nGREs (Figure 2A), in which individual bases had been systematically changed one by one, were then used to study whether non-canonical IR1 nGREs could function as efficient nGREs (Figure 2F). With one exception, at least a one base pair change was “tolerable” at any position of the TSLP IR1 nGRE and did not impair its activity *in vitro*, suggesting that GR bound to “degenerate” IR1 elements might also mediate GC-induced transrepression *in vivo* (see below). A similar analysis carried out with luciferase plasmids containing

IR2 nGREs showed that at least a one base pair change was “tolerable” at any position of IR2 nGRE (Figure S2).

G) Mouse genes that contain IR0, IR1 and IR2 nGREs conserved in their human orthologues are repressed upon GC agonist treatment in vivo.

Bioinformatics analyses of mouse and human genomes revealed the presence of thousands of genes containing IR elements made up of inverted repeated motifs identical to those of TSLP (CTCC and GGAGA) with either no (IR0), 1 (IR1) or 2 (IR2) base pair spacers (Table 1A). A comparison of mouse and human orthologues indicated that a number of such IR elements were conserved (51 IR0, 379 IR1 and, 566 IR2; Table 1A and Table S1). Within each orthologue gene family containing either IR0, IR1 or IR2 nGREs, we randomly chose 15 mouse genes (Table 1B) to determine whether they were expressed in either epidermis or/and intestinal epithelium, and to investigate whether their expression was inhibited by GCs (Dexamethasone, Dex), whether this inhibition could be relieved by RU486 co-administration, and also if it could be correlated to GR and corepressor binding to their putative IR nGRE. Out of the 15 “IR1” genes, 10 were expressed in epidermis and 12 in intestine, 7 being expressed in both epidermis and intestinal epithelium. Among these 7 genes, 3 genes were “repressed” in both tissues, 2 were “repressed” in intestine only, and 2 were not “repressed” in either tissue. Moreover, 3 genes were selectively expressed and “repressed” in epidermis, 3 other genes selectively expressed and “repressed” in intestine epithelium, while two genes expressed in intestine only were not “repressed” (Figures 3A and B, and Table 1B).

For a number of the above “IR1” genes, we tested the repressing activity of their putative IR1 nGREs *in vitro* using the luciferase plasmid assay (Figures 2 and 3C). In all tested cases, and irrespective of the tissue pattern of GC-induced repression, these putative IR1 nGREs “repressed” luciferase

activity, indicating that all of these IR1 nGREs elements are *bona fide* IR1 nGREs (Figure 3C; see BCL2L1 and NKRF genes which are not "repressed" in either tissue, Figures 3A and B). Importantly, upon GC treatment *in vivo,* there was a tight correlation between repression of a given gene in a given tissue (and its relief by RU486 co-administration), and GR and corepressor association with the IR1 nGRE of that gene in that tissue (compare ChIP assays in Figures 3D and E with Figures 3A and B, respectively). In contrast there was no GR and corepressor association with the IR1 element of BCL2L1 and NKRF genes which are not "repressed" in either tissue (ChIP assays in Figure S3A). Taken together, these data indicate that, not only could the tissue-specific expression of genes which potentially can be negatively controlled by GCs subjected to epigenetic control (e.g. BCL2L1 and NKRF), but also that their GC-repression itself could also be epigenetically controlled, which suggests that additional mechanisms operate in the negative control of gene expression mediated by IR nGREs (compare USF1 and JunD in Figure 3A, B, C and D). Along the same lines, note that, depending on the gene and the time of exposure of the animal to FA or Dex (6 and 18 hours), the corepressor components of the repressing complex may change (see Figures 3D and E).

Out of the chosen 15 "IR0" genes (Figures S3 B and C, and Table 1B), 12 were expressed in epidermis and 15 in intestine, 12 being expressed in both tissues. Among these 12 genes, 2 were "repressed" in both tissues, one was "repressed" in intestinal epithelium, 2 were "repressed" in epidermis, and 7 were not "repressed". With respect to the chosen 15 "IR2" genes (Figures S3 F and G, and Table 1B), 7 were expressed in epidermis and 13 in intestinal epithelium, 5 being expressed in both tissues. One gene was "repressed" in epidermis, and 6 others were "repressed" in intestine. Like for "IR1" genes, we tested the GC-induced repressing potential of putative IR nGREs of some of the selected "IR0" and "IR2" genes using the luciferase assay, and found (Figures S3 D and H) that they exhibited a repressing activity, irrespective of their activity *in vivo*. Importantly, upon mouse Dex treatment, a decrease in gene expression in a given tissue always correlated with GR and corepressor association

with the IR0 or IR2 element in that tissue (see ChIP assays in Figures S3 E and I). Note also that in all cases the GC-induced repression was relieved by co-administration of RU486. Taken together, we conclude from these results that, as expected from our *in vitro* luciferase assays, not only IR1, but also IR0 and IR2 nGREs can efficiently mediate the cis-acting GC agonist-induced repressing activity of the GR, *in vivo*.

H) IR nGREs of mouse and human orthologues may differ by a "tolerable" one base pair mutation.

As many one base pair changes within IR1 and IR2 nGREs had little effect on their activity *in vitro* (see above), we wondered whether such changes would also be "tolerable" *in vivo*. As Keratin 5 (K5), which is known to be down-regulated by GCs (see Ramot et al., 2009, and also Figure 4B which shows that Dex treatment-induced decrease in epidermal K5 transcript levels can be prevented by RU486 co-administration), was not present in the list of human/mouse orthologues that contain a canonical nGRE (Table S1), we looked whether this absence could reflect the presence of a canonical IR1 nGRE in human K5, while a "tolerable" change would exist in its mouse orthologue, or vice-versa. We found one canonical IR1 nGRE in human K5 gene and 3 putative nGREs (mK5 IR1 nGRE 1, 2 and 3) in its mouse orthologue, each of them exhibiting one "tolerable" base pair change *in vitro* (Figure 4A). ChIP assays revealed that only one of them (mK5 IR1 nGR3) allowed formation of a GR-SMRT repressing complex in epidermis of Dex-treated mice (Figure 4C), thus suggesting that some, but not all *in vitro* "tolerable" IR1 nGRE variants could be functional in a given tissue.

Similarly, we looked at the insulin (ins) and insulin receptor (insr) genes, as expression of both of them has been reported to be down-regulated by GCs (Delaunay et al., 1997, Caro and Amatruda, 1982; see also Figure 4B, which shows that these GC-induced down-regulations - in pancreas for insulin, and in liver for insulin receptor - can be prevented by co-treatment with the GC antagonist

RU486). A canonical IR1 nGRE was found in the human insulin receptor gene (hinsr IR1 nGRE), and two IR1 nGREs, each bearing one "tolerable" change, were present in its mouse counterpart (Figure 4A). ChIP assays of liver extracts revealed that upon Dex treatment, functional GR-SMRT/NCoR repressing complexes were assembled on both mouse insulin receptor IR1 nGRE variants (minsr IR1 nGRE1 and 2 in Figure 4C). Remarkably, in addition to a canonical IR2 nGRE present in both human and mouse insulin genes, a "tolerable" IR1 nGRE variant was present in the mouse insulin gene, whereas a canonical IR1 nGRE was present in the human insulin gene (Figure 4A). Interestingly, *in vitro* studies suggested 20 years ago that this latter human element could act as a negative GRE (Boam et al., 1990; Goodman et al, 1996). Upon Dex treatment, repressing complexes were bound, in mouse pancreas, to both the IR1 nGRE variant and the IR2 nGRE of the insulin gene. However, in the absence of Dex treatment, this complex could be detected (albeit fainter) on the IR1 nGRE variant, but not on the IR2 nGRE (Figure 4C), suggesting that the affinity of the latter for the liganded GR could be lower.

We also looked at the Reverbα gene, as its expression has been found to be down-regulated by GCs (Duez and Staels, 2008, and Refs therein) . A canonical IR1 nGRE was found in the mouse, but not in the human gene, which instead contains 3 IR1 nGREs each bearing one "tolerable" variant (Figure 4A). Note in this respect that, in the mouse, this gene also contains an IR1 nGRE variant (mReverbα IR1 nGRE2 in Figure 4A), that is identical to one of the human nGREs variant (hReverbα IR1 nGRE2 in Figure 4A) and appears to be as functional as the mouse canonical IR1 nGRE1, as judged from ChIP assays of liver extracts (Figure 4C).

I) Failure of "dissociated GCs" to prevent systemic undesirable side effects of GC treatment could be at least in part due to IR nGREs-mediated transrepression

Long-term clinical use of GCs is limited by debilitating side effects (see below), which have been thought to be due to (+)GRE-mediated gene transactivation, whereas GC beneficial anti-inflammatory effects were essentially ascribed to "tethered" transrepression mediated through DNA-bound transcription factors, such as NF-κB and AP1 (Karin, 1998; Kassel and Herrlich, 2007). This possibility led to a search for so-called "dissociated" GR ligands which would preferentially induce "tethered" transrepression, but only reduced or no transactivation. Such a ligand, RU24858, was initially identified and shown to exhibit the expected dissociated profile *in vitro* (Vayssière et al., 1997). However, upon RU24858 administration to whole animals, pathophysiological studies failed to confirm this dissociation (Belvisi et al., 2001). In the light of our present study, we posited that GC-induced transcriptional repression of IR nGRE-containing genes could be instrumental in generating at least some of the undesirable side effects induced by GC treatment.

To investigate whether the expression of IR nGRE-containing genes could be repressed by RU24858, we examined the activities exhibited *in vitro* by RU24858 in IL-1β-"activated" A549 cells transfected with pGL4- and pGL3-based reporter plasmids for (i) "tethered" transrepression (Figure 5A; NF-κBluc and AP1luc plasmids), (ii) (+)GRE-mediated transactivation [Figure 2A; (+)GRE pGL3 luciferase plasmid], and (iii) IR0, IR1 or IR2 nGRE-mediated transrepression (VDRE/IR0, IR1 or IR2 nGRE pGL3 luciferase plasmids, see Figures 2A and 2E). As expected from its published "dissociated" profile *in vitro,* RU24858 was as efficient as Dex at repressing IL-1β-induced activation of transcription by NF-κB (Figure 5B, left panel) and AP1 (Figure 5B, right panel). RU24858 was also as efficient as Dex at inducing recruitment of a repressing complex tethered to NF-κB bound to its cognate elements in the NF-κBluc plasmid (Figure 5C). Most interestingly, RU24858 was again as efficient as Dex at inducing repression mediated by IR0, IR1 and IR2 nGREs in VDRE/IR0, IR1 and IR2 nGRE pGL3 luciferase plasmids (Figure 5D), as well as at recruiting GR and SMRT to form repressing complexes on nGRE-containing regions (see ChIP assays in Figure 5E). In contrast, as expected from the study of

Vayssière et al. (1997), RU24858 was much less efficient than Dex at inducing transactivation of the (+)GRE pGL3 luciferase plasmid (Figure 5D).

These *in vitro* results prompted us to investigate the "activity profile" of RU24858 *in vivo*. Unlike Dex, a topical treatment of dorsal skin with RU24858 did not activate GC-dependent expression of the (+)GRE-containing gene GPX3 in epidermis (Figure 5F), and did not induce assembly of an activating complex on its (+)GRE (ChIP assays in Figure 5H). In contrast, RU24858 was as efficient as Dex at down-regulating, through NF-κB-mediated "tethered" transrepression, genes of which the skin expression was enhanced by topical TPA treatment (Figure 5G, and data not shown). Most interestingly, and as *in vitro*, RU24858 was also as efficient as Dex at inducing transrepression of IR0 (CCND1), IR1 (TSLP, CYP26A1, K14, PRKCB) and IR2 (DPAGT1) nGRE-containing genes, through recruitment of GR-SMRT/NCoR repressing complexes on nGRE regions (Figures 5F and H).

Taken together the above data clearly indicate that in the animal, as well as in cell-based assays *in vitro*, the so-called "dissociated" GR receptor ligand RU24858 could not, or only poorly induce transactivation mediated by (+)GREs, whereas it was as efficient as Dex at inducing "tethered" transrepression activity. However, this RU24858 anti-inflammatory activity was not dissociated from its IR nGRE-mediated transrepression activity, thus supporting our initial assumption that GC-induced repression of IR nGRE-containing genes is the source of at least some of the undesirable side-effects generated by GC treatment.

J) IR nGRE-containing genes exert physiological homeostatic functions related to debilitating and anti-inflammatory effects of glucocorticoid therapy.

Long-term treatments with GCs generate numerous debilitating side effects which affect skin homeostasis, bone and cartilage development and homeostasis, glucose metabolism and insulin signaling, muscle homeostasis, HPA (hypothalamus-pituitary-adrenal) axis homeostasis, circadian rhythm, cell cycle regulation and apoptosis, immunity, as well as behavior (see Table 2A, and Refs therein). An ontology search revealed that the known or putative functions of almost 15% of IR nGRE-containing orthologue genes could possibly be implicated in physiological homeostatic processes leading to these GC side-effects upon GC therapy (Table S2). Moreover, there is evidence that repression of expression of a number of these latter genes could actually be instrumental to the generation of defects subsequent to GC administration, either because their expression is known to be decreased upon GC treatment, and/or because their decreased expression is known to generate defects related to those produced by GC-therapy (Table 2A; see also references in Table S2).

The anti-inflammatory and immune-suppressant properties of GCs represent the central target of pharmacological GC therapy. Up to now, there has been a consensus that these effects are predominantly mediated through indirect “tethered” transrepression of genes encoding regulatory components (e.g. cytokines) of the immune system. Interestingly, many of these genes, which all contain both NF-κB and AP1 binding sites, also contain IR nGREs (Table 2B and S2). It is also noteworthy that the expression of factors involved in protection from apoptosis (the anti-apoptotic proteins Bcl2 and Bcl-XL), as well as factors involved in cell cycle progression at the G1/S phase (the mitogenic proteins Cyclin D1 and Cdk4), can also be GC-transrepressed through IR nGREs (see Table 2A and Table S2).

Discussion

While investigating the molecular mechanism underlying transcriptional repression of the TSLP gene in mouse skin epidermis, we unveiled the existence of a widespread and conserved family of

"negative" glucocorticoid response elements (IR nGREs) that mediate transrepression through direct binding of agonist-liganded GR. We discuss below some structural and functional salient features of these novel nGRE family, as well as the importance of their physiological and pathophysiological involvement in glucocorticoid signaling.

A) IR nGREs act as conformational effectors of bound agonist-liganded GR to generate repressing complexes on GC target genes.

Taken together, results displayed in Figures 1 and S1 demonstrate that expression of the TSLP gene in mouse epidermal keratinocytes is transcriptionally repressed *in vivo* by agonist-liganded GR. Interestingly, this repression, is relieved by co-administration of RU486, a well-known antagonist of activation of transcription by GC agonist-liganded GR. A search for a possible GR binding site in regions surrounding the promoter of both mouse and human TSLP genes revealed a palindromic sequence with a 1 bp spacer, to which a recombinant human GR protein did bind *in vitro* with a lower efficiency than to the unrelated canonical (+)GRE sequence. Most interestingly, as shown by ChIP assays (Figures 1 and S1), not only both mouse and human GR bind *in vivo* to the region containing this palindromic element in the presence of a GC agonist, but in addition, a repressing complex is formed by association of SMRT/NCoR corepressors and HDACs with the GR. Importantly, RU486 did not allow the formation of this GC-induced repressing complex, further supporting the conclusion that this complex is instrumental *in vivo* in transrepression mediated by the GR-binding palindromic sequence. Inserting on its own this TSLP palindromic GR binding sequence (that we termed IR1 nGRE) into a reporter plasmid that was transfected in A549 cells, proved that no additional DNA element is required for generating an active repressing complex in the presence of FA, thus suggesting that the TSLP IR1 nGRE is not a composite element (see below). Importantly, the addition of RU486 to FA, prevented the formation of the repressing complex, and RU486 on its own

did not induce the binding of GR to the inserted TSLP IR1 nGRE (Figures 2A-D). What could be the mechanism underlying this repression was clearly indicated by ChIP and Chromosome Conformation Capture (3C) assays which showed that the presence of the agonist-liganded GR repressing complex prevents interaction, through chromatin-looping, between the region harboring an activating complex and the proximal promoter region (Figures 1K and S1 J). In this respect, we note that there is no evidence, from our present 3C assays, for the existence of a competitive chromatin looping between the region harboring the repressing complex and the proximal promoter region, perhaps because this looping is not stable enough.

Experiments aimed at investigating *in vitro* whether the integrity of the TSLP IR1 nGRE is important for its function revealed (i) that an IR nGRE with a 2bp spacer between the palindromic repeated motifs (IR2 nGRE) is as efficient as the TSLP IR1 nGRE, whereas an IR nGRE lacking a spacer (IR0 nGRE) is less efficient, and nGREs with a 3 (IR3 nGRE), 4 (IR4 nGRE) or 5 (IR5 nGRE) base spacer are inefficient (Figures 2C-E), and (ii) that, with one exception, at least a one base pair change is "tolerable" at any position of the repeated motifs of TSLP IR1 nGRE (Figure 2F), while in the case of IR2 nGREs, at least a one base pair change is "tolerable" at any position of the repeated motifs (Figure S2). A question of paramount importance was then, how frequent is, in vertebrates, GC-inducible gene transrepression mediated by IR nGREs. Mouse and human genome-wide analyses revealed the presence of thousands of genes containing IR0, IR1 and IR2 nGREs sequences (Table 1A), as well as that of hundreds of mouse and human orthologue genes containing conserved IR0, IR1 and IR2 nGREs (Table 1B). Importantly, in no case are these latter elements located in the near vicinity (<100bp) of a binding site for a known transregulatory factor, and many of them are also conserved in vertebrates (orangutan, elephant, horse, rabbit, dolphin, chicken, and zebra fish; data not shown). We have characterized *in vivo* a number of these "IR0", "IR1", and "IR2" genes, either expressed or non-expressed in epidermis and/or intestinal epithelium (Table 1B) for (i) inhibition of

their expression by dexamethasone and relief of this inhibition by RU486, (ii) association of their IR nGREs with GR and corepressors, and (iii) repressing activity of their IR nGREs *in vitro* using a luciferase reporter plasmid transfection assay (Figures 3 and S3). Taken together, the results of these experiments demonstrate that not only IR1, but also IR0 and IR2 nGRE-containing genes can be efficiently transrepressed by agonist-liganded GR bound to their respective nGREs together with SMRT/NCoR corepressors. It must be pointed out that, as a one base pair changes within IR1 and IR2 nGREs has little effect on their repressing activity (Figures 2F and S2), the existence of point mutations in IR nGREs of human and/or mouse orthologue genes could result in underestimating by several hundreds the actual number of IR nGRE-containing orthologue genes (see Figure 4, and Result section).

Structural studies are obviously required to unveil the detailed mechanism that underlies this agonist-liganded GR-mediated direct transrepression. The role played by an agonistic GC in this transrepression cannot be simply to ensure the translocation of the GR into the nucleus, as the GC antagonist RU486 which is known to promote such a translocation acts as an antagonist of IR nGRE-mediated transrepression. Moreover, ChIP assays *in vivo* (Figures 1 and S1) and *in vitro* (see Figure 2) show clearly that binding of a GR corepressor complex to IR nGREs requires the presence of a glucocorticoid agonist which “normally” is known to induce a GR conformational change that allows the formation of a GR coactivator complex that binds to a (+)GRE (see Figure 1I). Thus, a possible mechanism that may account for the formation of a repressing complex could be that the IR nGRE DNA binding site acts as a conformational “allosteric” effector of GR, enabling it to bind corepressors in the presence of a GC-agonist. We note in this respect that it has been recently proposed that distinct (+)GRE genomic GR binding sequences (GBS) to which the agonist-liganded GR binds to activate transcription are sequence-specific-allosteric ligands of GR, that tailors the activity of the receptor toward specific target genes (Meijsing et al., 2009). Whether the diversity of IR nGREs DNA

sequences could similarly allow such an allosteric fine-tuning of IR nGRE-mediated transrepression remains to be seen. Finally, it is tempting to speculate that 'tethered" transrepression could also be allosterically fine-tuned as single nucleotide difference in NF-κB binding sequences has been shown to act allosterically to determine cofactor specificity for NF-κB dimers (Leung et al., 2004).]

B) Importance of physiological and pathophysiological involvement of GC-inducible direct transrepression of IR nGRE-containing genes.

GCs that act as end-effectors of the HPA (hypothalamus-pituitary-adrenal) axis, are secreted by adrenal glands in a circadian and stress related manner. They are known to influence the functions of virtually all organs and tissues throughout life span, and to be essential for maintenance of their homeostasis and important biological activities such as intermediary metabolism and immune and inflammatory reactions, as well as circadian clock and stress systems (Chrousos, 2009; Nader et al., 2010). Interestingly, our ontology search (Table S2) has revealed that a number of IR nGRE-containing genes are known to be involved in such functions. Due to lack of space, we will focus here on a few examples illustrated by the present study.

Our present data (see Figure 4 and table 2A) are the first to unequivocally demonstrate that GC-induced IR nGRE-mediated transrepressions of both the insulin precursor gene (in pancreas β cells) and insulin receptor gene (in liver) are early stress-induced events. This ensures that, upon occurrence of a stress, an elevation of blood glucose level will rapidly follow the surge of GC secretion, thereby providing the increased nutrition of brain, heart and skeletal muscles, which is required for the central coordination of stress response (Chrousos, 2009). On the other hand, under conditions of chronic stress, the GC-induced IR nGRE-mediated repression of the insulin receptor gene may cause the insulin resistance that leads to diabetes. Our present data also reveal the existence of IR1 GREs in the ACTH receptor (melacortin 2 receptor, MC2R) gene (Tables 2A and S2),

as well as in the ACTH receptor accessory protein (MRAP) gene (Table 2A and Figure 4B), thereby adding, at the adrenal level, another step to the closed negative feedback loop that reset the HPA axis by regulating the synthesis of secreted GCs through GR-mediated repression of CRH and POMC gene expression in hypothalamus and pituitary, respectively (Dostert and Heinzel, 2004). Interestingly, we also found GC-induced IR nGRE-mediated repression for the Reverbα gene (Figure 4 and Table 2A), as well as for the RORα gene (Table1B; Figure S3 F to I), which both intervene in the control of the circadian timing system and are likely to play an important role in communication of the Clock and Stress systems with intermediary metabolism, which are all fundamental for survival (Duez and Staels, 2008; Le Martelot et al. 2009; Nader et al., 2010; and Refs therein).

Importantly, the expression of several of the IR nGRE-containing genes was known to be decreased upon GC therapy (Table 2A, and refs therein), but the underlying pathophysiological molecular mechanisms were unknown. Interestingly, our present data demonstrate that, upon GC therapy, the skin decreases in keratins 5 and 14, as well as those in cyclin D and cdk4, are due to GC-induced direct transrepression through IR nGREs (Table 2A, and Figure 4). Along the same lines, diabetes, one of the disease associated with chronic stress and a major debilitating side-effect of GC therapy, is known to result in an activation of the Protein kinase Cβ enzyme (PrkCb gene) that has been shown to be involved in the development of several clinical complications, such as retinopathy, kidney disorders and neuropathy (Avignon and Sultan, 2006). Interestingly, there is a functional IR1 nGRE in the Prkcb gene (Table 2A, Figure 3A to E), which is likely to reduce the occurrence of these complications by allowing transrepression of this gene under the conditions of elevated circulating glucocorticoids that prevail in chronic stress and GC therapy. Hsd11b2 is another important gene that we found to be repressed by IR1 nGRE-mediated GC-treatment in both skin and colon tissues (Figure 3A, and data not shown). The 11β-HSD2 enzyme (encoded in Hsd11β2 gene) is responsible for inactivating glucocorticoids in mineralocorticoid receptor (MR) target tissues (Reviewed in Gross

and Cidlowski, 2008). In the absence of this enzyme, GCs (corticosterone in mice) activate MR despite the absence of aldosterone, resulting in hypertension (Stewart et al., 1996). Thus, our finding that Hsd11b2 is a GC-repressed IR1 nGRE-containing gene provides a possible molecular explanation for GC therapy-induced hypertension.

Finally, It is generally believed that the anti-inflammatory therapeutic effect of GC is related to indirect "tethered" transrepression of chemokines and cytokine expression. In fact, we have found that many of the genes which contain both NF-κB and AP1 binding sites also bear IR nGREs (Table 2B). Interestingly, preliminary experiments performed with cultured cells *in vitro* and on epidermis *in vivo* have shown that repressing complexes can be concomitantly assembled on NF-κB and IR nGRE sites present in IL-6 and TSLP genes (data not shown), and therefore could possibly cooperate to achieve efficient anti-inflammatory therapy and immunosupression.

C) Towards improved anti-inflammatory "dissociated" glucocorticoid agonists.

As already mentioned, the discovery of "tethered" transrepression and the subsequent assumption that it was essentially responsible for the beneficial anti-inflammatory effects of GCs, led to differential screenings aimed at identifying "dissociated" glucocorticoids which would preferentially induce "tethered" transrepression, but little or no (+)GRE-mediated transactivation. Synthetic glucocorticoids exhibiting such a "dissociated" profile were obtained, but failed to prevent the appearance of a number of systemic debilitating side effects *in vivo* (in the mouse) (see Table 2A for references). Our present data indicate that it is likely that this failure is at least in part due to the fact that these so-called dissociated GCs have kept their IR nGRE-dependent transrepression activity. Our present study clearly paves the way to improved screenings of anti-inflammatory "dissociated" glucocorticoids. Ideally, one would like to screen for compounds that would repress gene expression

through “tethered” transrepression, but would be devoid of IR nGRE-mediated transrepression activity, as well as of (+)GRE-mediated transactivation activity. In this respect, we note that our luciferase-expressing reporter plasmids could be used for such screening assays. We note also that these assays could be useful to characterize the mode of action of some non GC-derived compounds that may exhibit some of the beneficial therapeutic activities of “dissociated” glucocorticoids, but not their detrimental side effects (De Bosscher and Haegeman, 2009).

Conclusion

That a single hormone (cortisol in human and corticosterone in rodents) bound to a single nuclear receptor, the glucocorticoid receptor, can finely and coordinately tune transcription of thousands of genes involved in vital functions, in essentially all cells throughout the life span of vertebrates, remains an amazing conundrum to be solved at the molecular level. Although significant advance has been recently made concerning how distinct (+)GRE binding site sequences of different target genes may induce subtle conformational changes in bound GR to direct its transactivation function (Meijsing et al., 2009), similar progress has not been made concerning possible mechanisms involved in GC-induced direct repression. In this respect, our present study clearly demonstrates the existence of a novel mechanism of control of gene expression by glucocorticoids, namely GC-induced transrepression through direct binding of agonist-liganded GR associated with SMRT/NCoR corepressors to an evolutionary conserved family of “simple” negative DNA binding sites (IR nGREs), which are apparently unrelated to the “simple” (+)GRE binding site family that mediates activation of transcription. Thus, our study introduces a new paradigm for GR action through which variations in the level of a single ligand can differentially turn on or off two sets of genes widely differing in their response element DNA sequences [(+)GRE and IR nGRE, respectively]. Interestingly, this possibility remarkably suits GR signaling as GC adrenal secretion varies in a circadian and stress related fashion. Indeed, increases in GC levels will concomitantly turn on transactivation of (+)GRE-

containing genes, and turn off transrepression of IR nGRE-containing genes, whereas decreases in GC levels will have the opposite effects on the two sets of genes. Whether the different cell-specific GR isoforms (Gross and Cidlovski, 2008) generate additional specificity in these controls remains to be seen, as well as the possible existence of similar mechanisms of control of gene expression by other members of the NR superfamily.

Experimental Procedures

Additional details on methods are available online in Extended Experimental Procedures.

Mice. For topical treatment on ear and dorsal skin, 1 nmole/cm2 of MC903, at-RA or TPA; 6 nmoles/cm2 of FA, Dex or RU24858; and 90 nmoles/cm2 of RU486 were used. For systemic treatment, 8 mg/kg body weight of active Vitamin D3 or Dex, and 64 mg/kg body weight of RU486 emulsified in sunflower oil were intraperitoneally injected. Breeding and maintenance of mice were performed under institutional guidelines, and all of the experimental protocols were approved by the Animal Care and Use Committee of the Institut de Génétique et de Biologie Moléculaire et Cellulaire.

Isolation of epidermis and intestinal epithelium from mouse. The inner side of dorsal skin was scraped off fat and floated over 0.8% trypsin solution (0.8% trypsin (w/v) dissolved in PBS) for 30 minutes at 37 0C. Epidermal sheets were recovered in cell culture medium (EMEM without calcium + 10% FCS), incubated at 37 0C for 15 minutes and filtered through a 70µm nylon cell strainer (BD falcon). For nuclear run-on assay, epidermal cells were pelleted (400g, 5 minutes) at 4 0C, washed twice in ice-cold PBS and used for preparation of nuclei. For ChIP and 3C assays, epidermal cells were cross-linked for 10 minutes in 1% or 2% formaldehyde, respectively. Intestinal epithelial cells were prepared as described (Flores- Langarica et al., 2005), followed by cross-linking for 10 minutes in 1% formaldehyde for ChIP assay. Details are given in Extended Experimental procedure.

ChIP, Nuclear run-on, EMSA, 3C, Real time PCR and Luciferase assay. ChIP assay (Vaisanen et al., 2005), Nuclear Run-on assay and EMSA (Carey and Smale., 2001), 3C assay (Liu et al., 2005), Real time PCR (Li et al., 2005) and Luciferase assay (Promega kit) were essentially done as reported. Details are given in Extended Experimental procedures.

Statistics and Bioinformatics analysis. Statistical analysis was done as described (Li et al., 2009). Details of bioinformatics analysis are described in Extended Experimental procedures.

Acknowledgements

This study is dedicated to the memory of Dr. Régine Losson, who untimely died early this year. She was a wonderful colleague and an outstanding scientist. We thank the staff of the animal and cell culture facilities of the IGBMC/ICS for their kind help, Dr. Hinrich Gronemeyer and Leo Pharmaceutical for kind gifts of RU24858 and MC903, respectively, Dr. S. Kato for floxed VDR mice, as well as Estelle Meyer for secretariat help. This work was supported by the CNRS, the INSERM, the Agence Nationale de la Recherche (No. ANR 07-Physio 002-01), and the Association pour la Recherche à l'IGBMC (A.R.I). M.S., A.M., and G.H. were supported by ARI post-doctoral fellowships, and K.G. by predoctoral fellowship from ARI.

References

Avignon, A., and Sultan, A. (2006). PKC-B inhibition: a new therapeutic approach for diabetic complications? Diabetes Metab. *32*, 205-213.

Bechtold, D.A., Gibbs, J.E., and Loudon, A.S. (2010). Circadian dysfunction in disease. Trends Pharmacol. Sci. *31*, 191-198.

Belvisi, M.G., Wicks, S.L., Battram, C.H., Bottoms, S.E., Redford, J.E., Woodman, P., Brown, T.J., Webber, S.E., and Foster, M.L. (2001). Therapeutic benefit of a dissociated glucocorticoid and the relevance of In Vitro separation of transrepression from transactivation activity. J. Immunol. *166*, 1975-1982.

Bieber T. (2008). Atopic dermatitis. N. Engl. J. Med. *358*, 1483-1494.

Boam, D.S., Clark, A.R., and Docherty, K. (1990). Positive and negative regulation of the human insulin gene by multiple trans-acting factors. J. Biol. Chem. *265*, 8285-8296.

Caro, J.F., and Amatruda, J.M. (1982). Glucocorticoid-induced insulin resistance. J. Clin. Invest. *69*, 866-875.

Chrousos, G.P. (2009). Stress and disorders of the stress system. Nat. Rev. Endocrinol. *5*, 374-381.

De Bosscher, K., and Haegeman, G. (2009). Minireview: latest perspectives on antiinflammatory actions of glucocorticoids. Mol. Endocrinol. *23*, 281-291.

Delaunay, F., Khan, A., Cintra, A., Davani, B., Ling, Z.C., Andersson, A., Ostenson, C.G., Gustafsson, J., Efendic, S., and Okret, S. (1997). Pancreatic beta cells are important targets for the diabetogenic effects of glucocorticoids. J. Clin. Invest. *100*, 2094-2098.

Dostert, A., and Heinzel, T. (2004). Negative glucocorticoid receptor response elements and their role in glucocorticoid action. Curr. Pharm. Des. *10*, 2807-2816.

Duez, H., and Staels, B. (2008) Rev-erb alpha gives a time cue to metabolism. FEBS Lett. *582*, 19-25.

Flores-Langarica, A., Meza-Perez, S., Calderon-Amador, J., Estrada-Garcia, T., Macpherson, G., Lebecque, S., Saeland, S., Steinman, R.M., and Flores-Romo, L. (2005). Network of dendritic cells within the muscular layer of the mouse intestine. Proc. Natl. Acad. Sci. USA *102*, 19039-19044.

Goodman, P.A., Medina-Martinez, O., and Fernandez-Mejia, C. (1996). Identification of the human insulin negative regulatory element as a negative glucocorticoid response element. Mol. Cell. Endocrinol. *120*, 139-146.

Gross, K.L., and Cidlowski J.A. Tissue-specific glucocorticoid action: a family affair. (2008). Trends Endocrinol. Metab. *19*, 331-339.

Karin, M. (1998). New Twists in Gene Regulation by Glucocorticoid Receptor: Is DNA Binding Dispensable? Cell *93*, 487-490.

Kassel, O., and Herrlich, P. (2007). Crosstalk between the glucocorticoid receptor and other transcription factors: Molecular aspects. Mol. Cell. Endocrinol. *275*, 13-29.

Kleiman, A., and Tuckermann, J.P. (2007). Glucocorticoid receptor action in beneficial and side effects of steroid therapy: Lessons from conditional knockout mice. Mol. Cell. Endocrinol. *275*, 98-108.

Le Martelot, G., Claudel, T., Gatfield, D., Schaad, O., Kornmann, B., Sasso, G.L., Moschetta, A., and Schibler, U. (2009). REV-ERBalpha participates in circadian SREBP signaling and bile acid homeostasis. PLoS Biol. *7*, e1000181.

Leung, T.H., Hoffmann, A., and Baltimore, D. (2004). One nucleotide in a kappaB site can determine cofactor specificity for NF-kappaB dimers. Cell *118*, 453-464.

Li, M., Messadeq, N., Teletin, M., Pasquali, J.L., Metzger, D., and Chambon, P. (2005). Retinoid X receptor ablation in adult mouse keratinocytes generates an atopic dermatitis triggered by thymic stromal lymphopoietin. Proc. Natl. Acad. Sci. USA *102*, 14795-14800.

Li, M., Hener, P., Zhang, Z., Kato, S., Metzger, D., and Chambon, P. (2006). Topical vitamin D3 and low-calcemic analogs induce thymic stromal lymphopoietin in mouse keratinocytes and trigger an atopic dermatitis. Proc. Natl. Acad. Sci. USA *103*, 11736-11741.

Li, M., Hener, P., Zhang, Z., Ganti, K.P., Metzger, D., and Chambon, P. (2009). Induction of thymic stromal lymphopoietin expression in keratinocytes is necessary for generating an atopic dermatitis upon application of the active vitamin D3 analogue MC903 on mouse skin. J. Invest. Dermatol. *129*, 498-502.

Lonard, D.M., and O'Malley, B.W. (2007). Nuclear receptor coregulators: judges, juries and executioners of cellular regulation. Mol. Cell *27*, 691-700.

Meijsing, S.H., Puffal, M.A., So, A.Y., Bates, D.L., Chen, L., and Yamamoto, K.R. (2009). DNA binding site sequence directs glucocorticoid receptor structure and activity. Science *324*, 407-410.

Nader, N., Chrousos, G.P., and Kino, T. (2010). Interactions of the circadian CLOCK system and the HPA axis. Trends Endocrinol. Metab. *21*, 277-286.

Pratt, W.B., Morishima, Y., Murphy, M., and Harrell, M. (2005). Chaperoning of glucocorticoid receptor. Handb. Exp. Pharmacol. *172*, 111-138.

Preitner, N., Damiola, F., Lopez-Molina, L., Zakany, J., Duboule, D., Albrecht, U., and Schibler, U. (2002). The orphan nuclear receptor REV-ERBalpha controls circadian transcription within the positive limb of the mammalian circadian oscillator. Cell *110*, 251-260.

Ramot, Y., Paus, R., Tiede, S., and Zlotogorski, A. (2009). Endocrine controls of keratin expression. Bioessays *31*, 389-399.

Rhen, T., and Cidlowski, J.A. (2005). Antiinflammatory action of glucocorticoids--new mechanisms for old drugs. N. Engl. J. Med. *353*, 1711-23.

Ricketson, D., Hostick, U., Fang, L., Yamamoto, K.R., and Darimont, B.D. (2007). A conformational switch in the ligand-binding domain regulates the dependence of the glucocorticoid receptor on Hsp90. J. Mol. Biol. *368*, 729-741.

Schake, H., Docke, W.D., and Asadullah, K. (2002). Mechanisms involved in the side effects of glucocorticoids. Pharmacol. Ther. *96*, 23-43.

Schakman, O., Gilson, H., and Thissen, J.P. (2008a). Mechanisms of glucocorticoid-induced myopathy. J. Endocrinol. *197*, 1-10.

Stewart, P.M., Krozowski, Z.S., Gupta, A., Milford, D.V., Howie, A.J., Sheppard, M.C., and Whorwood, C.B. (1996). Hypertension in the syndrome of apparent mineralocorticoid excess due to mutation of the 11 beta-hydroxysteroid dehydrogenase type 2 gene. Lancet *347*, 88-91.

Tuckermann, J.P., Reichardt, H.M., Arribas, R., Richter, K.H., Schutz, G., and Angel, P. (1999). The DNA binding-independent function of the glucocorticoid receptor mediates repression of AP-1-dependent genes in skin. J. Cell Biol. *147*, 1365-1370.

Vayssiere, B.M., Dupont, S., Choquart, A., Petit, F., Garcia, T., Marchandeau, C., Gronemeyer, H., and Resche-Rigon, M. (1997). Synthetic glucocorticoids that dissociate transactivation and AP-1 transrepression exhibit antiinflammatory activity in vivo. Mol. Endocrinol. *11*, 1245-1255.

Wang J.C., Derynck M.K., Nonaka, D.F., Khodabakhsh D.B., Haqq, C., and Yamamoto, K.R. (2004). Chromatin immunoprécipitation (ChIP) scanning identifies primary glucocorticoid receptor target genes. Proc. Natl. Acad. Sci. USA *101*, 15603-15608.

Wrange, O., Eriksson, P., and Perlmann, T. (1989). The purified activated glucocorticoid receptor is a homodimer. J. Biol. Chem. *264*, 5253-5259.

Figure Legends

Figure 1. Glucocorticoid-induced inhibition of TSLP transcription is mediated through binding of GR and corepressors to a negative GRE (nGRE).

(A) Quantitative-RT-PCR (Q-PCR) of TSLP, Cyp24A1 and GPX3 RNA from ear epidermis of WT mice topically treated for 6 hours, as indicated. Values are mean ± SEM.

(B) TSLP Q-PCR from RXRαβ$^{ep-/-}$ and WT mouse ear epidermis, FA-treated twice a day for 3 days (Left panel). TSLP Q-PCR from GR$^{ep-/-}$ and WT mouse ear epidermis, treated for 6 hours, as indicated (right panel).

(C) Nuclear run-on assays using dorsal epidermis from WT mice treated as indicated. Autoradiograms of labelled transcripts hybridized with TSLP, β actin or pSK+ vector DNA are displayed in upper panels. Lower panel is ethidium bromide (etbr) staining of DNA probes.

(D) Left panels: EMSA with recombinant human GR protein and GR antibody (ab) supershift assays using [32P] 5'-labelled oligonucleotide probes as indicated (panel E and Extended Experimental procedures). Arrow and arrowhead point to the position of shifted [32P]- GREs in absence and presence of GR ab. Right panel: Competition EMSA and GR ab supershift assays using either cold (+)GREc and [32P]- TSLP nGRE probes or cold TSLP nGREc and [32P]- (+)GRE probes, as indicated. 10X, 25X and 50X refers to 10, 25 or 50 - fold molar excess of cold oligonucleotide probe.

(E) Comparison of putative mouse (m) and human (h) TSLP nGRE sequences with that of TAT (+) GRE. Palindromes are underlined. Conserved bases in nGREs are in bold letters. N: any base. Mutant residues are in smaller font size.

(F) Representation of mTSLP promoter region. The “A” base of the translation initiation codon (ATG) was taken as position +1. A, B, C, D and E are Nla III digested DNA fragments. Numbers 1 to 6 denote Nla III sites. Boxes represent promoter elements, with their coordinates. DNA segment (region) coordinates PCR-amplified in ChIP assays are indicated.

(G) ChIP assays using dorsal skin from WT and $GR^{ep-/-}$ mice treated as indicated, showing (1) FA-induced binding of GR and corepressors to TSLP nGRE region and its reversion by RU (RU486), (2) MC-induced binding of VDR and cofactors to TSLP VDRE region and (3) binding of Pol II and cofactors to TSLP and PP region. IP antibody indicates antibodies used for immunoprecipitation. Control is rabbit IgG. 10% input indicates the signal obtained after PCR amplification of the relevant DNA region contained in 10% of chromatin used for immunoprecipitation with a given antibody.

(H) Colocalization of GR and its corepressors on TSLP region encompassing the nGRE. Topically FA-treated epidermis was processed for ChIP using antibodies and primers 1 to 7 to amplify amplicons 1 to 7, as indicated. Amplicon 5 encompasses the nGRE.

(I) ChIP assays with aliquots of samples used in panel (G) showing GR and coactivators (SRC2 and SRC3) bound to (+)GRE of GPX3 gene.

(J) Binding of histone deacetylases (HDAC) to TSLP nGRE region. ChIP assays were as in panel (G) with indicated HDAC antibodies.

(K) Chromosome conformation capture (3C) assay using WT epidermis shows that FA prevents MC-induced interaction between Nla III segments A and E containing the VDRE (DR3d) and the proximal promoter (PP), respectively. Upper, middle and lower panels reveal interaction between nGRE and PP regions, VDRE and nGRE regions and VDRE and PP regions, respectively.

See also Figure S1.

Figure 2. The TSLP nGRE is not a composite element, but its activity is affected by changes in spacing and/or sequence of its inverted repeated (IR) motifs.

(A) pGL3 luciferase reporter plasmids.

(B) TSLP nGRE is sufficient to repress basal as well as VitD3-induced expression of the luciferase gene. A549 cells were transiently transfected with pGL3 luciferase plasmids, treated with FA and VD3 (vitD3), as indicated followed by luciferase assay (mean ± SEM).

(C) ChIP assays showing GR and SMRT recruitment to the IR1 nGRE element present in transfected pGL3 IR1 nGRE luciferase plasmid following FA and RU treatments.

(D) ChIP assays to detect GR binding to IR0, IR1, IR2, IR3, IR4, IR5 nGRE and (+) GRE elements present in transfected pGL3 luciferase plasmids following FA and RU treatment.

(E) Luciferase assay showing that deleting the 1 base spacer in IR1 nGRE (IR0) or having a 2 base spacer (IR2), but not a 3 base spacer (IR3) between the IR motifs does not affect its repressing activity.

(F) Luciferase assay to show the *in vitro* functionality of various mutant IR1 nGRE elements bearing a 1 base pair change. Sequences of the canonical IR1 nGRE and its variants are listed as numbers 1 to 28 on the right panel. Circled numbers indicate untolerable mutations. Big letters indicate the sequence of canonical IR nGRE, smaller letters indicate “tolerable” base changes.

See also Figure S2.

Figure 3. Glucocorticoid-induced repression of mouse genes that contain IR1 nGREs conserved in mouse and human orthologues is relieved by RU486 co-administration.

(A) Q-PCR (mean ± SEM) for transcripts of IR1 nGRE-containing genes (see table 1B) in WT mouse epidermis topically-treated with dexamethasone (Dex) and/or RU486 (RU) for 18 hours.

(B) As under (A), but using intestinal epithelium of WT mice intraperitoneally-injected with Dex and/or RU for 18 hours.

(C) Luciferase assay to test *in vitro* functionality of IR1 nGREs conserved in mouse and human orthologues. A549 cells transfected with pGL3 luciferase plasmids (Figure. 2A) containing IR1 nGREs from various genes as indicated, were treated for 6 hours with VitD3 (VD3) and FA, as indicated.

(D) ChIP assay of mouse epidermis showing FA- and Dex- induced binding of GR and corepressors to IR1 nGRE regions of genes analyzed in panel A

(E) ChIP assay of mouse intestinal epithelial cells showing Dex- induced binding of GR and corepressors to the IR1 nGRE regions of genes analyzed in panel B.

See also Figure S3.

Figure 4. IR nGREs of mouse and human orthologues may differ by a "tolerable" one base pair mutation.

(A) Sequence and position (from the +1 transcription startsite) of nGRE motifs present in human (h) and mouse (m) genes. Bold letters in low case denote non canonical bases in IR1 and IR2 nGREs.

(B) Q-PCR of various gene transcripts, as indicated (see also Table 2A and S2), in WT mice topically-treated (epidermis) or intra-peritoneally-injected (for other tissues) with Dex and/or RU (RU486), for 18 hours (mean ± SEM).

(C) ChIP assays of mouse epidermis, pancreas and liver showing the binding of GR and corepressors to the IR nGRE regions of indicated genes. WT mice were topically-treated with

vehicle or Dex (in the case of K5 ChIP) or intra-peritoneally-injected with vehicle or Dex (in the case of ins, insr and Reverbα ChIP) for 18 hours.

Figure 5. Transrepression of nGRE-containing genes by the so-called "dissociated" glucocorticoid RU 24858.

(A) NF-κBluc and AP1luc luciferase reporter plasmids.

(B) Both Dex and RU24858 treatment repress NF-κB and AP1-driven transcriptional activation *in vitro,* with similar efficiency. Transfected A549 cells with NF-κBluc were treated as indicated for 6 hours, followed by luciferase assay. BAY and JNK I denote addition of a NF-κB-specific inhibitor (BAY 11-7082) and of a JNK inhibitor (JNK inhibitor II), respectively (mean ±SEM).

(C) ChIP assays using NF-κBluc plasmid-transfected A549 cells demonstrate the recruitment of NF-κB p65 and Pol II to the proximal promoter region upon IL-1β addition. Addition of Dex or RU24858 resulted in the formation of a similar transrepressing complex, while Pol II was released.

(D) Dex or RU24858 treatment enable efficient IR nGRE-mediated transrepression, whereas RU24858 is a weak inducer of (+)GRE-mediated transactivation, *in vitro*. Transfected A549 cells were treated for 6 hours as indicated, followed by luciferase assay (mean ±SEM).

(E) ChIP assays show that 6 hour treatment of Dex and RU24858 recruit SMRT and GR to nGREs in A549 cells transfected as indicated with pGL3 VDRE/IR0/IR1/IR2 nGRE plasmids (see Figure 2A and 2D).

(F) Dex and RU24858 repress the expression of IR nGRE-containing genes, whereas RU24858 does not induce the expression of the (+)GRE- containing GPX3 gene. Relative RNA levels were

determined by Q-PCR analysis in dorsal epidermis of WT mice topically-treated with Dex or RU24858 for 18 hours (mean ±SEM).

(G) Q-PCR analysis shows that Dex and RU24858 similarly repress *in vivo* the expression of cytokines, in dorsal skin of WT mice topically treated for 18 hours with TPA, Dex or RU24858, as indicated (mean ±SEM).

(H) Both Dex and RU24858 treatment in vivo promote GR and corepressor binding to nGRE regions of repressed genes, whereas RU24858 is unable to promote binding of GR and of the coactivators SRC2 and SRC3 to the GPX3 (+)GRE region. Dorsal skin of WT mice was topically-treated with Dex and RU24858 for 18 hours, followed by epidermis isolation and ChIP assay using indicated antibodies. Aliquots of the ChIP DNA was PCR-amplified using primers flanking nGRE or (+) GRE regions of the indicated genes.

Table 1

(A) Distribution of mouse and human IR0, IR1 and IR2 nGREs.

	IR0	IR1	IR2
mouse genes containing a putative nGRE	**1105**	**3303**	**3949**
human genes containing a putative nGRE	**1169**	**4281**	**5443**
mouse and human orthologue genes containing identical IR nGREs	**51**	**379**	**566**

(B) Repression, upon mouse treatment with a GC agonist, of genes containing IR0, IR1 and IR2 nGREs conserved in their human orthologues.

IR1 nGRE containing Genes	Epidermis			Intestinal epithelium			IR0 nGRE containing genes	Epidermis			Intestinal epithelium			IR2 nGRE containing genes	Epidermis			Intestinal epithelium		
	repressed	*not repressed*	*expressed*	*repressed*	*not repressed*	*expressed*		*repressed*	*not repressed*	*expressed*	*repressed*	*not repressed*	*expressed*		*repressed*	*not repressed*	*expressed*	*repressed*	*not repressed*	*expressed*
PRKCB	●		+	●		+	CCND1	●		+	●		+	DPAGT1	●		+			
STRA13	●		+	●		+	ADAMTS19	●		+	●		+	CCR10				●		+
TNFRSF 19	●		+	●		+	NDUFA4L2	●		+		♦	+	FKBP2		♦	+	●		+
USF1		♦	+	●		+	SPARC	●		+		♦	+	FOXJ1				●		+
JUND		♦	+	●		+	NEU1		♦	+	●		+	POMGNT1		♦	+	●		+
CYP26A1	●		+				FBXL18		♦	+		♦	+	RDH5				●		+
HSD11B2	●		+				KLF5		♦	+		♦	+	RORA		♦	+	●		+
KRT14	●		+				AIP		♦	+		♦	+	SLC2A8		♦	+		♦	+
BTG2				●		+	TCF25		♦	+		♦	+	GPR68					♦	+
GBA2				●		+	MTG1		♦	+		♦	+	MUC20					♦	+
RDH11				●		+	SLC25A5		♦	+		♦	+	SLC25A34					♦	+
SOCS3					♦	+	TRPM7		♦	+		♦	+	PRKRA		♦	+		♦	+
BCL2L1		♦	+		♦	+	CITED1					♦	+	SOCS1					♦	+
NKRF		♦	+		♦	+	MAPK4					♦	+	TNFRSF25					♦	+
SGK3					♦	+	SP9					♦	+	COL4A3BP		♦	+			

RNA isolated from 18 hr- Dex-treated WT mice epidermis and intestinal epithelium was analyzed by Q-RT-PCR. Genes, for which no signal could be detected in tissue samples from vehicle treated mice after 60 cycles of amplification, were considered to be not expressed in that tissue. (+) indicates that the gene was expressed in that tissue while “Repressed” denotes statistically ($p<0.05$) significant decrease in transcript levels after Dex treatment.

Table 2

A. IR nGRE- containing genes whose GC-induced transrepression could generate side effects related to those produced by GC therapy (see also Table S2)

Debilitating side effects upon GC therapy	Gene symbol	Gene name	a	b	References (For full reference, see Table S2)
Skin atrophy, bruising, thinning, brittle skin, disturbed wound healing (Schacke et al., 2002)	*Krt 14, Krt 5*	Keratin 14 **(IR1)**, Keratin 5 **(IR1)**	+	-	Ramot et al., 2009, This study (see Fig. 3A and 4B)
	TGFβ1	Transforming growth factor beta 1 precursor **(IR1)**	+	-	Frank et al., 1996
	Smad4	SMAD family member 4 **(IR2)**	-	+	Chen et al., 2000
	Tnc	Tenascin C **(IR2)**	+	-	Fassler et al., 1996
	Trpv3	Transient receptor potential cation channel subfamily V member 3 **(IR2)**	-	+	Cheng et al., 2010
	Ccnd1	Cyclin D1 **(IR0)**	+	+	This study (see Fig. S3B)
	Cdk4	Cyclin-dependent kinase 4 **(IR2)**	+	+	Rogatsky et al., 1997
Impaired skeletal growth and osteoporosis (Schacke et al., 2002, Kleiman and Tuckermann, 2007)	*Tnfrsf11b*	Osteoprotegerin **(IR2)**	+	+	Sasaki et al., 2001
	Bcl2	Bcl- 2 **(IR1)**	+	-	Mocetti et al., 2001
	Bcl2l1	Bcl- XL **(IR1)**	+	-	Lu et al., 2007
	TGFβ1	Transforming growth factor beta 1 precursor **(IR1)**	-	+	Geiser et al., 1998
	Smad 4	SMAD family member 4 **(IR2)**	-	+	Tan et al., 2007
	Ghr	Growth hormone receptor **(IR1)**	+	+	Gevers et al., 2002
	Gnas	Adenylate cyclase stimulating G-alpha protein **(IR1)**	-	+	Weinstein et al., 2004
	Wnt5a	Wingless-related MMTV integration site 5A **(IR1)**	-	+	Yang et al., 2003
	Ahsg	Alpha -2- HS- glycoprotein precursor **(IR0)**	-	+	Szweras et al., 2002
	Col11a2	Collagen, type XI, alpha 2 chain precursor **(IR2)**	-	+	Li et al., 2001
Hyperglycemia and Diabetes (Schacke et al., 2002, Kleiman and Tuckermann, 2007)	*Ins*	Insulin precursor **(IR1, IR2)**	+	+	Delaunay et al., 1997, This study (see Fig. 4B)
	Insr	Insulin receptor **(IR1)**	+	+	Caro and Amatruda., 1982, This study (see Fig. 4B)
Muscle atrophy/Myopathy (Schakman et al., 2008a)	*ctnnb1*	Beta –catenin **(IR1)**	+	+	Schakman et al., 2008b
	Akt1	Protein kinase B **(IR2)**	-	+	Schakman et al., 2008a
	Tpm2	Tropomysin beta chain **(IR1)**	-	+	Ochala et al., 2007
Impaired HPA axis, Adrenal insufficiency (Schacke et al., 2002)	*Mc2r*	ACTH receptor **(IR1)**	+	+	Chida et al., 2007, This study (see Fig. 4B)
	Mrap	ACTH receptor accessory protein **(IR1)**	+	+	Metherell et al., 2005, This study (see Fig. 4B)
Circadian rhythm disorder, metabolic syndrome, bipolar disorder and mania (Bechtold et al., 2010, Duez and Staels, 2008)	*Clock*	Circadian locomoter output cycle kaput protein **(IR1)**	-	+	Roybal et al., 2007
	Nr1d1	Reverbα **(IR1)**	+	-	Torra et al., 2000, Preitner et al., 2002, This study (see Fig. 4B)
	Rora	RORα **(IR2)**	+	-	This study (see Fig. S3G)
Anxiety and depression (Schacke et al., 2002)	*Ucn2*	Urocortin 2 **(IR1)**	+	+	Chen et al., 2004, 2006
	Crhr2	Corticotropin releasing hormone receptor 2 **(IR1)**	-	+	Bale et al., 2000
Hypertension (Schacke et al., 2002)	*Hsd11b2*	Corticosteroid 11-beta-dehydrogenase isozyme 2 (11β-HSD2) **(IR1)**	+	+	Stewart et al., 1996, This study (see Fig. 3A)

a.Genes whose expression is known to be decreased upon GC treatment.

b.Genes, whose decreased expression is known to generate effects related to those produced by GC treatment.

(IR0), **(IR1)** and **(IR2)** indicate the type of nGRE motif present in that gene.

B. IR nGRE- containing genes involved in GC-anti-inflammatory therapy (see also Table S2)

Gene symbol	Gene name*	Gene symbol	Gene name*
C1qb	Complement C1q subcomponent subunit B Precursor **(IR2)**	*Il16*	Interleukin-16 Precursor **(IR1)**
C1ql1	C1q-related factor Precursor **(IR1)**	*Il17rb*	Interleukin-17 receptor b **(IR1)**
C3	Complement C3 Precursor **(IR1)**	*Il11ra1*	Interleukin-11 receptor **(IR1)**
Cfd	Complement factor D Precursor **(IR1)**	*Il17b*	Interleukin-17b Precursor **(IR1)**
Il6	Interleukin-6 Precursor **(IR1)**	*Il17f*	Interleukin-17f Precursor **(IR1)**
Il20	Interleukin-20 Precursor **(IR2)**	*Il28a*	Interleukin-28a Precursor **(IR1)**
Ccr10	C-C chemokine receptor type 10 **(IR2)**	*Il28b*	Interleukin-28b Precursor **(IR1)**
Stat3	Signal transducer and activator of transcription 3 **(IR2)**	*Il24*	Interleukin-24 Precursor **(IR1)**
Nfatc1	Nuclear factor of activated T-cells, cytoplasmic 1 **(IR1)**	*Il34*	Interleukin-34 Precursor **(IR1)**
Il8ra	Interleukin-8 receptor a **(IR1)**	*Il1rn*	Interleukin-1 receptor antagonist protein Precursor **(IR2)**
Il12rb1	Interleukin-12 receptor b1 **(IR1)**	*Il22ra1*	interleukin-22 receptor a1 **(IR1)**
Il17ra	Interleukin-17 receptor a **(IR1)**	*TSLP*	Thymic Stromal Lymphopoietin **(IR1)**

* All of these genes also contain NF-κB and AP1 binding sites.

Figure 1

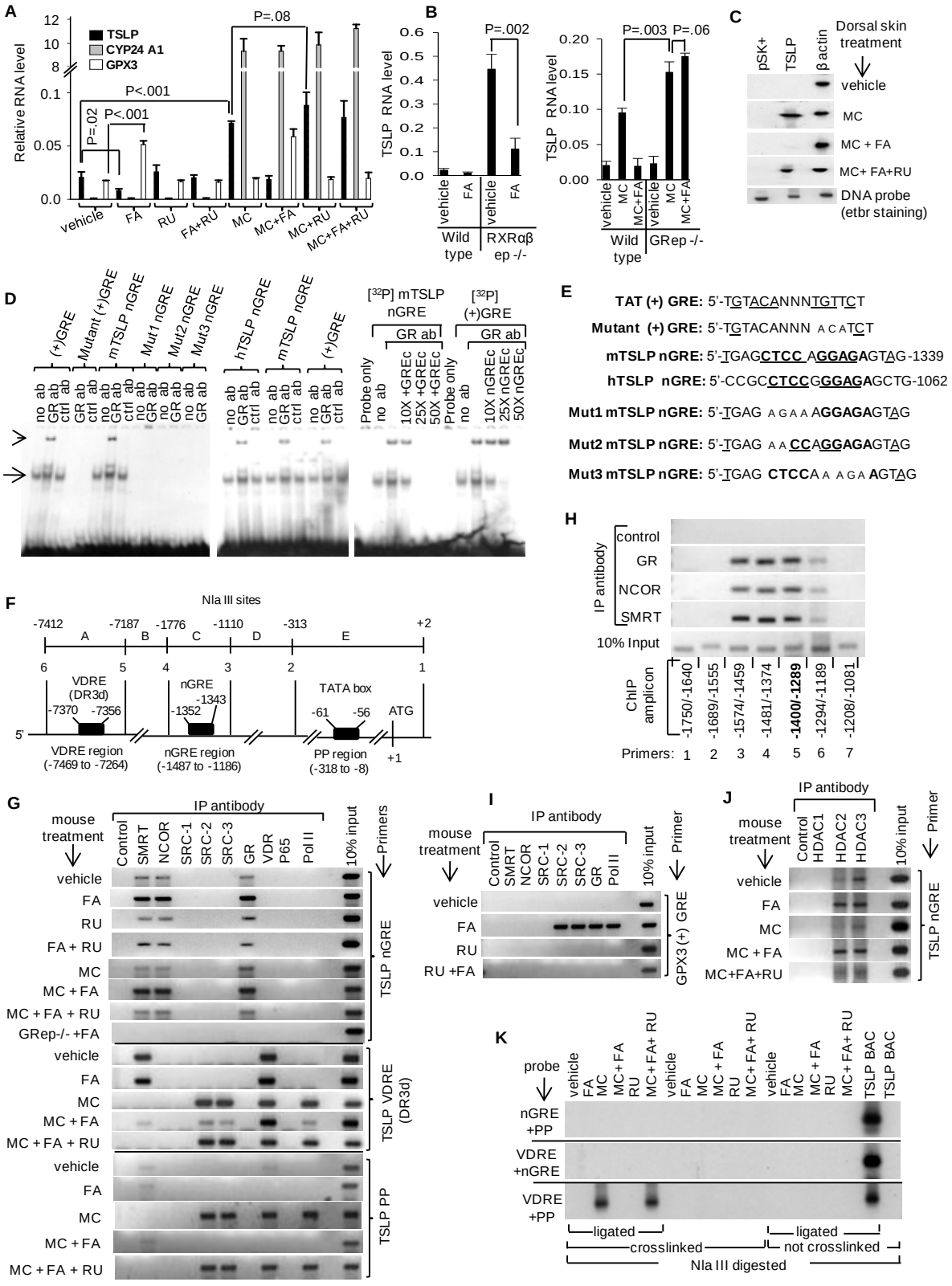
A
TSLP
CYP24 A1
GPX3
Relative RNA level
P=.08
P<.001
P=.02
P<.001
vehicle
FA
RU
FA+RU
MC
MC+FA
MC+RU
MC+FA+RU
B
TSLP RNA level
P=.002
vehicle
FA
Wild type
RXRαβ ep -/-
P=.003
P=.06
MC
MC+FA
GRep -/-
C
pSK+
TSLP
β actin
Dorsal skin treatment
vehicle
MC
MC + FA
MC+ FA+RU
DNA probe (etbr staining)
D
(+)GRE
Mutant (+)GRE
mTSLP nGRE
Mut1 nGRE
Mut2 nGRE
Mut3 nGRE
hTSLP nGRE
mTSLP nGRE
(+)GRE
[32P] mTSLP nGRE
[32P] (+)GRE
GR ab
no ab
GR ab
ctrl ab
Probe only
10X +GREc
25X +GREc
50X +GREc
10X nGREc
25X nGREc
50X nGREc
E
TAT (+) GRE: 5'-TGTACANNNTGTTCT
Mutant (+) GRE: 5'-TGTACANNN ACATCT
mTSLP nGRE: 5'-TGAGCTCC AGGAGAGTAG-1339
hTSLP nGRE: 5'-CCGCCTCCGGGAGAGCTG-1062
Mut1 mTSLP nGRE: 5'-TGAG AGAA AGGAGAGTAG
Mut2 mTSLP nGRE: 5'-TGAG AA CCAGGAGAGTAG
Mut3 mTSLP nGRE: 5'-TGAG CTCCA A AGA AGTAG
F
NIa III sites
-7412
-7187
-1776
-1110
-313
+2
A
B
C
D
E
6
5
4
3
2
1
VDRE (DR3d)
-7370
-7356
nGRE
-1343
-1352
TATA box
-61
-56
ATG
5'
+1
VDRE region (-7469 to -7264)
nGRE region (-1487 to -1186)
PP region (-318 to -8)
H
IP antibody
control
GR
NCOR
SMRT
10% Input
ChIP amplicon
-1750/-1640
-1689/-1555
-1574/-1459
-1481/-1374
-1400/-1289
-1294/-1189
-1208/-1081
Primers: 1 2 3 4 5 6 7
G
IP antibody
mouse treatment
Control
SMRT
NCOR
SRC-1
SRC-2
SRC-3
GR
VDR
P65
Pol II
10% input
Primers
vehicle
FA
RU
FA + RU
MC
MC + FA
MC + FA + RU
GRep-/- +FA
TSLP nGRE
TSLP VDRE (DR3d)
TSLP PP
I
IP antibody
mouse treatment
Control
SMRT
NCOR
SRC-1
SRC-2
SRC-3
GR
Pol II
10% input
Primer
vehicle
FA
RU
RU +FA
GPX3 (+) GRE
J
IP antibody
mouse treatment
Control
HDAC1
HDAC2
HDAC3
10% input
Primer
vehicle
FA
MC
MC + FA
MC+FA+RU
TSLP nGRE
K
probe
vehicle
FA
MC
MC+ FA
RU
MC+ FA+ RU
TSLP BAC
nGRE +PP
VDRE +nGRE
VDRE +PP
ligated
crosslinked
not crosslinked
NIa III digested

Figure 2

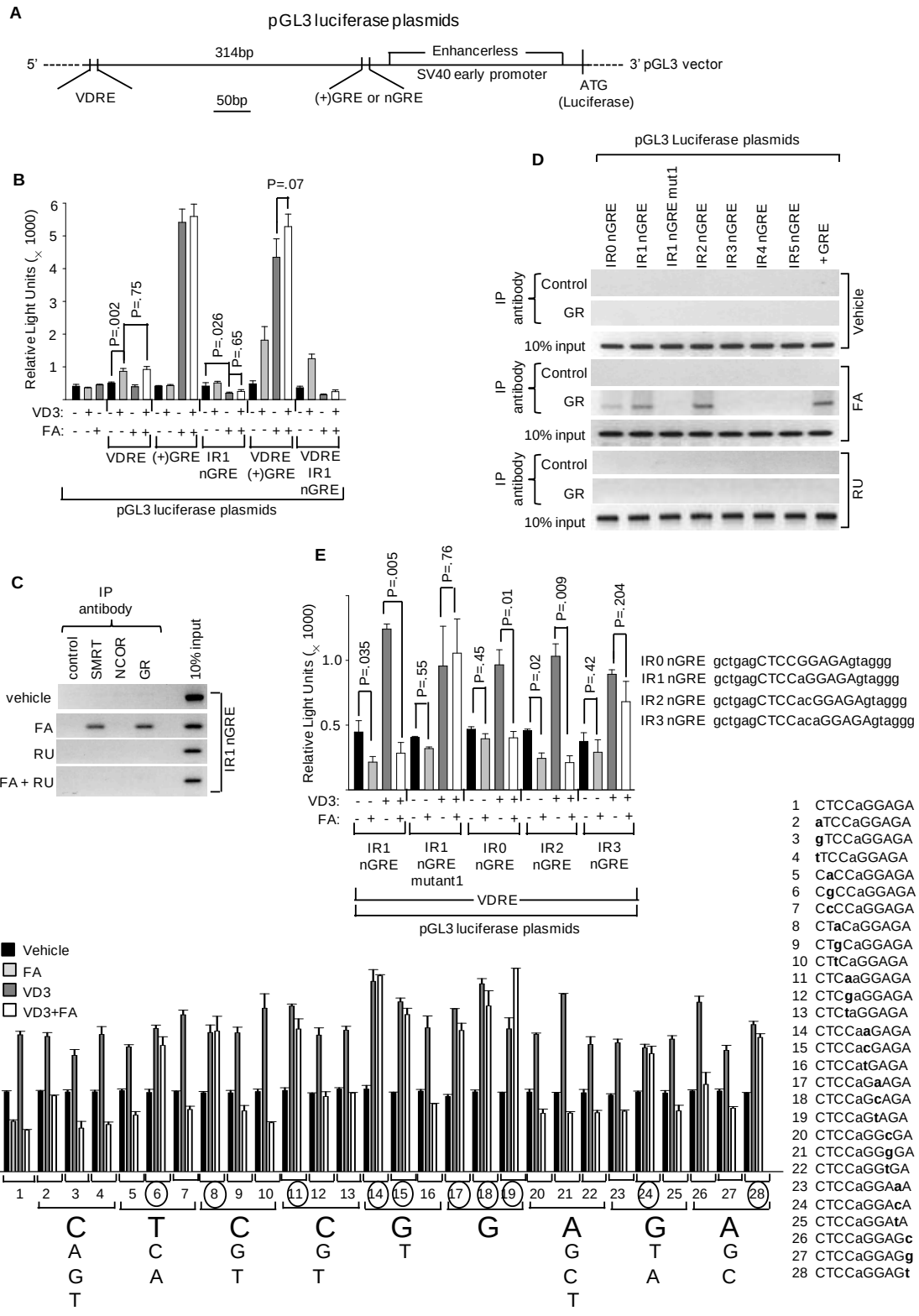
A
pGL3 luciferase plasmids
5'
314bp
Enhancerless
SV40 early promoter
3' pGL3 vector
ATG
(Luciferase)
VDRE
50bp
(+)GRE or nGRE
B
Relative Light Units (X 1000)
P=.002
P=.75
P=.026
P=.65
P=.07
VD3:
FA:
VDRE
(+)GRE
IR1 nGRE
VDRE
(+)GRE
VDRE
IR1 nGRE
pGL3 luciferase plasmids
C
IP antibody
control
SMRT
NCOR
GR
10% input
vehicle
FA
RU
FA + RU
IR1 nGRE
D
pGL3 Luciferase plasmids
IR0 nGRE
IR1 nGRE
IR1 nGRE mut1
IR2 nGRE
IR3 nGRE
IR4 nGRE
IR5 nGRE
+ GRE
IP antibody
Control
GR
10% input
Vehicle
FA
RU
E
Relative Light Units (X 1000)
P=.035
P=.005
P=.55
P=.76
P=.45
P=.01
P=.02
P=.009
P=.42
P=.204
VD3:
FA:
IR1 nGRE
IR1 nGRE mutant1
IR0 nGRE
IR2 nGRE
IR3 nGRE
VDRE
pGL3 luciferase plasmids
IR0 nGRE gctgagCTCCGGAGAgtaggg
IR1 nGRE gctgagCTCCaGGAGAgtaggg
IR2 nGRE gctgagCTCCacGGAGAgtaggg
IR3 nGRE gctgagCTCCacaGGAGAgtaggg
F
Relative Light Units (X 1000)
Vehicle
FA
VD3
VD3+FA
1 CTCCaGGAGA
2 aTCCaGGAGA
3 gTCCaGGAGA
4 tTCCaGGAGA
5 CaCCaGGAGA
6 CgCCaGGAGA
7 CcCCaGGAGA
8 CTaCaGGAGA
9 CTgCaGGAGA
10 CTtCaGGAGA
11 CTCaaGGAGA
12 CTCgaGGAGA
13 CTCtaGGAGA
14 CTCCaaGAGA
15 CTCCacGAGA
16 CTCCatGAGA
17 CTCCaGaAGA
18 CTCCaGcAGA
19 CTCCaGtAGA
20 CTCCaGGcGA
21 CTCCaGGgGA
22 CTCCaGGtGA
23 CTCCaGGAaA
24 CTCCaGGAcA
25 CTCCaGGAtA
26 CTCCaGGAGc
27 CTCCaGGAGg
28 CTCCaGGAGt

Figure 3

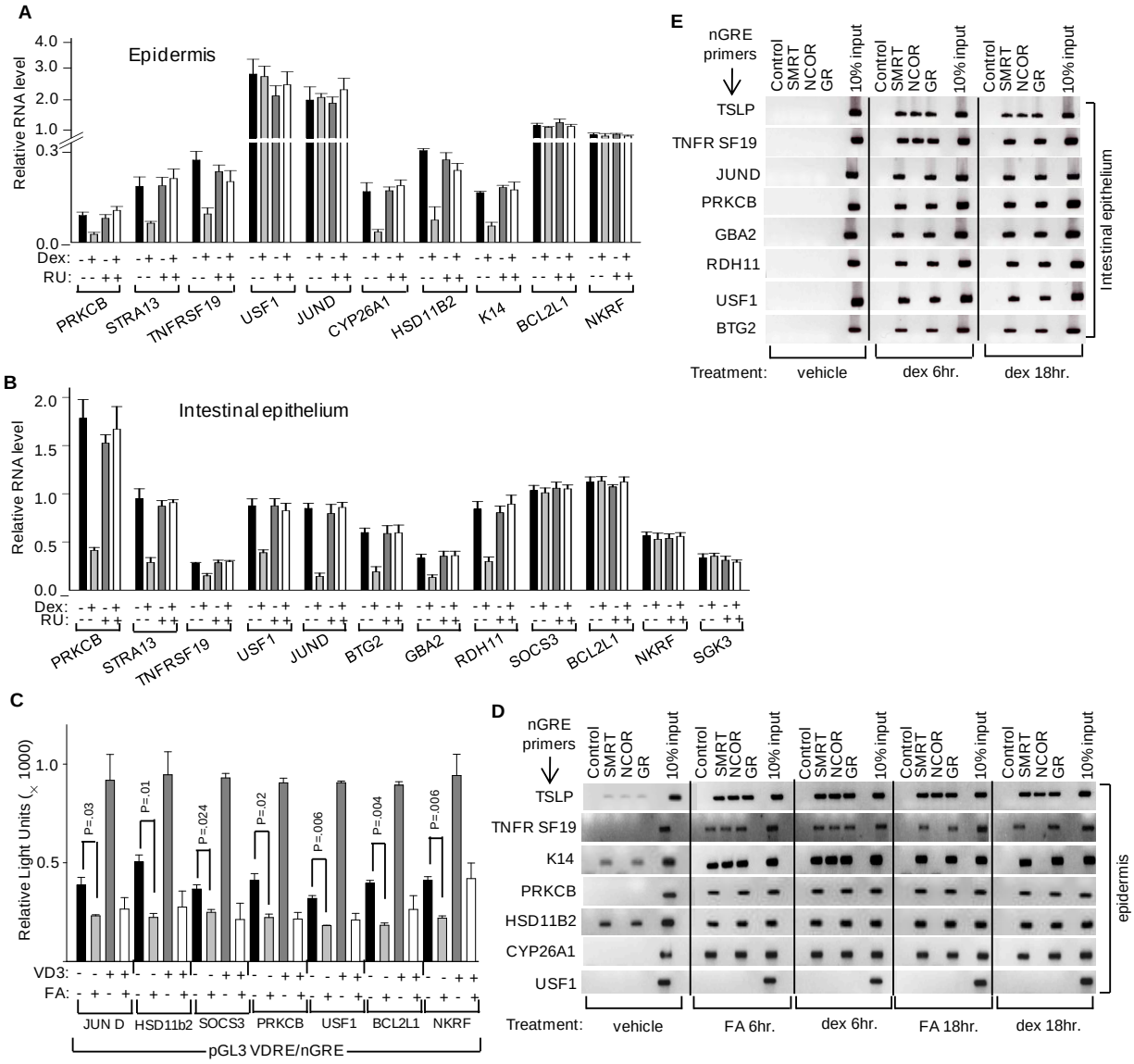
A
Epidermis
Relative RNA level
Dex:
RU:
PRKCB
STRA13
TNFRSF19
USF1
JUND
CYP26A1
HSD11B2
K14
BCL2L1
NKRF
B
Intestinal epithelium
Relative RNA level
PRKCB
STRA13
TNFRSF19
USF1
JUND
BTG2
GBA2
RDH11
SOCS3
BCL2L1
NKRF
SGK3
C
Relative Light Units (X 1000)
P=.03
P=.01
P=.024
P=.02
P=.006
P=.004
P=.006
VD3:
FA:
JUN D
HSD11b2
SOCS3
PRKCB
USF1
BCL2L1
NKRF
pGL3 VDRE/nGRE
D
nGRE primers
Control
SMRT
NCOR
GR
10% input
TSLP
TNFR SF19
K14
PRKCB
HSD11B2
CYP26A1
USF1
epidermis
Treatment:
vehicle
FA 6hr.
dex 6hr.
FA 18hr.
dex 18hr.
E
nGRE primers
Control
SMRT
NCOR
GR
10% input
TSLP
TNFR SF19
JUND
PRKCB
GBA2
RDH11
USF1
BTG2
Intestinal epithelium
Treatment:
vehicle
dex 6hr.
dex 18hr.

Figure 4

A

Human (h) and mouse (m) putative nGREs in keratin 5 (K5) gene

hK5 IR1 nGRE1: gtgt CTCCaGGAGA gcaa 3017

mK5 IR1 nGRE1: tgct CTCCtGGAG**g** cgga 2194

mK5 IR1 nGRE2: gaag CTCCtGGAG**g** gatg -1990

mK5 IR1nGRE3: tttg **a**TCCaGGAGA gctg -7804

Human (h) and mouse (m) putative nGREs in insulin receptor (insr) and insulin (ins) gene

hinsr IR1 nGRE : ttct CTCCtGGAGA cctg 3856

minsr IR1 nGRE1 : tggg CT**t**CgGGAGA ggat 5

minsr IR1 nGRE2 : tgta CTCCtGG**g**GA acca -7700

hins IR1 nGRE: tgct CTCCtGGAGA catt -202

mins IR1 nGRE : caac CT**g**CaGGAGA ccta -12625

hins IR2 nGRE : aggc CTCCctGGAGA ggct -25700

mins IR2 nGRE : tagg CTCCacGGAGA acct -11925

Human (h) and mouse (m) putative nGREs in Reverbα (Nr1d1) gene

hReverbα IR1 nGRE1 : agag C**c**CCaGGAGA tcat -12043

hReverbα IR1 nGRE2 : cctt CTCCgGGAG**g** atgg -12984

hReverbα IR1 nGRE3: agcc CTCCaGG**t**GA ttct -14522

mReverbα IR1 nGRE1 : ccga CTCCtGGAGA acaa -7637

mReverbα IR1 nGRE2 : tgaa CTCCaGGAG**g** gagt -2177

B

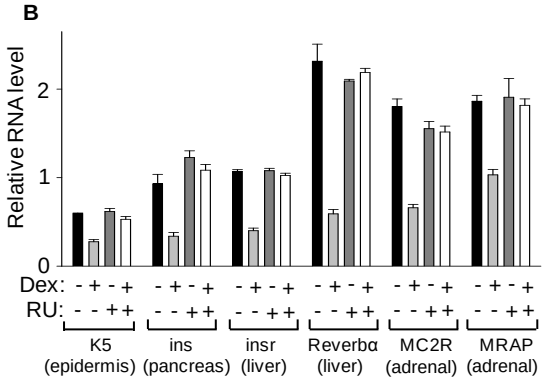

C

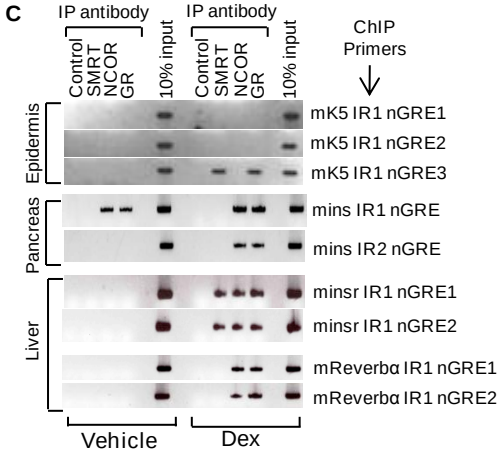

Figure 5

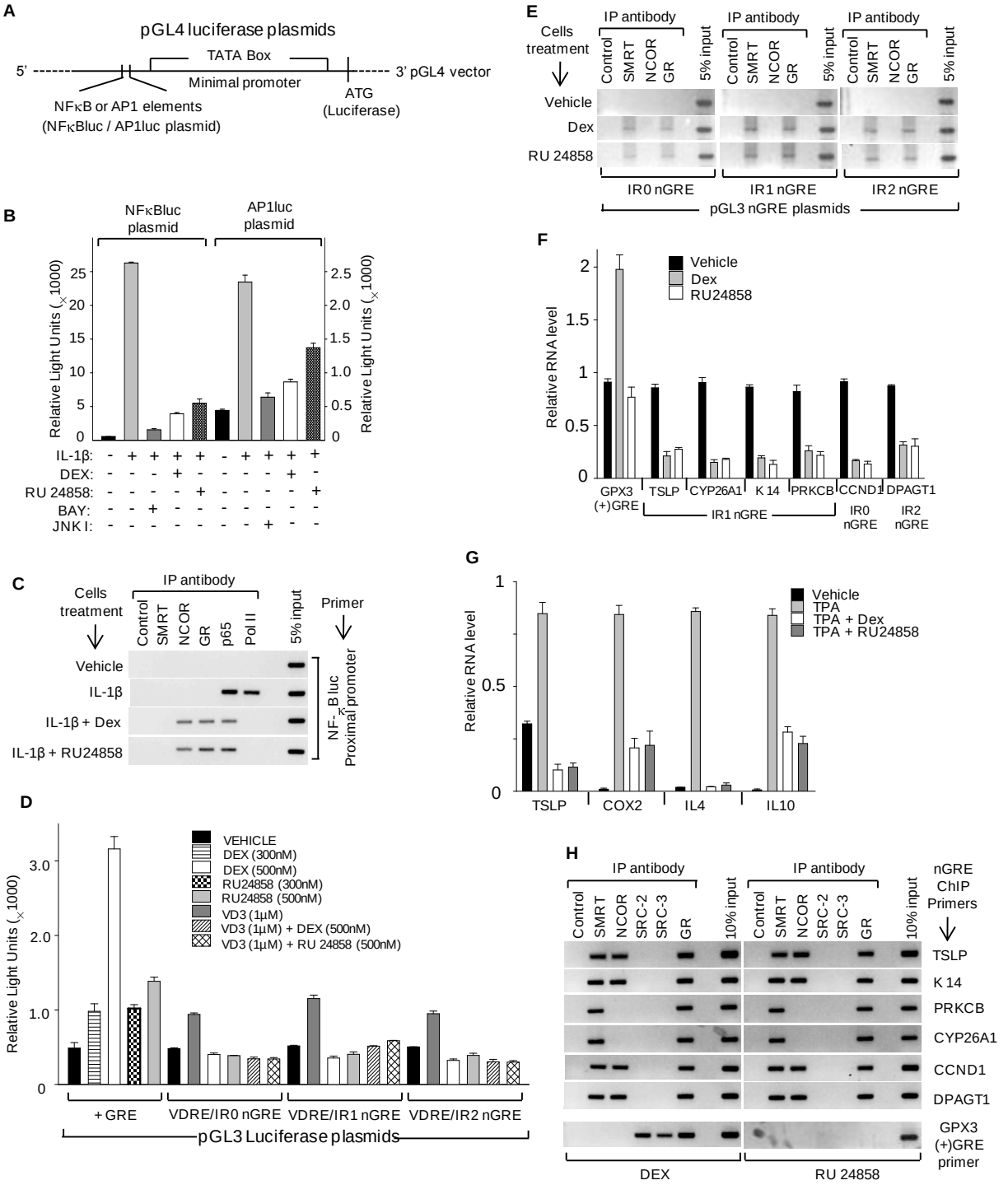
A
pGL4 luciferase plasmids
TATA Box
5'
3' pGL4 vector
Minimal promoter
NFκB or AP1 elements
(NFκBluc / AP1luc plasmid)
ATG
(Luciferase)
B
NFκBluc plasmid
AP1luc plasmid
Relative Light Units (X1000)
IL-1β:
DEX:
RU 24858:
BAY:
JNK I:
C
Cells treatment
IP antibody
Control
SMRT
NCOR
GR
p65
Pol II
5% input
Primer
Vehicle
IL-1β
IL-1β + Dex
IL-1β + RU24858
NF-κB luc Proximal promoter
D
VEHICLE
DEX (300nM)
DEX (500nM)
RU24858 (300nM)
RU24858 (500nM)
VD3 (1μM)
VD3 (1μM) + DEX (500nM)
VD3 (1μM) + RU 24858 (500nM)
+ GRE
VDRE/IR0 nGRE
VDRE/IR1 nGRE
VDRE/IR2 nGRE
pGL3 Luciferase plasmids
E
Cells treatment
IP antibody
Control
SMRT
NCOR
GR
5% input
Vehicle
Dex
RU 24858
IR0 nGRE
IR1 nGRE
IR2 nGRE
pGL3 nGRE plasmids
F
Vehicle
Dex
RU24858
Relative RNA level
GPX3 (+)GRE
TSLP
CYP26A1
K 14
PRKCB
CCND1
DPAGT1
IR1 nGRE
IR0 nGRE
IR2 nGRE
G
Vehicle
TPA
TPA + Dex
TPA + RU24858
Relative RNA level
TSLP
COX2
IL4
IL10
H
IP antibody
Control
SMRT
NCOR
SRC-2
SRC-3
GR
10% input
nGRE ChIP Primers
TSLP
K 14
PRKCB
CYP26A1
CCND1
DPAGT1
GPX3 (+)GRE primer
DEX
RU 24858

Figure S1

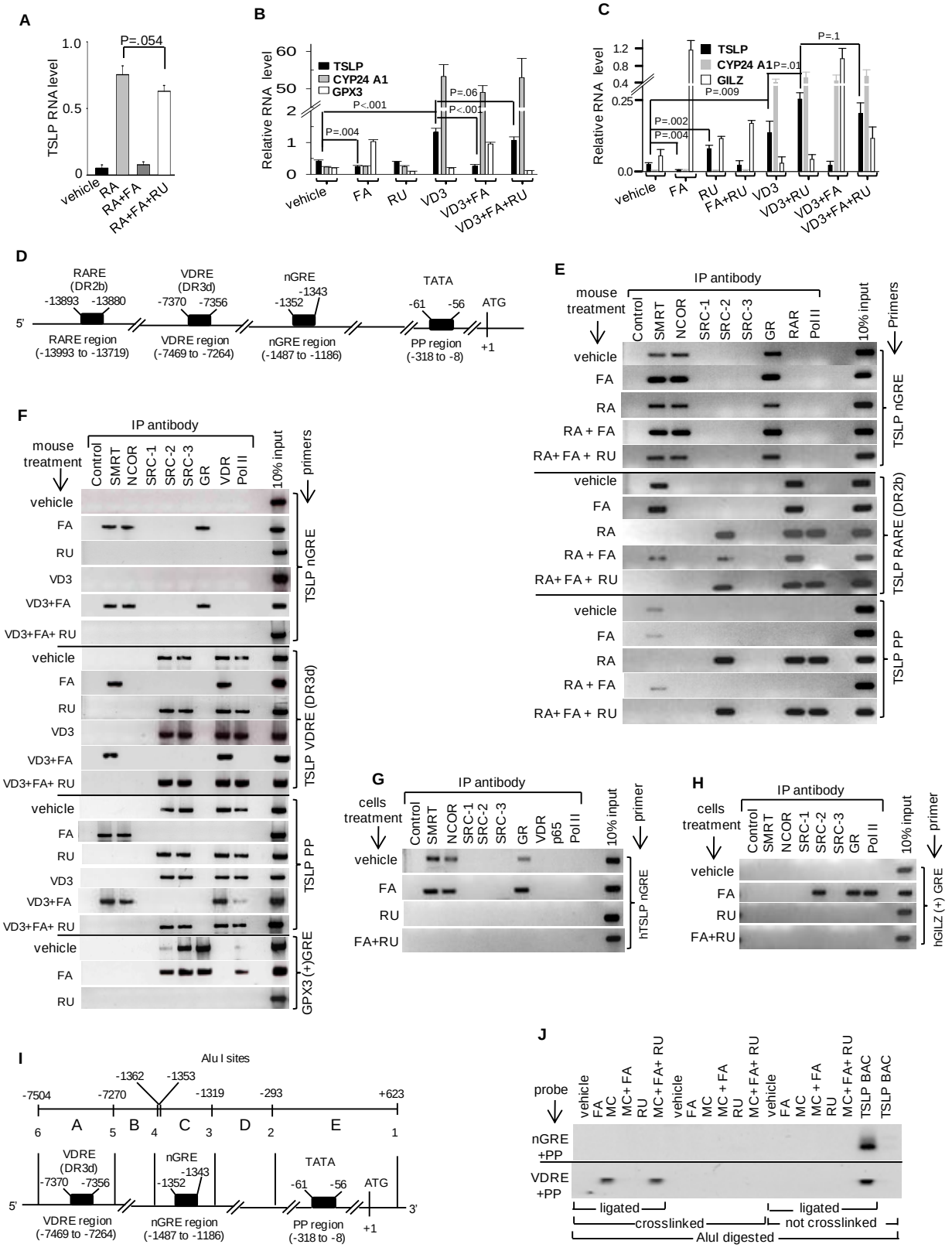
A
TSLP RNA level
P=.054
vehicle
RA
RA+FA
RA+FA+RU
B
Relative RNA level
TSLP
CYP24 A1
GPX3
P<.001
P=.004
P=.06
P<.001
vehicle
FA
RU
VD3
VD3+FA
VD3+FA+RU
C
Relative RNA level
TSLP
CYP24 A1
GILZ
P=.1
P=.01
P=.009
P=.002
P=.004
vehicle
FA
RU
FA+RU
VD3
VD3+RU
VD3+FA
VD3+FA+RU
D
RARE (DR2b)
-13893
-13880
VDRE (DR3d)
-7370
-7356
nGRE
-1343
-1352
TATA
-61
-56
ATG
+1
5'
RARE region (-13993 to -13719)
VDRE region (-7469 to -7264)
nGRE region (-1487 to -1186)
PP region (-318 to -8)
E
IP antibody
mouse treatment
Control
SMRT
NCOR
SRC-1
SRC-2
SRC-3
GR
RAR
Pol II
10% input
Primers
vehicle
FA
RA
RA + FA
RA+ FA + RU
TSLP nGRE
TSLP RARE (DR2b)
TSLP PP
F
IP antibody
mouse treatment
Control
SMRT
NCOR
SRC-1
SRC-2
SRC-3
GR
VDR
Pol II
10% input
primers
vehicle
FA
RU
VD3
VD3+FA
VD3+FA+ RU
TSLP nGRE
TSLP VDRE (DR3d)
TSLP PP
GPX3 (+)GRE
G
IP antibody
cells treatment
Control
SMRT
NCOR
SRC-1
SRC-2
SRC-3
GR
VDR
p65
Pol II
10% input
primer
vehicle
FA
RU
FA+RU
hTSLP nGRE
H
IP antibody
cells treatment
Control
SMRT
NCOR
SRC-1
SRC-2
SRC-3
GR
Pol II
10% input
primer
vehicle
FA
RU
FA+RU
hGILZ (+) GRE
I
AluI sites
-1362
-1353
-7504
-7270
-1319
-293
+623
6
A
5
B
4
C
3
D
2
E
1
VDRE (DR3d)
-7370
-7356
nGRE
-1343
-1352
TATA
-61
-56
ATG
+1
5'
3'
VDRE region (-7469 to -7264)
nGRE region (-1487 to -1186)
PP region (-318 to -8)
J
probe
vehicle
FA
MC
MC+ FA
RU
MC+ FA+ RU
TSLP BAC
nGRE +PP
VDRE +PP
ligated
crosslinked
not crosslinked
AluI digested

Figure S2

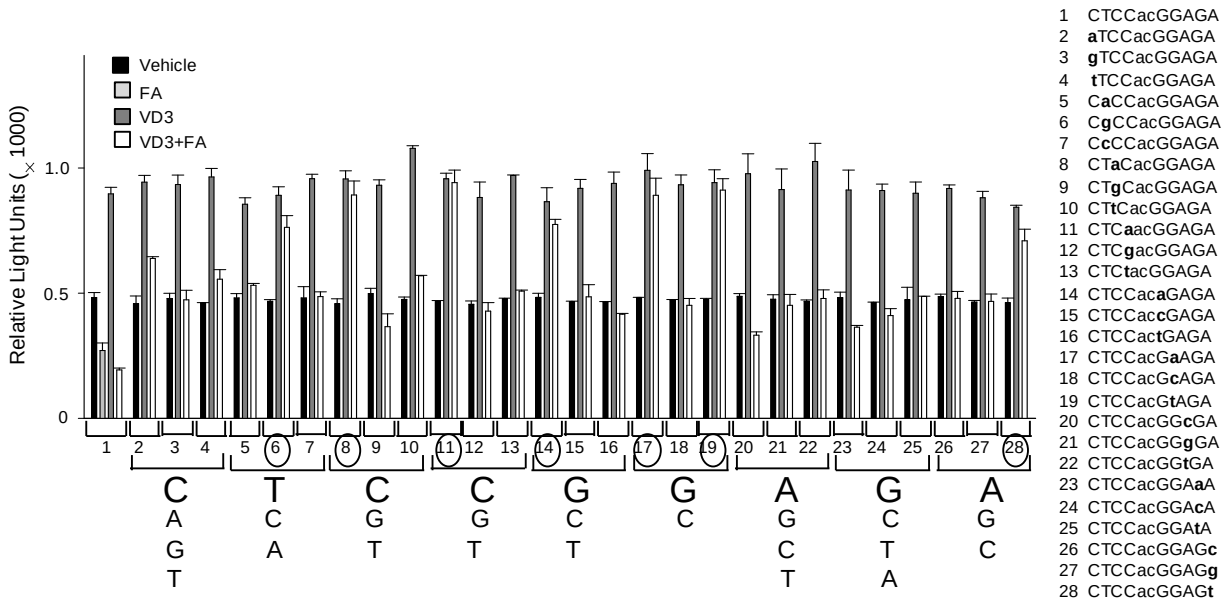
Vehicle
FA
VD3
VD3+FA
Relative Light Units (× 1000)
1.0
0.5
0
1 2 3 4 5 6 7 8 9 10 11 12 13 14 15 16 17 18 19 20 21 22 23 24 25 26 27 28
C A G T
T C A
C G T
C G T
G C T
G C
A G C T
G C T A
A G C
1 CTCCacGGAGA
2 aTCCacGGAGA
3 gTCCacGGAGA
4 tTCCacGGAGA
5 CaCCacGGAGA
6 CgCCacGGAGA
7 CcCCacGGAGA
8 CTaCacGGAGA
9 CTgCacGGAGA
10 CTtCacGGAGA
11 CTCaacGGAGA
12 CTCgacGGAGA
13 CTCtacGGAGA
14 CTCCacaGAGA
15 CTCCaccGAGA
16 CTCCactGAGA
17 CTCCacGaAGA
18 CTCCacGcAGA
19 CTCCacGtAGA
20 CTCCacGGcGA
21 CTCCacGGgGA
22 CTCCacGGtGA
23 CTCCacGGAaA
24 CTCCacGGAcA
25 CTCCacGGAtA
26 CTCCacGGAGc
27 CTCCacGGAGg
28 CTCCacGGAGt

Figure S3

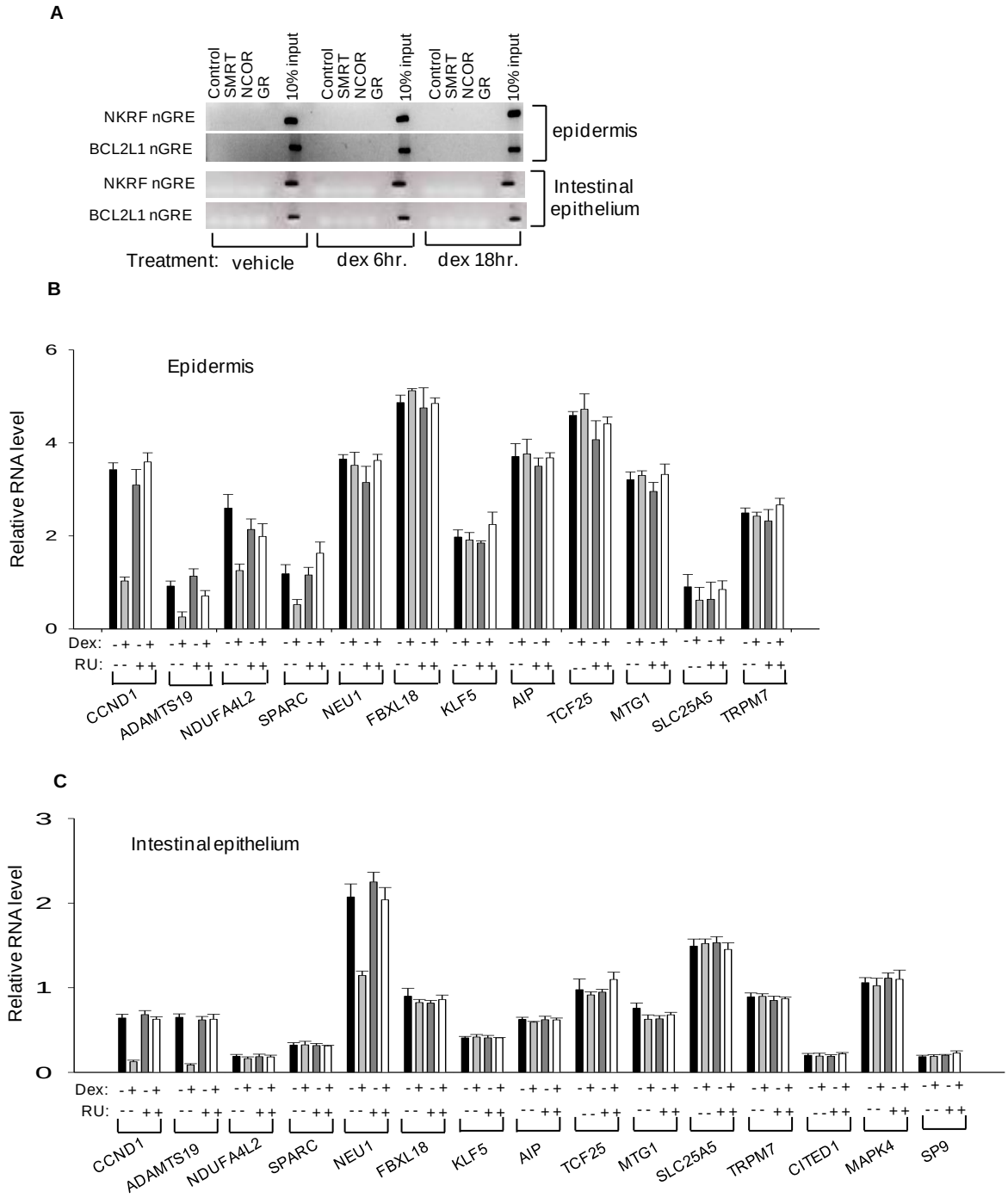
A
Control
SMRT
NCOR
GR
10% input
NKRF nGRE
BCL2L1 nGRE
epidermis
Intestinal epithelium
Treatment: vehicle
dex 6hr.
dex 18hr.
B
Epidermis
Relative RNA level
Dex:
RU:
CCND1
ADAMTS19
NDUFA4L2
SPARC
NEU1
FBXL18
KLF5
AIP
TCF25
MTG1
SLC25A5
TRPM7
C
Intestinal epithelium
CITED1
MAPK4
SP9

Figure S3

D

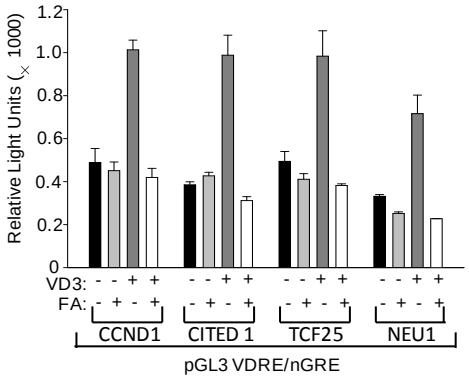
Relative Light Units (x 1000)
1.2
1.0
0.8
0.6
0.4
0.2
0
VD3: - - + + - - + + - - + + - - + +
FA: - + - + - + - + - + - + - + - +
CCND1
CITED 1
TCF25
NEU1
pGL3 VDRE/nGRE

E

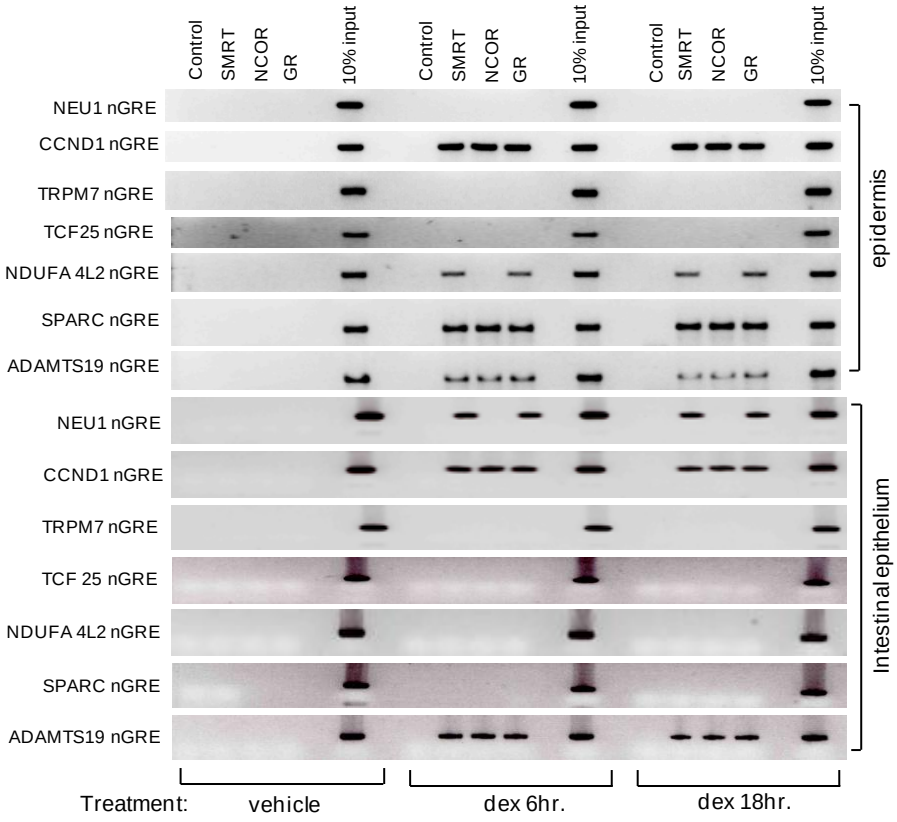
Control
SMRT
NCOR
GR
10% input
NEU1 nGRE
CCND1 nGRE
TRPM7 nGRE
TCF25 nGRE
NDUFA 4L2 nGRE
SPARC nGRE
ADAMTS19 nGRE
epidermis
TCF 25 nGRE
Intestinal epithelium
Treatment:
vehicle
dex 6hr.
dex 18hr.

Figure S3

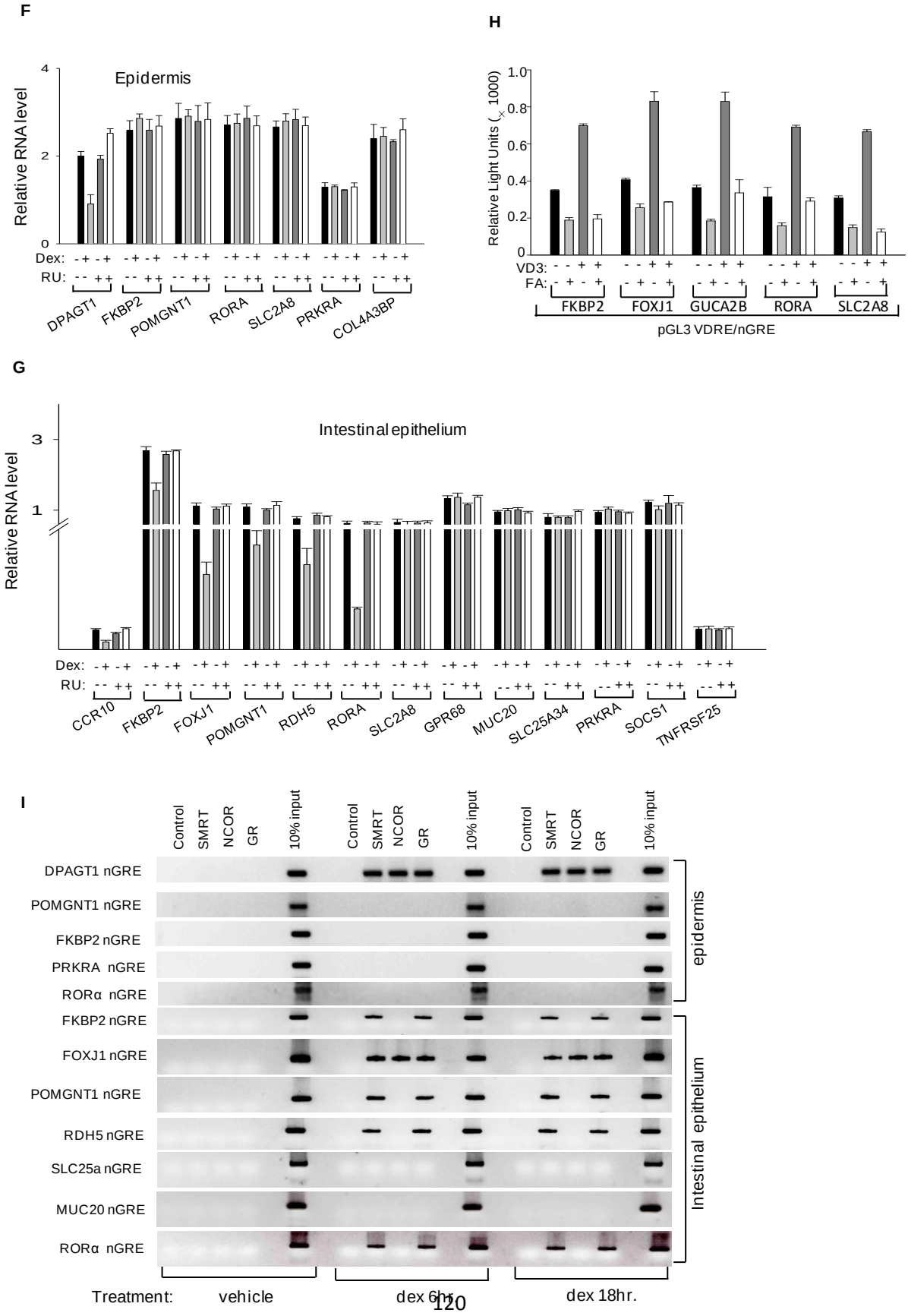
F
Epidermis
Relative RNA level
Dex:
RU:
DPAGT1
FKBP2
POMGNT1
RORA
SLC2A8
PRKRA
COL4A3BP
H
Relative Light Units (x 1000)
VD3:
FA:
FKBP2
FOXJ1
GUCA2B
RORA
SLC2A8
pGL3 VDRE/nGRE
G
Intestinal epithelium
Relative RNA level
CCR10
FKBP2
FOXJ1
POMGNT1
RDH5
RORA
SLC2A8
GPR68
MUC20
SLC25A34
PRKRA
SOCS1
TNFRSF25
I
Control
SMRT
NCOR
GR
10% input
DPAGT1 nGRE
POMGNT1 nGRE
FKBP2 nGRE
PRKRA nGRE
RORα nGRE
FKBP2 nGRE
FOXJ1 nGRE
POMGNT1 nGRE
RDH5 nGRE
SLC25a nGRE
MUC20 nGRE
RORα nGRE
epidermis
Intestinal epithelium
Treatment:
vehicle
dex 6hr.
dex 18hr.

Legend to supplementary figures:

Figure S1. Glucocorticoid-induced recruitment of GR and corepressors to the TSLP IR1 nGRE prevent RA and active VD3-induced recruitment of RAR, VDR, coactivators and pol II to the TSLP DR2b RARE, DR3d VDRE and proximal promoter (PP) regions in epidermis and intestinal epithelium of wild type mouse and in human A549 cells, related to Figure 1.

(A) Q-PCR of TSLP RNA from skin of WT mice topically-treated for 6 hours with the indicated compounds (mean ± SEM). FA, fluocinolone acetonide; RA, all-trans retinoic acid; VD3, active Vitamin D3; RU, glucocorticoid antagonist RU486. All values were normalized with respect to those obtained for HPRT.

(B) Q-PCR of TSLP, GPX3 and Cyp24A1 RNA in epithelial cells of WT mouse ileum (mean ± SEM). Mice were intraperitoneally (I.P.)-injected with vehicle, FA, RU 486 (RU) and/or VD3, as indicated. All values were normalized with respect to those obtained for HPRT.

(C) Q-PCR of TSLP, GILZ and Cyp24A1 RNA in A549 cells, treated for 6 hours as indicated. Values were normalized with respect to those obtained for GAPDH (mean ± SEM).

(D) Mouse TSLP promoter region showing the position of DR2b RARE with respect to other sequence elements. Related to Figure 1F.

(E) Glucocorticoid-induced repression of the TSLP promoter is initiated *in vivo* through binding of the GR to the nGRE, along with corepressors. ChIP assays showing the FA-induced binding of GR and corepressors to the TSLP nGRE region and its reversion by RU 486 (RU). Dorsal skin from WT mice was topically treated with vehicle, RA, FA and RU for 6 hours prior to epidermis isolation. ChIP-immunoprecipitated DNA from epidermal whole cell extracts was PCR-amplified using primers flanking the TSLP nGRE, TSLP RARE (DR2b) and TSLP PP (Proximal Promoter) regions (see panel D). IP antibody indicates the antibodies used for immunoprecipitation. Control antibody corresponds to rabbit IgG. 10% input indicates the signal obtained after PCR amplification of a given DNA region contained in 10% of the chromatin used for immunoprecipitation of each sample with a given antibody.

(F) ChIP assays of intestine epithelium of WT mouse, intraperitoneally-injected as indicated with vehicle, VD3, FA and RU, for 6 hours prior to removal of intestine. Epithelial cells were isolated and processed through ChIP assays using indicated antibodies. ChIP immunoprecipitated DNA was PCR- amplified using primers flanking the TSLP nGRE, DR3d and PP regions, as well as the GPX3 (+) GRE region.

(G) ChIP assays of A549 whole cell extract (WCE) showing the FA-induced binding of GR and corepressors to the human TSLP nGRE (hTSLP nGRE) region and its reversion by RU.

(H) ChIP assays of A549 WCE showing the FA-induced binding of GR and coactivators to the hGILZ (+) GRE region, and its reversion by RU. Aliquots of the immunoprecipitated DNA described in panel (G) were PCR-amplified using primers flanking the (+) GRE region of the human GILZ gene.

(I) Schematic representation of the Alu I sites flanking the PP, nGRE and DR3d VDRE regions of the TSLP promoter.

(J) Chromosome conformation capture (3C) assay using MC 903-treated WT mouse dorsal epidermis shows that topical treatment with FA prevents the interaction of the Alu I region A that contains the VDRE (DR3d) with the Alu I region E that contains the proximal promoter (PP) region (see panel I). Dorsal skin was topically treated with vehicle, MC, FA and/or RU for 6 hours, prior to isolation of epidermis. Non-cross linked and cross-linked chromatin were digested with Alu I enzyme, diluted and incubated with T4 DNA ligase. Ligated DNA was PCR-amplified using primers flanking the junction between either VDRE (Alu I fragment A) or nGRE (Alu I fragment C) regions with the PP (Alu I fragment E) region. PCR product was separated in a 2% agarose gel and Southern-hybridized to a [^{32}P]-5' labeled probe corresponding to 20 nucleotides upstream and 20 nucleotides downstream from the junction between the Alu I regions A and E and C and E. Upper and lower panels reveal interaction between region C containing the nGRE and region E containing the PP region, and between region A containing the VDRE and region E. A BAC containing a 50kb genomic DNA sequence encompassing the TSLP coding and flanking sequences was processed along as a positive control for efficiency of ligation (TSLP BAC).

Figure S2. Mutational analysis of the canonical IR2 nGRE motif, related to Figure 2.

Luciferase assay in A549 cells treated as indicated in Figure 2B, show the in vitro functionality of various mutant IR2 nGRE elements bearing a 1 base substitution as indicated. Sequence of the canonical IR2 nGRE and its mutants are listed as numbers 1 to 28 in the right panel. Circled numbers in the graph indicate the mutations that abolish the ability of nGRE to inhibit luciferase expression. Big letters in the lower panel indicate the sequence of canonical residues and smaller letters indicate “tolerable” base substitutions at different positions.

Figure S3. Glucocorticoid-induced repression of mouse genes that contain IR0, IR1 or IR2 nGREs conserved in mouse and human orthologues, related to Figure 3.

(A) ChIP assay of mouse epidermis and intestinal epithelium WCE topically-treated or intraperitoneally-injected with dexamethasone (Dex) for 6 or 18 hours with the indicated antibodies. PCR amplification was done using primers flanking the IR1 nGRE regions of NKRF and BCL2L1 genes.

(B) Expression of putative IR0 nGRE-containing genes in WT mice topically-treated with Dex and/or RU for 18 hours (mean ± SEM). Relative RNA levels were determined by Q-PCR of epidermal RNA (mean± SEM).

(C) As under (B), but using intestinal epithelium of WT mice intraperitoneally-injected with Dex and/or RU for 18 hours (mean ± SEM).

(D) Luciferase assay to test the in vitro functionality of conserved IR0 nGREs present in mouse and human orthologues. A549 cells were transiently transfected with the pGL3 vector (see fig. 2A) containing a consensus VDRE and IR0 nGREs from different genes (as indicated). Cells were treated with VD3 and/or FA as indicated, for 6 hours. Luciferase activity was normalised and expressed as relative light units (mean ± SEM).

(E) ChIP assays of mouse skin epidermis and intestinal epithelium WCE showing FA and Dex-induced binding of GR and corepressors to the nGRE regions of genes (analyzed in panel B and C) exhibiting an IR0 nGRE motif.

(F) Expression of IR2 nGRE-containing genes in epidermis of WT mice topically-treated with dexamethasone (Dex) and/or RU for 18 hours (mean ± SEM). Relative transcript levels were determined by Q-PCR of epidermal RNA (mean± SEM).

(G) As under (F), but using intestinal epithelium of WT mice intraperitoneally-injected with Dex and/or RU for 18 hours (mean ± SEM).

(H) Luciferase assay to test the in vitro functionality of conserved IR2 nGREs present in mouse and human orthologues. A549 cells were transiently transfected with the pGL3 vector (see fig. 2A) containing a consensus VDRE and IR2 nGREs from different genes (as indicated). Cells were treated with VD3 and/or FA as indicated, for 6 hours. Luciferase activity was normalised and expressed as relative light units (mean ± SEM).

(I) ChIP assays of mouse skin epidermis and intestinal epithelium WCE showing FA and Dex-induced binding of GR and corepressors to the nGRE regions of genes (analyzed in panel F and G) exhibiting an IR2 nGRE motif.

EXTENDED EXPERIMENTAL PROCEDURES.

Materials. GR (SC-1004X, used in ChIP assay), P65 (SC-372X), pan-RAR (SC-773X), HDAC3 (SC-11417X) and SRC3 (SC-9119X) rabbit polyclonal antibodies were from Santacruz Biotechnology. Control rabbit IgG (ab46540), SRC1 (ab84) mouse monoclonal, HDAC1 (ab7028), HDAC2 (ab7029) and GR (ab3671, used in supershift assay) rabbit polyclonal antibodies were from Abcam. RNA polymerase II (05-623) mouse monoclonal antibody was from Millipore Corporation. SMRT, NCoR and TIF2 (SRC2) mouse monoclonal antibodies, and VDR rabbit polyclonal antibodies were generated in-house. All in-house generated antibodies were tested by ELISA, immunoprecipitation, western blotting and absence of reaction in null mutant mice to ensure specificity. All other antibodies were tested by immunoprecipitation and western blotting. Active vitamin D3 [1α, 25 (OH)2 Vitamin D3,], Fluocinolone acetonide (FA), Dexamethasone, RU 486, all trans retinoic acid (RA) and BAY 11-7082 were from Sigma Aldrich. MC 903, JNK inhibitor II and recombinant human IL-1β was from Leo pharma, Calbiochem and R&D systems, respectively. RU24858 was a gift from Dr. Hinrich Gronemeyer. Source of all other materials is indicated in parentheses at appropriate places.

Mouse genotyping. Wild type BALB/c ByJ and C57BL/6J female mice, 6-8 week-old, were purchased from Charles River Laboratories. K14-Cre-ERT^2/floxed RXRαβ (RXRα $^{L2/L2}$ RXRβ $^{L2/L2}$) and K14-Cre-ERT^2/ floxed GR (GR$^{L2/L2}$) mice (6-8 weeks-old) were intraperitoneally injected with 0.1mg tamoxifen for 5 days to ablate RXR α and β (RXRαβ$^{ep-/-}$ mice) or GR (GR$^{ep-/-}$ mice) in keratinocytes. Genotyping of RXRαβ$^{ep-/-}$ mutants was as described (Li et al., 2005). Primer pairs BAD837/BAD838 were used to detect GR L2 alelle (347 bp) and GR wild type (208 bp), while AED182/BAD838 primers were used to detect GR L- allele (193 bp) and GR wild type allele (1115 bp) bands. Primer sequences are given below.

GR genotyping primers	**Sequence**
BAD837	5' GACTGACAAAATCAGTGACCCTGGG
BAD838	5' GTCAACACATGATCACCTTGCAGTC
AED182	5' CCAGAGAACTAATTGGCTCTTGCAC

ChIP assay. ChIP assay was as reported (Vaisanen et al., 2005) with few modifications. Formaldehyde was added to epidermal or intestinal epithelial cells in suspension to a final concentration of 1% and incubated on a flip-flop rocker for 10 minutes at room temperature, followed by addition of 2M glycine (0.125M final concentration) and incubation for 5 minutes (room temperature). Cells were pelleted (400g, 5 minutes) at 4 ^{0}C, washed twice in ice-cold PBS, followed by lysis. Similarly, pancreas and liver tissues were dissected from vehicle or dexamethasone injected mice, washed in ice cold PBS, cut into small pieces and kept in PBS. Formaldehyde was added [1% final concentration (v/v)] to the PBS containing tissues and incubated on a flip-flop rocker for 10 minutes at room temperature, followed by addition of 2M glycine (0.125M final concentration) and incubation for 5 minutes (room temperature). Tissues were pelleted (400g, 5 minutes) at 4 ^{0}C, washed twice in ice-cold PBS and resuspended in 300µl ice-cold lysis buffer [50 mM Tris-HCl, pH 8.1, 1% (w/v) SDS, 10 mM EDTA, 1X protease inhibitor cocktail (Roche)]. Cross-linked epidermal cells from dorsal skin, intestinal epithelial cells, or A549 cells were also resuspended in 300µl ice-cold lysis buffer and all lysates were sonicated at 4^{0}C to generate 300-500 base pair chromatin fragments (Bioruptor sonicator, Diagenode). Cellular debri were removed by spinning (10000g,10 min) at 4 ^{0}C

and the supernatant was pre-cleared by incubating with 60 µl protein G-agarose beads (pre-blocked with salmon sperm DNA and BSA) for 20 min at 4 ^{0}C over a flip-flop rocker. Beads were pelleted (100g, 1 minute) at 4 ^{0}C and discarded. Equal amounts of lysates were used for immunoprecipitation. 10 % of the lysate amount used for each immunoprecipitation reaction was saved to be used as input DNA in PCR amplification. Individual samples were diluted 1:8 (v/v) in ChIP dilution buffer [16.7 mM Tris-HCl, pH 8.1, 0.01% (w/v) SDS, 1.1% (v/v) Triton-X 100, 1.2 mM EDTA, 16.7 mM NaCl, 1X protease inhibitor cocktail] and incubated overnight with different primary antibodies at 4 ^{0}C on a flip-flop rocker, followed by incubation with 60 µl protein G-agarose beads (pre blocked with salmon sperm DNA and BSA) for 90 minutes. Immunoabsorbed complexes were recovered by centrifugation (100g, 1 minute) at 4 ^{0}C. Protein G beads were then washed once in low salt buffer [20mM Tris-HCl, pH 8.1, 0.1% (w/v) SDS, 1% (v/v) triton X -100, 2mM EDTA, 150mM NaCl], once in high salt buffer [20mM Tris-HCl, pH 8.1, 0.1% (w/v) SDS, 1% (v/v) triton X -100, 2mM EDTA, 500mM NaCl], once in LiCl buffer [10mM Tris-HCl, pH 8.1, 250mM LiCl, 1% (v/v) NP-40, 1% (w/v) sodium deoxycholate, 1mM EDTA], and finally washed twice in 1ml TE buffer (10mM Tris-HCl, pH 8.0, 1mM EDTA). Chromatin was released from the beads by incubation with 150 µl elution buffer [1% (w/v) SDS, 100mM NaHCO3] for 15 minutes at room temperature with intermittent vortexing. The elution step was repeated and both eluates were pooled. 1 µl of 10 mg/ml RNase and 5M NaCl (200mM final concentration) was added to the eluate and incubated at 65 ^{0}C overnight. 1µl of 30mg/ml Proteinase K was then added to the samples and incubated at 50^{0}C for 1hour. DNA was subsequently purified from the eluate using Qiagen PCR purification kit (Qiagen corp.) in a final volume of 50 µl. 3 µl of the purified DNA was used as template in different PCR amplifications (Applied Biosystems Thermocycler). Sequence of the various primers is listed below. The number of PCR cycles was optimized to maintain linear amplification in all experiments. PCR products were resolved by 2% agarose gel electrophoresis. Images of ethidium bromide-stained DNA was acquired using an UV trans-illuminator equipped with a digital camera.

Primers for ChIP assay.

mTSLPnGRE fp	5' GTGGAGCACCCAACATCATC
mTSLPnGRE rp	5' CTGGTTGGGGTTTGAAAGG
hTSLPnGRE fp	5' CCCCAGGTGACAGACGTTTT
hTSLPnGRE rp	5' CCACCTTCACAGTCCCACTC
mGPX3 (+) GRE fp	5' AACCAATGCAACCAAGCACT
mGPX3 (+) GRE rp	5' AAAGAACCTGGAGACCAGGAA
mTSLP DR3d fp	5' AGGTCCAGATACTGCATGCTC
mTSLP DR3d rp	5' CAGCAGCTGATGCAAACAGA
mTSLP PP fp	5' GCATGTAGCAAGTGTTTAGGGCAGA
mTSLP PP rp	5' GCCTGAACGTGGAGTCTTCCTGAT
mTSLP DR2b fp	5' TGAGGTATTTTATCAGAACAATGGAC
mTSLP DR2b rp	5' CCAAGTGCTGGGATTAAAGG
hGILZ (+) GRE fp	5' AGCCAAATGCAGTCTGAAGG
hGILZ (+) GRE rp	5' CACATGTCTTAGTGCAAACACC
mTNFRSF19 fp	5’ AGAAACGGTGGGATTCTGTT
mTNFRSF19 rp	5’ AGCCTGGCTTGGGTATTTTT
mK14 fp	5’ GGGGGCACGGTAAGAGATAG
mK14 rp	5’ GAAAGGGGTGAGCATGAGAA
mHSD11B2 fp	5' TCTCCATAGAGACGGCGAGT
mHSD11B2 rp	5’ TGGCCTCTGGTTGACTCTCT
mPRKCB fp	5’ CTGCAGACCTTGGTGTGTGT
mPRKCB rp	5’ AGATGAGCACCTCGGTTGAT
mCYP26A1 fp	5’ GCTCATCCTCAAAGCGACAT
mCYP26A1 rp	5’ TGGCCCTCTTACTGTGTCTTG
mUSF1 fp	5’ CAAACCACAGTTTGCCAAGA
mUSF1 rp	5’ TGCTACAAGGAGGGGTTCTG
mJUND fp	5’ GGTTAGGCCAAAGCAACAAA
mJUND rp	5’ CTCCCTCCAGCCTCATAAAA

mGBA2 fp	5’ GTGGGCAGCACTTCACTGTA
mGBA2 rp	5’ CTGCCTCCACTTGCTGTGT
mRDH11 fp	5’ CGCTGTCTCCCAGACAAAAT
mRDH11 rp	5’ TGGCGGTGATACATTCAGAG
mBTG2 fp	5’ CCAGACCGTCATCATCGTT
mBTG2 rp	5’ TAAAGACACCCCAGGCAAGA
mBCL2L1 fp	5’ ACCCCCTCGCTCTAGCAC
mBCL2L1 rp	5’ ATCACAGATCCGAGGCTGTC
mNKRF fp	5’ TTGTTATGTTTATGGTTCCCTTGA
mNKRF rp	5’ AACTGCAATGGGCTGTGTTT
mNEU1 fp	5’ AGGAACTGTAGAGGACCACAGG
mNEU1 rp	5’ TCCTCTGTCAGGATCCAACC
mCCND1 fp	5’ CACAGGAGCTGGTGTTCCAT
mCCND1 rp	5’ CACACGGACTACAGGGGAGT
mTRPM7 fp	5’ GCTCCGTACCATTCTCCTCA
mTRPM7 rp	5’ GCTGGTCGCACAATTATGAA
mTCF25 fp	5’ ACACTGCTGCTCTTCCTCGT
mTCF25 rp	5’ GGTTGTTGACACGGACTCCT
mNDUFA4L2 fp	5’ AACACTGGAAATGCAGAGCA
mNDUFA4L2 rp	5’ AGGTGAGGGAAAGCGAGAGT
mSPARC fp	5’ CCTCAGTCAGTGCTCAGTGG
mSPARC rp	5’ AGACAGCCTGGGACCAGAT
mADAMTS19 fp	5’ CTGCCCAGCAAGAGGAAC
mADAMTS19 rp	5’ TAAAAGCAGGAGGCATCTGG
mDPAGT1 fp	5’ AGAAAATGCTGGGCCAACT
mDPAGT1 rp	5’ GCCTGACACTGTTCCCTGTT

mPOMGNT1 fp	5’ CCTCCTGAGAGCTGGGATT
mPOMGNT1 rp	5’ GGAGGAGCTCAGTGTGACTGT
mFKBP2 fp	5’ TGGCTCCCATCACACTTACA
mFKBP2 rp	5’ AGGCTGAAGGAGCTGAATGA
mPRKRA fp	5’ GCGAAGCTGACAAGTACCAA
mPRKRA rp	5’ TCCATACAACCCCTGTTAGGTT
mRORA fp	5’ TCTCCGCCGATCTCTACATT
mRORA rp	5’ GTCGCAGCGTCTCCTACCT
mFOXJ1 fp	5’ GGACCGGCATTAAGTAGACG
mFOXJ1 rp	5’ GCGGGAATGCACAGAGTC
mRDH5 1 fp	5’ TGCCTGGCTGAAGTTAGGTT
mRDH5 1 rp	5’ GGCTGTGCTAAGCAGTGTCA
mMUC20 fp	5’ TCTAGCCCCAGTCTGGATTTT
mMUC20 rp	5’ TGCAATTTGTAATCCCAGCA
mSLC25A34 fp	5’ GATGGAAGCTTCATGGATGG
mSLC25A34 rp	5’ AGGTCGACTGGAGAGCTGAG
mK5nGRE1 fp	5’ GTAGGCAGCATCCACATCCT
mK5nGRE1 rp	5’ GTCCCTTTGACCACCAGGTA
mK5nGRE2 fp	5’ CAAACACACACACACACACACA
mK5nGRE2 rp	5’ CTGGGATTGGAGTGTGGCTA
mK5nGRE3 fp	5’ CAGGTCTCCTTTCCCATCC
mK5nGRE3 rp	5’ TTGGAGGATCATGGGAAGTC
mins IR1 nGRE fp	5’ ATGTTATGCCTTGAGCATGTTT
mins IR1 nGRE rp	5’ ACCTTGGAAAGGCCTTAGGT
mins IR2 nGRE fp	5’ TTACTGGGGCCTTAGGCTTT
mins IR2 nGRE rp	5’ AGGCCACAGTGAGACCTTTG
minsr nGRE1 fp	5’ ACCCTCTCCAGGGTACAGGT

minsr nGRE1 rp	5’ CGTGGAAGAGAAGGACGTG
minsr nGRE2 fp	5’ TGTTGAAGCTTTGGGGAAAT
minsr nGRE2 rp	5’ GAGGACGAGGAGGAGAGGAG
mrev- erb alpha nGRE1 fp	5’ GGGGCCAATGGATTGTAAG
mrev- erb alpha nGRE1 rp	5’ AAGTAGGGGCTCTGGGGTTA
mrev- erb alpha nGRE2 fp	5’ CAGGCTGGATGAATTTCTGG
mrev- erb alpha nGRE2 rp	5’ ATATCGCTCACTCCCCTGCT
pGL3 VDRE/nGRE luc fp	5’ TGGACAGTCGTCACAGTCATC
pGL3 VDRE/nGRE luc rp	5’ CCTCGGCCTCTGCATAAATA
NF-κB luc proximal promoter fp	5’ CTAACTGGCCGGTACCTGAG
NF-κB luc proximal promoter rp	5’ GCTGGGCCCTTCTTAATGTT

Primers used in Figure 1H ChIP assays to detect colocalization of GR and its corepressors.

Figure 1H primer 1 fp	5' GCAGGACTCCAGAAAAGTCC
Figure 1H primer 1 rp	5' CCCAGTTCTCTGGCATTAGG
Figure 1H primer 2 fp	5' CTGCCACCGCTACAATCTTT
Figure 1H primer 2 rp	5' GATTCTATTCGGGGGAAAGC
Figure 1H primer 3 fp	5' GCTTTCCCCCGAATAGAATC
Figure 1H primer 3 rp	5' GCTCAGAACGATGATGTTGG
Figure 1H primer 4 fp	5' CACCCAACATCATCGTTCTG
Figure 1H primer 4 rp	5' CCTCCTGAGACCCAGTTCAC
Figure 1H primer 5 fp	5' GGGGAGAGTGAACTGGGTCT
Figure 1H primer 5 rp	5' CAGTACTGGGAGCAGGAAAGA
Figure 1H primer 6 fp	5' GTACTGTACTGGCGCTGCTC
Figure 1H primer 6 rp	5' GGTTGGGGTTTGAAAGGAAG
Figure 1H primer 7 fp	5' CTTCCTTTCAAACCCCAACC
Figure 1H primer 7 rp	5' TCAGCCAGTAAATCGTTGGA

Nuclear run-on assay. pSK+ empty vector and pSK+ β actin (2 kb β actin cDNA cloned into pSK+ vector at EcoRI, BamHI sites) plasmids were linearised by digestion with BamHI. A 4 kb region of mouse TSLP gene coding sequence was amplified by PCR from a BAC construct (Invitrogen) [forward primer: 5'-AGTTCTTCTCAGGAGCCTCTTCATC-3' (+165 to +190 with respect to 'A' of the translation initiation codon ATG as +1), reverse primer: 5'-CCAGATTCCACAATCTTCTTTCAGA-3' (+4157 to +4181 with respect to 'A' of ATG as +1)]. Approximately 10 µg each of pSK+ empty vector, pSK+ β actin and TSLP DNA was separated by 0.8% agarose gel electrophoresis, and transferred to 0.45µm nitrocellulose membranes. Membranes containing the transferred DNA probes were baked for 2 hours at 80 ^{0}C in a vacuum oven, followed by washing in 2X SSC.

Run-on assay was as described (Carey and Smale., 2001). Approximately 10^8 epidermal cells were resuspended in 5 ml ice cold NP-40 lysis buffer [10 mM Tris-HCl, pH 7.4, 10 mM NaCl, 3 mM MgCl2, 0.5% (v/v) NP-40] and incubated for 5 minutes on ice. Nuclei were pelleted (100g, 10 minutes) at 4 ^{0}C. The nuclear pellet was resuspended in 250 µl of nuclear freezing buffer [50 mM Tris-HCl, pH 8.3, 40% (v/v) glycerol, 5 mM MgCl2, 0.1 mM EDTA]. 225 µl of the nuclei were added to 60 µl of 5X run-on buffer [25 mM Tris-HCl, pH 8.0, 12.5 mM MgCl2, 750 mM KCl, and 12.5 mM each of ATP, GTP and CTP]. 150 µCi of α-[^{32}P] UTP was added and the reaction was incubated at 37 ^{0}C for 30 minutes. 20 µl of 10 mM CaCl2 and 10 µl of 1 mg/ml of RNase-free DNase were added and incubated at 30 ^{0}C for 5 minutes, followed by addition of 35 µl of proteinase K buffer [10% (w/v) SDS, 50mM EDTA, 10mM Tris-HCl, pH 7.4, 3 mg/ml proteinase K] and incubation at 37 ^{0}C for 45 minutes. Reaction mixture was extracted twice with phenol-chloroform and once with chloroform, followed by 1:1 dilution with 5 M ammonium acetate and precipitation with isopropanol. Precipitated pellet was resuspended in 100 µl TE (pH 8.0) followed by addition of 100 µl solution containing 10 mM MgCl2 and 5 mM CaCl2. 10 µl of 1 mg/ml RNase-free DNase was added and reaction mix was incubated at 37 ^{0}C for 5 minutes followed by chilling on ice for 5 minutes. 50 µl of 1N NaOH was added and the reaction mixture was incubated on ice for another 2 minutes. Alkali was neutralized by addition of 77µl of 1M HEPES (free acid) followed by precipitation of RNA in isopropanol and resuspension in 100 µl TE. 90 µl of the radiolabelled RNA was hybridised to the nitrocellulose filter containing the above DNA

probes for 24 hours at 65 ^{0}C in 2 ml hybridization buffer [6X SSC, 5X Denhardt's reagent, 50% formamide, 0.5% (w/v) SDS, 200 µg salmon sperm DNA, 2 µg polyA]. Membrane was washed 4 times in 2X SSC, excess liquid removed, wrapped in saran and exposed to X-ray films for 48 hours in presence of an intensifying screen at -70 ^{0}C.

Chromosome conformation capture (3C) assay. 3C assay was as described (Liu et al., 2005). Formaldehyde cross-linked or not-cross linked (negative control for ligation efficiency) epidermal cells (10^7 cells, see epidermis isolation section) were resuspended in lysis buffer [10mM Tris-HCl, pH 8.0, 10mM NaCl, 0.2% (v/v) NP-40, and 1X protease inhibitor cocktail] and incubated for 5 minutes on ice, followed by centrifugation (100g, 10 minutes) at 4 ^{0}C. The nuclear pellet was resuspended in 200µl digestion buffer [1X Nla III or Alu I restriction enzyme digestion buffer (NEB) + 0.3% (w/v) SDS] and incubated at 37 ^{0}C for 1 hour on a flip-flop rocker. 1.8% (v/v) triton X-100 (final concentration) was then added to the samples and incubated for 1 hour under similar conditions. Precipitate was removed by short spinning. 400 units Nla III or Alu I restriction enzyme (NEB) was added and incubated at 37 ^{0}C for 2 hours, followed by addition of another 200 units of the respective enzymes and overnight incubation at 37 ^{0}C. Restriction enzyme was inactivated by addition of SDS (1.6% v/v, final concentration) and incubation at 70 ^{0}C for 20 minutes. SDS was quenched by addition of triton X-100 (1% v/v, final concentration) and 1 hour incubation at 37 ^{0}C. Individual samples were then diluted 12 times in ligase buffer (final DNA concentration approximately 3 ng/µl). Ligation was done for 4.5 hour at 16 ^{0}C followed by 30 minute incubation at room temperature using 400units T4 DNA ligase (NEB). For mock-ligated sample, no ligase was added. Next, 1µl of 10mg/ml RNase and 5M NaCl (final concentration 200mM) were added to the samples which were incubated overnight at 65 ^{0}C. Proteinase K (200µg/ml) was added to the samples, which were incubated for 30 minutes at 50 ^{0}C, and DNA was purified by phenol-chloroform extraction and isopropanol precipitation. DNA amount was estimated by spectrophotometry and equal amounts of DNA were used for PCR amplification (primer sequences are listed below). PCR-amplified DNA was separated by 2% agarose gel electrophoresis, followed by Southern hybridization (Sambrook et al., 1989) to a probe designed to contain 20 nucleotides on each side (5' and 3', probe length: 40 nucleotides) of a possible junction between 2 Nla III or Alu I fragments of the TSLP gene region of interest (see Figure 1 F and Figure

S1 I). The probe was 5'- end labelled using γ- [^{32}P] ATP and purified through sephadex G-50 column to remove free γ- [^{32}P] ATP. As a positive control for Nla III and Alu I digestion, ligation, PCR amplification and Southern hybridization, a BAC DNA encompassing the region of interest was simultaneously processed (denoted as TSLP BAC).

Primers and probes for chromosome conformation capture (3C) assay

Junctions	PCR primers/southern probe sequence	Product length
Nla III fragments C and E	Forward primer: -1208 CTTCCTTTCAAACCCCAACC -1189	260bp
	Reverse primer: -93 AGGCCAATGATTTTCCTTGA -112	
	Southern probe: 5'- **TCGTGCTGCTGGGAC<u>GCATG</u>**TAGCAAGTGTTTAGGGCAGA -3' (-1130 to -1111) (-313 to -294)	
Nla III fragments A and E	Forward primer: -7267 GCTGGGTGAAACCTCTTTGA -7248	249bp
	Reverse primer: -93 AGGCCAATGATTTTCCTTGA -112	
	Southern probe: 5'- **GAGGCCGGCTCTCTC<u>CCATG</u>**TAGCAAGTGTTTAGGGCAGA -3' (-7207 to -7188) (-313 to -294)	
Nla III fragments A and C	Forward primer: -7365 CCTCTGGCTCCCTCAATTCT -7346	260bp
	Reverse primer: -1640 CCCAGTTCTCTGGCATTAGG -1659	
	Southern probe: 5'- **GAGGCCGGCTCTCTC<u>CCATG</u>**GTATCATAACCTAAATTTAA -3' (-7207 to -7188) (-1775 to -1756)	
Alu I fragments C and E	Forward primer: -1360 GGCTGAGCTCCAGGAGAGTA -1341	247bp
	Reverse primer: -87 TCCCCTAGGCCAATGATTTT -106	
	Southern probe: 5'- **GTTGGGTTCGTGTCAAC<u>AG</u>**CTAAAAAATAAATAAATAAAT -3' (-1377 t -1316) (-294 to -272)	
Alu I fragments A and E	Forward primer: -7365 CCTCTGGCTCCCTCAATTCT -7346	301bp
	Reverse primer: -87 TCCCCTAGGCCAATGATTTT -106	
	Southern probe: 5'- **CCACATCTGTTTGCATC<u>AG</u>**CTAAAAAATAAATAAATAAAT -3' (-7288 to -7268) (-294 to -272)	

Electrophoretic mobility shift assay (EMSA). Synthetic oligonucleotides encompassing different DNA elements were annealed and double-stranded oligonucleotides were purified by 15%

polyacrylamide gel electrophoresis. 50ng of purified oligonucleotides were 5'-end labelled using γ-[^{32}P] ATP which was removed by purifying the probe through sephadex G 50 column. 8 fmoles of probe was mixed with 250ng recombinant human GR protein (ab3582, abcam) in EMSA buffer [20mM hepes, pH 7.9, 60mM KCL, 5mM MgCl2, 2mM DTT, 10% (v/v) glycerol, 200ng poly dI-dC]. The reaction mixture was incubated at room temperature for 20 minutes. Rabbit polyclonal human GR antibody (ab3671, abcam) or rabbit control IgG (ab46540, abcam) was added to the reaction mixture and incubation was continued for 20 minutes. Samples were electrophoresed on a 4.5% non-denaturing polyacrylamide gel in TBE buffer (90mM Tris-borate, 2.5mM EDTA, pH 8.3). Vacuum-dried gels were exposed to X-ray film overnight at -70 ^{0}C in the presence of an intensifying screen. In the case of competitor binding assay with a cold oligonucleotide probe, the excess amount of cold probe, which was added to the reaction mixture together with the [^{32}P]- labelled probe, is indicated in the figure (10X, 25X, 50X).

Probes used for EMSA.

TAT (+) GRE U (5'→3')	5' AGAGGATCTGTACAGGATGTTCTAGAT
TAT (+) GRE L (3'→5')	5' ATCTAGAACATCCTGTACAGATCCTCT
Mutant (+) GRE U	5' AGAGGATCTCAACAGGATCATCTAGAT
Mutant (+) GRE L	5' ATCTAGATGATCCTGTTGAGATCCTCT
hTSLP nGRE U	5' CTGCGCCGCCTCCGGGAGAGCTGAGCTT
hTSLP nGRE L	5' AAGCTCAGCTCTCCCGGAGGCGGCGCAG
mTSLP nGRE U	5' CTGGCTGAGCTCCAGGAGAGTAGGGGT
mTSLP nGRE L	5' ACCCCTACTCTCCTGGAGCTCAGCCAG
Mut1 mTSLP nGRE U	5' CTGGCTGAGAGAAAGGAGAGTAGGGGT
Mut1 mTSLP nGRE L	5' ACCCCTACTCTCCTTTCTCTCAGCCAG
Mut2 mTSLP nGRE U	5' CTGGCTGAGAACCAGGAGAATAGGGGT
Mut2 mTSLP nGRE L	5' ACCCCTATTCTCCTGGTTCTCAGCCAG
Mut3 mTSLP nGRE U	5' CTGGCTGAGCTCCAAAGAAGTAGGGGT
Mut3 mTSLP nGRE L	5' ACCCCTACTTCTTTGGAGCTCAGCCAG

Cell culture experiments. A549 human lung epithelial cells (CCL-185, ATCC) were maintained in DMEM/HAM F12 (1:1) medium containing 10% foetal calf serum (FCS) and gentamycin. Cells were transfected using Fugene 6 reagent, as instructed (Roche). For RNA isolation from A549 cells, cells were seeded at 50% density in 60mm plates. 24 hours post-seeding, complete medium was replaced with medium containing charcoal-treated serum. 24 hours later, 1μM active vitamin D3 [1α, 25 (OH)2 Vitamin D3,], 300 nM FA, 4.5 μM RU486 (final concentration) or vehicle (acetone) were added to the medium for 6 hours. RNA was isolated using TRI reagent (MRC Inc) following manufacturer's protocol.

For ChIP assay, cells were cross-linked by adding formaldehyde (1% final concentration) to the medium and incubation on a rotary shaker for 10 minutes at room temperature. Cross-linking was stopped by adding 2M glycine (0.125M final concentration) and incubation for 5 minutes under similar condition, followed by 2X washing in ice-cold PBS. Cells were scraped using a rubber policeman, pelleted (400g, 5 minutes) at 4 ^{0}C, washed once in ice-cold PBS, snap frozen in liquid nitrogen and stored at -70 ^{0}C before proceeding for ChIP assay.

For ChIP assays to test GR and cofactor binding to the nGRE, +GRE or NF-κB region of various luciferase reporter plasmids, ~60% confluent A549 cells in 100mm TC dish were transfected with 2μg of respective plasmids using fugene 6 reagent (Roche) and maintained in charcoal treated FCS containing medium. 44 hours post-transfection, 500nM FA or Dex or RU24858 and/or 7.5μM RU 486, 5ng/ml IL-1β (final conc.) was added to the medium for 4 hours, followed by formaldehyde treatment and processing as described above.

Luciferase reporter plasmids (see Figure 2A and 5A).

Oligonucleotides were designed in which (+) GRE and various putative IR nGRE elements and their mutants are flanked by Sma I and Bgl II sites at their 5' and 3' ends, respectively (sequences listed below). 5'-ends of these oligonucleotides were phosphorylated using T4 polynucleotide kinase and annealed to make double stranded oligonucleotides. pGL3 promoter vector (Promega) which contains

a SV40 enhancerless early promoter upstream of the luciferase coding region, was linearised with Sma I and Bgl II and double stranded oligonucleotides were ligated into it. These plasmids were named as pGL3 (+) GRE and pGL3 IR0, IR1 or IR2 nGRE.

Two tandem copies of consensus VDRE (VDR response element) was inserted into the pGL3 vector or pGL3 (+)GRE and pGL3 nGRE vectors, upstream of the (+)GRE or nGRE element (see Figure 2A). In order to separate the VDRE and GRE, a 314 bp DNA fragment was inserted between them. This 314 bp fragment was amplified from the mouse TSLP upstream region (-5359 to -5046 base pairs considering "A" of translation initiation codon ATG as +1) using primers that contained a KpnI restriction site and the VDRE sequence in the forward primer (5' CATAGGTACCAGGTCAGAGAGGTCAACCACTAGAAGACAGGTCAGAGAGGTCATGTGGAAATCA AAGGAAAGGA) and a SacI restriction site in the reverse primer (5' TACCGAGCTCGCAGTGCCTGTGTGCTCTTA). Bioinformatics analysis of this region did not indicate the presence of binding sites for any known transcription factor. PCR was carried out using a BAC encompassing the region of interest as template. The PCR product was digested with KpnI and SacI restriction enzymes and cloned into pGL3, pGL3 (+) GRE and pGL3 IR0, IR1, IR2, IR3, IR4 or IR5 nGRE plasmids digested with the same enzymes. These plasmids were named as pGL3 VDRE, pGL3 VDRE/(+)GRE and pGL3 VDRE/IR0, IR1, IR2, IR3, IR4 or IR5 nGRE.

pGL4 NFκB luc plasmid (pGL4.32 [luc2P/NFκB-RE/Hygro]) which contain 5 tandem copies of consensus NFκB response element upstream of a SV40 minimal promoter, was purchased from Promega. In order to construct the pGL4 AP1 luc plasmid, 6 tandem copies of consensus AP1 response element containing oligonucleotide was cloned into pGL4 (pGL4.27[luc2P/minP/Hygro]) vector (promega) at XhoI and Bgl II site. All the clones were verified by sequencing. Oligonucleotide sequences are given below.

Luciferase reporter cloning oligos	**Sequence**
+GRE luc assay oligo U (5'→3')	5' GGGAGAGGATCTGTACAGGATGTTCTAGATA
+GRE luc assay oligo L (3'→5')	5' GATCTATCTAGAACATCCTGTACAGATCCTCTCCC

IR1 ngre luc assay oligo U	5’ GGGGCTGAGCTCCAGGAGAGTAGGGA
IR1 ngre luc assay oligo L	5’ GATCTCCCTACTCTCCTGGAGCTCAGCCCC
IR1 ngre mut1 luc assay oligo U	5’ GGGGCTGAGAGAAAGGAGAGTAGGGA
IR1 ngre mut1 luc assay oligo L	5’ GATCTCCCTACTCTCCTTTCTCTCAGCCCC
IR0 ngre luc assay oligo U	5’ GGGGCTGAGCTCCGGAGAGTAGGGA
IR0 ngre luc assay oligo L	5’ GATCTCCCTACTCTCCGGAGCTCAGCCCC
IR2 ngre luc assay oligo U	5’ GGGGCTGAGCTCCACGGAGAGTAGGGA
IR2 ngre luc assay oligo L	5’ GATCTCCCTACTCTCCGTGGAGCTCAGCCCC
IR3 ngre luc assay oligo U	5’ GGGGCTGAGCTCCACAGGAGAGTAGGGA
IR3 ngre luc assay oligo L	5’ GATCTCCCTACTCTCCTGTGGAGCTCAGCCCC
IR4 ngre luc assay oligo U	5’ GGGGGCCCTCCAGCTGGAGAGAGGA
IR4 ngre luc assay oligo L	5’ GATCTCCTCTCTCCAGCTGGAGGGCCCCC
IR5 ngre luc assay oligo U	5’ GGGGAGCCTCCTGCATGGAGACTCAA
IR5 ngre luc assay oligo L	5’ GATCTTGAGTCTCCATGCAGGAGGCTCCCC
mJUND luc assay oligo U	5’ GGGGGTTTTCTCCGGGAGAGAGCCA
mJUND luc assay oligo L	5’ GATCTGGCTCTCTCCCGGAGAAAACCCCC
mHSD11B2 luc assay oligo U	5’ GGGCAAAGCCTCCTGGAGAATTGGA
mHSD11B2 luc assay oligo L	5’ GATCTCCAATTCTCCAGGAGGCTTTGCCC
mSOCS3 luc assay oligo U	5’ GGGGCCGCGCTCCTGGAGACCCAAA
mSOCS3 luc assay oligo L	5’ GATCTTTGGGTCTCCAGGAGCGCGGCCCC
mPRKCB luc assay oligo U	5’ GGGCCATCCCTCCAGGAGACGCATA
mPRKCB luc assay oligo L	5’ GATCTATGCGTCTCCTGGAGGGATGGCCC
mUSF1 luc assay oligo U	5’ GGGATGGGACTCCTGGAGAAAAAGA
mUSF1 luc assay oligo L	5’ GATCTCTTTTTCTCCAGGAGTCCCATCCC
mBCL2l1 luc assay oligo U	5’ GGGATACCTCCGGGAGAGTTCA
mBCL2l1 luc assay oligo L	5’ GATCTGAACTCTCCCGGAGGTATCCC
mNKRF luc assay oligo U	5’ GGGTGGACTCCTGGAGAGAGGA

mNKRF luc assay oligo L	5’ GATCTCCTCTCTCCAGGAGTCCACCC
mCCND1 luc assay oligo U	5’ GGGCGCGCTCCGGAGACCGGA
mCCND1 luc assay oligo L	5’ GATCTCCGGTCTCCGGAGCGCGCCC
mCITED1 luc assay oligo U	5’ GGGACTGCTCCGGAGACACTA
mCITED1 luc assay oligo L	5’ GATCTAGTGTCTCCGGAGCAGTCCC
mRBP3 luc assay oligo U	5’ GGGGACCCTCCGGAGAAATGA
mRBP3 luc assay oligo L	5’ GATCTCATTTCTCCGGAGGGTCCCC
mNEU1 luc assay oligo U	5’ GGGATCACTCCGGAGACTGAA
mNEU1 luc assay oligo L	5’ GATCTTCAGTCTCCGGAGTGATCCC
mGUCA2B luc assay oligo U	5’ GGGTCATCTCCTAGGAGATCTGA
mGUCA2B luc assay oligo L	5’ GATCTCAGATCTCCTAGGAGATGACCC
mFOXJ1 luc assay oligo U	5’ GGGCGGTCTCCTTGGAGACGTAA
mFOXJ1 luc assay oligo L	5’ GATCTTACGTCTCCAAGGAGACCGCCC
mFKBP2 luc assay oligo U	5’ GGGTCTGCTCCAGGGAGAGTAAA
mFKBP2 luc assay oligo L	5’ GATCTTTACTCTCCCTGGAGCAGACCC
mSLC2A8 luc assay oligo U	5’ GGGCCGACTCCATGGAGATCCGA
mSLC2A8 luc assay oligo L	5’ GATCTCGGATCTCCATGGAGTCGGCCC
mRORA luc assay oligo U	5’ GGGCGGGCTCCAGGGAGACCCCA
mRORA luc assay oligo L	5’ GATCTGGGGTCTCCCTGGAGCCCGCCC
AP1 luc assay oligo U	5’ TCGAGTGAGTCAGTGAGTCACTGACTCACTGACT CATGAGTCAGCTGACTCA
AP1 luc assay oligo L	5’ GATCTGAGTCAGCTGACTCATGAGTCAGTGAGT CAGTGACTCACTGACTCAC

Luciferase reporter assay. A549 cells seeded on 24-well tissue culture plates overnight at 70% confluency were transfected with 100 ng pCMV β galactosidase, 200 ng pGL3 reporter plasmids and

wherever indicated, with 600 ng pSG5 hVDR plasmid (Green et al., 1988) into each well and maintained in medium containing charcoal treated FCS. 24 hours post-transfection, medium was changed and different compounds were added to it for 6 hours. Final concentrations of the compounds are: FA, 500nM; Dex or RU24858, 300nM or 500 nM (wherever 300nM Dex or RU was used, it is indicated in the figure, in all other cases, 500nM concentration was used); active vitamin D3, 1μM; IL-1β, 5ng/ml; BAY 11-7082, 5μM, JNK inhibitor II, 25μM . Luciferase assay was carried out as instructed (Promega). Normalized values are reported as the mean ± SEM; each value originates from at least three individual transfections with assays performed in duplicate.

RNA isolation, Reverse transcription and real time PCR analysis. For RNA isolation from whole ears, liver, pancreas and adrenal, respective tissues were cut and immediately frozen in liquid nitrogen and stored at -70 ^{0}C until further use. For RNA isolation from ear epidermis, epidermis was separated from the dermis by splitting the ear longitudinally and incubating in 0.8% trypsin solution (0.8% trypsin (w/v) in PBS) at 4 ^{0}C for 2 hours. Epidermal sheets were recovered by using a forcep, directly put in TRI reagent (MRC Inc) at room temperature and used for RNA isolation as per the manufacturer's instruction. Similarly, RNA was isolated from intestinal epithelial cells using TRI reagent. Reverse transcription and Real time PCR analysis was done as described (Li et al., 2005). Primer sequences are listed below.

Primers used for real time PCR analysis.

Forward and reverse primers	**Sequence**
mHPRT fp	5' GTTGGATACAGGCCAGACTTTGTTG
mHPRT rp	5' GATTCAACTTGCGCTCATCTTAGGC
mTSLP fp	5' AGCTTGTCTCCTGAAAATCGAG
mTSLP rp	5' AGGTTTGATTCAGGCAGATGTT
mCYP24A1 fp	5' CCAGCGGCTAGAGATCAAAC
mCYP24A1 rp	5' CCCCATAAAATCAGCCAAGA

mGPX3 fp	5’ ATTCTACCCCACCCCAGATT
mGPX3 rp	5’ AGTTGTGCCAGGCTTGTCTT
hGAPDH fp	5’ GAGTCAACGGATTTGGTCGT
hGAPDH rp	5’ TTGATTTTGGAGGGATCTCG
hTSLP fp	5’ CCAGGCTATTCGGAAACTCA
hTSLP rp	5’ TGGTGCTGTGAAATATGACCA
hCYP24 fp	5’ GGCAACAGTTCTGGGTGAAT
hCYP24 rp	5’ TATTTGCGGACAATCCAACA
hGILZ fp	5’ AGCCAAATGCAGTCTGAAGG
hGILZ rp	5’ CACATGTCTTAGTGCAAACACC
mCOX2 fp	5’ TTCAAAAGAAGTGCTGGAAAAGGT
mCOX2 rp	5’ GATCATCTCTACCTGAGTGTCTTT
mIL4 fp	5’ GGCATTTTGAACGAGGTCAC
mIL4 rp	5’ AAATATGCGAAGCACCTTGG
mIL6 fp	5’ GAGGATACCACTCCCAACAGACC
mIL6 rp	5’ AAGTGCATCATCGTTGTTCATACA
mIL10 fp	5’ TGCTATGCTGCCTGCTCTTA
mIL10 rp	5’ TCATTTCCGATAAGGCTTGG
minsr fp	5’ AGACCAACTGTCCTGCCACT
minsr rp	5’ ACACACTTGGTGGGGTCATC
mins fp	5’ TGGAGGCTCTCTACCTGGTG
mins rp	5’ TCTACAATGCCACGCTTCTG
mRev-erb alpha fp	5’ AGCCACCCCAAGACCTTACT
mRev-erb alpha rp	5’ CGGTCATTCAAACTGGACCT
mMC2R fp	5’ TGACAAAGCCAAGGAGAGGA
mMC2R rp	5’ TGGTGTTTGCCGTTGACTTA
mMRAP fp	5’ GAAGCTGAAAGCCAACAAGC
mMRAP rp	5’ GAACATATTGGCTGGGGTTG

mK5 fp	5’ ACCTCCTCACCCCTCTGAAC
mK5 rp	5’ CACTTGGTGTCCAGGACCTT
mK14 fp	5’ CAGCCCCTACTTCAAGACCA
mK14 rp	5’ GGCTCTCAATCTGCATCTCC
mCYP26A1 fp	5’ TTCGGGTTGCTCTGAAGACT
mCYP26A1 rp	5’ TCCTCCAAATGGAATGAAGC
mPRKCB fp	5’ CCACTGCACCGACTTCATC
mPRKCB rp	5’ CATACAGCAGCGATCCACA
mSTRA13 fp	5’ CCATTTGCACTTCAGGGATT
mSTRA13 rp	5’ GCACTTTCTCCAGCTGATCC
mTNFRSF19 fp	5’ CACACACATTTTTGGGAAGG
mTNFRSF19 rp	5’ AAGAGAATGGCAGCGAAGAG
mUSF1 fp	5’ AAGGGGCAGCAGAAAACAG
mUSF1 rp	5’ CGTTGGGGTCAGGAAAAGT
mJUND fp	5’ ACGCAAGAACGCATCAAGG
mJUND rp	5’ CTGTTGACGTGGCTGAGGA
mBTG2 fp	5’ GTATGAGCCACGGGAAGAGA
mBTG2 rp	5’ CGGATACAGCGATAGCCAGA
mGBA2 fp	5’ CTCGGTATGGGCTTGAGGT
mGBA2 rp	5’ TGGTACATTCCAGGGTTGAG
mRDH11 fp	5’ ACTTGGTCACGCCAAAAATC
mRDH11 rp	5’ TCCCGGCAAGCTAAATACAC
mHSD11B2 fp	5’ GAAAGGGCCTGGATAAGAGG
mHSD11B2 rp	5’ CAGCCCCGCCTATATAGAGTT
mSOCS3 fp	5’ GGGAGCCCCTTTGTAGACTT
mSOCS3 rp	5’ GGAAACTTGCTGTGGGTGA
mBCL2L1 fp	5’ AAGTTCCCCCGGTCTCTTC
mBCL2L1 rp	5’ TGTCCAAAACACCTGCTCAC

mNKRF fp	5’ ATAGCCACGAAAGTGACTGG
mNKRF rp	5’ AAGGTTTGGGCAGCATTAGA
mSGK3 fp	5’ CAGAAGCGAGTGGTTTGTCTT
mSGK3 rp	5’ TGGATGGTTGTAAAGCTCTGG
mCCND1 fp	5’ CTCAAGACGGAGGAGACCTG
mCCND1 rp	5’ AGGAAGCGGTCCAGGTAGTT
mADAMTS19 fp	5’ TCCTCTACCAGCTAGGCTTCC
mADAMTS19 rp	5’ GATCCCGGGTCTGAGCTG
mNDUFA4L2 fp	5’ CCGGCAGATAAAAAGACACC
mNDUFA4L2 rp	5’ ACTGGTCATTGGGACTCAGG
mSPARC fp	5’ GGCCTGGATCTTCTTTCTCC
mSPARC rp	5’ CTGCACCGTCCTCAAATTCT
mNEU1 fp	5’ AGGATGACTTCAGCCTGGTG
mNEU1 rp	5’ CCTCATCGGATGCAGATTTT
mFBXL18 fp	5’ ACACATCCTGAGCCATGTCC
mFBXL18 rp	5’ CCAGTTGCTTCACCTTCTCC
mKLF5 fp	5’ CTCCGGAGACGATCTGAAAC
mKLF5 rp	5’ CTGGTCTACCACTGAGGCACT
mAIP fp	5’ ATCGCAAGACTTCGAGAGGA
mAIP rp	5’ TCGTGTTCGGCTGTCATCTA
mTCF25 fp	5’ AGGAGTCCGTGTCAACAACC
mTCF25 rp	5’ GGTCTCTGCGTTTCCATGTT
mMTG1 fp	5’ GCAGTCTGAAGTCGGTGGAT
mMTG1 rp	5’ TGCCAAGTCCATTTTGTTGA
mSLC25A5 fp	5’ ATCTCCAAGACAGCGGTAGC
mSLC25A5 rp	5’ CTGGGTGGGGAAGTATCTGA
mTRPM7 fp	5’ AAGCTCCAAAGACCCTCACA
mTRPM7 rp	5’ GTGTGCTTTTCCACAGACC

mCITED1 fp	5’ CCGATTTATCGGACTTCTGC
mCITED1 rp	5’ CGATCCAGAGGAGCTAGTGG
mMAPK4 fp	5’ TGCTCAAGATTGGGGATTTC
mMAPK4 rp	5’ CCCACATATCGATGGCTTTT
mSP9 fp	5’ CGTCTATACTTGGGGAAGAGC
mSP9 fp	5’ AGGTTGCAGCTGGACGAG
mDPAGT1 fp	5’ CTCACTGCCTCAGCTCTTCC
mDPAGT1 rp	5’ CACCGTCCTCACTCTCACCT
mCCR10 fp	5’ AAACCCTTGTAGCCAGAGATG
mCCR10 rp	5’ AGGTGGGAGATCGGGTAGTT
mFKBP2 fp	5’ TACCACAGAACCAGCCCTTT
mFKBP2 rp	5’ GCAGCTCCACCTCAAACAC
mFOXJ1 fp	5’ ACTATGCCACCAACCCACAC
mFOXJ1 rp	5’ CCTTCTCCCGAGGCACTT
mPOMGNT1 fp	5’ GTGTATGTGGCTGTGGATGG
mPOMGNT1 rp	5’ TTTGCTGTGTCCTTGAGGTG
mRDH5 fp	5’ CCTGGGAAGTCTAGGAGCAA
mRDH5 rp	5’ CAGCCAGTGATGAAGATGAAAG
mRORA fp	5’ TCAGTCACGAAGAAGACACACA
mRORA rp	5’ TCTGACGAGGACAGGAGTAGG
mSLC2A8 fp	5’ CTACCGGCATCTGTGTCCTC
mSLC2A8 rp	5’ AATGGGCTGTGACTTGTTCC
mPRKRA fp	5’ ACGGCATGAAGACCAAGAAC
mPRKRA rp	5’ AGGCATTAAGGGGTCAGGAA
mCOL4A3B fp	5’ TAGACGCCATTGAACAGCAC
mCOL4A3B rp	5’ CCATTTCAGCCAGTTTCTCAC
mGPR68 fp	5’ GGGTATGGGGCTGGATAGTT
mGPR68 rp	5’ TCCCTCTCTTGCCATCTTGT

mMUC20 fp	5’ CCACAGGCAATACAACCAAC
mMUC20 rp	5’ GTCAGCCGTACAAGGAGGAA
mSLC25A34 fp	5’ AATGGTGTCCGTTTCTACTGCT
mSLC25A34 rp	5’ CCTGATGCTGGTGCTGATG
mSOCS1 fp	5’ ACCTGAGTTCCTTCCCCTTC
mSOCS1 rp	5’ ATCTCACCCTCCACAACCAC
mTNFRSF25 fp	5’ GCTGCCAAGTCTGTGATGAA
mTNFRSF25 rp	5’ CAGATCAGGATAGCCCCAAA

Bioinformatics analysis. For identification of nGRE motifs present across the human and mouse genome, Human [hg19, Ensembl version: 56, downloaded from Ensembl (ftp://ftp.ensembl.org/pub/current_fasta/homo_sapiens/dna/] and mouse [mm9, Ensembl version: 48 (ftp://ftp.ensembl.org/pub/current_fasta/mus_musculus/dna/] repeat masked genome assembly was used. A homemade Java based application (written in Java, http://java.sun.com/) was used to parse the DNA sequences and reveal the motif CTCCNGGAGA (IR1 nGRE) with a regular expression research (Java class: Pattern, Matcher) using the pattern: CTCC[ACGT]GGAGA. By comparing with the Ensembl human and mouse gene annotations, (gene annotation: Ensembl Gene ID, Associated Gene Name, Chromosome Name, Gene Start, Gene End, chromosome strand and location), we chose the matches within -20kb upstream to 5kb downstream of the Gene Start site for each gene. 4281 genes for human and 3303 genes for mouse were thus selected (see Table 1A). Similar analysis was done using the patterns CTCCGGAGA and CTCCNNGGAGA to reveal IR0 and IR2 nGRE - containing genes, respectively. Orthologue analysis was done using the Ensembl orthologue database and genes containing conserved motifs both in human and mouse were sorted (see Table S1). Gene functional annotation was performed using DAVID programme (Huang et al., 2009).

REFERENCES

Carey, M. and Smale, S.T. (2001). Transcriptional Regulation in Eukaryotes: Concepts, Strategies, and Techniques (New York:Cold Spring Harbor Laboratory Press).

Green, S., Issemann, I., and Sheer, E. (1988). A versatile in vivo and in vitro eukaryotic expression vector for protein engineering. Nuc. Acid Res. *16*, 369.

Huang, Da.W., Sherman, B.T., and Lempicki, R.A. (2009). Systematic and integrative analysis of large gene lists using DAVID bioinformatics resources. Nat. Protoc. *4*, 44-57.

Li, M., Messaddeq, N., Teletin, M., Pasquali, J.L., Metzger, D., and Chambon, P. (2005). Retinoid X receptor ablation in adult mouse keratinocytes generates an atopic dermatitis triggered by thymic stromal lymphopoietin. Proc. Natl. Acad. Sci. USA *102*, 14795-14800.

Liu, Z. and Garrard, W. T. (2005). Long-range interactions between three transcriptional enhancers, active Vkappa gene promoters, and a 3' boundary sequence spanning 46 kilobases. Mol. Cell Biol. *25*, 3220-3231.

Sambrook, J., Fritsch, E. F., and Maniatis, T. (1989). Molecular Cloning: A Laboratory Manual, 2nd Ed. (New York : Cold Spring Harbor Laboratory Press).

Vaisanen, S., Dunlop, T. W., Sinkkonen, L., Frank, C., and Carlberg, C. (2005). Spatio-temporal activation of chromatin on the human CYP24 gene promoter in the presence of 1alpha,25-Dihydroxyvitamin D3. J. Mol. Biol. *350*, 65-77.

Table S1. Mouse and human orthologue genes containing conserved IR0, IR1 or IR2 nGREs (see Experimental Procedures), related to Table 1A and B.

Available upon request

(1) Genes containing IR0 nGREs

Species	Gene symbol	Sequence	Chromosomal location	Ensembl ID	Gene name	Description
Mouse	1110036O03Rik	aagaCTCCGGAGAaggg	chr11:100273887	ENSMUSG00000006931	1110036O03Rik	RIKEN cDNA 1110036O03 gene Gene [Source:MGI Symbol;Acc:MGI:1913430]
Human	AC130686.2	tcagCTCCGGAGAgccg	chr17:39968186	ENSG00000141696	AC130686.6	Synaptonemal complex protein SC65 (Nucleolar autoantigen No55) [Source:UniProtKB/Swiss-Prot;Acc:Q92791]
Mouse	1700054N08Rik	tgacCTCCGGAGAgcgg	chr8:126383756	ENSMUSG00000031971	1700054N08Rik	RIKEN cDNA 1700054N08 gene Gene [Source:MGI Symbol;Acc:MGI:1920670]
Human	C1orf96	acgcCTCCGGAGAcccc	chr1:229478607	ENSG00000154429	C1orf96	Uncharacterized protein C1orf96 [Source:UniProtKB/Swiss-Prot;Acc:Q6IQ19]
Mouse	2310066E14Rik	gaaaCTCCGGAGAaagc	chr8:108118017	ENSMUSG00000038604	Fam65a	family with sequence similarity 65, member A Gene [Source:MGI Symbol;Acc:MGI:1922937]
Human	FAM65A	gctgCTCCGGAGAcctg	chr16:67551706	ENSG00000039523	FAM65A	family with sequence similarity 65, member A [Source:HGNC Symbol;Acc:25836]
Mouse	2810012G03Rik	ttctCTCCGGAGAtggc	chr18:34911161	ENSMUSG00000034300	Fam53c	family with sequence similarity 53, member C Gene [Source:MGI Symbol;Acc:MGI:1913556]
Human	FAM53C	gtggCTCCGGAGAggct	chr5:137661002	ENSG00000120709	FAM53C	family with sequence similarity 53, member C [Source:HGNC Symbol;Acc:1336]
Mouse	Adamts19	gctgCTCCGGAGAgatg	chr18:58997546	ENSMUSG00000053441	Adamts19	a disintegrin-like and metallopeptidase (reprolysin type) with thrombospondin type 1 motif, 19 Gene [Source:MGI Symbol;Acc:MGI:2442875]
Human	ADAMTS19	gctgCTCCGGAGAgacg	chr5:128797259	ENSG00000145808	ADAMTS19	ADAM metallopeptidase with thrombospondin type 1 motif, 19 [Source:HGNC Symbol;Acc:17111]
Mouse	Ahsg	agtgCTCCGGAGAttgg	chr16:22889712	ENSMUSG00000022868	Ahsg	alpha-2-HS-glycoprotein Gene [Source:MGI Symbol;Acc:MGI:107189]
Mouse	Ahsg	aggtCTCCGGAGAgtga	chr16:22893672	ENSMUSG00000022868	Ahsg	alpha-2-HS-glycoprotein Gene [Source:MGI Symbol;Acc:MGI:107189]
Human	AHSG	agccCTCCGGAGAgctg	chr3:186333479	ENSG00000145192	AHSG	alpha-2-HS-glycoprotein [Source:HGNC Symbol;Acc:349]
Mouse	Aip	ccggCTCCGGAGAggcc	chr19:4127090	ENSMUSG00000024847	Aip	aryl-hydrocarbon receptor-interacting protein Gene [Source:MGI (curated);Acc:MGI:109622]
Human	AIP	ccggCTCCGGAGAggcc	chr11:67235522	ENSG00000110711	AIP	aryl hydrocarbon receptor interacting protein [Source:HGNC Symbol;Acc:358]
Mouse	Ano4	tgctCTCCGGAGAgtcc	chr10:88720371	ENSMUSG00000035189	Ano4	anoctamin 4 Gene [Source:MGI Symbol;Acc:MGI:2443344]
Human	AC079953.2	cgctCTCCGGAGAgtcc	chr12:101188573	ENSG00000151572	ANO4	anoctamin 4 [Source:HGNC Symbol;Acc:23837]
Mouse	C130039O16Rik	ccagCTCCGGAGAggaa	chr12:85552915	ENSMUSG00000042507	C130039O16Rik	RIKEN cDNA C130039O16 gene Gene [Source:MGI Symbol;Acc:MGI:2685106]
Human	C14orf43	ttgtCTCCGGAGAaaat	chr14:74252437	ENSG00000156030	C14orf43	Uncharacterized protein C14orf43 [Source:UniProtKB/Swiss-Prot;Acc:Q6PJG2]
Mouse	Ccnd1	cgcgCTCCGGAGAccgg	chr7:152125684	ENSMUSG00000070348	Ccnd1	cyclin D1 Gene [Source:MGI (curated);Acc:MGI:88313]
Human	CCND1	aggcCTCCGGAGActcc	chr11:69460010	ENSG00000110092	CCND1	cyclin D1 [Source:HGNC Symbol;Acc:1582]
Mouse	Cep76	ctgcCTCCGGAGAaagc	chr18:67800810	ENSMUSG00000073542	Cep76	centrosomal protein 76 Gene [Source:MGI Symbol;Acc:MGI:1923401]
Human	CEP76	ctgcCTCCGGAGAaagc	chr18:12702529	ENSG00000101624	CEP76	centrosomal protein 76kDa [Source:HGNC Symbol;Acc:25727]
Mouse	Cited1	actgCTCCGGAGAcact	chrX:99449475	ENSMUSG00000051159	Cited1	Cbp/p300-interacting transactivator with Glu/Asp-rich carboxy-terminal domain 1 Gene [Source:MGI (curated);Acc:MGI:108023]
Human	CITED1	actgCTCCGGAGAcact	chrX:71528956	ENSG00000125931	CITED1	Cbp/p300-interacting transactivator, with Glu/Asp-rich carboxy-terminal domain, 1 [Source:HGNC Symbol;Acc:1986]
Mouse	D630039A03Rik	ctggCTCCGGAGAtggc	chr4:57933151	ENSMUSG00000052117	D630039A03Rik	RIKEN cDNA D630039A03 gene Gene [Source:MGI Symbol;Acc:MGI:2442889]
Human	C9orf152	gacgCTCCGGAGAggaa	chr9:112976077	ENSG00000188959	C9orf152	Uncharacterized protein C9orf152 [Source:UniProtKB/Swiss-Prot;Acc:Q5JTZ5]
Mouse	Ddi1	gaggCTCCGGAGAgttt	chr9:6265641	ENSMUSG00000047619	Ddi1	DDI1, DNA-damage inducible 1, homolog 1 (S. cerevisiae) Gene [Source:MGI Symbol;Acc:MGI:1919079]
Human	DDI1	tatgCTCCGGAGAcatc	chr11:103908553	ENSG00000170967	DDI1	DNA-damage inducible 1 homolog 1 (S. cerevisiae) [Source:HGNC Symbol;Acc:18961]
Mouse	Dlat	gtcaCTCCGGAGAcggc	chr9:50467609	ENSMUSG00000000168	Dlat	dihydrolipoamide S-acetyltransferase (E2 component of pyruvate dehydrogenase complex) Gene [Source:MGI (curated);Acc:MGI:2385311]
Human	DLAT	gtcaCTCCGGAGAcggc	chr11:111896151	ENSG00000150768	DLAT	dihydrolipoamide S-acetyltransferase [Source:HGNC Symbol;Acc:2896]
Mouse	E030019B06Rik	gagaCTCCGGAGAaagg	chr7:146803645	ENSMUSG00000070357	E030019B06Rik	RIKEN cDNA E030019B06 gene Gene [Source:MGI Symbol;Acc:MGI:2685016]
Human	C10orf92	ggggCTCCGGAGAcaca	chr10:134752336	ENSG00000171811	C10orf92	Uncharacterized protein C10orf92 [Source:UniProtKB/Swiss-Prot;Acc:Q8IYW2]
Mouse	EG434402	tggtCTCCGGAGAtagc	chr9:48303780	ENSMUSG00000042293	Gm5617	predicted gene 5617 Gene [Source:MGI Symbol;Acc:MGI:3643566]
Human	C11orf71	tggtCTCCGGAGAcggc	chr11:114270938	ENSG00000180425	C11orf71	Uncharacterized protein C11orf71 [Source:UniProtKB/Swiss-Prot;Acc:Q6IPW1]
Mouse	Fbxl18	ctagCTCCGGAGAggta	chr5:143656790	ENSMUSG00000066640	Fbxl18	F-box and leucine-rich repeat protein 18 Gene [Source:MGI (curated);Acc:MGI:2444450]
Mouse	Fbxl18	tggaCTCCGGAGAcggg	chr5:143666355	ENSMUSG00000066640	Fbxl18	F-box and leucine-rich repeat protein 18 Gene [Source:MGI (curated);Acc:MGI:2444450]
Human	FBXL18	ccagCTCCGGAGAggta	chr7:5553289	ENSG00000155034	FBXL18	F-box and leucine-rich repeat protein 18 [Source:HGNC Symbol;Acc:21874]
Human	FBXL18	gggcCTCCGGAGAtggg	chr7:5569990	ENSG00000155034	FBXL18	F-box and leucine-rich repeat protein 18 [Source:HGNC Symbol;Acc:21874]
Mouse	Fsd2	tcttCTCCGGAGAaccc	chr7:88717288	ENSMUSG00000038663	Fsd2	fibronectin type III and SPRY domain containing 2 Gene [Source:MGI Symbol;Acc:MGI:2444310]
Human	FSD2	tctaCTCCGGAGAgagg	chr15:83492024	ENSG00000186628	FSD2	small Cajal body-specific RNA 15 [Source:HGNC Symbol;Acc:32572]
Mouse	Gli1	agccCTCCGGAGActgc	chr10:126788368	ENSMUSG00000025407	Gli1	GLI-Kruppel family member GLI1 Gene [Source:MGI Symbol;Acc:MGI:95727]
Human	GLI1	agccCTCCGGAGActac	chr12:57849545	ENSG00000111087	GLI1	GLI family zinc finger 1 [Source:HGNC Symbol;Acc:4317]
Mouse	Gm525	aggtCTCCGGAGAnnnn	chr11:88921921	ENSMUSG00000072553	Gm525	predicted gene 525 Gene [Source:MGI Symbol;Acc:MGI:2685371]

Table S2, Ontology search for IR nGRE-containing orthologue genes that could exert physiological homeostasis functions related to debilitating side effects of glucocorticoid treatment, related to table 2.

Gene symbol	species	sequence of nGRE	distance from TSS (putative)	Gene name
Genes involved in skin homeostasis				
Akt1	m	acgg CTCCagGGAGA ccct	-7273	Protein kinase B
	h	aggc CTCC tt GGAGA cagc	-1724	
Btg2	m	catg CTCCcGGAGA tcgc	84	B-cell translocation gene 2, anti-proliferative
	h	catg CTCCcGGAGA tcgc	196	
Cited1	m	actg CTCCGGAGA cact	-2027	Cbp/p300-interacting transactivator 1 (Melanocyte-specific protein 1)
	h	actg CTCCGGAGA cact	-1972	
Ctnnb1	m	agtt CTCCtGGAGA tgtc	-13621	Beta-catenin
	h	aggg CTCCtGGAGA ctgg	-18316	
Fgfr3	m	ctgc CTCCccGGAGA tggc	-16169	Fibroblast growth factor receptor 3 Precursor
	h	ctgc CTCCccGGAGA tggc	-14933	
Irf6	m	ctag CTCCttGGAGA agga	-9442	Interferon regulatory factor 6
	h	ccat CTCCtgGGAGA gtgt	-11439	
Jund	m	tttg CTCCtGGAGA ccgc	-16362	Transcription factor jun-D
	h	cctg CTCCtGGAGA gggc	-6563	
Krt14	m	gggc CTCCaGGAGA caat	-2920	Keratin-14 (Ramot, Y., Paus, R., Tiede, S., and Zlotogorski, A. (2009). Endocrine controls of keratin expression. BioEssays *31* , 389-399.)
	h	aaaa CTCCcGGAGA gcag	-16317	

* indicates the presence of a tolerable one base mutation within the cnonical IR nGRE sequence

* indicates t	m*	tttg **a**TCCaGGAGA gctg	-7804	Keratin-5 (Ramot, Y., Paus, R., Tiede, S., and Zlotogorski, A. (2009). Endocrine controls of keratin expression. BioEssays *31* , 389-399.)
	h	gtgt CTCCaGGAGA gcaa	3017	
Lama5	m	ttaa CTCCaGGAGA ctca	-13911	Laminin subunit alpha-5 Precursor
	h	gcac CTCCtGGAGA agct	-5201	
Nr2f1	m	ctag CTCCagGGAGA ttgt	1636	COUP transcription factor 1 (COUP-TF I)
	h	ctag CTCCagGGAGA tttt	3415	
Plxna1	m	ctgc CTCCgGGAGA gcag	-14581	Plexin-A1 Precursor
	h	agtc CTCCgGGAGA aggt	2792	
Ppp2r2b	m	cact CTCCtGGAGA tacc	-17088	Serine/threonine-protein phosphatase 2A 55 kDa regulatory subunit B beta isoform
	h	aaat CTCCaGGAGA actt	1757	
Sfn	m	ccat CTCCaaGGAGA cttc	-925	14-3-3 protein sigma (Stratifin)
	h	aggg CTCCgtGGAGA ggga	967	
Smad4	m	gagt CTCCtgGGAGA aggg	-11235	Mothers against decapentaplegic homolog 4 (Chen, S.J., Yuan, W., Lo, S., Trojanowska, M., and Varga, J. (2000). Interaction of Smad3 with a proximal smad-binding element of the human α2(I) procollagen gene promoter required for transcriptional activation by TGF-β. J. Cell Physiol. *183* , 381-392.)
	h	tctt CTCCtgGGAGA gcag	-12919	
Tgfb1	m	ccca CTCCcGGAGA gagc	-10900	Transforming growth factor beta-1 Precursor (Frank, S., Madlener, M., and Werner, S. (1996). Transforming growth factors β1, β2, and β3 and their receptors are differentially regulated during normal and impaired wound healing. J. Biol. Chem. *271* , 10188-10193.)
	h	tctc CTCCaGGAGA cgga	536	
Tgm3	m	taca CTCCtGGAGA gagt	-717	Transglutaminase-3
	h	tggg CTCCaGGAGA aaga	-4782	

Tnc	m	acga CTCCatGGAGA ttgc	-19030	Tenascin-C (Fassler, E., Sasaki, T., Timpl, E., Chu, M.L., and Werner, S. (1996). Differential regulation of fibulin, tenascin-C, and nidogen expression during wound healing of normal and glucocorticoid-treated mice. Exp. Cell Res. *222* , 111-116.)
	h	tgtt CTCCtaGGAGA atcc	4669	
Trpv3	m	ccca CTCCaaGGAGA tggc	2053	Transient receptor potential cation channel subfamily V member 3 (Cheng, X., Jin, J., Hu, L., Shen, S., Dong, X.P., Samie, M.A.A., Knoff, J., Eisinger, B., Liu, M.L., Huang, S.M., Caterina, M.J., Dempsey, P., Michal, L.E., Dlugosz, A.A., Andrews, N.C., Clapham, D.E., and Xu, H. (2010). TRP channel regulates EGFR signaling in hair morphogenesis and skin barrier formation. Cell *141* , 331-343.)
	h	tttc CTCC ct GGAGA agat	-7725	
Wnt5a	m	gcat CTCCcGGAGA aaaa	-160	Wingless-related MMTV integration site 5A
	h	gcat CTCCcGGAGA aaaa	2154	
Genes involved in bone and cartilage development and homeostasis				
Acan	m	actc CTCCctGGAGA cacc	-9592	Cartilage-specific proteoglycan core protein
	h	cagg CTCCagGGAGA aact	1881	
Ahsg	m	agtg CTCCGGAGA ttgg	-2351	Alpha-2-HS-glycoprotein Precursor (Fetuin-A) (Szweras, M., Liu, D., Partridge, E.A., Pawling, J., Sukhu, B., Clokie, C., Jahnen-Dechent, W., Tenenbaum, H.C., Swallow, C.J., Grynpas, M.D., and Dennis, J.W. (2002). α2-HS glycoprotein/fetuin, a transforming growth factor-β/Bone morphogenetic protein antagonist, regulates postnatal bone growth and remodeling. J. Biol. Chem. *277* , 19991-19997.)
	h	agcc CTCCGGAGA gctg	2820	
Akt1	m	acgg CTCCagGGAGA ccct	-7273	Protein kinase B
	h	aggc CTCC tt GGAGA cagc	-1724	
Barx2	m	tcct CTCCaaGGAGA cctg	219	Homeobox protein BarH-like 2

	h	tcct CTCCaaGGAGA cctg	197	
Bcl2	m	tgtc CTCCaGGAGA tggg	-14391	Apoptosis regulator Bcl-2 (Mocetti, P., Silvestrini, G., Ballanti, P., Patacchioli, F.R., Di Grezia, R., Angelucci, L., and Bonucci, E. (2001). Bcl-2 and Bax expression in cartilage and bone cells after high-dose corticosterone treatment in rats. Tissue and Cell *33* , 1-7.)
	h*	ggag CTCCgGGAG**g** cggc	167	
	h*	ctct CTCCtGG**g**GA ggcg	539	
	h*	aaga CTC**tt**GGAGA taaa	-1336	
Bcl2l1	m	atacCTCCgGGAGAgttc	941	Apoptosis regulator Bcl-XL (Lu, N.Z., Collins, J.B., Grissom, S.F., and Cidlowski, J.A. (2007). Selective regulation of bone cell apoptosis by translational isoforms of the glucocorticoid receptorα. Mol. Cell Biol. *27* , 7143-7160.)
	h	ccacCTCCgGGAGAgtac	964	
Bmp3	m	gaga CTCCtGGAGA agtg	3000	Bone morphogenetic protein 3 Precursor
	h	cttt CTCCtGGAGA aagc	4955	
Cdh11	m	gatt CTCCtGGAGA gcaa	-8249	Cadherin-11 Precursor (Osteoblast cadherin)
	h	ggtt CTCCtGGAGA gcca	-9011	
Col11a2	m	ggga CTCCagGGAGA tggt	1362	Collagen alpha-2(XI) chain Precursor (Li, S.W., Takanosu, M., Arita, M., Bao, Y., Ren, Z.X., Meier, A., Prockop, D.J., and Mayne, R. (2001). Targeted disruption of Col11a2 produces a mild cartilage phenotype in transgenic mice: comparison with the human disorder otospondylomegaepiphyseal dysplasia (OSMED). Dev. Dyn. *222* , 141-152.)
	h	caga CTCCtgGGAGA gctt	2293	
Ctnnb1	m	agtt CTCCtGGAGA tgtc	-13621	Beta-catenin
	h	aggg CTCCtGGAGA ctgg	-18316	
Fgfr3	m	ctgc CTCCccGGAGA tggc	-16169	Fibroblast growth factor receptor 3 Precursor
	h	ctgc CTCCccGGAGA tggc	-14933	

Ghr	m*	ccgt **g**TCCtGGAGA agtg	488	Growth hormone receptor (Gevers, E.F., Van der Eerden, B.C., Karperien, M., Raap, A.K., Robinson, I.C., and Wit, J.M. (2002). Localization and regulation of the growth hormone receptor and growth hormone-binding protein in the rat growth plate. J. Bone Miner. Res. *17*, 1408-1419.)
	m*	tgaa CTC**t**gGGAGA aata	-18197	
	m*	actc CTCCtGGA**a**A tatt	-17058	
	m*	gtat CTCCaGGAG**g** tctt	1412	
	h	aggt CTCCaGGAGA tcat	-14122	
Gnas	m	catt CTCCtGGAGA tcgg	-16791	Adenylate cyclase stimulating G-alpha protein (Weinstein, L.S., Liu, J., Sakamoto, A., Xie, T., and Chen, M. (2004). Minireview: GNAS: normal and abnormal functions. Endocrinology *145*, 5459-5464.)
	h	acag CTCCaGGAGA ggag	-3819	
Nkx3-2	m	ggta CTCCaGGAGA gggt	4675	Homeobox protein Nkx-3.2
	h	gcaa CTCCtGGAGA ccac	2721	
Ostm1	m	agcc CTCCGGAGA ctgc	-9779	Osteopetrosis-associated transmembrane protein 1 Precursor
	h	agcc CTCCGGAGA ctac	-4334	
Plxna1	m	ctgc CTCCgGGAGA gcag	-14581	Plexin-A1 Precursor
	h	agtc CTCCgGGAGA aggt	2792	
Prkra	m	cgat CTCCcaGGAGA atat	-2643	Interferon-inducible double stranded RNA-dependent protein kinase activator A
	h	ctgt CTCCtaGGAGA atat	-2133	
Smad4	m	gagt CTCCtgGGAGAa ggg	-11235	Mothers against decapentaplegic homolog 4 (Tan, X., Weng, T., Zhang, J., Wang, J., Li, W., Wan, H., Lan, Y., Cheng, X., Hou, N., Liu, H., Ding, J., Lin, F., Yang, R., Gao, X., Chen, D., and Yang, X. (2007). Smad4 is required for maintaining normal murine postnatal bone homeostasis. J. Cell Sci. *120*, 2162-2170.)
	h	tctt CTCCtgGGAGA gcag	-12919	

Sparc	m	gcca CTCCGGAGA cgac	-8383	Osteonectin
	h	ctcc CTCCGGAGA tttg	-6977	
Tgfb1	m	ccca CTCCcGGAGA gagc	-10900	Transforming growth factor beta-1 Precursor (Geiser, A.G., Zeng, Q.Q., Sato, M., Helvering, L.M., Hirano, T., and Turner, C.H. (1998). Decreased bone mass and bone elasticity in mice lacking the transforming growth factor-β1 gene. Bone *23*, 87-93.)
	h	tctc CTCCaGGAGA cgga	536	
Tnfrsf11b	m*	ggtt CT**t**CtgGGAGA gtcg	3095	Tumor necrosis factor receptor superfamily member 11B Precursor (Osteoprotegerin) (Sasaki, N., Kusano, E., Ando, Y., Yano, K., Tsuda, E., and Asano, Y. (2001). Glucocorticoid decreases circulating osteoprotegerin (OPG): possible mechanism for glucocorticoid induced osteoporosis. Nephrol. Dial. Transplant. *16*, 479-482.)
	m*	cctg CTCCcaGGAG**c** ataa	-2900	
	m*	ttag CTCC tt GGA**t**A cttt	-4828	
	m*	cagg **g**TCCtgGGAGA gttt	-16874	
	h	ctcc CTCCcaGGAGA ggct	411	
Tuft1	m	aaat CTCCttGGAGA gaca	-4989	Tuftelin
	h	aaat CTCCttGGAGA gaca	-4584	
Wnt5a	m	gcat CTCCcGGAGA aaaa	-160	Wingless-related MMTV integration site 5A (Yang, Y., Topol, L., Lee, H., and Wu, J. (2003). Wnt5a and Wnt5b exhibit distinct activities in coordinating chondrocyte proliferation and differentiation. Development *130*, 1003-1015.)
	h	gcat CTCCcGGAGA aaaa	2154	
Genes involved in glucose metabolism				
Akt1	m	acgg CTCCagGGAGA ccct	-7273	Protein kinase B
	h	aggc CTCC tt GGAGA cagc	-1724	

Dlat	m	gtca CTCCGGAGA cggc	222	Dihydrolipoyllysine-residue acetyltransferase component of pyruvate dehydrogenase complex, mitochondrial Precursor
	h	gtca CTCCGGAGA cggc	668	
Gaa	m	ctcc CTCCaGGAGA agca	-4829	Lysosomal alpha-glucosidase Precursor
	h	ccct CTCCtGGAGA ctca	-14274	
Galk2	m	gtct CTCCaGGAGA agat	-209	N-acetylgalactosamine kinase
	h	atgt CTCCaGGAGA ctca	-702	
Galt	m	gtct CTCCtgGGAGA caga	-15596	Galactose-1-phosphate uridylyltransferase
	h	ggtt CTCCagGGAGA aaga	-11088	
Gba2	m	ctcc CTCCaGGAGA ctta	-1923	Non-lysosomal glucosylceramidase
	h	ctcc CTCCaGGAGA ctta	-1604	
Gbe1	m	ccga CTCCtGGAGA ttga	211	1,4-alpha-glucan-branching enzyme
	h	caga CTCCtGGAGA tcga	690	
Man2b1	m	ggag CTCCgGGAGA gtgg	-9876	Lysosomal alpha-mannosidase Precursor
	h	ggag CTCCgGGAGA acgg	-13126	
Pcdh12	m	atgc CTCCcgGGAGA acct	2859	Protocadherin-12 Precursor
	h	atgc CTCCcgGGAGA acct	3741	
Pdha2	m	aatg CTCCcaGGAGA ctac	-3189	Pyruvate dehydrogenase E1 component subunit alpha, testis-specific form, mitochondrial Precursor
	h	aatg CTCCctGGAGA tctc	-1539	
Pfkfb4	m	gggt CTCCcgGGAGA gcgt	-17780	6-phosphofructo-2-kinase/fructose-2,6-biphosphatase 4
	h	gcat CTCCatGGAGA ggac	2430	

Phka2	m	tcat CTCCttGGAGA aact	-12928	Phosphorylase b kinase regulatory subunit alpha, liver isoform
	h	ttgt CTCCttGGAGA gacc	-13866	
Phkg2	m	aagc CTCCagGGAGA cata	-12482	Phosphorylase b kinase gamma catalytic chain, testis/liver isoform
	h	aagc CTCCagGGAGA cata	-8384	
Slc2a6	m	gcga CTCCtGGAGA gaga	69	solute carrier family 2 (facilitated glucose transporter), member 6
	h	gagc CTCCaGGAGA cctt	-7792	
Genes involved in insulin signaling				
Akt1	m	acgg CTCCagGGAGA ccct	-7273	Protein kinase B
	h	aggc CTCC tt GGAGA cagc	-1724	
Calml3	m	atgc CTCCtGGAGA cttt	-1248	Calmodulin-like protein 3
	h	gcac CTCCtGGAGA agtg	-19865	
Flot2	m	cttg CTCCatGGAGA atct	-11784	Flotillin-2 (Epidermal surface antigen)
	h	ttgc CTCCatGGAGA atct	-12504	
Ins	m*	caac CT**g**CaGGAGA ccta	-12625	Insulin Precursor (Delaunay, F., Khan, A., Cintra, A., Davani, B., Ling, Z.C., Andersson, A., Östenson, C.G., Gustafsson, J.A., Efendic, S., and Okret, S. (1997). Pancreatic b cells are important targets for the diabetogenic effects of glucocorticoids. J. Clin. Invest. *100* , 2094-2098.)
	h	tgct CTCCtGGAGA catt	-202	
	m	tagg CTCCacGGAGA acct	-11925	
	h	aggc CTCCctGGAGA ggct	-25700	
Insr	m*	tggg CT**t**CgGGAGA ggat	5	Insulin receptor (Caro, J.F., and Amatruda, J.M. (1982). Glucocorticoid-induced insulin resistance: the importance of postbinding events in the regulation of insulin binding, action, and degradation in freshly isolated and primary cultures of rat hepatocytes.. J. Clin. Invest. *69* , 866-875.)

	m*	tgta CTCCtGG**g**GA acca	-7700	
	h	ttct CTCCtGGAGA cctg	3856	
Mapkapk2	m	gtaa CTCCaGGAGA gaca	-3094	MAP kinase-activated protein kinase 2
	h	cctt CTCCaGGAGA atta	-19211	
Phka2	m	tcat CTCCttGGAGA aact	-12928	Phosphorylase b kinase regulatory subunit alpha, liver isoform
	h	ttgt CTCCttGGAGA gacc	-13866	
Phkg2	m	aagc CTCCagGGAGA cata	-12482	Phosphorylase b kinase gamma catalytic chain, testis/liver isoform
	h	aagc CTCCagGGAGA cata	-8384	
Shc4	m	ctta CTCCaGGAGA aatg	2759	Src homology 2 domain-containing-transforming protein C4
	h	tcaa CTCCaGGAGA aaac	-13400	
Socs1	m	ccgt CTCCagGGAGA gcct	-176	Suppressor of cytokine signaling 1
	h	aact CTCCagGGAGA gaaa	1879	
Socs3	m	cgcg CTCCtGGAGA ccca	577	Suppressor of cytokine signaling 3
	h	caca CTCCtGGAGA ccta	582	
Srebf1	m	ttgg CTCCtGGAGA gttg	-5437	Sterol regulatory element-binding protein 1
	h	ggct CTCCcGGAGA gggg	-6852	
Genes involved in muscle homeostasis				
Akt1	m	acgg CTCCagGGAGA ccct	-7273	Protein kinase B (Schakman, O., Gilson, H., and Thissen, J.P. (2008a). Mechanisms of glucocorticoid-induced myopathy. J. Endocrinol. *197* , 1-10.)
	h	aggc CTCC tt GGAGA cagc	-1724	
Barx2	m	tcct CTCCaaGGAGA cctg	219	Homeobox protein BarH-like 2
	h	tcct CTCCaaGGAGA cctg	197	

Ctnnb1	m	agtt CTCCtGGAGA tgtc	-13621	Beta-catenin (Schakman, O., Kalista, S., Bertrand, L., Lause, P., Verniers, J., Ketelslegers, J.M., and Thissen, J.P. (2008b). Role of Akt/GSK-3β/β-Catenin transduction pathway in the muscle anti-atrophy action of insulin-like growth factor-I in glucocorticoid-treated rats. Endocrinology *149* , 3900-3908.)
	h	aggg CTCCtGGAGA ctgg	-18316	
Tagln	m	ccga CTCCaGGAGA agtc	-9672	Transgelin (Smooth muscle protein 22-alpha)
	h	gccc CTCCaGGAGA actt	539	
Tagln2	m	ccag CTCCaGGAGA caca	-2325	Transgelin (Smooth muscle protein 22-beta)
	h	cctg CTCCaGGAGA cacc	-2548	
Tpm2	m	cgga CTCCtGGAGA ggcg	-1207	Tropomyosin beta chain (Ochala, J., Li, M., Tjsharghi, H., Kinber, E., Tulinius, M., Oldfors, A., and Larsson, L. (2007). Effects of a R133W b-tropomyosin mutation on regulation of muscle contraction in single human muscle fibres. J. Physiol. *581* , 1283-1292.)
	h	ggaa CTCCtGGAGA accc	-19898	
Genes involved in Hypothalamus Pituitary Adrenal (HPA) axis				
Mc2r	m*	gcag CTCCtGGAaA gaac	1385	ACTH receptor (Chida, D., Nakagawa, S., Nagai, S., Sagara, H., Kastumata, H., Imaki, T., Suzuki, H., Mitani, D., Ogishima, T., Shimizu, C., Kotaki, H., Kakuta, S., Sudo, K., Koike, T., Kubo, M., and Iwakura, Y. (2007). Melanocortin 2 receptor is required for adrenal gland development, steroidogenesis, and neonatal gluconeogenesis. Proc. Natl. Acad. Sci. USA *104* , 18205-18210.)
	h	ggag CTCCaGGAGA ggct	4217	

Mrap	m	tctg CTCCcGGAGA cccg	-10507	ACTH receptor accessory protein (Metherell, L.A., Chapple, J.P., Cooray, S., David, A., Becker, C., Rüschendorf, F., Naville, D., Begeot, M., Khoo, B., Nurnberg, P., Huebner, A., Cheetham, M.E., and Clark, A.J. (2005). Mutations in MRAP, encoding a nex interacting partner of the ACTH receptor, cause familial glucocorticoid deficiency type 2. Nat. Genet. *37* , 166-170.)
	h	agca CTCCtGGAGA acca	-8935	
Genes involved in circadian rhythm				
Clock	m	gaac CTCCaGGAGA ggaa	-456	Circadian locomoter output cycle kaput protein (Roybal. K., Theobold, D., Graham, A., DiNieri, A.A., Russo, S.J., Krishnan, V., Chakravarty, S., Peevey, J., Oehrlein, N., Birnbaum, S., Vitaterna, M.H., Orsulak, P., Takahashi, J.S., Nestler, E.J., Carlezon, W.A., and McClung, C.A. (2007). Mania-like behavior induced by disruption of CLOCK. Proc. Natl. Acad. Sci. USA *104* , 6406-6411.)
	h*	ccag C**a**CCaGGAGA ggaa	482	
	h*	agcg CTCCcGG**t**GA gagg	1102	
	h*	agat CTCCaGG**t**GA cacg	-6216	
Nr1d1	m*	tgaa CTCCaGGAG**g** gagt	-2177	Rev-erbα [Torra, P.I., Tsibulsky, V., Delauney, F., Saladin, R., Laudet, V., Fruchart, J., Kosykh, V., and Staels, B. (2000). Circadian and glucocorticoid regulation of Rev-erbα expression in liver. Endocrinology *141* , 3799-3806; Preitner, N., Damiola, F., Molina, L-L., Zakany, J., Duboule, D., Albrecht, U., and Schibler, U. (2002). The orphan nuclear receptor REV-ERBα controls circadian transcription within the positive limb of the mammalian circadian oscillator. Cell *110* , 251-260.]
	m	ccga CTCCtGGAGA acaa	-7637	
	h*	agag C**c**CCaGGAGA tcat	-12043	
	h*	cctt CTCCgGGAG**g** atgg	-12984	
	h*	agcc CTCCaGG**t**GA ttct	-14522	

Behaviour related genes				
Crhr2	m*	ctaa **g**TCCaGGAGA tgga	-17784	Corticotropin-releasing factor receptor 2 Precursor (Bale, T.L., Contarino, A., Smith, G.X., Chan, R., Gold, L.H., Sawchenko, P.E., Koob, G.F., Vale, W.W., and Lee, K.F. (2000). Mice deficient for corticotrophin-releasing hormone receptor-2 display anxiety-like behavior and are hypersensitive to stress. Nat. genet. *24* , 410-414.)
	m*	tggt **t**TCCaGGAGA gagg	1826	
	m*	gtat CTCCaGGA**a**A agcc	-720	
	h	gcat CTCCaGGAGA aagt	-1138	
Ucn2	m	gggc CTCCtGGAGA gaaa	-18502	Urocortin-2 Precursor [Chen, A., Blount, A., Vaughan, J., Brar, B., and Vale, W. (2004). Urocortin II gene is highly expressed in mouse skin and skeletal muscle tissues: localization, basal expression in corticotrophin-releasing factor receptor (CRFR) 1-and CRFR2-null mice, and regulation by glucocorticoids. Endocrinology *145* , 2445-2457; Chen, A., Zorrilla, E., Smith, S., Rousso, D., Levy, C., Vaughan, J., Donaldson, C., Robert, A., Lee, K.F., and Vale, W. (2006). Urocortin 2-deficient mice exhibit gender-specific alterations in circadian hypothalamus-pituitary-adrenal axis and depressive-like behavior. J. Neurosci. *26* , 5500-5510.]
	h	gggc CTCCtGGAGA gaag	-17598	
Genes involved in cell cycle regulation				
Ak1	m	gacc CTCCcgGGAGA ccct	-14078	Adenylate kinase isoenzyme 1
	h	gggc CTCCtaGGAGA gttc	-12805	
Ccnd1	m	cgcg CTCCGGAGA ccgg	92	G1/S-specific cyclin-D1
	h	aggc CTCCGGAGA ctcc	4192	
Cdc123	m	agca CTCCacGGAGA cagt	-7531	Cell division cycle protein 123 homolog
	h	agcg CTCCaaGGAGA ctcc	-528	

Cdc20	m	gagt CTCCaGGAGA tggt	2109	Cell division cycle protein 20 homolog
	h	tgcc CTCCaGGAGA atga	-19769	
Cdc25a	m	atga CTCCttGGAGA cctt	-12769	cell division cycle 25A
	h	aaga CTCCaaGGAGA ctct	-17956	
Cdc25b	m	acta CTCCcGGAGA acac	-14232	M-phase inducer phosphatase 2
	h	gggc CTCCtGGAGA actg	1106	
Cdc25c	m	gtct CTCCtGGAGA ttct	3355	M-phase inducer phosphatase 3
	h	cctg CTCCtGGAGA gaga	704	
Cdc6	m	aaag CTCCagGGAGA ctta	-7225	Cell division control protein 6 homolog
	h	ttac CTCCagGGAGA ggtg	-5927	
Cdk4	m	agcc CTCCgaGGAGA ataa	-4377	Cell division protein kinase 4 (Rogatsky, I., Hittelman, A.B., Pearce, S., and Garabedian, M.J. (1999). Distinct glucocorticoid receptor transcriptional regulatory surfaces mediate the cytotoxic and cytostatic effects of glucocorticoids. Mol. Cell Biol. *19* , 5036-5049.)
	h	cgct CTCCggGGAGA aagc	-3769	
Irf6	m	ctag CTCCttGGAGA agga	-9442	Interferon regulatory factor 6
	h	ccat CTCCtgGGAGA gtgt	-11439	
Ppp1r15a	m	cctg CTCCatGGAGA actt	-4400	Growth arrest and DNA damage-inducible protein GADD34
	h	tcat CTCCatGGAGA aggc	2982	
Smad4	m	gagt CTCCtgGGAGA aggg	-11235	Mothers against decapentaplegic homolog 4
	h	tctt CTCCtgGGAGA gcag	-12919	
Tgfb1	m	ccca CTCCcGGAGA gagc	-10900	Transforming growth factor beta-1 Precursor
	h	tctc CTCCaGGAGA cgga	536	

Wdr6	m	gcct CTCCccGGAGA ttgt	-2301	WD repeat domain 6
	h	gtcc CTCCaaGGAGA accg	1200	
Genes involved in regulation of apoptosis				
Adamtsl4	m	ccac CTCCctGGAGA cttg	-12475	ADAMTS-like protein 4 Precursor (Thrombospondin repeat-containing protein 1)
	h	gaga CTCCctGGAGA ggga	-15072	
Akt1	m	acgg CTCCagGGAGA ccct	-7273	Protein kinase B
	h	aggc CTCC tt GGAGA cagc	-1724	
Atf5	m	tttc CTCCaaGGAGA caac	450	Activating transcription factor 5-alpha/beta
	h	cctg CTCCctGGAGA cagg	-9390	
Bat2	m	gtgg CTCCgaGGAGA cgtt	-6677	HLA-B-associated transcript 2
	h	gtgg CTCCggGGAGA cgtt	-4185	
Bat3	m	acag CTCCccGGAGA attc	-7971	HLA-B-associated transcript 3
	h	acag CTCCtcGGAGA attc	-7184	
Bcl2	m	tgtc CTCCaGGAGA tggg	-14391	Apoptosis regulator Bcl-2
	h*	ggag CTCCgGGAG**g** cggc	167	
	h*	ctct CTCCtGG**g**GA ggcg	539	
	h*	aaga CTC**tt**GGAGA taaa	-1336	
Bcl2l1	m	atac CTCCgGGAGA gttc	941	Apoptosis regulator Bcl-XL
	h	ccac CTCCgGGAGA gtac	964	

Btg2	m	catg CTCCcGGAGA tcgc	84	B-cell translocation gene 2, anti-proliferative
	h	catg CTCCcGGAGA tcgc	196	
Cdk5	m	agcc CTCCgGGAGA tctg	788	Cyclin-dependent kinase 5
	h	cgcc CTCCgGGAGA tctg	1529	
Cdk5r1	m	ctgc CTCCtgGGAGA gggc	-4980	Cyclin-dependent kinase 5 activator 1 Precursor
	h	ctgc CTCCtgGGAGA gggc	-5520	
Cidec	m	ggag CTCCgGGAGA actt	-6883	Cell death-inducing DFFA-like effector protein C
	h	tttg CTCCtGGAGA gcag	34	
Dlg5	m	cttc CTCCaaGGAGA tata	-10097	Dlg5 protein
	h	ggag CTCC tt GGAGA ggga	-897	
Eef1a2	m	cccc CTCCtGGAGA gata	181	Elongation factor 1-alpha 2
	h	cccc CTCCcGGAGA taaa	-14	
Ifih1	m	cacc CTCCaaGGAGA gctt	-18015	Interferon-induced helicase C domain-containing protein 1
	h	acaa CTCCcaGGAGA gatg	-1452	
Il6	m	ttct CTCCaGGAGA accc	-8214	Interleukin-6 Precursor
	h	aggg CTCCaGGAGA cctg	486	
Ints1	m	aggt CTCCatGGAGA ggaa	-566	Integrator complex subunit 1
	h	gcct CTCCagGGAGA cagt	-9554	
Muc20	m	tgct CTCCtgGGAGA attt	-16409	Mucin-20 Precursor
	h	ccac CTCCgtGGAGA catc	4098	
Pak7	m	gcat CTCCtaGGAGA tgcc	413	p21-activated kinase 7
	h	gcat CTCCtaGGAGA tgca	383	

Plagl2	m	caga CTCCctGGAGA ccca	362	pleiomorphic adenoma gene-like 2
	h	tagg CTCCctGGAGA ccca	408	
Prkra	m	cgat CTCCcaGGAGA atat	-2643	Interferon-inducible double stranded RNA-dependent protein kinase activator A
	h	ctgt CTCCtaGGAGA atat	-2133	
Sgk3	m	tgtg CTCCgGGAGA gctc	246	Serum/glucocorticoid-regulated kinase 3
	h	ccgg CTCCcGGAGA gttt	376	
Tgfb1	m	ccca CTCCcGGAGA gagc	-10900	Transforming growth factor beta-1 Precursor
	h	tctc CTCCaGGAGA cgga	536	
Uaca	m	gatg CTCCaGGAGA cacc	-3900	Uveal autoantigen with coiled-coil domains and ankyrin repeats
	h	cccg CTCCtGGAGA agga	-15562	
Vcp	m	atac CTCCatGGAGA ttct	-6814	Valosin-containing protein
	h	tcac CTCCatGGAGA gagg	-5305	
Vdac2	m	cttg CTCCtgGGAGA gaaa	-1576	Voltage-dependent anion-selective channel protein 2
	h	agtt CTCCctGGAGA agat	4376	
Genes involved in inflammation and immunity				
Akt1	m	acgg CTCCagGGAGA ccct	-7273	Protein kinase B
	h	aggc CTCC tt GGAGA cagc	-1724	
C1qb	m	gaca CTCCagGGAGA ttag	-8501	Complement C1q subcomponent subunit B Precursor
	h	ggga CTCCcaGGAGA tctg	-4033	

C1ql1	m	nnnc CTCCaGGAGA ccgg	200	C1q-related factor Precursor (Complement component 1 Q subcomponent-like 1)
	h	aact CTCCtGGAGA attt	-3742	
C3	m	cagc CTCCaGGAGA caga	-18762	Complement C3 Precursor
	h	tcac CTCCtGGAGA atct	-12489	
Ccr10	m	tggt CTCCcaGGAGA gttc	-17350	C-C chemokine receptor type 10
	h	tcat CTCCtgGGAGA ggca	-19371	
Cfd	m	cgtt CTCCaGGAGA ttat	-10133	Complement factor D Precursor
	h	gggg CTCCgGGAGA cagg	-11498	
Cyr61	m	cagg CTCCgGGAGA actc	-843	Insulin-like growth factor-binding protein 10
	h	cagc CTCCcGGAGA actc	-896	
Il11ra1	m	cggc CTCCaGGAGA gagc	-3594	interleukin-11 receptor
	h*	gtgg **g**TCCtGGAGA aggc	-18256	
Il12rb1	m*	taag C**a**CCaGGAGA ggca	-15564	interleukin-12 receptor b1
	m*	tgag CT**t**C t GGAGA ggtc	-11208	
	m*	ctat CTCCaGGA**a**A ccct	-19041	
	m*	gcag CTCCtGGAG**g** actc	-10567	
	h	ctgc CTCCtGGAGA aatg	1800	
Il16	m*	gctg **t**TCCtGGAGA gctt	-8773	cytokine activity
	m*	ggat CTC**g**aGGAGA aaaa	-11359	
	m*	cact CTCCtGG**t**GA tctc	1089	
	h	tcag CTCCgGGAGA agtg	-13476	

Il17b	m	ctgt CTCCaGGAGA gcac	-8301	cytokine activity
	m	gttt CTCCgGGAGA tagt	-383	
	h*	ataa **t**TCCaGGAGA tccc	-10368	
	h*	gccg CTC**t**t GGAGA aaga	-2868	
Il17f	m	tcag CTCCtGGAGA agtg	598	cytokine activity
	h	gtca CTCCtGGgGA ggcc	-4395	
Il17ra	m*	ggac CT**t**CgGGAGA gcag	-5793	interleukin-17 receptor a
	h	agac CTCCaGGAGA tcca	-17503	
Il17rb	m	ctca CTCCaGGAGA cttg	2717	interleukin-17 receptor b
	m	agaa CTCCaGGAGA acaa	-19210	
	h	catt CTCCaGGAGA gacc	-15856	
	h*	ccct CTCCaGG**g**GA gatg	-7981	
	h*	ctgg CTCCcGGA**a**A gcat	-15287	
Il1rn	m	gggc CTCCaaGGAGA cagg	-18289	Interleukin-1 receptor antagonist protein Precursor
	h	agtg CTCCcaGGAGA cgga	-2627	
Il20	m	cgga CTCCtaGGAGA ccag	-6171	Interleukin-20 Precursor
	h	cagg CTCCtaGGAGA ccag	-1733	
Il22ra1	m*	tgac tTCCaGGAGA atca	-17163	interleukin-22 receptor a1
	m*	agtt tTCCtGGAGA tgga	240	
	m*	cttc CTtCaGGAGA aaaa	-11612	
	m*	gtgg CTCCtGGgGA aaga	-17654	
	h	cagg CTCCaGGAGA cccc	-13251	

Il24	m	gttt CTCCaGGAGA aacc	-7331	cytokine activity
	h*	tctg **a**TCCaGGAGA gttt	-3416	
	h*	ccgt CTCCtGG**g**GA ggag	1397	
Il28a	m	tgct CTCCaGGAGA agag	590	cytokine activity
	m	tctt CTCCtGGAGA gcag	-13172	
	h*	cctg C**a**CCaGGAGA gact	-11971	
	h*	tcac CTCCtGGAG**g** taaa	-16061	
	h*	ccgg CTCCaGGAG**g** cccc	1284	
Il28b	m	tctt CTCCtGGAGA gcag	-13065	cytokine activity
	m	tgct CTCCaGGAGA agag	697	
	h*	cagc C**c**CCaGGAGA tcct	-18465	
	h*	ttac CTCCaGGAG**g** tgaa	-7335	
	h*	ccgg CTCCaGGAG**g** cccc	1285	
Il34	m	acct CTCCtGGAGA gagt	-4275	cytokine activity
	h*	aaag CTCCaGGAG**g** ggtg	2058	
Il6	m	ttct CTCCaGGAGA accc	-8214	Interleukin-6 Precursor
	h	aggg CTCCaGGAGA cctg	486	
Il8ra	m*	acca C**c**CCaGGAGA caag	-4717	interleukin-8 receptor a
	m*	gaat CT**t**C t GGAGA aaag	-11676	
	h	actt CTCCtGGAGA cccc	-2398	
Itpr3	m	ggag CTCCcGGAGA gctt	-4158	Inositol 1,4,5-trisphosphate receptor type 3
	h	ccaa CTCCtGGAGA ggga	-43	

Jund	m	tttg CTCCtGGAGA ccgc	-16362	Transcription factor junD
	h	cctg CTCCtGGAGA gggc	-6563	
Mapkapk2	m	gtaa CTCCaGGAGA gaca	-3094	MAP kinase-activated protein kinase 2
	h	cctt CTCCaGGAGA atta	-19211	
Nfatc1	m	ggct CTCCtGGAGA agtg	-15543	Nuclear factor of activated T-cells, cytoplasmic 1
	h	tgcg CTCCaGGAGA aggg	-2166	
Orm1	m	gcct CTCCtGGAGA cctg	318	Alpha-1-acid glycoprotein 1 Precursor
	h	atgg CTCCaGGAGA ggca	-12227	
Orm2	m	gcct CTCCtGGAGA cctg	-17565	Alpha-1-acid glycoprotein 2 Precursor
	h	atgg CTCCaGGAGA ggca	-19040	
Pak4	m	ttgc CTCCtGGAGA ggtg	-9656	p21-activated kinase 4
	h	ttcc CTCCtGGAGA ggtg	-15442	
Pak7	m	gcat CTCCtaGGAGA tgcc	413	p21-activated kinase 7
	h	gcat CTCCtaGGAGA tgca	383	
Pla2g2c	m	gcat CTCCtGGAGA ggtc	-17227	Group IIC secretory phospholipase A2 Precursor
	h	gagg CTCCaGGAGA taca	-5047	
Plcg1	m	gccc CTCCccGGAGA gggt	-9	Phospholipase C-gamma-1
	h	gccc CTCCcgGGAGA gggc	45	
Prkcb	m	atcc CTCCaGGAGA cgca	-421	Protein kinase C beta
	h	atcc CTCCaGGAGA cgcg	-387	
Prkch	m	tgct CTCCggGGAGA ctat	99	Protein kinase C eta
	h	ggtc CTCCccGGAGA caaa	-946	

Rac3	m	tctt CTCCtGGAGA tgca	3008	Ras-related C3 botulinum toxin substrate 3 Precursor
	h	gtct CTCCgGGAGA agct	-937	
Stab1	m	agta CTCCaGGAGA gaca	-2004	Stabilin-1 Precursor
	h	cggg CTCCtGGAGA cgca	-14268	
Stat3	m	cctt CTCCaaGGAGA agat	-19731	Signal transducer and activator of transcription 3
	h	cctt CTCCaaGGAGA agat	-16701	
Tgfb1	m	ccca CTCCcGGAGA gagc	-10900	Transforming growth factor beta-1 Precursor
	h	tctc CTCCaGGAGA cgga	536	
Tgm6	m	cagg CTCCctGGAGA agtt	-4373	transglutaminase 6
	h	ttgg CTCCctGGAGA aagc	-4671	
Tirap	m	cagc CTCCttGGAGA gcag	-9343	Toll/interleukin-1 receptor domain-containing adapter protein
	h	ggcc CTCCgaGGAGA atgt	361	
Genes involved in signal transduction				
Akt1	m	acgg CTCCagGGAGA ccct	-7273	Protein kinase B
	h	aggc CTCC tt GGAGA cagc	-1724	
Arhgap6	m	tctt CTCCtaGGAGA tggc	562	Rho GTPase-activating protein 6
	h	cctc CTCCacGGAGA gcgc	34	
Fev	m	ctgt CTCCtgGGAGA caag	-11317	PC12 ETS domain-containing transcription factor 1
	h	caca CTCCcaGGAGA aact	4464	
Fgfr3	m	ctgc CTCCccGGAGA tggc	-16169	Fibroblast growth factor receptor 3 Precursor
	h	ctgc CTCCccGGAGA tggc	-14933	

Hsd11b2	m	cttt CTCCtGGAGA cttc	-7888	Corticosteroid 11-beta-dehydrogenase isozyme 2 (Stewart, P.M., Krozowski, A.S., Gupta, A., Milford, D.V., Howie, A.J., Sheppard, M.C., and Whorwood, C.B. (1996). Hypertension in the syndrome of apparent mineralcorticoid excess due to mutation of the 11beta-hydroxysteroid dehydrogenase type 2 gene. Lancet *347*, 88-91.)
	h*	ttta **a**TCCtGGAGA cagt	-5308	
	h*	gcta CTCCtGGAG**c** tcag	2234	
Itpr3	m	ggag CTCCcGGAGA gctt	-4158	Inositol 1,4,5-trisphosphate receptor type 3
	h	ccaa CTCCtGGAGA ggga	-43	
Mapkapk2	m	gtaa CTCCaGGAGA gaca	-3094	MAP kinase-activated protein kinase 2
	h	cctt CTCCaGGAGA atta	-19211	
Nfatc1	m	ggct CTCCtGGAGA agtg	-15543	Nuclear factor of activated T-cells, cytoplasmic
	h	tgcg CTCCaGGAGA aggg	-2166	
Pla2g2c	m	gcat CTCCtGGAGA ggtc	-17227	Group IIC secretory phospholipase A2 Precursor
	h	gagg CTCCaGGAGA taca	-5047	
Plcg1	m	gccc CTCCccGGAGA gggt	-9	Phospholipase C-gamma-1
	h	gccc CTCCcgGGAGA gggc	45	
Ppp2r2b	m	cact CTCCtGGAGA tacc	-17088	Serine/threonine-protein phosphatase 2A 55 kDa regulatory subunit B beta isoform
	h	aaat CTCCaGGAGA actt	1757	
Ppp2r2c	m	ccca CTCCctGGAGA ggga	747	Serine/threonine-protein phosphatase 2A 55 kDa regulatory subunit B gamma isoform
	h	ccct CTCCctGGAGA agaa	679	
Prkcb	m	atcc CTCCaGGAGA cgca	-421	Protein kinase C beta
	h	atcc CTCCaGGAGA cgcg	-387	

Prkch	m	tgct CTCCggGGAGA ctat	99	Protein kinase C eta
	h	ggtc CTCCccGGAGA caaa	-946	
Prl	m*	caag CTCCc**t**GAGA ggtt	-4752	Prolactin-releasing hormone
	m*	catt **t**TCCtGGAGA catc	-9199	
	m*	atgc CTCCa**t**GAGA tcca	-9871	
	h	gggg CTCCtGGAGA gcca	-16043	
	h	ggca CTCCatGGAGA tccg	141	
Prlr	m	ctag CTCCaGGAGA tctg	-18599	Prolactin-releasing hormone receptor
	m	cggg CTCCtGGAGA gaac	503	
	h	cctg CTCCctGGAGA ttct	2132	
	h	gtct CTCCcaGGAGA attc	-9135	
Rab25	m	aaac CTCCgGGAGA tctc	-7141	Ras-related protein Rab-25
	h	aaac CTCCgGGAGA tttc	-9272	
Rac3	m	tctt CTCCtGGAGA tgca	3008	Ras-related C3 botulinum toxin substrate 3 Precursor
	h	gtct CTCCgGGAGA agct	-937	
Srgap1	m	gctt CTCCacGGAGA ctgg	-4	SLIT-ROBO Rho GTPase-activating protein 1
	h	gcct CTCCaaGGAGA acgg	40	
Stat3	m	cctt CTCCaaGGAGA agat	-19731	Signal transducer and activator of transcription
	h	cctt CTCCaaGGAGA agat	-16701	

RESULT II

Functional dissection of the Thymic Stromal Lymphopoietin (TSLP) promoter.

(Manuscript in preparation)

Functional dissection of the Thymic Stromal Lymphopoietin (TSLP) promoter

Milan Surjit[1], Krishna Priya Ganti[1], Mei Li, Daniel Metzger and Pierre Chambon*.

Institut de Génétique et de Biologie Moléculaire et Cellulaire (CNRS UMR7104, Inserm U964, Université de Strasbourg, Collège de France), Illkirch, 67404, France.

***Correspondence:** chambon@igbmc.fr (P.C.)

[1] These authors contributed equally to this work

Introduction

Previous studies from our laboratory have shown that keratinocyte-selective ablation of RXR α and β (RXRαβ$^{ep-/-}$ mutant) in the mouse results in the development of a skin and systemic syndrome mimicking human atopic dermatitis (AD), preceded by an enhanced expression of the cytokine Thymic stromal lymphopoietin (TSLP) in epidermal keratinocytes (Li *et al*, 2005). TSLP, the master regulator of allergic inflammation (Liu, 2006), is highly expressed in human AD skin lesions (Soumelis *et al*, 2002), and several lines of evidence have demonstrated that TSLP expression is both necessary and sufficient to induce atopic inflammation in mouse (Li *et al*, 2005, 2006, 2009; Yoo *et al*, 2005).

The TSLP promoter was found to contain putative nuclear receptor (NR) response elements. Topical treatment with either active Vitamin D3 [1α, 25 (OH)2 Vitamin D3] (VD3) or its low calcemic analogue MC903 (MC) and BMS961, which are agonistic ligands for VDR and RARγ, respectively, could on their own or synergistically induce TSLP expression in mouse keratinocytes (Li *et al*, 2006). MC903 treatment was more efficient at inducing TSLP expression in a cell-autonomous manner, and long term treatment with MC903 resulted in development of AD-like symptoms similar to those observed in RXRαβ$^{ep-/-}$ mice. Based on these evidence, we proposed the following molecular model (*see below, scheme A*) to explain how RXRα or β/VDR and RXRα or β/RARγ heterodimers could modulate TSLP expression (note that RXRγ is not expressed in keratinocytes). Because, under homeostatic conditions in vivo, there is no RA and very little, if any VD3 in epidermal keratinocytes, the activity of the TSLP promoter would be repressed by unliganded RXRα or β/VDR and RXRα or β/RARγ heterodimers associated with corepressors. RXRα and -β ablation which releases both heterodimers from their binding sites, would thus abolish repression and allow basal promoter-bound transcription factors to stimulate TSLP transcription to an activity that is sufficient to trigger the generation of an AD-like phenotype. Moreover, the topical application of MC903 would generate RXR/VDR-coactivator complexes, the transcriptional activity of which would be efficient enough to relieve the repression exerted by RXR/RARγ-corepressor complexes, and to enhance the basal promoter activity, whereas, RXR/RARγ-coactivator complexes formed upon application of BMS961 would be much less efficient at activating the basal TSLP promoter.

In the present study, we demonstrate the validity of the mechanism through which RXRα(β)/VDR and RXRα(β)/RARγ heterodimers regulate TSLP expression and also prove that this regulation is conserved in mouse and human. Furthermore, we have characterized several additional transcription factor binding elements, which are also conserved in mouse and human TSLP genes, and can function independently of RARγ and VDR. Taken together, our studies unveil the complexity of TSLP promoter organization and provide important insight into the mechanisms that regulate TSLP expression in mouse and human.

(A) Schematic model of RXRα(β)/VDR- and RXRα(β)RAR-mediated regulation of TSLP expression in mouse keratinocytes.

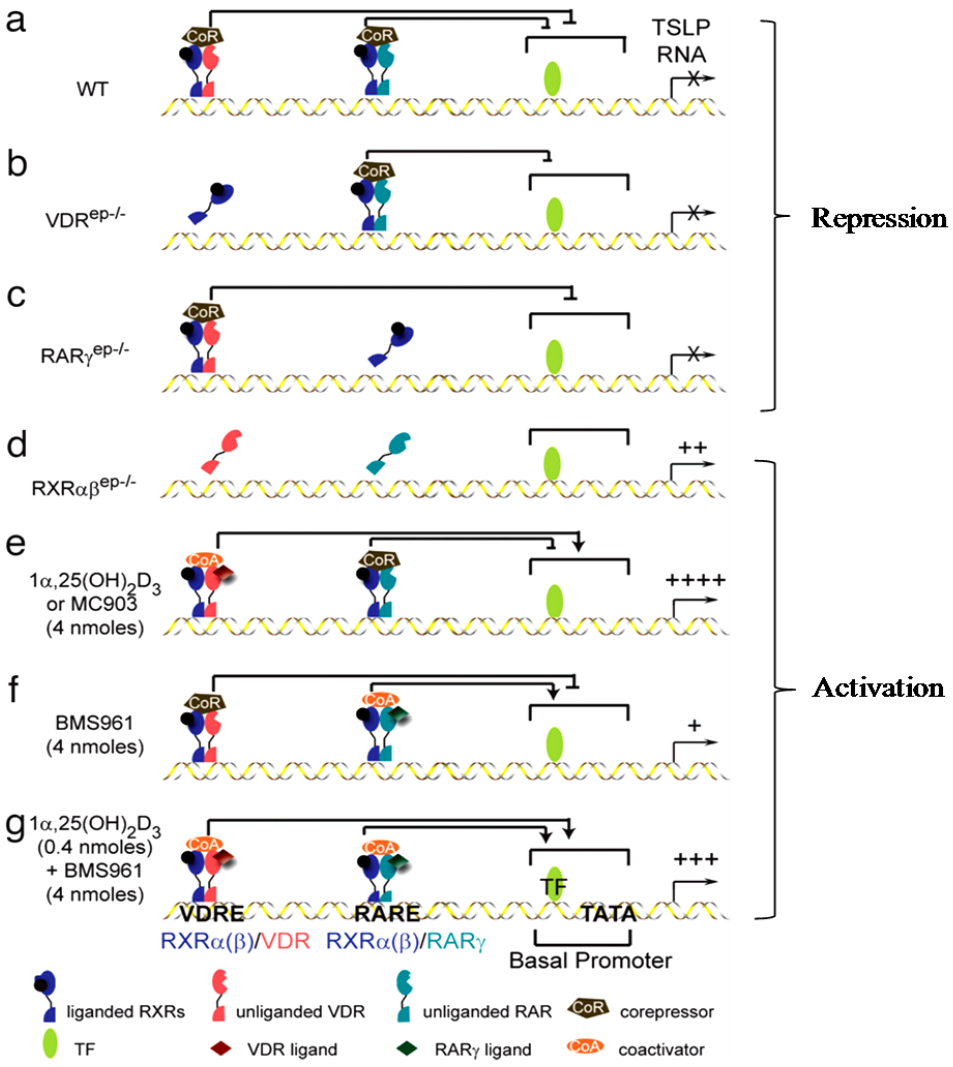

Results and Discussion

(A) VDR, RARs and RXRs control TSLP expression at the transcriptional level in epidermal keratinocytes of the mouse.

To determine whether MC (MC903, a low calcemic analog of active vitamin D3) or RA (all-trans retinoic acid)-mediated increase in TSLP RNA level in the epidermis of wild type (WT) mice (Li *et al*, 2006) is due to increased transcription, nuclear run-on assays were performed using nuclei isolated from the dorsal skin epidermis of WT C57Bl/6J mice topically treated with vehicle (ethanol), MC or RA. TSLP transcript specific autoradiogram signals were detected in MC and RA-treated samples, whereas no signal was detected in ethanol-treated sample (Figure 1A, Panel 1, 2, 3, lane 2). Moreover, run-on transcripts from MC treated mice produced a more intense "TSLP" signal than those from RA-treated mice, indicating that the higher level of TSLP RNA achieved with MC than with RA (Li *et al*, 2006, and see below) treatment corresponds to a higher rate of transcription. Similarly, cotreatment with MC and RA generated a stronger "TSLP" signal in agreement with the synergistic increase observed at the RNA level (Li *et al*, 2006, and panel 4). To determine whether increased TSLP RNA production in the RXRαβ$^{ep-/-}$ mice (Li *et al*, 2005) was due to increased transcription, nuclear run-on assays were performed using epidermis from these mice. Epidermis from RARγ/VDR$^{ep-/-}$ and RARαγ/VDR$^{ep-/-}$ mice was also subjected to nuclear run-on assay to investigate whether the increased TSLP RNA production in these animals (see figure 2 H) could also be due to increased transcription. In all cases, increased TSLP expression corresponded to increased transcription from the TSLP promoter (Figure 1A, panel 5, 8, 9, 10). As a positive control to ensure that an equal amount of nuclei was used across different samples, the rate of β actin transcription was measured in the same samples, which produced equal signal intensity in all cases (lane 3). pSK+ vector was used as a negative control to ensure specificity of the signal (lane 1).

(B) Unliganded RXRα/VDR and RARγ/RXRα or RXRβ heterodimers bind to their cognate response elements and mediate ligand-dependent activation of TSLP transcription in mouse epidermis.

We previously reported the presence of putative NR binding sites in the mouse TSLP gene upstream promoter region ((Li *et al*, 2006). We have now performed a detailed "manual" and bioinformatics analysis of 100kb upstream and 20kb downstream DNA sequence from the mouse TSLP +1 position (considering "A" of the translation initiation codon ATG as position +1) allowing 2 base mismatch in NR consensus motifs, and observed the existence of 7 putatuive VDREs (denoted DR3a-g), 2 putative RAREs (denoted DR2a and DR2b) and 3 putative DR1 elements (denoted DR1a-c; which are known to associate with heterodimers of RXR associated with PPAR/LXR/PXR/FXR among others) (Figure 1B, Table 1). Note that DR3b, DR3c and DR3e and DR3d, DR3f and DR3g elements contain identical sequence (Table 1). DR3f and DR3g are present within a 2.13kb long repeated sequence which spans from -32824 to -30694bp (encompassing DR3f) and -44655 to -42526bp (encompassing DR3g).

The ability of these elements to bind their cognate NRs was verified in vitro by Electrophoretic Mobility Shift Assay (EMSA) and supershift assay using nuclear extract from mouse epidermis and respective antibodies. Only DR3d, DR3f and DR3g associated with a nuclear protein complex that could be supershifted with antibodies specific to RXRα and VDR [Note that all 3 elements contain identical sequence (Table 1), so only DR3d was tested]. Importantly, this complex was absent when nuclear extract from $VDR^{ep-/-}$ mice epidermis was used in the assay, thus confirming that these are bonafide VDREs (Figure S1A and data not shown). Both DR2a and DR2b element bound nuclear protein complex could be supershifted using RXRα and RARγ antibodies (Figure S1B), whereas only DR1a and DR1b-bound nuclear protein complex could be supershifted using RXRα, PPARα and PPARγ antibodies (Figure S1 C and data not shown). Note that no efficient antibody for supershift assay against PPARβ was available. Interestingly, although none of these NR binding elements were perfect elements, only those with a consensus motif at least in one of the repeated motifs could associate with the corresponding NR (see Table 1).

We then tested whether DR3, DR2 and DR1 elements were associated with their corresponding NR partners in vivo, in the mouse epidermis. Using RXRα and VDR antibodies, Chromatin immunoprecipitation (ChIP) assay of epidermal whole cell extract (WCE) from vehicle-treated skin revealed association of VDR and RXRα with DR3d, DR3f, and/or DR3g elements (Figure 1C). (As DR3f and DR3g are present within a 2.13kb long repeat sequence, unique primers could not be designed to specifically assess VDR and RXRα binding to the DR3f and DR3g regions) Treatment with MC did not alter the binding efficiency of RXRα and VDR with various DR3 elements (Figure 1C). The specificity of the ChIP assay was confirmed by testing VDR and RXRα association with the DR3d element in the epidermis of $VDR^{ep-/-}$ mice,

which gave negative result (Figure 1D). Similar results were obtained for DR3 f and DR3g elements (data not shown).

To determine whether RAR is associated with DR2 elements, a pan-RAR antibody (which reacts with all 3 RAR isotypes) was used, since no ChIP grade antibody specific against different RAR isotypes was available. ChIP assay revealed that irrespective of RA treatment, neither RAR nor RXRα were associated with the DR2a element. However, under identical conditions, RAR was associated with the DR2b element (Figure 1E). To identify the RAR isotype that associates with the TSLP DR2b element, we performed ChIP assays using epidermis from RARγ$^{-/-}$ mice. No binding of RAR with DR2b was detectable in these animals, indicating that RARγ specifically associated with DR2b (Figure 1F). The specific involvement of the RARγ isotype in regulation of TSLP transcription was confirmed by using the isotype-specific RAR agonistic ligands BMS961 and BMS753, selective for RARγ and RARα, respectively. Measurement of TSLP transcript level in WT and RARγ$^{-/-}$ mice topically treated with the above ligands revealed that both RA (a pan-RAR isotype agonist) and BMS961, but not BMS753 enhanced TSLP level in WT animals. None of the ligands could enhance TSLP levels in the skin of RARγ$^{-/-}$ animals (Figure 1G). As a control, we tested the ability of the above ligands to induce CRABP II transcription. In WT mice, RA, BMS961 and BMS753 could increase CRABP II transcript level, although RA and BMS961 were much more efficient than BMS753. As expected, in the RARγ$^{-/-}$ mice, only RA and BMS753 could induce CRABP II transcript level (Figure 1G).

As RXRα could not be detected on the DR2b element, we tested whether RXRα/RAR could associate with the DR2 element present in the CRABP II gene (which is a known target of RA in epidermal suprabasal cells), using aliquots of the same immunoprecipitated samples. Both RXRα and RAR could be detected on the CRABP II DR2 (Figure 1E), thus indicating that absence of RXRα on the TSLP DR2b is a property specific to the TSLP gene. In the epidermis, RXRα is the major isotype to be expressed, followed by RXRβ whereas no RXRγ can be detected (Li *et al*, 2000; Chapellier *et al*, 2002; Fisher and Voorhees, 1996). To investigate whether any specificity could exist between RXRα and RXRβ for heterodimerizing with VDR and RARγ, ChIP assays were carried out using epidermis from RXRα$^{ep-/-}$, RXRβ$^{ep-/-}$ and RXRαβ$^{ep-/-}$ mice. In the RXRα$^{ep-/-}$ mice, VDR did not associate with the DR3d, DR3f and/or DR3g regions, whereas RARγ association with the DR2b region was decreased by ~50 %. On the other hand, VDR binding was unaffected in the RXRβ$^{ep-/-}$ mice and RARγ binding was decreased by ~90% in the same animals (Figure 1 H and data not shown). As expected, neither VDR nor RARγ could associate with the corresponding elements in the RXRαβ$^{ep-/-}$ mice. As a control for RAR immunoprecipitation, its

association with CRABP II DR2 element was assessed in the above samples. RAR could associate with the CRABP II DR2 with equal efficiency in both WT and RXRβ$^{ep-/-}$ mice, whereas RAR binding was decreased by at least ~80% in the RXRα$^{ep-/-}$ mice and no binding was detected in the RXRαβ$^{ep-/-}$ mice (Figure 1H). To identify the NRs bound to the TSLP DR1 elements in mouse epidermis, we performed ChIP assays using RXRα, PPARα and PPARγ antibodies. Only RXRα binding to the DR1a element could be detected (Figure 1I, and data not shown).

Taken together, these results clearly demonstrated that (i) RXRα specifically heterodimerizes with the VDR on the TSLP DR3d, f and/or g elements (ii) RXRβ is the predominant heterodimerization partner of RARγ on the TSLP DR2b element (iii) RXRα may partially complement the deficiency of RXRβ on the TSLP DR2b element (iv) RXRα is the predominant partner of RAR on the CRABP II DR2 element (v) RXRβ may partially complement the deficiency of RXRα on the CRABP II DR2 element.

It is noteworthy that despite RXRβ being the predominant heterodimerization partner of RARγ on the TSLP DR2b, we could detect as much as ~50% decrease in RARγ binding to the DR2b element in RXRα$^{ep-/-}$ mice. This may be attributed to a redundancy among RXRα and RXRβ isotypes, if we assume that in the absence of RXRα, RXRβ could in-part replace RXRα by heterodimerizing with NR partners, to which RXRα is normally heterodimerized. Such a competition may result in limiting the amount of RXRβ available for binding to the TSLP DR2b element.

(C) VDR/RXRα and RARγ/RXRβ assemble repressing and activating complexes on TSLP VDRE and RARE elements, in the absence and presence of their cognate ligands, respectively.

As we found, in the absence of RA and MC903 treatment, a "constitutive" association of RXR/VDR and RXR/RARγ on their DNA binding sites (DBS) on the TSLP regulatory region, we investigated whether these heterodimers were functionally active in repressing TSLP transcription in mouse epidermis. DNA-bound RXR/VDRs and RXR/RARγ are known to assemble corepressor complexes containing SMRT, NCoR, Sin3A and Histone Deacetylases (HDACs) in the absence of agonistic ligands, thereby establishing a transcriptionally inactive chromatin state. ChIP assays using WT mouse epidermis revealed the presence of SMRT on

DR3d, f and/or g and DR2b elements. We also tested if HDACs were associated with the above complex using HDAC1, HDAC2, HDAC3 and HDAC7 antibodies in ChIP assays, which revealed the presence of HDAC2 (Figure 2A, and data not shown). ChIP assay of MC-treated epidermis revealed the disappearance of SMRT and HDAC2 and appearance of SRC2 and SRC3, as well as p300, pCAF, CDK7, and RNA polymerase II on DR3d region. However, DR3f and/or DR3g as well as DR2b regions were still associated with SMRT and HDAC2. On the other hand, treatment with RA resulted in disappearance of SMRT and HDAC2, and recruitment of SRC2, as well as p300, pCAF, CDK7, and RNA polymerase II to the DR2b region, whereas, DR3d, f and/or g remain associated with the corepressor SMRT and HDAC2 (Figure 2A). In order to assess the overall transcription status of TSLP promoter in these experiments, we amplified a fragment from the proximal promoter region (-318 to -8bp from +1 position, denoted "PP" hereafter). PP region was associated with SMRT, HDAC2, pCAF and VDR (comparatively weaker signal) in vehicle treated mouse epidermis. Treatment with MC or RA resulted in dissociation of SMRT and HDAC2 and association of SRC2 and SRC3 (SRC3 is seen only in MC-treated samples), as well as p300, pCAF, CDK7, and RNA polymerase II on the PP region (Figure 2A).

DR3d and PP and DR2b and PP regions displayed a similar cofactor dynamics in the presence of agonists, suggesting that DR3d and DR2b may be interacting with the PP region in the presence of their respective agonists. Direct interaction between enhancer complex and PP is known to be a crucial determinant for transcription activation in several genes. To verify if such a mechanism holds true for TSLP, we designed a chromatin conformation capture (3C) assay to test the possible interaction between DR3d, f and/or g and DR2b elements with the PP region. Formaldehyde cross-linked chromatin was digested with AluI restriction enzyme to generate small DNA fragments encompassing various regions of interest (Figure 2B). These fragments were then re-ligated in such a manner that only if two fragments are held together by protein-protein interaction, they would be preferentially re-ligated. To ensure specificity of the assay, we used several controls (i) epidermis from $VDR^{ep-/-}$ or $RAR\gamma^{-/-}$ mice was simultaneously processed, which should produce negative result, (ii) AluI digested chromatin was "de-crosslinked" to release the protein complexes and then ligated (if 2 fragments could randomly ligate with each other, then we should detect that event in these samples, denoted as D+NC+L), (iii) Southern hybridized the PCR product with a probe spanning the AluI junction, and (iv) unligated (D) and undigested (ND+L) samples were used as negative controls. A BAC DNA was used as a positive control to check 3C efficiency in each case (TSLP BAC).

In the absence of MC, no or very weak interaction was observed between DR3d and PP region in WT mouse epidermis (Figure 2C, upper panel, lane 1 from left). This interaction was strongly increased in the presence of MC (lane 2). As expected, no interaction between DR3d and PP region was observed in VDR$^{ep-/-}$ mice treated with MC or WT mice treated with RA and TPA (lanes 7, 8, 9). Further, DR3f and/or DR3g, which did not show any coactivator or Pol II binding in ChIP assay, failed to interact with the PP region (Figure 2C, lower panel). 3C assay using DR2b region specific probe revealed a weaker interaction between DR2b and PP region only in the presence of RA (Figure 2D, lane 2).

As DNA bound VDR and RARγ complexes were associated with SMRT and HDAC2 in WT mice, we aimed at identifying the dominant repressor complex among these two. WT or RARγ$^{-/-}$ mice were treated with a limiting dose of MC (0.25 nmoles/cm^2). No significant increase in TSLP transcript was observed in the WT mice, whereas a ~5 fold increase was observed in the RARγ$^{-/-}$ mice (Figure 2E). On the other hand, treatment of WT or VDR$^{ep-/-}$ mice with 1 nmoles/cm^2 RA resulted in ~1.5 and 2 fold increase in the TSLP transcript level, respectively, (Figure 2F), suggesting that RARγ associated repressor complex played a dominant role in repressing TSLP transcription. In agreement with these results, treatment of RXRβ$^{ep-/-}$ mice with 4 nmoles/cm^2 MC resulted in ~150 fold increase in TSLP transcript level, in comparison to only ~50 fold increase in the WT mice (Figure 2G).

As DR3 and DR2 bound VDR and RARγ associated complexes appeared to constitutively repress TSLP transcription in WT mice, we hypothesized that selective ablation of VDR and RARγ in the keratinocytes should result in increased TSLP expression, as observed in RXRαβ$^{ep-/-}$ mice. To investigate this possibility, we generated keratinocyte selective conditional knock-out mice lacking RARγ and VDR (RARγ/VDR$^{ep-/-}$). Although, increase in TSLP transcript and protein level were observed in these mice, relative levels were much lower than that observed in RXRαβ$^{ep-/-}$ mice (Figure 2H, I, and J). Moreover, these mice did not develop pathophysiological characteristics typical to RXRαβ$^{ep-/-}$ mice (Figure S2, 2J, and data not shown). Interestingly, mice lacking RARα in addition to RARγ and VDR selectively in the keratinocytes (RARαγ/VDR$^{ep-/-}$) developed a phenotype and pathophysiology similar to those observed in the RXRαβ$^{ep-/-}$ mice (Figure S2 and 2J). As expected, level of TSLP transcript and protein in these triple mutants was comparable to those of RXRαβ$^{ep-/-}$ mice (Figure 2H, I, and J).

Taken together, these results demonstrate that in the absence of an agonistic ligand, which is the condition prevalent in WT mice epidermis, heterodimers of VDR/RXRα and RARγ/ RXRα or RXRβ are bound to their respective response elements on the TSLP promoter upstream

regulatory region along with corepressor SMRT and HDAC2, thereby maintaining TSLP gene in a transcriptionally inactive state. Upon MC or RA binding to VDR or RARγ respectively, SMRT and HDAC2 are released from the DNA bound NR complexes, followed by recruitment of SRC2 and/or SRC3 bearing coactivator complexes and interaction of the DR3d VDRE or DR2b RARE with the PP region, leading to activation of TSLP transcription. Relative contribution of SMRT, SRC2 and SRC3 in regulating TSLP transcription may be evaluated by measuring TSLP transcription in mice lacking these factors selectively in the epidermal keratinocytes.

Inability of RARγ/VDR$^{ep-/-}$ mutant mice to generate the phenotype of RXRαβ$^{ep-/-}$ mutant mice may be attributed to the redundancy between RARα and RARγ isotypes in this artificial condition. Thus, when RARγ is ablated, RARα may be able to complement some of its repressor activity. However, as treatment of RARγ/VDR$^{ep-/-}$ mice with BMS753 did not result in any further increase in TSLP transcript; and we did not detect any RARα at the DR2b element in these mutants (data not shown), therefore, an alternate possibility may be that ablation of RARαγ/VDR or RXRαβ in the keratinocytes activates some other transcription factors (TFs), which could in turn induce TSLP transcription.

It is noteworthy that although MC treatment resulted in the recruitment of both SRC2 and SRC3, RA treatment could recruit only SRC2. One possible explanation may be that, owing to the presence of a heterogeneous population of cells in the epidermis, different populations may be responsive to MC and RA treatment and there may be selective enrichment of either SRC2 or SRC3 in one of them. Presence of a heterogeneous population of cells in the epidermis may also explain why DR3f and/or g elements remain "constitutively" associated with a corepressor complex.

SMRT, HDAC2, pCAF and VDR were detectable at the PP region in the WT mice without MC or RA treatment. SMRT and HDAC2 seem to be associated with some other DNA bound factors at the PP region rather than VDR because (i) we did not detect a clear interaction between DR3d and PP in the absence of MC (ii) if SMRT, HDAC2 and VDR are part of the same complex, their band intensities should have been almost similar. Function of pCAF on the TSLP PP region in vehicle treated mice remains to be explored.

(D) TSLP upstream regulatory sequence contains multiple Smad, NF-κB, AP1 and STAT binding elements.

To characterize additional regulatory elements present in the TSLP gene, bioinformatics analysis was carried out spanning 100kb upstream and 20kb downstream DNA sequence from the TSLP +1 position, which revealed the presence of several putative Smad, NF-κB, AP1 and STAT binding elements (Figure 3A & Table 1).

TSLP upstream promoter region contains 2 putative Smad binding elements with the characteristic "CAGA" motif. In EMSA, both Smad 3a and Smad 3b elements could associate with Smad3 and Smad4 (Figure S3A). ChIP assay of WT mouse epidermis as well as MLE12 cells demonstrated that Smad2, Smad3 and Smad4 are associated with Smad3a and Smad3b elements (Figure 3B). Additionally, pCAF was also constitutively bound to these regions. However, no Smad binding was detected at the PP region in the mouse epidermis, although they could be readily detected at the PP region in MLE12 cells along with p300 and pCAF. Smad binding to their cognate elements and PP was further enhanced by TGFβ treatment of the MLE12 cells (Figure 3B). A functional role of Smads in regulating TSLP transcription was further investigated by treating MLE12 cells with either TGFβ or Smad3 specific inhibitor (SIS3) or TGFβ receptor specific inhibitor (TGFR In). Treatment with either SIS3 or TGFR inhibitor repressed the basal level of TSLP transcript to some extent. Also, TGFβ treatment stimulated TSLP transcript level by ~30%, which could be repressed by the inhibitors (Figure 3C). As a control to ensure the specificity of these inhibitors, Smad7 (a target of TGFβ pathway) RNA level was measured in these samples, which showed expected result (Figure 3C).

TSLP promoter contains 1 consensus NF-κB element (NF-κBa) and 5 putative NF-κB elements (Table 1). In EMSA, NF-κBa element exhibited a stronger affinity for association with p65 and p50 NF-κB proteins. Of the imperfect NF-κB elements, only NF-κBc could associate with p65 and p50 (Figure S3B, and data not shown). Ability of NF-κBa and NF-κBc elements to associate with p65 protein was tested in vivo by ChIP assays. In vehicle, MC or RA-treated mouse epidermis, p65 or p50 was not bound to any of the TSLP NF-κB binding sites (Figure 3D). We reasoned that absence of p65 or p50 binding to any of the TSLP NF-κB binding sites may be due to absence of these factors in the nucleus in the absence of an activating signal. Therefore, we treated mouse dorsal skin with TPA, a known activator of NF-κB signalling. ChIP assay using TPA-treated epidermal extract revealed that both p65 and p50 could bind to NF-κBa and NF-κBc regions (Figure 3D). NF-κBa element was more efficient than NF-κBc element for binding with p65 and p50 (Figure 3D). A functional role of NF-κB in activating TSLP transcription in mouse

epidermis was determined by co-treatment of mouse skin with TPA and BAY (a specific inhibitor of IKKβ activity), which resulted in ~70% decrease in TSLP transcript level (Figure 3G). Note that, we have earlier confirmed by nuclear run-on assay that TPA enhances the rate of TSLP transcription (Figure 1A, panel 5). In order to determine whether NF-κB similarly regulated TSLP promoter when induced by a physiologically relevant activator, MLE12 mouse lung epithelial cells were treated with IL-1β, which increased the level of TSLP transcript (Figure 3H) and p65 and p50 proteins were bound to both NF-κBa and NF-κBc elements (Figure 3I).

Mouse TSLP gene contains 4 consensus (AP1 b, e, f and g) and 3 with one base mismatch (AP1 a, c and d, all three containing the same sequence) AP1 elements (Table 1). In EMSA, both types of AP1 elements equally bound with c-fos and c-jun (Figure S3C). In ChIP assays using vehicle, MC or RA-treated mouse epidermis, c-fos or c-jun was not bound to any of the TSLP AP1 binding sites (Figure 3E, and data not shown), We reasoned that absence of c-fos or c-jun binding to any of the TSLP AP1 binding sites may be due to absence of these factors in the nucleus in the absence of an activating signal. Therefore, we treated mouse dorsal skin with TPA, which is also known to activate AP1 signalling. ChIP assay using TPA-treated epidermal extract revealed that both c-fos and c-jun could bind to AP1b, AP1c, AP1d, AP1f and AP1g elements (Figure 3E & 3F). As expected, co-treatment of mouse skin with TPA and ERK (Extra-cellular Regulated Kinase) inhibitor U0126 or JNK (Jun Kinase) inhibitor resulted in ~50% and 70% decrease in the level of TSLP transcript, respectively (Figure 3G). Note that both ERK and JNK control the activity of c-fos and c-jun by phosphorylating them. Association of c-fos and c-jun with the AP1 elements was also tested in IL1β treated MLE12 cells, which showed similar results (Figure 3J and data not shown).

ChIP assays were performed using TPA-treated mouse epidermis to identify the coactivators present at the NF-κB and AP1 elements. Owing to the close proximity of NF-κBa element with the PP region (-237 bp), PCR with PP primers was used to detect factors present at the NF-κBa and PP regions in ChIP assay. TPA treatment resulted in the binding of p300, CDK7, pol II, p65 and c-jun to the PP region (Figure 3K) in addition to pCAF, which was also detected in the absence of TPA (Figure 2A). None of these factors except p65 were detectable at the NF-κBc element (data not shown). AP1b and AP1g elements were also associated with the same factors except that HDAC2 was present at the AP1g in addition (Figure 3K). Interestingly, both DR3d and DR2b elements were associated with their respective NRs and corepressor in the presence of TPA (Figure 3K), suggesting that dissociation of corepressors from these elements is not a prerequisite for transcriptional activation of TSLP promoter by NF-κB and AP1.

We then performed a 3C assay to determine if AP1 elements could interact with the PP region in TPA treated samples. AluI was used to generate fragments of DNA encompassing the different AP1 elements and the PP region (Figure 3L), which were then re-ligated to reveal the interaction between PP and a particular AP1 element. Only AP1b and AP1g elements were able to associate with the PP region specifically in the TPA treated samples (Figure 3M and Figure 5C).

We discovered 8 consensus STAT5/6 binding elements in the TSLP regulatory region (denoted STAT a-h). STAT5 and STAT6 bind to ttc(n3)gaa and/or ttc(n4)gaa motifs (Boucheron *et al*, 1998; Ehret *et al*, 2001). ChIP assays revealed that STAT5 was bound to STATa, STATb, STAT5c, STATd, STATf, STATg and STATh regions after overnight TPA treatment of mouse skin. In contrast, only after 3 days of MC treatment (once daily), STAT5 could be detected at some elements. No STAT5 association was detected after 3 days of RA treatment (Figure 4A). STAT6 was not bound at any of these elements under any condition (data not shown). These observations were further verified in MLE12 cells treated with VD3, IL-1β or TPA, which revealed a constitutive association of STAT5 and STAT6 at STATa, STATb, STATd and STATe regions. VD3 treatment did not alter this pattern. However, treatment with IL-1β resulted in disappearance of STAT5 and increased association of STAT6 at the same elements (Figure 4B). Thus, it appears that activation of STAT5 is a property specific to TPA treatment. Because STAT5 is abundantly available in TPA-treated samples, they bind to both STAT5 and STAT6 elements by default.

(E) Analysis of TSLP gene in keratinocyte-selective mutants of RARγ/VDR, RXRαβ and RARαγ/VDR reveals association of AP1 and STAT5 with their respective response elements.

ChIP assays performed using p65 antibody revealed no association with either NFkBa or NFkBc region in RXRα$^{ep-/-}$, RXRβ$^{ep-/-}$, RXRαβ$^{ep-/-}$, RARγ/VDR$^{ep-/-}$ or RARαγ/VDR$^{ep-/-}$ mice (Figure 5A, middle left panel). Simultaneous processing of a set of TPA treated samples served as a positive control (Figure 5A, left panel). On the other hand, c-jun was bound to the AP1b, AP1c, AP1d, AP1f and AP1g elements only in the RXRαβ$^{ep-/-}$ mice (Figure 5A, middle right panel & Figure 5B). Whether the observed AP1 binding was a consequence of global increase in AP1

activity in these animals was confirmed by in vitro gel shift assays using consensus AP1 probes, which revealed an increase in AP1 factor binding (data not shown). Further, a 3C assay (to test the interaction of different AP1 elements with the PP region in the epidermis of RXRαβ$^{ep-/-}$ mice) revealed that only the AP1b element could interact with the PP region (Figure 5C). ChIP assays using STAT5 antibody demonstrated that it was bound to all of the STAT elements except "STATe" in RXRαβ$^{ep-/-}$ mice, and except "STATe" and "STATh" in RARαγ/VDR$^{ep-/-}$ mice (Figure 5D). No association of STAT5 was detected in the RARγ/VDR$^{ep-/-}$ mice. Also, STAT6 was not detectable on any of the elements in these mice (data not shown). As in WT mice, Smad3a and Smad3b elements of different mutant mice were associated with Smad2, Smad3 and Smad4 (Figure 5E). Note that Smad binding appears to be enhanced in the RARαγ/VDR$^{ep-/-}$ mice in comparison to others.

In summary, these results indicate that higher TSLP expression observed in both RXRαβ$^{ep-/-}$ and RARαγ/VDR$^{ep-/-}$ mutant mice may be a consequence of activation of other TFs in these animals. We may assume that in addition to relief from NR mediated repression, activation by AP1 and STAT5 in RXRαβ$^{ep-/-}$ mice and STAT5 and Smads in the RARαγ/VDR$^{ep-/-}$ mice may be responsible for stronger activation of the TSLP promoter, whereas in the RARγ/VDR$^{ep-/-}$ mice, only NR mediated repression is relieved, resulting in comparatively weaker activation of TSLP promoter. Nevertheless, the actual contribution of AP1, STAT5 and Smads in driving TSLP transcription needs to be confirmed by co-ablating these factors in the RXRαβ$^{ep-/-}$ and RARαγ/VDR$^{ep-/-}$ mice.

(F) Organization of TSLP regulatory elements is conserved in mouse and human.

To determine whether TSLP expression in both human and mouse is regulated in a similar manner, a bioinformatics search was carried out to identify orthologue elements in the human TSLP gene. As expected, human TSLP gene was found to contain similar regulatory elements (Table S1), the functionality of which was validated in A549 human lung epithelial cells.

Treatment of A549 cells with active Vitamin D3 (VD3), RA, TPA, IL-1β or TNFα for 6 hours, resulted in an increase in TSLP RNA level, indicating that both NR dependent and independent pathways that control TSLP expression in mouse, are functional in these cells (

Figure 6A). EMSA and ChIP assays were carried out to identify and characterize various elements.

Of the 8 putative DR3 elements, 7 could associate with RXRα and VDR in EMSA and supershift assay (Table S1), however only DR3 b, c, d and e could associate with RXRα and VDR in vivo, as revealed by ChIP assay (Figure 6B). Similarly, of the 4 putative DR2 elements, only DR2b could associate with RAR and RXRα in vivo, although all of them associated with RXRα and RARγ in vitro (Figure 6C and Table S1). Treatment of cells with agonistic ligands of VDR and RAR did not alter this binding pattern (data not shown). Among the two DR1elements, both could associate with RXRα, PPARα and PPARγ in vitro, but neither was associated with these factors in vivo (data not shown).

An earlier report has characterized the role of an imperfect NF-κB element in regulating human TSLP expression (denoted NF-κBb, Lee *et al*, 2007). We observed the presence of an additional consensus NF-κB element (NF-κBa) close to the TATA box, which is also perfectly conserved in mouse (see Table 1). ChIP assay of IL-1β treated cells demonstrated p65 and p50 binding at these elements, expectedly NF-κBa element was bound to p65/p50 with a higher affinity (Figure 6D).

Human TSLP gene also contains 7 AP1 elements, all of which could associate with c-fos and c-jun in EMSA. However, in ChIP assays using IL-1β treated cells, only AP1a and AP1e could associate with c-fos and c-jun (Figure 6E). Similarly, of the 8 consensus STAT5/6 elements, only STATe and STATg could associate with STAT5 or STAT6 in TPA or IL-1β treated cells, respectively (Figure 6F) and of the 2 putative Smad binding elements, only Smad3a element could associate with Samd2 and Smad4 proteins in TGFβ treated cells (Figure 6G). TGFβ treatment also resulted in an increase in TSLP RNA level, which could be blocked with a TGFR inhibitor but not with SIS3 (Smad3 specific inhibitor), further supporting that Smad3 is not involved in regulating TSLP expression in these cells (data not shown). Note that none of the NF-κB, AP1, STAT or Smad elements were associated with cognate TFs in the absence of their activating stimulus.

Collectively, these results demonstrate that similar cis-acting regulatory elements are present in the TSLP promoter of both mouse and human. Therefore, transcription of the human TSLP gene may be controlled in a manner similar to that in the mouse.

Conclusion

In the present study, we have investigated the molecular mechanisms involved in the activation and repression of transcription of the TSLP gene in epidermal keratinocytes *in vivo*. The following conclusions can be drawn from this study:

A) Role of NRs in modulating TSLP transcription.

- RXRα, RXRβ, VDR, RARγ, and to some extent RARα, transcriptionally regulate the expression of TSLP in mouse keratinocytes *in vivo*. In basal state (WT), unliganded VDR/RXRα and RARγ(α)/RXRβ are bound to the DR3d (VDRE) and DR2b (RARE) sites, respectively, along with SMRT corepressor and HDAC2, thus maintaining the TSLP promoter in an inactive state. Topical application of RA and/or MC903 results in the replacement of corepressor complexes by coactivator complexes containing SRC2 (TIF2), or SRC2 (TIF2) and SRC3, for RA or MC903, respectively, thereby inducing TSLP transcription (see *scheme B*).
- **Our work shows unequivocally that unliganded and liganded heterodimers do bind efficiently and similarly to DR2 and DR3 elements, *in vivo.***
- **Our study also demonstrates for the first time that the function of RXR isotypes is not redundant within RXR/NR heterodimers *in vivo,* as in epidermal suprabasal keratinocytes and irrespective of the presence of their cognate ligands:**

    1. **VDR is heterodimerized with RXRα on the DR3d, -f and -g VDREs of the TSLP promoter.**
    2. **RARγ is heterodimerized with RXRβ on the DR2b RARE of the TSLP gene.**
    3. **RARγ is heterodimerized with RXRα on the DR2b RARE of the CRABP II gene.**

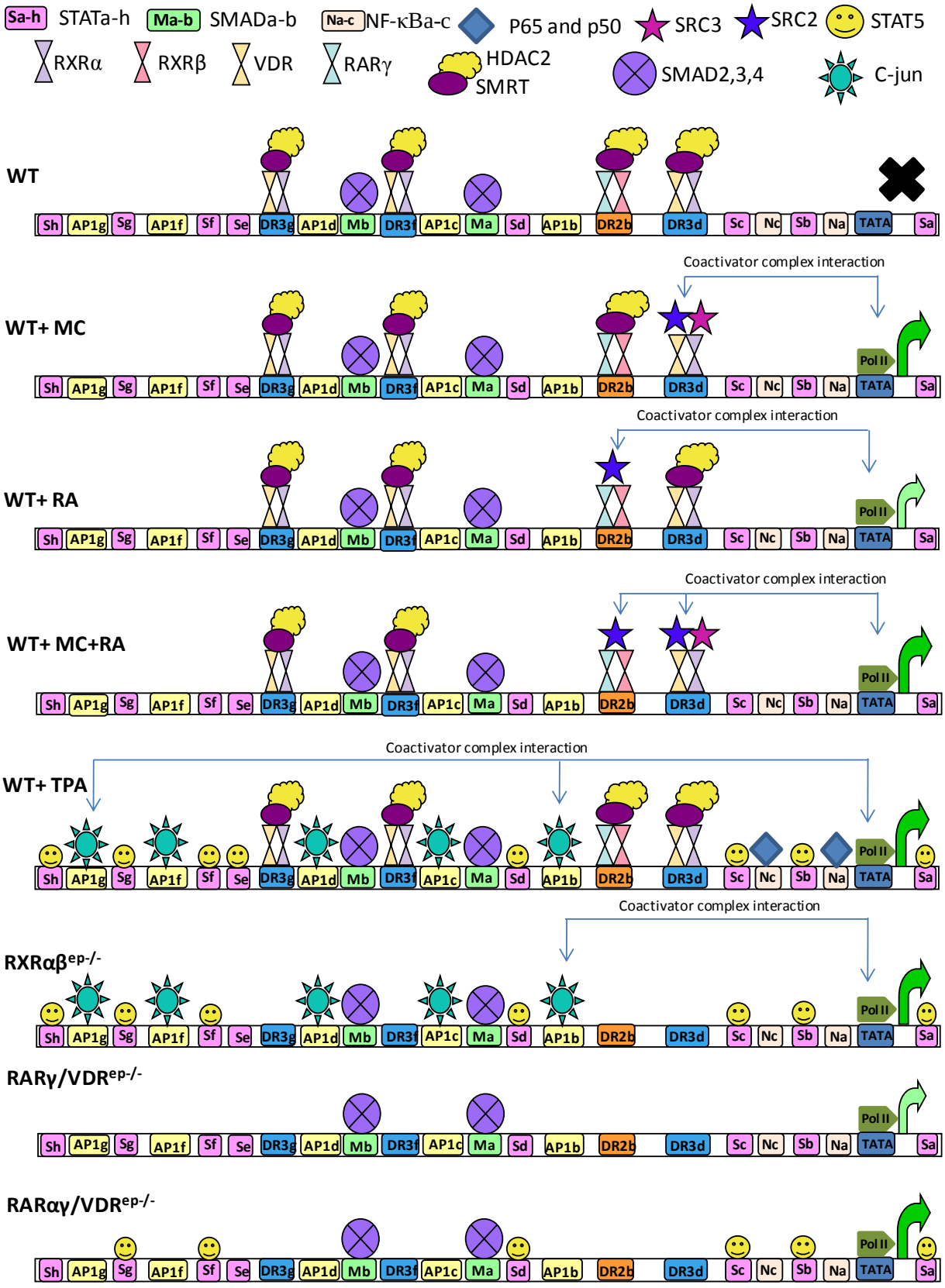

(B) Schematic representation of the distribution of transcription factors regulating

TSLP gene transcription in the keratinocytes of "wild type" untreated (WT), MC, RA, MC + RA, TPA- treated or in RXRαβ$^{ep-/-}$ RARγ/VDR$^{ep-/-}$ and RARγα/VDR$^{ep-/-}$ mutant mice.

- Derepression by keratinocyte selective ablation of either RXRα and RXRβ (RXRαβ$^{ep-/-}$) or RARγ(α) and VDR (RARγ/VDR$^{ep-/-}$ or RARγα/VDR$^{ep-/-}$) results in the release of repressor complexes from their respective response elements and recruitment of basal transcriptional machinery, thus enhancing the TSLP transcription.
  - The role of RARα remains unclear, as neither we detect its binding to the DR2b element nor is there an increase in TSLP transcript level by topical application of RARα specific agonist.
  - Though VDR/RXRα associated repressor complex could be detected on DR3d, -f and/or -g element, only DR3d recruits a coactivator complex upon MC903 treatment. This raises important questions regarding the role of these DR3 elements. Does DR3d alone modulate TSLP transcription? Does DR3f/g behave only as repressors or do they recruit coactivator complex under specific instances? In order to clarify this point we are generating mice bearing mutation in the DR3d element of the TSLP promoter.
  - In case of DR2 elements, we detect a repressor complex only on the DR2b element, which is replaced with a coactivator complex upon RA treatment. In order to definitely establish the specific role of DR2b element in regulating TSLP transcription, mice bearing mutation in this element is being generated.
  - As we detect NR-associated repressor complexes on both DR2b and DR3d elements in the basal state and ablation of either NR partners from both of these heterodimers results in increased expression of TSLP, it would be interesting to check if mice bearing both DR2b and DR3d element mutations show similar rate of TSLP transcription as in RXRαβ$^{ep-/-}$ or RARαγ/VDR$^{ep-/-}$ mutant mice.
- In addition, the actual role played by corepressors and coactivators in regulating TSLP transcription will be investigated using the keratinocyte-selective mouse mutants, SMRT$^{ep-/-}$, SRC2$^{ep-/-}$ and SRC$^{ep-/-}$, which are available in our laboratory.

B) Role of other transcription factors in modulating TSLP transcription.

- Mouse TSLP gene contains binding sites for the transcription factors Smad, NF-κB, AP1 and STAT.
- We detected "constitutive" binding of Smad2, 3 and 4 to the Smad binding elements in the TSLP gene in wild type as well as in RXRαβ$^{ep-/-}$, RARγ/VDR$^{ep-/-}$ and RARαγ/VDR$^{ep-/-}$ mutant mice. However, their functional relevance in regulating TSLP transcription *in vivo* remains unclear. We are generating keratinocyte-selective Smad2/3 null mice to address this issue. Further, ablation of Smad 2 and 3 in RXRαβ$^{ep-/-}$, RARγ/VDR$^{ep-/-}$ and RARαγ/VDR$^{ep-/-}$ mutant mice would enable us to delineate the role of Smads, if any, in inducing TSLP transcription in these mice.
- We are currently generating mice bearing mutation in NF-κBa element in the TSLP promoter to reveal the *in vivo* significance of this element in regulating TSLP expression, in particular with respect to the NF- κBc element.
- We have also shown that STAT5 or STAT6 is recruited to STAT binding element depending on the stimulus (TPA treatment induces STAT5 binding, whereas IL1β induces STAT6 binding to its response element, while MC903 also induces STAT5 binding to its response element). Interestingly, reports have shown that TSLP induces STAT5 activity in cultured cells. We will investigate how TSLP could be involved in regulating STAT5 activity at the TSLP promoter. Additionally, we are generating keratinocyte-selective STAT5 null mice to establish its role in regulating TSLP expression.

  STAT5 is also bound to STAT binding elements in RXRαβ$^{ep-/-}$ and RARαγ/VDR$^{ep-/-}$ mutant mice (see scheme B). Co-ablation of STAT5 in RXRαβ$^{ep-/-}$ and RARαγ/VDR$^{ep-/-}$ mice would clarify its role in regulating TSLP transcription in these mice.

- Our work demonstrates that between mouse and human, there are structural similarities of cis-acting regulatory elements in the TSLP gene. We are planning functional studies on human epidermis to investigate if additional mechanisms could have evolved in the course of evolution to ensure a tighter control of TSLP expression.

Materials and Methods

Mice. Wild type C57BL/6J female mice, 6-8 week-old, were purchased from Charles River Laboratories. RXRα$^{ep-/-}$, RXRβ$^{ep-/-}$, RXRαβ$^{ep-/-}$, RARγ$^{-/-}$and VDR$^{ep-/-}$ are described (Chapellier *et al,* 2002; Li *et al,* 2000, 2005, 2006). RARγ/VDR$^{ep-/-}$ and RARαγ/VDR$^{ep-/-}$ was obtained by injecting 0.1 mg/day tamoxifen intra-peritoneally for 5 days to respective floxed animals. Age- and sex- matched littermates were used as wild type controls. For topical treatment on ear and dorsal skin, 1 nmole/cm^2 MC903 or TPA, 2 nmoles/cm^2 at-RA, BMS961 or BMS753, 500 nmoles/cm^2 BAY, 125 nmoles/cm^2 U0126 and 500 nmoles/cm^2 JNKI were used.

Isolation of epidermis from mouse dorsal skin. Inner side of shaved dorsal skin was scraped off fat and floated over 0.8% trypsin solution (0.8% trypsin (w/v) dissolved in PBS) for 30 minutes at 37 ^{0}C. Epidermal sheets were recovered in cell culture medium (EMEM without calcium + 10% FCS), incubated at 37 ^{0}C for 15 minutes and filtered through a 70μm nylon cell strainer (BD falcon). Epidermal cells were recovered by centrifugation (400g, 5 minutes) at 4 ^{0}C.

ChIP, Nuclear run-on, EMSA and Chromosome conformation capture (3C) assays. ChIP assay (Vaisanen *et al,* 2005), Nuclear Run-on assay and EMSA (Carey and Smale, 2001) and 3C assay (Liu *et al*, 2005) was done as described. Details of the procedure are given in supplementary data.

Quantitative RT-PCR (Q-PCR), Serum TSLP determination, Hematoxylin and Eosin staining and TSLP immunohistochemistry. as described in Li *et al*, 2005.

References

1. Boucheron C, Dumon S, Santos SC, Moriggl R, Hennighausen L, Gisselbrecht S, Gouilleux F. A single amino acid in the DNA binding regions of STAT5A and STAT5B confers distinct DNA binding specificities. J Biol Chem. 1998 Dec 18;273(51):33936-41.

2. Chapellier, B., Mark, M., Messaddeq, N., Calleja, C., Warot, X., Brocard, J., Gerard, C., Li, M., Metzger, D., Ghyselinck, N. B., *et al.* (2002) *EMBO J.* **21,** 3402–3413.

3. Ehret GB, Reichenbach P, Schindler U, Horvath CM, Fritz S, Nabholz M, Bucher P. DNA binding specificity of different STAT proteins. Comparison of in vitro specificity with natural target sites. J Biol Chem. 2001 Mar 2;276(9):6675-88.

4. Lee HC, Ziegler SF. Inducible expression of the proallergic cytokine thymic stromal lymphopoietin in airway epithelial cells is controlled by NFkappaB. Proc Natl Acad Sci U S A. 2007 Jan 16;104(3):914-9.

5. Li M, Hener P, Zhang Z, Kato S, Metzger D, Chambon P (2006) Topical vitamin D3 and low-calcemic analogs induce thymic stromal lymphopoietin in mouse keratinocytes and trigger an atopic dermatitis. *Proc Natl Acad Sci USA* **103**:11736–41

6. Li M, Messaddeq N, Teletin M, Pasquali JL, Metzger D, Chambon P (2005) Retinoid X receptor ablation in adult mouse keratinocytes generates an atopic dermatitis triggered by thymic stromal lymphopoietin. *Proc Natl Acad Sci USA* **102,** 14795–14800.

7. Li, M., Indra, A. K., Warot, X., Brocard, J., Messaddeq, N., Kato, S., Metzger, D. & Chambon, P. (2000) *Nature* **407,** 633–636.

8. Li, M., Pierre Hener, Zhikun Zhang, Krishna P. Ganti, Daniel Metzger and Pierre Chambon. (2009) Induction of Thymic Stromal Lymphopoietin Expression in Keratinocytes Is Necessary for Generating an Atopic Dermatitis upon Application of the Active Vitamin D3 Analogue MC903 on Mouse Skin. *J Invest Dermatol.* **129**, 498–502.

9. Liu, Y. J. (2006) Thymic stromal lymphopoietin: master switch for allergic inflammation. *J. Exp. Med.* **203,** 269–273.

10. Soumelis, V., Reche, P. A., Kanzler, H., Yuan, W., Edward, G., Homey, B., Gilliet, M., Ho, S., Antonenko, S., Lauerma, A., Smith K, Gorman D, Zurawski S, Abrams J, Menon S, McClanahan T, de Waal-Malefyt Rd R, Bazan F, Kastelein RA, Liu YJ. (2002) Human epithelial cells trigger dendritic cell mediated allergic inflammation by producing TSLP. *Nat. Immunol.* **3,** 673–680.

11. Yoo, J., Omori, M., Gyarmati, D., Zhou, B., Aye, T., Brewer, A., Comeau, M. R.,Campbell, D. J. & Ziegler, S. F. (2005) Spontaneous atopic dermatitis in mice expressing an inducible thymic stromal lymphopoietin transgene specifically in the skin. *J. Exp. Med.* **202,** 541–549.

Figure Legends

Figure1. TSLP expression is transcriptionally regulated in the mouse skin epidermis by RXR, RAR and VDR.

(A) Nuclear run-on assay using epidermis from WT mice-treated as indicated (panels 1-5 and panel 7) or epidermis from different keratinocyte selective mutant mice (panels 8-10). Autoradiograms of labelled transcripts hybridized with TSLP, β actin and control vector DNA are displayed in panels 1-5 and 7-10. Panels 6 and 11 show ethidium bromide (EtBr) staining of DNA probes.

(B) Schematic representation of nuclear receptor binding elements present in mTSLP gene. 'A' base of translation initiation codon (ATG) was taken as +1. Underlined elements bind to their respective NRs in ChIP assays.

(C) ChIP assays using WT mouse skin epidermis, treated as indicated, show the binding of RXRα and VDR to different DR3 elements present in TSLP gene. 10% input indicates the signal obtained after PCR amplification of the relevant DNA region contained in 10% of the chromatin that was used for immuonprecipitation (IP) with a given antibody. Ab IP: antibodies used for IP.

(D) ChIP assays of skin epidermis from WT or VDR ep -/- mice to detect VDR and RXRα binding to TSLP DR3d region.

(E) ChIP assays of ethanol or RA treated WT mice skin epidermis to detect RAR and RXRα binding to DR2a and DR2b regions.

(F) ChIP assays of skin epidermis from WT or RARγ-/- mice to detect RAR and RXRα binding to the TSLP DR2b region.

(G) Qunatitative RT-PCR (Q-PCR) of TSLP and CRABPII RNA from ears of WT and RARγ-/- mice topically treated, as indicated, for 16 hours (mean ± SEM).

(H) ChIP assays using skin epidermis from WT or various keratinocyte selective NR mutant (mut) mice to detect VDR and RAR binding to different elements, as indicated.

(I) ChIP assays of WT mice skin epidermis to detect RXRα binding to TSLP DR1 elements, as indicated.

Figure 2. Repressing and activating complexes are assembled by RARγ/RXRβ and VDR/RXRα on the TSLP DR2 and the DR3 elements, in the absence and in the presence of their cognate ligands, respectively.

(A) ChIP assays of WT mice skin epidermis, treated as indicated. IP was done using different antibodies, as indicated (Ab IP), followed by PCR with different primers, as indicated.

(B) Schematic representation of mTSLP upstream regulatory region. All bases are numbered with respect to +1. A, B, C, D and E are fragments generated by Alu I digestion of genomic DNA. Numbers in the upper panel denote the position of Alu I sites. Boxes represent promoter elements, whose coordinates are indicated.

(C) Chromosome conformation capture (3C) assay using WT or VDR ep-/- mice skin epidermis, treated as indicated. Upper, middle and lower panels reveal interaction between the regions containing DR3d and PP, DR3f and PP, and DR3g and PP, respectively. A BAC DNA encompassing the TSLP coding and flanking sequences was processed along, as a positive control for ligation efficiency (TSLP BAC). D- Alu I digested, L- ligated, ND- not digested and NC-uncrosslinked. FPCR + AluI denote that final PCR product was digested with AluI, followed by southern blotting.

(D) 3C assay using WT or RARγ -/- mice skin epidermis, treated as indicated, to detect the interaction between the region encompassing the DR2b element and PP. TSLP BAC and other abbreviations are same as in (C).

(E) TSLP Q-PCR from ears of WT or RARγ -/- mice treated with 0.25 nmole MC903, as indicated, for 16 hours (mean ± SEM).

(F) TSLP Q-PCR from ears of WT or VDR ep-/- mice treated with 1 nmole RA, as indicated, for 16 hours (mean ± SEM).

(G) TSLP Q-PCR from ears of WT or mutant mice treated with 4 nmole MC903, as indicated, for 16 hours (mean ± SEM).

(H) TSLP Q-PCR from ears of WT or mutant mice, as indicated (mean ± SEM).

(I) Measurement of serum TSLP level in the same animals used for TSLP Q-PCR in figure 1-J.

(J) TSLP immunohistochemistry (upper panel) and Hematoxylin and Eosin (HE) staining (lower panel) images of ear sections of the same animals, used for TSLP Q-PCR in figure 1-J. Scale bar represents 25µm and 100µm for upper and lower panels,

respectively. Yellow and cyan colours indicate staining of TSLP and nucleus of the cell, respectively.

Figure 3. TSLP expression is regulated by multiple NF-κB, AP1, STAT and Smad binding elements.

(A) Schematic representation of transcription factor (TF) binding sites present in mTSLP gene. Underlined elements bind respective TFs in ChIP assay.

(B) ChIP assay of WT mice dorsal skin or MLE 12 cells treated as indicated, to detect Smad2, Smad3 and Smad4 binding to indicated regions.

(C) Q-PCR of TSLP (left panel) and Smad7 (right panel) RNA from MLE 12 cells, treated as indicated, for 6 hours (mean ± SEM).

(D) ChIP assay of WT mice skin epidermis, treated as indicated, to detect the binding of p65 with NF-κB elements.

(E) ChIP assay of WT mice skin epidermis, treated as indicated, to detect the binding of c-fos or c-jun with the AP1a and AP1b elements.

(F) Aliquots of TPA treated samples from (C) were PCR-amplified using primers flanking the different AP1 elements present in TSLP gene, as indicated.

(G) TSLP Q-PCR from ears of WT mice, treated as indicated, for 6 hours (mean ± SEM).

(H) TSLP Q-PCR from MLE 12 cells, treated as indicated, for 6 hours (mean ± SEM).

(I) ChIP assays of MLE 12 cells, treated as indicated, to detect p65 and p50 binding to TSLP NF-κBa and NF-κBc elements.

(J) ChIP assays of MLE 12 cells, treated as indicated, to detect c-fos and c-jun binding to TSLP AP1b and AP1g elements.

(K) ChIP assays of TPA treated WT mice skin epidermis. IP was done using various antibodies, as indicated, followed by PCR using primers flanking indicated elements.

(L) Schematic representation of AP1 elements present in mTSLP gene, which can associate with with AP1 factors. A, B, C, D, E and F are fragments generated by Alu I digestion of genomic DNA. Numbers in upper panel denote Alu I sites. Boxes represent AP1 elements, whose coordinates are indicated.

(M) 3C assay using WT mouse skin epidermis, treated as indicated, to detect the interaction between AP1b and PP (upper panel) and AP1g and PP (lower panel). TSLP BAC and other abbreviations are same as in Figure 2 C.

Figure 4. STAT5/6 and Smad2/3/4 associates with the mouse TSLP STAT and Smad binding elements, respectively.

(A) ChIP assays of WT mice skin epidermis, treated as indicated, to detect STAT5 binding to various STAT elements present in the TSLP gene.
(B) ChIP assays of MLE 12 cells, treated as indicated, to detect STAT3, STAT5 and STAT6 binding to various STAT elements.

Figure 5. Analysis of keratinocyte selective knock-out mutants of RXRα, RXRβ, RXRαβ, RARγ/VDR and RARαγ/VDR to test the occupancy of NF-κB, AP1, STAT5 and Smads at their corresponding response elements present in the TSLP gene.

(A) ChIP assays of skin epidermis from WT and various keratinocyte selective mutants (mut) or TPA treated WT mice to detect the binding of p65 with NF-κBa and NF-κBc (left panel) elements and c-jun with AP1b and AP1g elements (right panel).
(B) Aliquots of ChIP-DNA from WT and RXRαβ ep-/- mice, used in (A) were PCR amplified using primers flanking the AP1c, d, f and g elements of the TSLP gene.
(C) 3C assay using skin epidermis from WT and RXRαβ ep-/- or TPA treated WT mice to detect the interaction between the region containing different AP1 elements and proximal promoter (PP). TSLP BAC and other abbreviations are same as in Figure 2(C).
(D) ChIP assays of skin epidermis from WT or various keratinocyte selective mutant mice, as indicated, to detect STAT5 binding to various STAT elements.
(E) As in (D), but IP was done using Smad 2, Smad 3 and Smad 4 antibodies, followed by PCR with primers flanking the Smad 3a and Smad 3b elements.

Figure 6. Organization of the TSLP gene regulatory elements is conserved in both mouse and human.
(A) TSLP Q-PCR from A549 cells treated as indicated, for 6 hours (mean ± SEM).
(B) ChIP assay of A549 cells to detect VDR and RXRα binding to various DR3 elements present in hTSLP (human TSLP gene).

(C) ChIP assay of A549 cells to detect RAR and RXRα binding to the hTSLP DR2b element.

(D) ChIP assay of IL1β treated A549 cells to detect p65 or p50 binding to the NF-κBa and NF-κBb elements present in hTSLP.

(E) ChIP assay of IL-1β treated A549 cells to detect c-fos or c-jun binding to the AP1a and AP1e elements present in hTSLP.

(F) ChIP assay of A549 cells treated as indicated, to detect STAT binding to STATe and STATg elements present in hTSLP.

(G) ChIP assay of A549 cells treated as indicated, to detect smad binding to hTSLP smad3a element.

Table I. Position, sequence and functional characteristic of various transcription factor binding elements present in mouse TSLP gene.

Name of the element	Position from ATG (A= +1)	Sequence	EMSA+ antibody shifting	**ChIP**(IP antibody)
Consensus DR1		**RggtcanRggtca**		
DR1a	-2176 to -2164	gggtcaggggaca	RXRα, PPARα, PPARγ	RXRα
DR1b	-5727 to -5715	atggcaaaggtca	RXRα, PPARα, PPARγ	-
DR1c	-14702 to -14690	aggtaagatgtca	-	-
Consensus DR2		**RggtcannRggtca**		
DR2a	-1063 to -1050	agctcaacaggtca	RXRα, RARγ	-
DR2b	-13892 to -13879	aggtcatgagttca	RXRα, RARγ	pan-RAR
Consensus DR3		**RggtcannnRggtca**		
DR3a	-4038 to -4024	agttcattccggtca	-	-
DR3b	-4121 to -4107	aggacagccagggct	-	-
DR3c	-6506 to -6492	aggacagccagggct	-	-
DR3d	-7369 to -7355	gagccagaggggtca	RXRα, VDR	RXRα, VDR
DR3e	-13658 to -13644	aggacagccagggct	-	-
DR3f	-32704 to -32690	gagccagaggggtca	RXRα, VDR	RXRα, VDR
DR3g	-44535 to -44521	gagccagaggggtca	RXRα, VDR	RXRα, VDR
Consensus NF-κB		**gggRNNYYCC**		
NF-κBa	-237 to -218	gggaaattcc	p65, p50	p65, p50
NF-κBb	-1447 to -1438	aggaacttcc	-	-
NF-κBc	-3587 to -3578	caggaatttc	p65, p50	p65, p50
NF-κBd	-3771 to -3762	gaaaattacc	-	-
NF-κBe	-3997 to -3988	gagaatcccc	-	-
NF-κBf	-4612 to -4601	agggactctc	-	-
Consensus AP1		**tgagtca**		
AP1a	-1235 to -1228	tgactca	c-fos, c-jun	-
AP1b	-16647 to -16640	tgagtca	c-fos, c-jun	c-fos, c-jun
AP1c	-29950 to -29943	tgactca	c-fos, c-jun	c-fos, c-jun
AP1d	-41783 to -41776	tgactca	c-fos, c-jun	c-fos, c-jun
AP1e	-46283 to -46276	tgagtca	c-fos, c-jun	-
AP1f	-71999 to -71992	tgagtca	c-fos, c-jun	c-fos, c-jun
AP1g	-77688 to -77681	tgagtca	c-fos, c-jun	c-fos, c-jun
Consensus smad3		**agccagaca**		
Smad3a	-27191 to -27183	agacagaca	Smad3, smad4	Smad2, 3 and 4
Smad3b	-38999 to -38991	agacagaca	Smad3, smad4	Smad2, 3 and 4
Consensus STAT5/6		**ttcnnn(n)gaa**		
STATa	+2918 to +2927	ttcgtgtgaa	+	Stat5/6
STATb	-623 to -614	ttccagtgaa	+	Stat5/6
STATc	-6967 to -6959	ttcggggaa	+	Stat5
STATd	-20262 to -20253	ttccctagaa	+	Stat5/6
STATe	-48832 to -48823	ttcctctgaa	+	Stat5/6
STATf	-61255 to -61246	ttcccaagaa	+	Stat5/6
STATg	-72700 to -72691	ttctcaagaa	+	Stat5
STATh	-84196 to -84187	ttcctgagaa	+	Stat5

n= a/c/g/t; R= purine; Y= pyrimidine

Figure 1

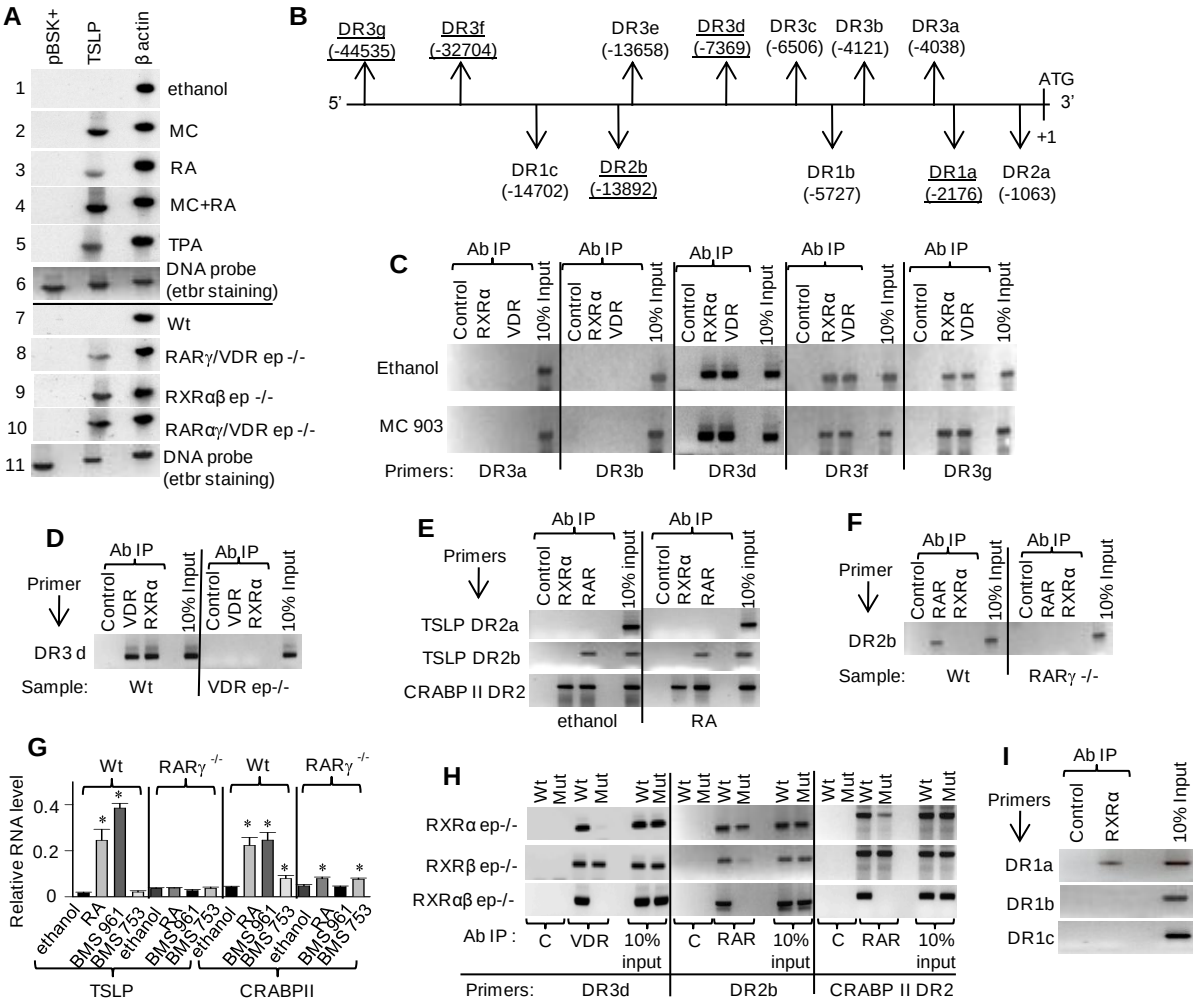
A
pBSK+
TSLP
β actin
1 ethanol
2 MC
3 RA
4 MC+RA
5 TPA
6 DNA probe (etbr staining)
7 Wt
8 RARγ/VDR ep -/-
9 RXRαβ ep -/-
10 RARαγ/VDR ep -/-
11 DNA probe (etbr staining)
B
DR3g (-44535)
DR3f (-32704)
DR3e (-13658)
DR3d (-7369)
DR3c (-6506)
DR3b (-4121)
DR3a (-4038)
5'
ATG
3'
+1
DR1c (-14702)
DR2b (-13892)
DR1b (-5727)
DR1a (-2176)
DR2a (-1063)
C
Ab IP
Control
RXRα
VDR
10% Input
Ethanol
MC 903
Primers: DR3a DR3b DR3d DR3f DR3g
D
Primer
DR3 d
Sample: Wt VDR ep-/-
E
Primers
TSLP DR2a
TSLP DR2b
CRABP II DR2
ethanol
RA
F
DR2b
Sample: Wt RARγ -/-
G
Wt
RARγ -/-
Relative RNA level
ethanol
RA
BMS 961
BMS 753
TSLP
CRABPII
H
Wt
Mut
RXRα ep-/-
RXRβ ep-/-
RXRαβ ep-/-
Ab IP :
C
VDR
10% input
RAR
Primers: DR3d DR2b CRABP II DR2
I
Primers
DR1a
DR1b
DR1c

Figure 2

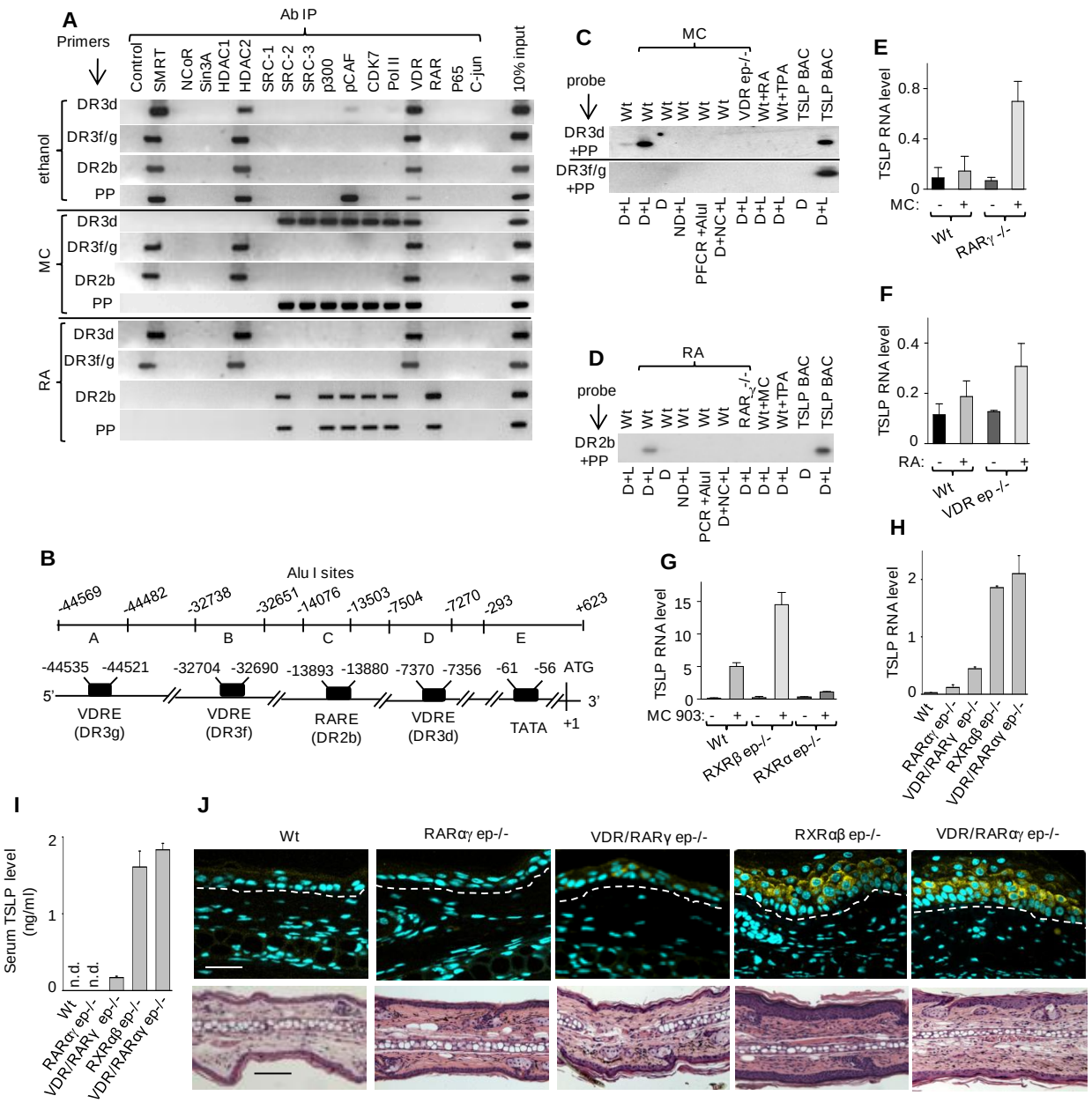
A
Ab IP
Primers
Control
SMRT
NCoR
Sin3A
HDAC1
HDAC2
SRC-1
SRC-2
SRC-3
p300
pCAF
CDK7
Pol II
VDR
RAR
P65
C-jun
10% input
ethanol
MC
RA
DR3d
DR3f/g
DR2b
PP
B
Alu I sites
-44569
-44482
-32738
-32651
-14076
-13503
-7504
-7270
-293
+623
A
B
C
D
E
-44535
-44521
-32704
-32690
-13893
-13880
-7370
-7356
-61
-56
ATG
5'
3'
VDRE (DR3g)
VDRE (DR3f)
RARE (DR2b)
VDRE (DR3d)
TATA
+1
C
MC
probe
DR3d +PP
DR3f/g +PP
Wt
VDR ep-/-
Wt+RA
Wt+TPA
TSLP BAC
D+L
ND+L
PFCR +AluI
D+NC+L
D
D
RA
DR2b +PP
RAR-/-
Wt+MC
E
TSLP RNA level
MC:
Wt
RARγ -/-
F
RA:
VDR ep -/-
G
MC 903:
RXRβ ep-/-
RXRα ep-/-
H
RARαγ ep-/-
VDR/RARγ ep-/-
RXRαβ ep-/-
VDR/RARαγ ep-/-
I
Serum TSLP level (ng/ml)
n.d.
J
Wt
RARαγ ep-/-
VDR/RARγ ep-/-
RXRαβ ep-/-
VDR/RARαγ ep-/-

Figure 3

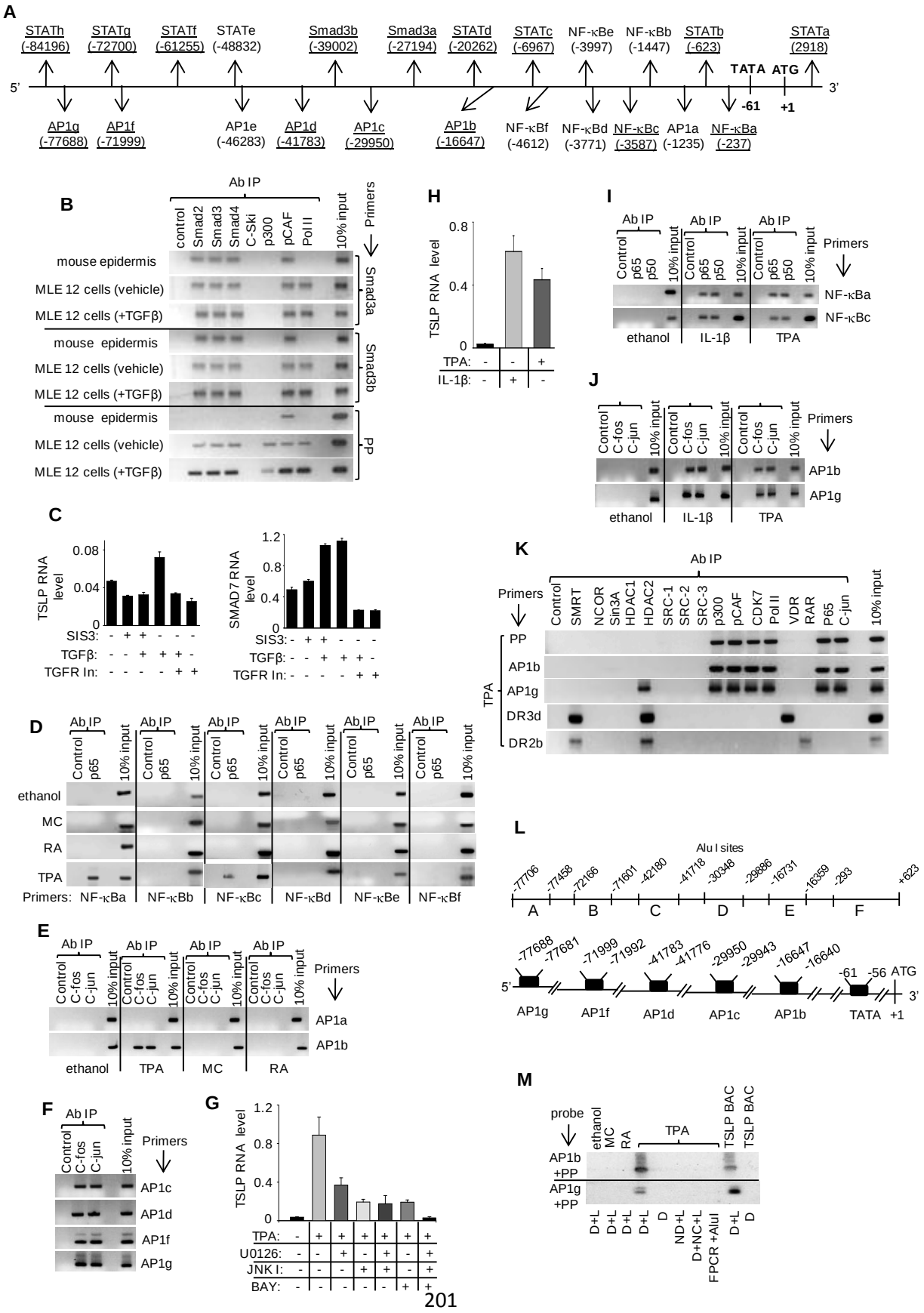
A
STATh (-84196)
STATg (-72700)
STATf (-61255)
STATe (-48832)
Smad3b (-39002)
Smad3a (-27194)
STATd (-20262)
STATc (-6967)
NF-κBe (-3997)
NF-κBb (-1447)
STATb (-623)
STATa (2918)
TATA
ATG
5'
3'
-61
+1
AP1g (-77688)
AP1f (-71999)
AP1e (-46283)
AP1d (-41783)
AP1c (-29950)
AP1b (-16647)
NF-κBf (-4612)
NF-κBd (-3771)
NF-κBc (-3587)
AP1a (-1235)
NF-κBa (-237)
B
Ab IP
control
Smad2
Smad3
Smad4
C-Ski
p300
pCAF
Pol II
10% input
Primers
mouse epidermis
MLE 12 cells (vehicle)
MLE 12 cells (+TGFβ)
Smad3a
Smad3b
Pol II
C
TSLP RNA level
SIS3:
TGFβ:
TGFR In:
SMAD7 RNA level
D
Ab IP
Control
p65
10% input
ethanol
MC
RA
TPA
Primers: NF-κBa NF-κBb NF-κBc NF-κBd NF-κBe NF-κBf
E
Ab IP
Control
C-fos
C-jun
10% input
Primers
AP1a
AP1b
ethanol
TPA
MC
RA
F
Ab IP
Control
C-fos
C-jun
10% input
Primers
AP1c
AP1d
AP1f
AP1g
G
TSLP RNA level
TPA:
U0126:
JNK I:
BAY:
H
TSLP RNA level
TPA:
IL-1β:
I
Ab IP
Control
p65
p50
10% input
Primers
NF-κBa
NF-κBc
ethanol
IL-1β
TPA
J
Control
C-fos
C-jun
10% input
Primers
AP1b
AP1g
ethanol
IL-1β
TPA
K
Ab IP
Primers
Control
SMRT
NCOR
Sin3A
HDAC1
HDAC2
SRC-1
SRC-2
SRC-3
p300
pCAF
CDK7
Pol II
VDR
RAR
P65
C-jun
10% input
TPA
PP
AP1b
AP1g
DR3d
DR2b
L
Alu I sites
-7706
-7458
-72166
-71601
-42180
-41718
-30348
-29886
-16731
-16359
-293
+623
A
B
C
D
E
F
-77688
-77681
-71999
-71992
-41783
-41776
-29950
-29943
-16647
-16640
-61
-56
ATG
5'
3'
AP1g
AP1f
AP1d
AP1c
AP1b
TATA
+1
M
probe
ethanol
MC
RA
TPA
TSLP BAC
TSLP BAC
AP1b +PP
AP1g +PP
D+L
D+L
D+L
D+L
D
ND+L
D+NC+L
FPCR +AluI
D+L
D

Figure 4

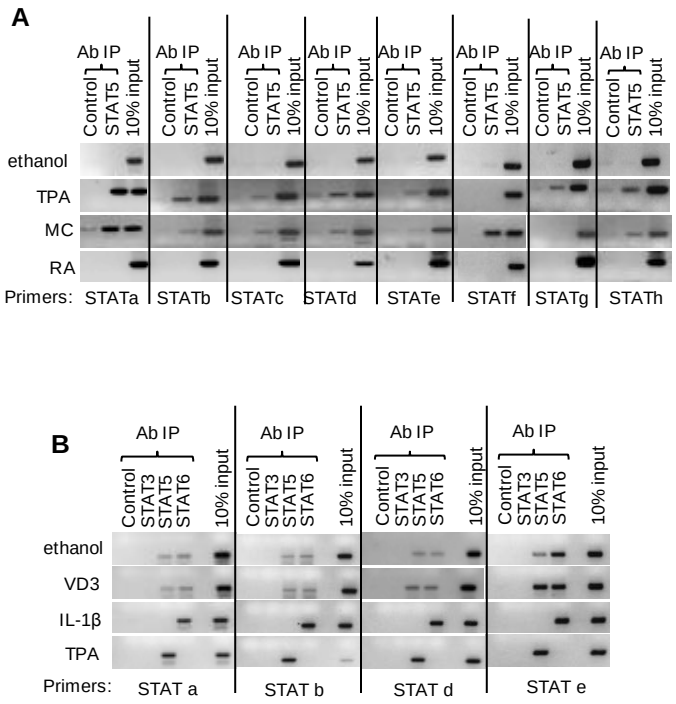
A
Ab IP
Control
STAT5
10% input
ethanol
TPA
MC
RA
Primers:
STATa
STATb
STATc
STATd
STATe
STATf
STATg
STATh
B
Ab IP
Control
STAT3
STAT5
STAT6
10% input
ethanol
VD3
IL-1β
TPA
Primers:
STAT a
STAT b
STAT d
STAT e

Figure 5

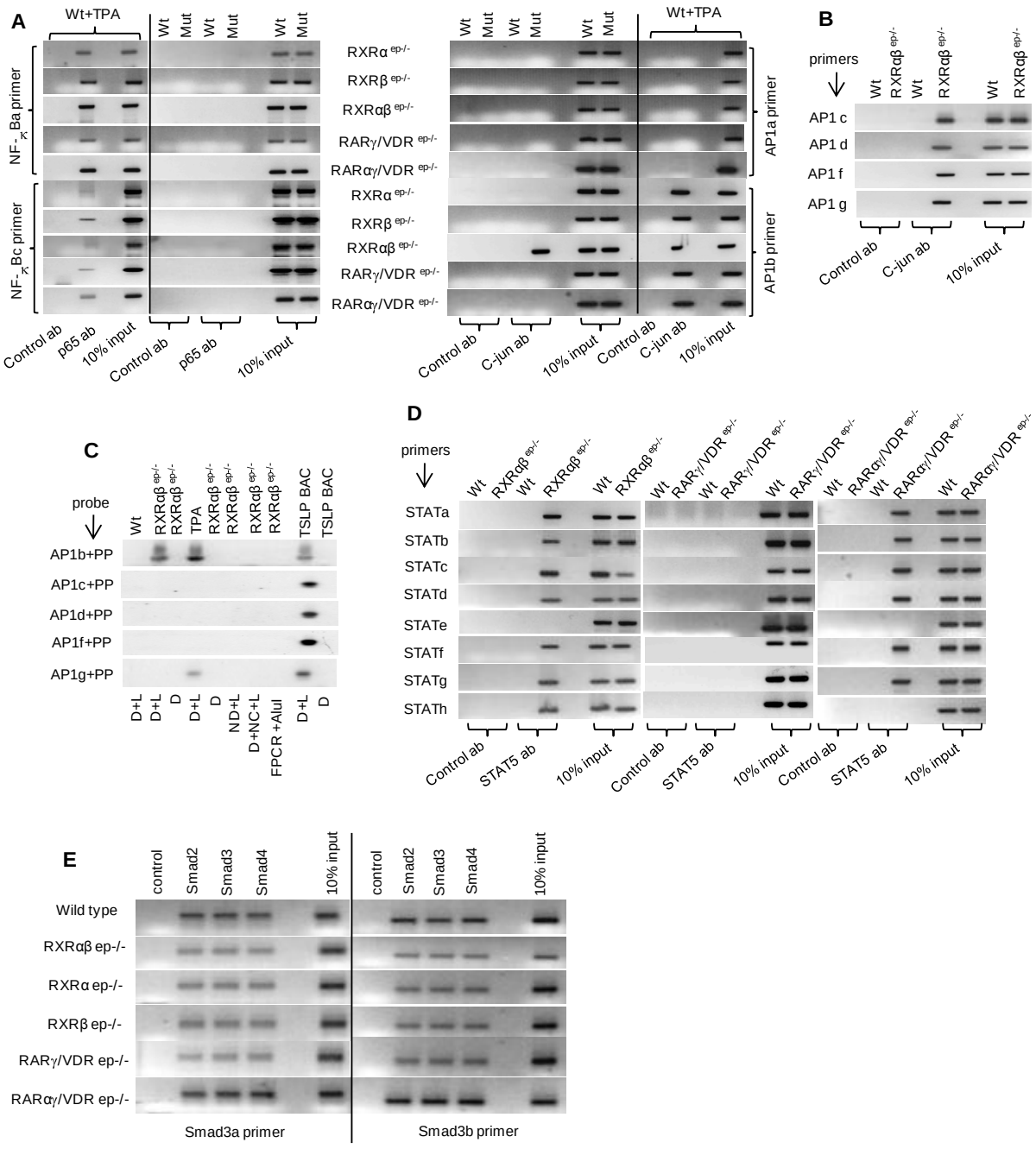
A
Wt+TPA
Wt
Mut
NF-κBa primer
NF-κBc primer
Control ab
p65 ab
10% input
RXRα ep-/-
RXRβ ep-/-
RXRαβ ep-/-
RARγ/VDR ep-/-
RARαγ/VDR ep-/-
AP1a primer
AP1b primer
C-jun ab
B
primers
AP1 c
AP1 d
AP1 f
AP1 g
C
probe
Wt
TPA
TSLP BAC
AP1b+PP
AP1c+PP
AP1d+PP
AP1f+PP
AP1g+PP
D+L
D
ND+L
D+NC+L
FPCR +AluI
D
STAT5 ab
STATa
STATb
STATc
STATd
STATe
STATf
STATg
STATh
E
control
Smad2
Smad3
Smad4
10% input
Wild type
RXRαβ ep-/-
RXRα ep-/-
RXRβ ep-/-
RARγ/VDR ep-/-
RARαγ/VDR ep-/-
Smad3a primer
Smad3b primer

Figure 6

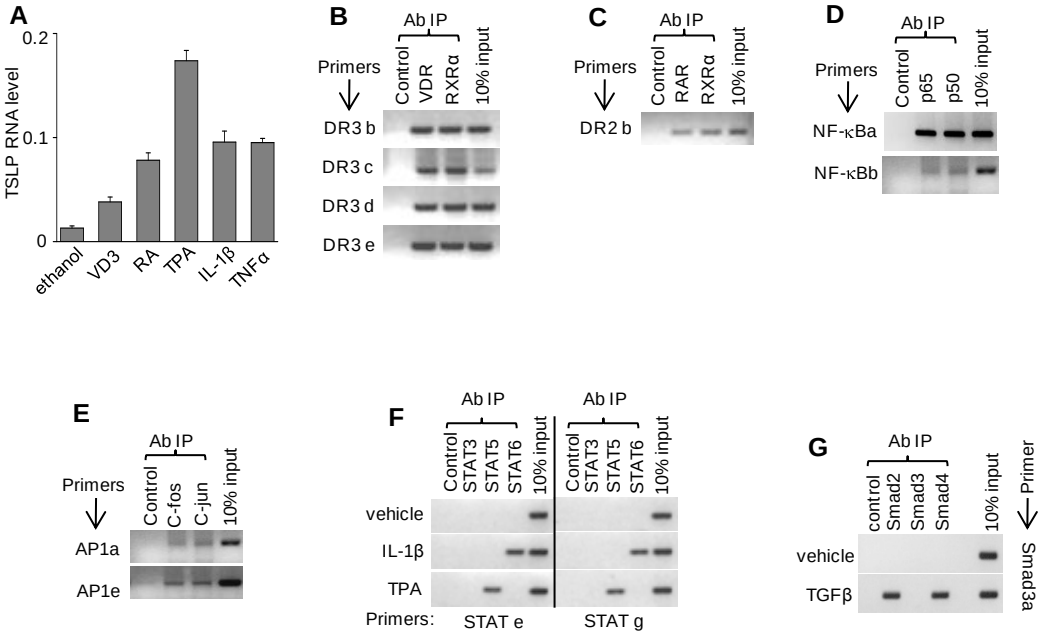
A
TSLP RNA level
0.2
0.1
0
ethanol
VD3
RA
TPA
IL-1β
TNFα
B
Ab IP
Primers
Control
VDR
RXRα
10% input
DR3 b
DR3 c
DR3 d
DR3 e
C
Ab IP
Primers
Control
RAR
RXRα
10% input
DR2 b
D
Ab IP
Primers
Control
p65
p50
10% input
NF-κBa
NF-κBb
E
Ab IP
Primers
Control
C-fos
C-jun
10% input
AP1a
AP1e
F
Ab IP
Ab IP
Control
STAT3
STAT5
STAT6
10% input
vehicle
IL-1β
TPA
Primers:
STAT e
STAT g
G
Ab IP
control
Smad2
Smad3
Smad4
10% input
Primer
Smad3a
vehicle
TGFβ

Figure S1

A

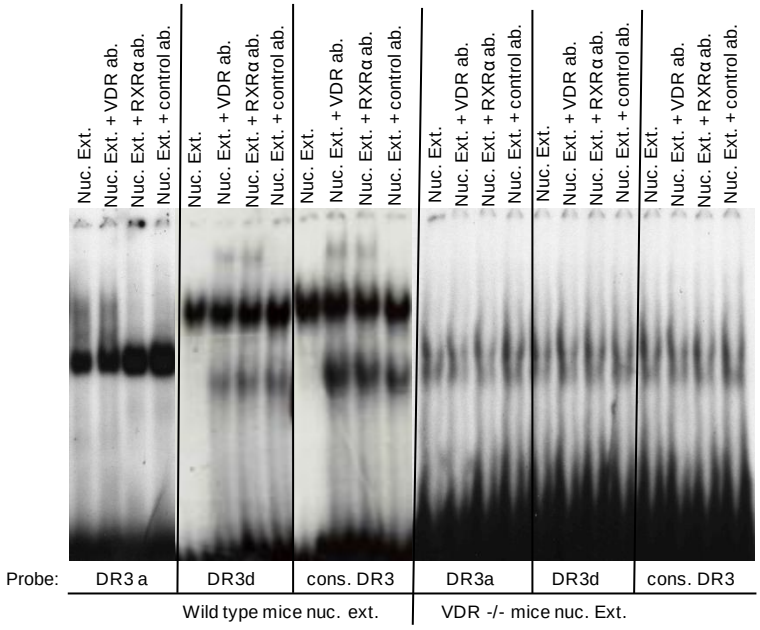
Nuc. Ext.
Nuc. Ext. + VDR ab.
Nuc. Ext. + RXRα ab.
Nuc. Ext. + control ab.
Probe:
DR3 a
DR3d
cons. DR3
DR3a
DR3d
cons. DR3
Wild type mice nuc. ext.
VDR -/- mice nuc. Ext.

B

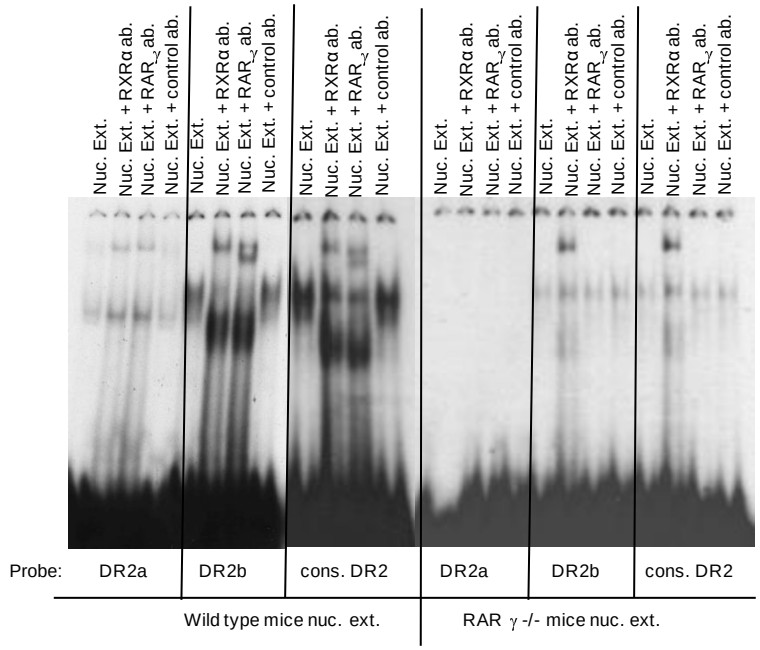
Nuc. Ext.
Nuc. Ext. + RXRα ab.
Nuc. Ext. + RARγ ab.
Nuc. Ext. + control ab.
Probe:
DR2a
DR2b
cons. DR2
DR2a
DR2b
cons. DR2
Wild type mice nuc. ext.
RAR γ -/- mice nuc. ext.

Figure S1

C

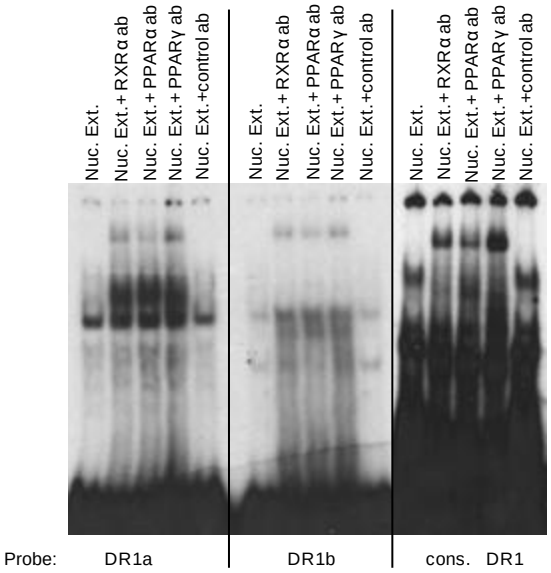
Nuc. Ext.
Nuc. Ext.+ RXRα ab
Nuc. Ext.+ PPARα ab
Nuc. Ext.+ PPARγ ab
Nuc. Ext.+control ab
Nuc. Ext.
Nuc. Ext.+ RXRα ab
Nuc. Ext.+ PPARα ab
Nuc. Ext.+ PPARγ ab
Nuc. Ext.+control ab
Nuc. Ext.
Nuc. Ext.+ RXRα ab
Nuc. Ext.+ PPARα ab
Nuc. Ext.+ PPARγ ab
Nuc. Ext.+control ab
Probe: DR1a DR1b cons. DR1

Figure S2

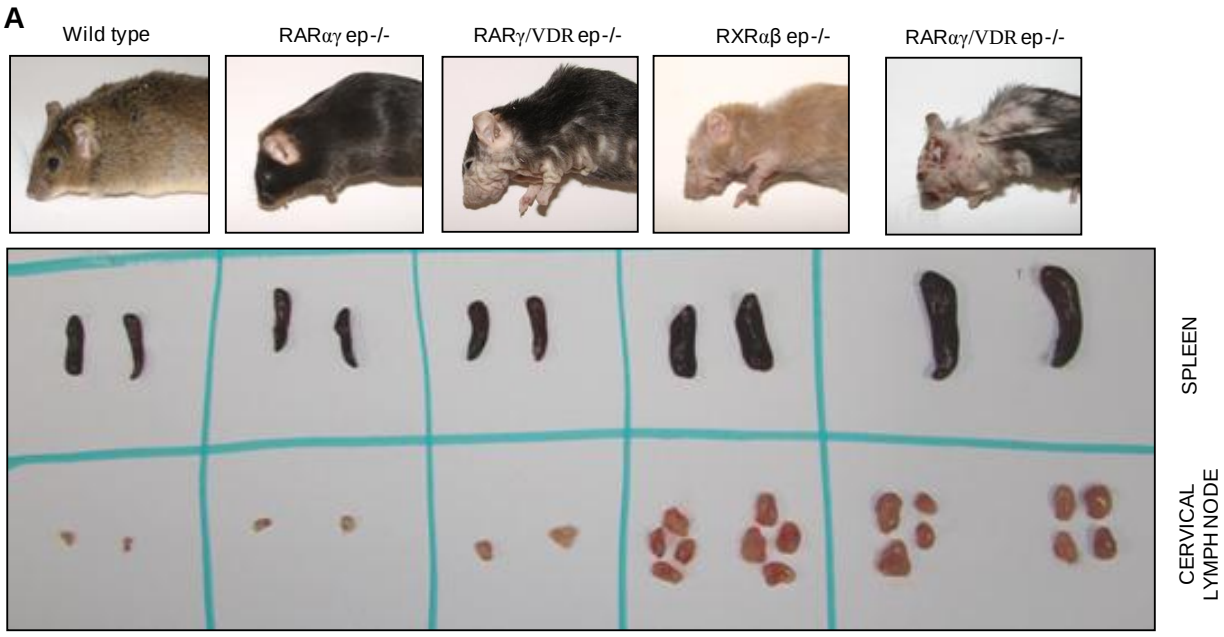
A
Wild type
RARαγ ep-/-
RARγ/VDR ep-/-
RXRαβ ep-/-
RARαγ/VDR ep-/-
SPLEEN
CERVICAL LYMPH NODE

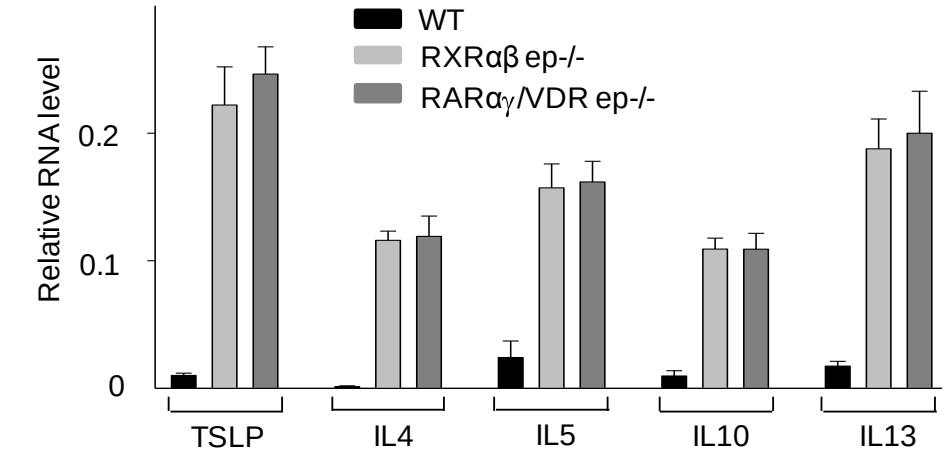
B
WT
RXRαβ ep-/-
RARαγ/VDR ep-/-
Relative RNA level
0
0.1
0.2
TSLP
IL4
IL5
IL10
IL13

Figure S3

A

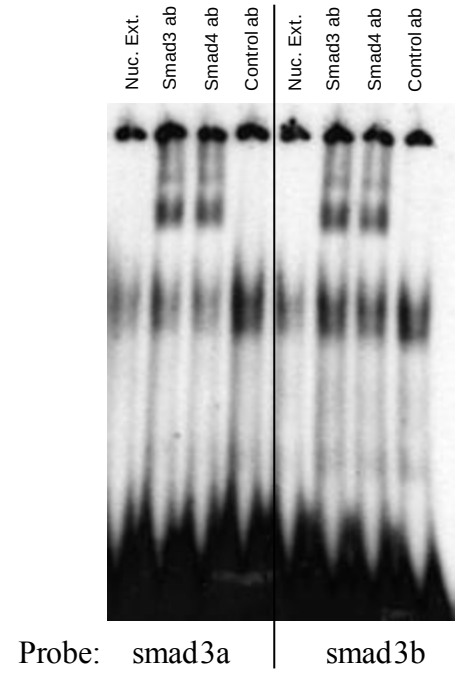
Nuc. Ext.
Smad3 ab
Smad4 ab
Control ab
Nuc. Ext.
Smad3 ab
Smad4 ab
Control ab
Probe: smad3a
smad3b

B

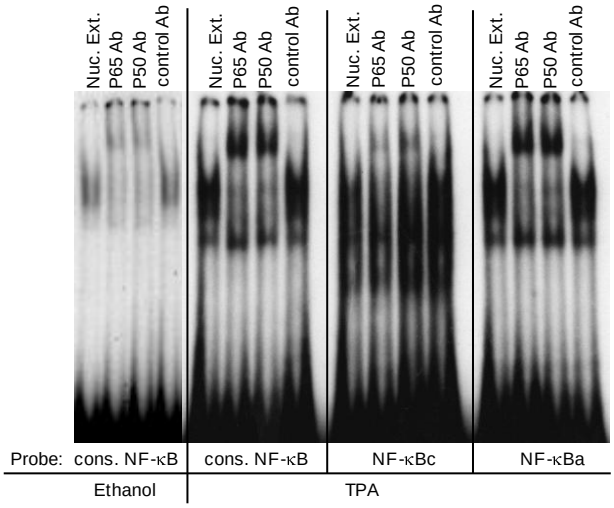
Nuc. Ext.
P65 Ab
P50 Ab
control Ab
Nuc. Ext.
P65 Ab
P50 Ab
control Ab
Nuc. Ext.
P65 Ab
P50 Ab
control Ab
Nuc. Ext.
P65 Ab
P50 Ab
control Ab
Probe: cons. NF-κB
cons. NF-κB
NF-κBc
NF-κBa
Ethanol
TPA

Figure S3

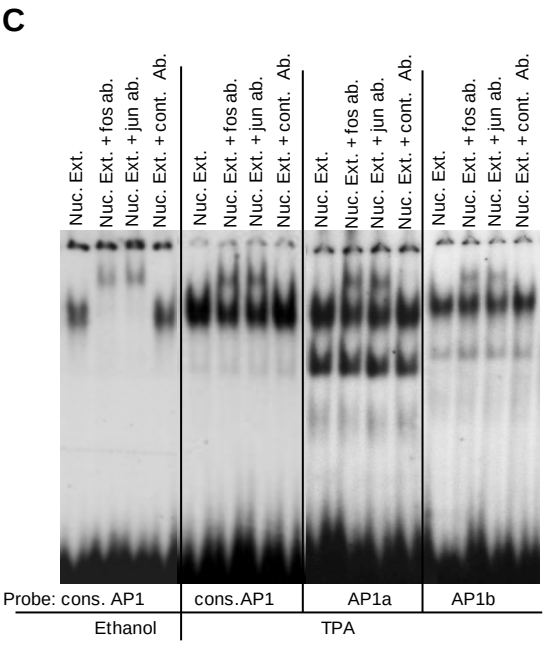
C
Nuc. Ext.
Nuc. Ext. + fos ab.
Nuc. Ext. + jun ab.
Nuc. Ext. + cont. Ab.
Probe: cons. AP1
cons.AP1
AP1a
AP1b
Ethanol
TPA

Table S I. Position, sequence and functional characteristic of various transcription factor binding elements present in human TSLP gene.

Name of the element	Position from ATG (A= +1)	Sequence	EMSA+ antibody shifting	CHIP (IP antibody)
Consensus DR1		**RggtcanRggtca**		
DR1a	-19878 to -19866	atgtcagagttca	RXRα, PPARα, PPARγ	-
DR1b	-25203 to -25191	tggtcagtggtct	RXRα, PPARα, PPARγ	-
Consensus DR2		**RggtcannRggtca**		
DR2a	-6459 to -6446	aggccaggagttca	RXRα, RARγ	-
DR2b	-11446 to 11433	aggtcaagagttca	RXRα, RARγ	RXRα, pan-RAR
DR2c	-29710 to -29697	tgaactcctgacct	RXRα, RARγ	-
DR2d	-66093 to -66080	tgaactcctgacct	RXRα, RARγ	-
Consensus DR3		**RggtcannnRggtca**		
DR3a	+6060 to +6074	cggtcagttatgtca	-	-
DR3b	-7055 to -7041	tgaacctttagaact	RXRα, VDR	RXRα, VDR
DR3c	-23442 to -23428	tgaacttcctgaaca	RXRα, VDR	RXRα, VDR
DR3d	-35899 to -35885	aggtcatctgggtaa	RXRα, VDR	RXRα, VDR
DR3e	-49949 to -49935	gggtcaggtatgtga	RXRα, VDR	RXRα, VDR
DR3f	-64244 to -64230	tgacccagatgaacc	RXRα, VDR	-
DR3g	-64290 to -64276	tgacccagatgaacc	RXRα, VDR	-
DR3h	-64650 to -64636	tgacccagatgaacc	RXRα, VDR	-
Consensus NF-κB		**gggRNNYYCC**		
NF-κBa	-391 to -382	gggaaattcc	p65, p50	p65, p50
NF-κBb	-4013 to -4004	ggaaactcca	p65, p50	p65, p50
Consensus AP1		**tgagtca**		
AP1a	-1276 to -1269	tgagtca	c-fos, c-jun	c-fos, c-jun
AP1b	-5788 to -5781	tgactca	c-fos, c-jun	-
AP1c	-20557 to -20550	tgagtca	c-fos, c-jun	-
AP1d	-26590 to -26582	tgagtca	c-fos, c-jun	-
AP1e	-28137 to -28130	tgactca	c-fos, c-jun	c-fos, c-jun
AP1f	-55376 to -55369	tgagtca	c-fos, c-jun	-
AP1g	-65353 to -65346	tgagtca	c-fos, c-jun	-
Consensus smad3		**agccagaca**		
Smad3a	-1304 to -1296	agacagaca	Smad3, smad4	Smad2, smad4
Smad3b	-5512 to -5504	aggcagaca	-	-
Consensus STAT5/6		**ttcnnn(n)gaa**		
STATa	-3201 to -3193	ttcatagaa	+	-
STATb	-3236 to -3227	ttcaatggaa	+	-
STATc	-3291 to -3283	ttccaggaa	+	-
STATd	-3761 to -3753	ttcaaggaa	+	-
STATe	-4693 to -4685	ttctaagaa	+	STAT5/6
STATf	-6004 to -5996	ttctcagaa	+	-
STATg	-9751 to -9742	ttcttaagaa	+	STAT5/6
STATh	-20582 to -20573	ttcagtagaa	+	

n= a/c/g/t; R= purine; Y= pyrimidine

Supplementary figure legends

Figure S1. EMSA and antibody shift analysis of NR binding elements present in the mouse TSLP gene.

(A) EMSA and antibody shift assay using epidermal nuclear extract from wild type (WT) and VDR-/- mice shows the binding of VDR and RXRα to various DR3 elements, as indicated.

(B) EMSA and antibody shift assay using epidermal nuclear extract from WT and RARγ-/- mice shows the binding of RXRα and RARγ to various DR2 elements, as indicated.

(C) EMSA and antibody shift assay using WT mouse epidermal nuclear extract shows the binding of RXRα, PPARα and PPARγ to various DR1 elements, as indicated.

Figure S2. Comparison of skin and systemic inflammation in WT, RXRαβ ep-/- and RARαγ/VDR ep-/- mice.

(A) Appearance of skin, spleen and cervical lymph node in WT, RARαγep-/-, RARγ/VDR ep-/-, RXRαβ ep-/- and RARαγ/VDR ep-/- mice, 22 weeks post tamoxifen injection. Upper panel shows the representative images of appearance of AD like skin inflammation on ear, dorsal skin and face. Lower panel shows splenomegaly and cervical lymph node hyperplasia in 2 mice from each corresponding genotype at the same age.

(B) Measurement of TSLP, IL4, IL5, IL10 and IL13 transcript levels in ear samples of WT, RXRαβ ep-/- and RARαγ/VDR ep-/- mice, 4 weeks post tamoxifen injection.

Figure S3. EMSA and antibody shift analysis of NF-κB, AP1 and Smad binding elements present in the mouse TSLP gene.

(A) EMSA and antibody shift assay using WT mouse epidermis nuclear extract shows the binding of smad3 and smad4 to Smad3a and Smad3b elements.

(B) EMSA and antibody shift assay using untreated or TPA treated mouse epidermis nuclear extract shows the binding of p50 and p65 proteins to various NF-κB elements, as indicated.

(C) EMSA and antibody shift assay using untreated or TPA treated mouse epidermis nuclear extract shows the binding of c-fos and c-jun to various AP1 elements, as indicated.

Supplementary Materials and Methods

Materials. P65 (SC-372X), P50 (SC-1192X), c-jun (SC-44X), c-fos (SC-52X), STAT3 (SC-482X), STAT5 (SC-835X), STAT6 (SC-981X), Smad2 (ab71109), Smad3 (SC-8332X), Smad4 (SC-7154X), c-ski (SC-9140X), SnoN (SC-9141X), P300 (SC-584X), pan-RAR (SC-773X), HDAC3 (SC-11417X) and SRC3 (SC-9119X) rabbit polyclonal antibodies were from Santacruz Biotechnology. Control rabbit IgG (ab46540), SRC1 (ab84) mouse monoclonal, HDAC1 (ab7028), and HDAC2 (ab7029) rabbit polyclonal antibodies were from Abcam. RNA polymerase II (05-623) mouse monoclonal antibody was from Millipore Corporation. SMRT, NCoR and TIF2 (SRC2) mouse monoclonal antibodies, and VDR rabbit polyclonal antibodies were generated in-house. All in-house generated antibodies were tested by ELISA, immunoprecipitation, western blotting and absence of reaction in null mutant mice to ensure specificity. All other antibodies were tested by immunoprecipitation and western blotting. Active vitamin D3 [1α, 25 (OH)2 Vitamin D3,], all trans retinoic acid (RA) and BAY 11-7082 were from Sigma Aldrich. MC 903 was from Leo pharma, U0126, JNK inhibitor II was from Calbiochem and recombinant human IL-1β was from R&D systems. Source of all other materials is indicated in parentheses at appropriate places. BMS961 and BMS753 are as described (Chapellier *et al,* 2002).

Mice Genotyping. Genomic DNA was isolated from the tail using Direct PCR (Tail) reagent (VIAGEN) and PCR was performed using respective primers as given below. For RXRα and RARα genotyping, all the mentioned primers were added together in the same reaction mixture and PCR was performed to yield wt, L2 and L- bands.

Gene	Allele	Size(bp)	Primer Sequences
RXRα	L2	250	P1 5' GTGTTGGAGACAGATGAGG
	L-	300	P2 5' AGCGCATGCTCCAGACTGC
	Wt	400	P3 5' GGGTACAGAGAAGCAAGAG
			P4 5' ACCTGGACTTGTCACCTAG
RXRβ	L2	260	FP 5' CCTCCACTGCACACAGCCC
	Wt	225	RP 5' CCGGGAGGGCTGACTTTCATC
RXRβ	L-	200	FP 5' CGTGCAAGGAAGGCCCTTTA
	Wt	1200	RP 5' TTAAAGCAGGAATTGGACCA
VDR	L2	350	FP 5’ TCTTCTGACTCCCACAAGTGTACC
	Wt	250	RP 5’ CTGTTGATGGACAGGAACACACAGC
VDR	L-	320	FP 5’ TCTTCTGACTCCCACAAGTGTACC
			RP 5’ CTTTGTACTACCAGGCTGAGCTTCG
RARα	L2	480	P1 5’ CTCCCTGTGACCAGAAGCTC
	L-	350	P2 5’ GGAAGGAAATAGGGCAGAGG
	Wt	400	P3 5’ TATCCTGTTGACCCCAGCTC
RARγ	L2	768	FP 5’ TGCTTAGCATACTTGAGAAC
	Wt	700	RP 5’ ACCGCACGACACGATAGGAC
RARγ	L-	495	FP 5’ GTAGATGCTGGGAATGGAAC
			RP 5’ ACCGCACGACACGATAGGAC

ChIP assay. ChIP assay was as carried out as described (Vaisanen *et al*, 2005) with few modifications. Epidermal cells from mouse dorsal skin were cross-linked by adding Formaldehyde to

a final concentration of 1%, and incubation on a flip-flop rocker for 10 minutes at 25 ^{0}C, followed by addition of 2M glycine (0.125M final concentration) and incubation for 5 minutes. Cells were pelleted (400g, 5 minutes) at 4 ^{0}C and washed twice in ice-cold PBS. Cross-linked mouse epidermal cells or A549 or MLE12 cells were resuspended in 300µl ice-cold lysis buffer [50 mM Tris-HCl, pH 8.1, 1% (w/v) SDS, 10 mM EDTA, 1X protease inhibitor cocktail (Roche)] and all lysates were sonicated at 4^{0}C to generate 300-500 base pair chromatin fragments (Bioruptor sonicator, Diagenode). Cellular debri were removed by spinning (10000g, 10 min) at 4 ^{0}C and the supernatant was pre-cleared by incubating with 60 µl protein G-agarose beads (pre-blocked with salmon sperm DNA and BSA) for 20 min at 4 ^{0}C over a flip-flop rocker. Beads were pelleted (100g, 1 minute) at 4 ^{0}C and discarded. Equal amounts of lysates were used for immunoprecipitation. 10 % of the lysate amount used for each immunoprecipitation reaction was saved to be used as input DNA in PCR amplification. Individual samples were diluted 1:8 (v/v) in ChIP dilution buffer [16.7 mM Tris-HCl, pH 8.1, 0.01% (w/v) SDS, 1.1% (v/v) Triton-X 100, 1.2 mM EDTA, 16.7 mM NaCl, 1X protease inhibitor cocktail] and incubated overnight with different primary antibodies at 4 ^{0}C on a flip-flop rocker, followed by incubation with 60 µl protein G-agarose beads (pre blocked with salmon sperm DNA and BSA) for 90 minutes. Immunoabsorbed complexes were recovered by centrifugation (100g, 1 minute) at 4 ^{0}C. Protein G beads were then washed once in low salt buffer [20mM Tris-HCl, pH 8.1, 0.1% (w/v) SDS, 1% (v/v) triton X -100, 2mM EDTA, 150mM NaCl], once in high salt buffer [20mM Tris-HCl, pH 8.1, 0.1% (w/v) SDS, 1% (v/v) triton X -100, 2mM EDTA, 500mM NaCl], once in LiCl buffer [10mM Tris-HCl, pH 8.1, 250mM LiCl, 1% (v/v) NP-40, 1% (w/v) sodium deoxycholate, 1mM EDTA], and finally washed twice in 1ml TE buffer (10mM Tris-HCl, pH 8.0, 1mM EDTA). Chromatin was released from the beads by incubation with 150 µl elution buffer [1% (w/v) SDS, 100mM NaHCO3] for 15 minutes at room temperature with intermittent vortexing. The elution step was repeated and both eluates were pooled. 1 µl of 10 mg/ml RNase and 5M NaCl (200mM final concentration) was added to the eluate and incubated at 65 ^{0}C overnight. 1µl of 30mg/ml Proteinase K was then added to the samples and incubated at 50^{0}C for 1hour. DNA was subsequently purified from the eluate using Qiagen PCR purification kit (Qiagen corp.) in a final volume of 50 µl. 3 µl of the purified DNA was used as template in different PCR amplifications (Applied Biosystems Thermocycler). Sequence of the various primers is listed below. The number of PCR cycles was optimized to maintain linear amplification in all experiments. PCR products were resolved by 2% agarose gel electrophoresis. Images of ethidium bromide-stained DNA was acquired using an UV trans-illuminator equipped with a digital camera.

ChIP assay primers.

mTSLP DR1a fp	5’ TCTAAAAATCCCTGAAGGGGGCC
mTSLP DR1a rp	5’ CCCCTGTAGGGAACCCACTTCTTT
mTSLP DR1b fp	5’ TATGTCTCTTTGGGCGCATT
mTSLP DR1b rp	5’ TTTCAGCTAGCAGGGGAATC
mTSLP DR1c fp	5’ TTCCAGTCTTTCTTGGTTTGG
mTSLP DR1c rp	5’ GCATGGTCATTGTCCTGAGA
mTSLP DR2a fp	5’ CAACCAGGGGAGCGCAAATCTT
mTSLP DR2a rp	5’ CAGCCGCCCTCGAAACTCATTA
mTSLP DR2b fp	5' TGAGGTATTTTATCAGAACAATGGAC
mTSLP DR2b rp	5' CCAAGTGCTGGGATTAAAGG
mTSLP DR3a fp	5’ GAAAAATGAAGTTCAGGACCAA
mTSLP DR3a rp	5’ TCTCCCTCCTCTTTCTCCTTC
mTSLP DR3b fp	5’ CACCTTTAATCCCAGCACCT
mTSLP DR3b rp	5’ TTGCTTCTTTAATTGGTCCTGAA
mTSLP DR3c fp	5’ GCCTTTAATCCCAGCACTTG
mTSLP DR3c rp	5’CTTGACTCCCATGAAAGATGC
mTSLP DR3d fp	5' AGGTCCAGATACTGCATGCTC
mTSLP DR3d rp	5' CAGCAGCTGATGCAAACAGA
mTSLP DR3e fp	5’ AAATACCTGGGCGGTGGT
mTSLP DR3e rp	5’ GTTTCCAGTGTTAAATTACATTGTTT
mTSLP DR3f and g fp	5’ AGACCAAAGCAGACTCCATGA
mTSLP DR3f and g rp	5’ CGACCTAGGATGGAACCAAA
mTSLP PP/ NF-κBa fp	5' GCATGTAGCAAGTGTTTAGGGCAGA
mTSLP PP/ NF-κBa rp	5' GCCTGAACGTGGAGTCTTCCTGAT
mTSLP NF-κBb fp	5’ CACCTCTGACTCCAGTCTGT
mTSLP NF-κBb rp	5’ GTACTGGGAGCAGGAAAGAA
mTSLP NF-κBc d fp	5’ AGGAGGGAGAAGTAAACAAAGC
mTSLP NF-κBc d rp	5’ CTCACTGCTGCCACCTTCTT
mTSLP NF-κBe fp	5’ AGAAGAGAAAGATGAGAGAA
mTSLP NF-κBe rp	5’ CTAGAAAAACATTCACTTGC
mTSLP NF-κBf fp	5’ ATGTAACTAGCAACTGAAGATC
mTSLP NF-κBf rp	5’ TGAGACAGCCAAATTTCTAT
mTSLP AP1a fp	5’ AGGAGAGTAGGGGTTGGGTTCGTGT
mTSLP AP1a rp	5’ AGGGGAGGAACAGCTTCTGACCTGT
mTSLP AP1b fp	5’ GTTACCACCTCCGTGGCTACT
mTSLP AP1b rp	5’ TATCCACAGGTTATTTTGGGAAA
mTSLP AP1c fp	5’ TTGCTTCCTTGTGATCTTGC
mTSLP AP1c rp	5’ AAAGGAGAGTGGCCATGGTA
mTSLP AP1d fp	5’ CATCCTTTCCCCTTCACTCA
mTSLP AP1d rp	5’ AGCTCACACCCGAATAATCAA
mTSLP AP1e fp	5’ GCCCATCCTTGTTGTGGATA
mTSLP AP1e rp	5’ TGAGACCCCTTAGAACTTGTGG
mTSLP AP1f fp	5’ TGATAAATCATCCCTTATTTTCCAA
mTSLP AP1f rp	5’ AGAAGACATAGGCCAATTCACA
mTSLP AP1g fp	5’ TGCCAAAGTTTCCCATTCTC

mTSLP AP1g rp	5’ TGTGATAGTGGCCCAAACAT
mTSLP STATa fp	5’ GGCAGGACTTTGCCTTCTTT
mTSLP STATa rp	5’ CTGACGTTTTCTGGCTCACA
mTSLP STATb fp	5’ CCTCTGAGTCCCAAGAGCTG
mTSLP STATb rp	5’ CTGGCAGTGTTCCTCTTCGT
mTSLP STATc fp	5’ TGGAAGTCCTGCCTGGTTAC
mTSLP STATc rp	5’ AGAATCACATGGCTGCTGGT
mTSLP STATd fp	5’ GACATGCATCTCTTCTGCTTTC
mTSLP STATd rp	5’ GTCCCTTCACTTCCCTGTCA
mTSLP STATe fp	5’ TCAAAGTCCCTTGGTACCTAACAT
mTSLP STATe rp	5’ TCCTGTTTTCTCCTCCCAAA
mTSLP STATf fp	5’ CCAAGAGCCACGACTTTACTG
mTSLP STATf rp	5’ GGTGTGGCCTTGTTAAAGGA
mTSLP STATg fp	5’ GCACTACTCCATTGCTGGTG
mTSLP STATg rp	5’ TGGGGCATCTTTTGTTTTGT
mTSLP STATh fp	5’ GGGTGGATCCCAACATAAGA
mTSLP STATh rp	5’ TGTGCCAAGTTATTCCACCA
mTSLP Smad3a fp	5’ GGGTTTCATTGCTGTGAAGAG
mTSLP Smad3a rp	5’ TGGCACTATTAGGAGGTGTGG
mTSLP Smad3b fp	5’ CATTGCTGTGAAGAGACACCA
mTSLP Smad3b rp	5’ GGAGTGGCACTATTAGGAGGTG
m Smad7 fp	5’ CTGGGAGAGGGTGGCAGTA
m Smad7 rp	5’ CCTCTGCTCGGCTGGTTC
mCRABPII DR2 fp	5’ CCTTCCTCCCTCATCCTCTC
mCRABPII DR2 fp	5’ AACAACGTTGCTCTGTGCTG
hTSLP DR1a fp	5’ GAGGTCAGCCAGCAGTCTCT
hTSLP DR1a rp	5’ CCTATGTAACAAACCTGCACATTC
hTSLP DR1b fp	5’ AAGCAAAGCAACACATTCCA
hTSLP DR1b rp	5’ CCTCGAACAAATGGATGATT
hTSLP DR2a fp	5’ CAGATAGGTAAGCAGAATTTAGCC
hTSLP DR2a rp	5’ GACAGATCTTGCTTCTGTTGC
hTSLP DR2b fp	5’ AGCTCCACAGAAAAGCATGG
hTSLP DR2b rp	5’ TTTGTGAGACAGAGTCTTACTGTGC
hTSLP DR2c fp	5’ ACAGGTGCATGTCATGATGC
hTSLP DR2c rp	5’ TGGACAAAAATTAACTCAAGATCAA
hTSLP DR2d fp	5’ CCAGGTTCAAGCAATTCTCC
hTSLP DR2d rp	5’ CACCAAGTCTCTTAAGGGGAAA
hTSLP DR3a fp	5’ CAGGTTTTGTAAAATCGCAAAG
hTSLP DR3a rp	5’ CCGAAACCTGCAATTTCTCC
hTSLP DR3b fp	5’ ATTGCCCAACTGGACAAGAC
hTSLP DR3b rp	5’ CAAATAGGTGGGACCACAGG
hTSLP DR3c fp	5’ TAGTGGAGCTGGCATTTCAA
hTSLP DR3c rp	5’ CACATTGGACCTGTGCAGTTA
hTSLP DR3d fp	5’ GAGCTGAAGAGTAGACAGTACAAAGC
hTSLP DR3d rp	5’ ATAGCCCCCTGAGCTTCATT

hTSLP DR3e fp	5’ TGCAGGCAATATCCATGTGT
hTSLP DR3e rp	5’ CGAGAGAGGACTGGGAGAAA
hTSLP DR3f fp	5’ CTGGTTCAATGTGCTCCTTTC
hTSLP DR3f rp	5’ GGAAGGGTTTATGGGGAAAA
hTSLP DR3g fp	5’ GCCAGCAACTTGGCTGATA
hTSLP DR3g rp	5’ GACACACAGTTGTTTACACTTGCT
hTSLP PP/ NF-κBa fp	5’ AGTTGAAAGTGGCCACAGGA
hTSLP PP/ NF-κBa rp	5’ TGGAATTTTAACATCAGTAAAGTCATC
hTSLP NF-κBb fp	5’ TGAGCATATGAAAACCAAGAAG
hTSLP NF-κBb rp	5’ TTGAAAAATAGTTGCCAAAAGGA
hTSLP AP1a fp	5’ TCATCTCAGCAACCTGATCG
hTSLP AP1a rp	5’ ACGCTTTAGTGCGCTCTGC
hTSLP AP1b fp	5’ GGGTGATTGCTTAACCCAGA
hTSLP AP1b rp	5’ AAAGCTTCTAGCTGTGAAAGATGA
hTSLP AP1c fp	5’ TGATGCAGGCAAATTTGAAG
hTSLP AP1c rp	5’ TGAATCGTGGATGCTATGTTTT
hTSLP AP1d fp	5’ TCAGCCGGACTAAGGTCAAT
hTSLP AP1d rp	5’ GCATCTTTACATTTCTATCATTAGGG
hTSLP AP1e fp	5’ TTGATATTTCCTGTTGTGACCA
hTSLP AP1e rp	5’ CACTGGCCCCAGAGATAAGA
hTSLP AP1f fp	5’ CAGAAAATGGCAAATCTTCG
hTSLP AP1f rp	5’ TGAGCTCATATAATGGAATGACAGA
hTSLP AP1g fp	5’ TGGGAAGAAACCAAAAGAAAA
hTSLP AP1g rp	5’ GGAACTCCTTTATTTTTATGGCTTAGA
hTSLP STATa b c fp	5’ TCACTCCTTCAGCATTTGGA
hTSLP STATa b c rp	5’ TCATAACCACAATAGGGCTGTC
hTSLP STATd fp	5’ CCAATCTCCTTTTGGCAACT
hTSLP STATd rp	5’ TTCTTGTTTTAATAATGCTTCTCACTG
hTSLP STATe fp	5’ AGGGAAGGACAGAGATTAGACC
hTSLP STATe rp	5’ CGGTGGGGGTAAAACAAGT
hTSLP STATf fp	5’ TCCCAATTCTTTGCTATCCA
hTSLP STATf rp	5’ GGTTAAGCAATCACCCCAAG
hTSLP STATg fp	5’ TGAACAAGGTTATTCACTGAAGC
hTSLP STATg rp	5’ CATACATAGGTTTACATATCCAGAAAA
hTSLP STATh fp	5’ TGATGCAGGCAAATTTGAAG
hTSLP STATh rp	5’ CCAAAGGGAGCCAAGTAAAA
hTSLP Smad3a fp	5’ TCATCTCAGCAACCTGATCG
hTSLP Smad3a rp	5’ TGGAAAACGTCTGTCACCTG
hTSLP Smad3b fp	5’ GGAAAACAAAGAAAATGGCAGA
hTSLP Smad3b rp	5’ ATGCTCCTTGTTTCCTGTGG

Nuclear run-on assay. pSK+ empty vector and pSK+ β actin (2 kb β actin cDNA cloned into pSK+ vector at EcoRI, BamHI sites) plasmids were linearised by digestion with BamHI. A 4 kb region of mouse TSLP gene coding sequence was amplified by PCR from a BAC construct (Invitrogen)

[forward primer: 5'-AGTTCTTCTCAGGAGCCTCTTCATC-3' (+165 to +190 with respect to 'A' of the translation initiation codon ATG as +1), reverse primer: 5'-CCAGATTCCACAATCTTCTTTCAGA-3' (+4157 to +4181 with respect to 'A' of ATG as +1)]. Approximately 10 µg each of pSK+ empty vector, pSK+ β actin and TSLP DNA was separated by 0.8% agarose gel electrophoresis, and transferred to 0.45µm nitrocellulose membranes. Membranes containing the transferred DNA probes were baked for 2 hours at 80 ^{0}C in a vacuum oven, followed by washing in 2X SSC.

Run-on assay was as described (Carey and Smale, 2001). Approximately 10^8 epidermal cells were resuspended in 5 ml ice cold NP-40 lysis buffer [10 mM Tris-HCl, pH 7.4, 10 mM NaCl, 3 mM MgCl2, 0.5% (v/v) NP-40] and incubated for 5 minutes on ice. Nuclei were pelleted (100g, 10 minutes) at 4 ^{0}C. The nuclear pellet was resuspended in 250 µl of nuclear freezing buffer [50 mM Tris-HCl, pH 8.3, 40% (v/v) glycerol, 5 mM MgCl2, 0.1 mM EDTA]. 225 µl of the nuclei was added to 60 µl of 5X run-on buffer [25 mM Tris-HCl, pH 8.0, 12.5 mM MgCl2, 750 mM KCl, and 12.5 mM each of ATP, GTP and CTP]. 150 µCi of α-[^{32}P] UTP was added and the reaction was incubated at 37 ^{0}C for 30 minutes. 20 µl of 10 mM CaCl2 and 10 µl of 1 mg/ml of RNase-free DNase were added and incubated at 30 ^{0}C for 5 minutes, followed by addition of 35 µl of proteinase K buffer [10% (w/v) SDS, 50mM EDTA, 10mM Tris-HCl, pH 7.4, 3 mg/ml proteinase K] and incubation at 37 ^{0}C for 45 minutes. Reaction mixture was extracted twice with phenol-chloroform and once with chloroform, followed by 1:1 dilution with 5 M ammonium acetate and precipitation with isopropanol. Precipitated pellet was resuspended in 100 µl TE (pH 8.0) followed by addition of 100 µl solution containing 10 mM MgCl2 and 5 mM CaCl2. 10 µl of 1 mg/ml RNase-free DNase was added and reaction mix was incubated at 37 ^{0}C for 5 minutes followed by chilling on ice for 5 minutes. 50 µl of 1N NaOH was added and the reaction mixture was incubated on ice for another 2 minutes. Alkali was neutralized by addition of 77µl of 1M HEPES (free acid) followed by precipitation of RNA in isopropanol and resuspension in 100 µl TE. 90 µl of the radiolabelled RNA was hybridised to the nitrocellulose filter containing the above DNA probes for 24 hours at 65 ^{0}C in 2 ml hybridization buffer [6X SSC, 5X Denhardt's reagent, 50% formamide, 0.5% (w/v) SDS, 200 µg salmon sperm DNA, 2 µg polyA]. Membrane was washed 4 times in 2X SSC, excess liquid removed, wrapped in saran and exposed to X-ray films for 48 hours in presence of an intensifying screen at -70 ^{0}C.

Electrophoretic mobility shift assay (EMSA). Synthetic oligonucleotides encompassing different DNA elements were annealed and double-stranded oligonucleotides were purified by 15% polyacrylamide gel electrophoresis. 50ng of purified oligonucleotides were 5'-end labelled using γ-

[^{32}P] ATP which was removed by purifying the probe through sephadex G 50 column. Nuclear extract was prepared as described (Carey and Smale, 2001). 8 fmoles of radiolabelled probe was mixed with 10ug wild type mouse epidermis or A549 cell nuclear extract in EMSA buffer [20mM hepes, pH 7.9, 150mM KCL, 5mM MgCl2, 2mM DTT, 10% (v/v) glycerol, 2ug poly dI-dC, 10ug BSA] and incubated for 20 minutes at room temperature. For supershift assay, specific antibody or rabbit IgG were added to the reaction mixture, and incubation continued further at room temperature for 20 minutes. Samples were electrophoresed on a 4.5% non-denaturing polyacrylamide gel in TBE buffer (90mM Tris-borate, 2.5mM EDTA, pH 8.3). Vacuum-dried gels were exposed to X-ray film overnight at -70 ^{0}C in the presence of an intensifying screen.

Chromosome conformation capture (3C) assay. 3C assay was carried out as described (Liu *et al,* 2005). Epidermal cells were cross-linked by adding Formaldehyde to a final concentration of 2%, and incubation on a flip-flop rocker for 10 minutes at 25 ^{0}C, followed by addition of 2M glycine (0.125M final concentration) and incubation for 5 minutes. Cells were pelleted (400g, 5 minutes) at 4 ^{0}C, washed twice in ice-cold PBS and resuspended in lysis buffer [10mM Tris-HCl, pH 8.0, 10mM NaCl, 0.2% (v/v) NP-40, and 1X protease inhibitor cocktail] and incubated for 5 minutes on ice, followed by centrifugation (100g, 10 minutes) at 4 ^{0}C. The nuclear pellet was resuspended in 200µl digestion buffer [1X Alu I restriction enzyme digestion buffer (NEB) + 0.3% (w/v) SDS] and incubated at 37 ^{0}C for 1 hour on a flip-flop rocker. 1.8% (v/v) triton X-100 (final concentration) was then added to the samples and incubated for 1 hour under similar conditions. Precipitate was removed by short spinning. 400 units Alu I restriction enzyme (NEB) was added and incubated at 37 ^{0}C for 2 hours, followed by addition of another 200 units of the respective enzymes and overnight incubation at 37 ^{0}C. Restriction enzyme was inactivated by addition of SDS (1.6% v/v, final concentration) and incubation at 70 ^{0}C for 20 minutes. SDS was quenched by addition of triton X-100 (1% v/v, final concentration) and 1 hour incubation at 37 ^{0}C. Individual samples were then diluted 12 times in ligase buffer (final DNA concentration approximately 3 ng/µl). Ligation was done for 4.5 hour at 16 ^{0}C followed by 30 minute incubation at room temperature using 400 units T4 DNA ligase (NEB). For mock-ligated sample, no ligase was added. Next, 1µl of 10mg/ml RNase and 5M NaCl (final concentration 200mM) was added to the samples which were incubated overnight at 65 ^{0}C. Proteinase K (200µg/ml) was added to the samples, which were incubated for 30 minutes at 50 ^{0}C, and DNA was purified by phenol-chloroform extraction and isopropanol precipitation. DNA amount was estimated by spectrophotometry and equal amounts of DNA were used for PCR amplification (primer sequences are listed below). PCR-amplified DNA was separated by 2% agarose gel electrophoresis, followed by Southern hybridization (Sambrook et al., 1989) to a probe designed to contain 20

nucleotides on each side (5' and 3', probe length: 40 nucleotides) of a possible junction between 2 Alu I fragments of the TSLP gene region of interest. The probe was 5'- end labelled using γ- [^{32}P] ATP and purified through sephadex G-50 column to remove free γ- [^{32}P] ATP. As a positive control for Alu I digestion, ligation, PCR amplification and Southern hybridization, a BAC DNA encompassing the region of interest was simultaneously processed (denoted as TSLP BAC).

3C assay Primers and probes

Junctions	PCR primers/southern probe sequence	Product length
DR2b and PP	Forward primer: -13711 GAGGCAGGTGGATTTCTGAG -13692	324bp
	Reverse primer: -200 AGCCAGCCAAATCTATGGAA -181	
	Southern probe: 5'-**CAGAACAACACAGTCTT<u>AGCT</u>**AAAAAATAAATAAATAAATA-3' (-13521 to -13501) (-294 to -272)	
DR3d and PP	Forward primer: -7365 CCTCTGGCTCCCTCAATTCT -7346	301bp
	Reverse primer: -87 TCCCCTAGGCCAATGATTTT -106	
	Southern probe: 5'-**CCACATCTGTTTGCATC<u>AGCT</u>**AAAAAATAAATAAATAAATA-3' (-7288 to -7268) (-294 to -272)	
DR3f/g and PP	Forward primer: -32702 ACCCCTCTGGCTCCTACAAT -32683	163bp
	Reverse primer: -53 CCAGTGTTCTCTGCCTCCAT -34	
	Southern probe: 5'-**CCTTCCTTAGGATCCCCTCA<u>AGCT</u>**AAAAAATAAATAAAT-3' (-32672 to -32652) (-294 to -268)	
AP1b and PP	Forward primer: -16618 CAGGGCCCAGAACATAGAAA -16599	374bp
	Reverse primer: -250 CCCTCACCTTTTTCCTTTCC -231	
	Southern probe: 5'-**AGTTTCTCTGTGTAGCCCT<u>AGCT</u>**AAAAAATAAATAAAT-3' (-16379 to -16357) (-294 to -268)	
AP1c and PP	Forward primer: -30007 TTCCCATGGTGACAGAATTT -29988	237bp
	Reverse primer: -113 GCCAATGATTTTCCTTGATG -94	
	Southern probe: 5'- **CCCCTCACCGAGGTTCTC<u>AGCT</u>**AAAAAATAAATAAAT -3' (-29904 to -29883) (-294 to -268)	
AP1d and PP	Forward primer: -41912 CTAGAGAACCCCAGGATTGC -41893	309bp
	Reverse primer: -200 AGCCAGCCAAATCTATGGAA -181	
	Southern probe: 5'-**ACCCCTCACGGAGGTTCTC<u>AGCT</u>**AAAAAATAAATAAAT-3' (-41738 to -41716) (-294 to -268)	
AP1f and PP	Forward primer: -71660 TCGATTAACCTATCCCCATGTC -71639	174bp
	Reverse primer: -53 CCAGTGTTCTCTGCCTCCAT -34	
	Southern probe: 5'-**TCTGAAGAGTGACTGAAG<u>AGCT</u>**AAAAAATAAATAAAT-3' (-71620 to -71599) (-294 to -268)	
AP1g and PP	Forward primer: -77526 TGGGCCTTAAATCCAACAAG -77507	183bp
	Reverse primer: -84 CTAAACGCCTACGGGCTCTC -65	
	Southern probe: 5'-**CACTATCACACTAGC<u>AGCT</u>**AAAAAATAAATAAAT-3' (-77474 to -77456) (-294 to -268)	

Cell culture experiments. A549 human lung epithelial cells (CCL-185, ATCC) were maintained in DMEM/HAM F12 (1:1) medium containing 10% foetal calf serum (FCS) and gentamycin. MLE12 mouse lung epithelial cells (CRL-2110, ATCC) were maintained in DMEM/Ham-F12 (1:1) medium containing 2% FCS, 5ug/ml insulin, 10ug/ml apo trans bovine, 35 nM sodium selenite, 10nM β estradiol, 10mM HEPES and gentamycin. HaCaT human keratinocytes (8) were maintained in medium containing DMEM 1g/l glucose, 10% FCS and gentamycin. For RNA isolation, cells were seeded at 50% density in 60mm plates. 24 hours post-seeding, complete medium was replaced with medium containing charcoal-treated serum. 24 hours later, 1μM active vitamin D3 [1α, 25 (OH)2 Vitamin D3,], 100ng/ml TPA, 1μM at-RA, 5ng/ml IL1β, (final concentration) or vehicle (ethanol) were added to the medium for 6 hours. RNA was isolated using TRI reagent (MRC Inc) following manufacturer's protocol. For ChIP assay, cells were cross-linked by adding formaldehyde (1% final concentration) to the medium and incubation on a rotary shaker for 10 minutes at room temperature. Cross-linking was stopped by adding 2M glycine (0.125M final concentration) and incubation for 5 minutes under similar condition, followed by 2 times washing in ice-cold PBS. Cells were scraped using a rubber policeman, pelleted (400g, 5 minutes) at 4 ^{0}C, washed once in ice-cold PBS, snap frozen in liquid nitrogen and stored at -70 ^{0}C before proceeding for ChIP assay.

Quantitative-RT-PCR Primers.

Forward and reverse primers	**Sequence**
mHPRT fp	5' GTTGGATACAGGCCAGACTTTGTTG
mHPRT rp	5' GATTCAACTTGCGCTCATCTTAGGC
mTSLP fp	5' AGCTTGTCTCCTGAAAATCGAG
mTSLP rp	5' AGGTTTGATTCAGGCAGATGTT
mCRABPII fp	5' CCAGCAGTCGAGATCAAACA
mCRABPII rp	5' TTCCACTCTCCCATTTCACC
mSmad7 fp	5' TCGGACAGCTCAATTCGGAC
mSmad7 fp	5' GGTAACTGCTGCGGTTGTAA
hGAPDH fp	5' GAGTCAACGGATTTGGTCGT
hGAPDH rp	5' TTGATTTTGGAGGGATCTCG
hTSLP fp	5' CCAGGCTATTCGGAAACTCA
hTSLP rp	5' TGGTGCTGTGAAATATGACCA

mIL4 fp	5′ GGCATTTTGAACGAGGTCAC
mIL4 rp	5′ AAATATGCGAAGCACCTTGG
mIL5 fp	5′ AGCACAGTGGTGAAAGAGACCTT
mIL5 rp	5′ TCCAATGCATAGCTGGTGATTT
mIL10 fp	5′ TGCTATGCTGCCTGCTCTTA
mIL10 rp	5′ TCATTTCCGATAAGGCTTGG
mIL13 fp	5′ GGAGCTGAGCAACATCACACA
mIL13 rp	5′ GGTCCTGTAGATGGCATTGCA

Statistical analysis. Data are represented as mean ± SD of at least three independent experiments, and were analyzed using sigmastat (Systat Software, Point Richmond, CA) by the Student *t* test or the Mann-Whitney rank sum nonparametric test depending on results from the Kolmogorov-Smirnov test (with Lilliefors' correction) for normality and Levene Median test for equal variance. $P < 0.05$ was considered significant.

RESULT III

Induction of Thymic Stromal Lymphopoietin Expression in Keratinocytes Is Necessary for Generating an Atopic Dermatitis upon Application of the Active Vitamin D3 Analogue MC903 on Mouse Skin. (Published)

Induction of Thymic Stromal Lymphopoietin Expression in Keratinocytes Is Necessary for Generating an Atopic Dermatitis upon Application of the Active Vitamin D3 Analogue MC903 on Mouse Skin

Journal of Investigative Dermatology (2009) **129,** 498–502; doi:10.1038/jid.2008.232; published online 24 July 2008

TO THE EDITOR

Thymic stromal lymphopoietin (TSLP) appears to be a master switch for T helper (Th)2 allergic inflammation such as atopic dermatitis (AD) and asthma (Liu, 2006). TSLP expression is increased in keratinocytes in skin lesions of patients with AD (Soumelis *et al.*, 2002), and various mouse models have established a link between TSLP expression and the pathogenesis of AD (Li *et al.*, 2005, 2006; Yoo *et al.*, 2005).

Abbreviations: AD, atopic dermatitis; LN, lymph node; Th2, T helper 2; TSLP, thymic stromal lymphopoietin; WT, wild-type

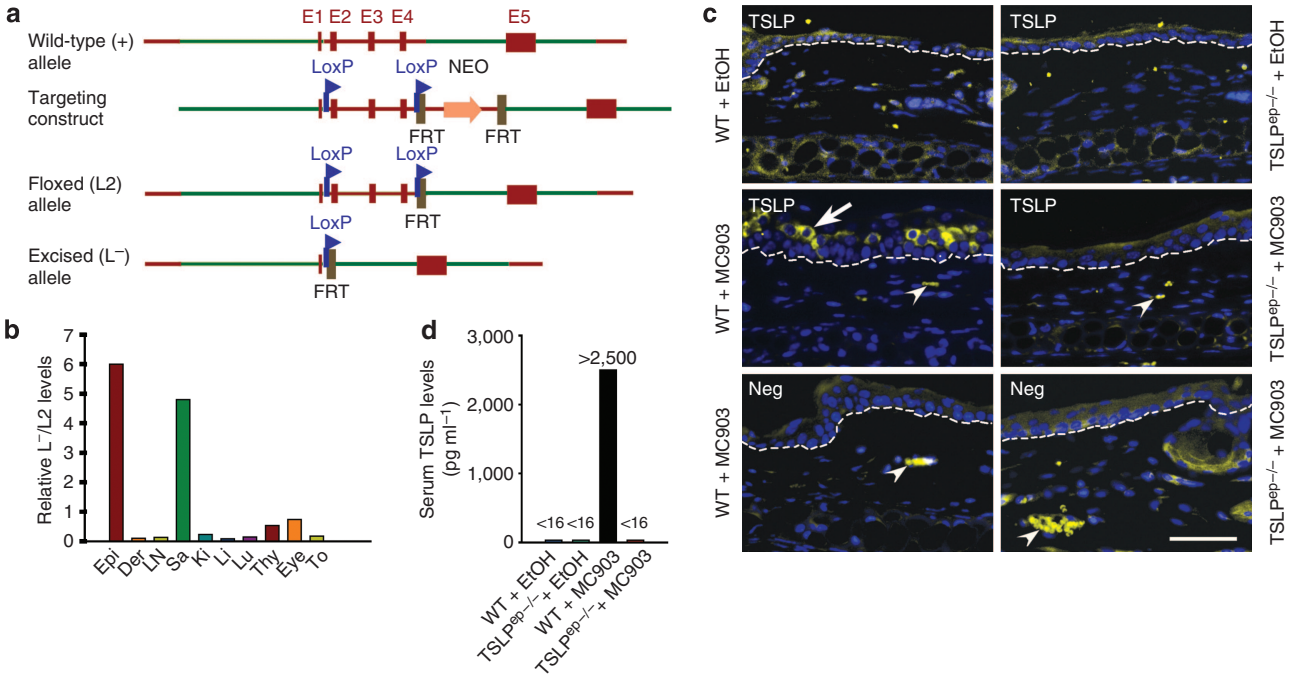

Figure 1. Generation and characterization of TSLP$^{ep-/-}$ mice in which TSLP is selectively ablated in keratinocytes. (**a**) Schematic drawing of the TSLP wild-type allele (+), the targeting construct (containing the FRT-flanked neomycin (Neo) resistance gene), the floxed (L2) allele after FLP-mediated excision of Neo, and the excised (L$^-$) allele after Cre-mediated excision of exons 2–4. Red boxes stand for exons (E). LoxP and FRT sites are indicated. (**b**) L$^-$ and L2 alleles were quantified by PCR on DNA extracted from various tissues of a TSLP$^{ep-/-}$ (K14-Cre$^{tg/0}$/TSLP$^{L2/L2}$) mouse. The L$^-$/L2 ratio shows that the excision occurred in epidermis (Epi), as well as in salivary gland (Sa), thymus (Thy), and tongue (To), but not in dermis (Der), lymph node (LN), kidney (Ki), liver (Li), lung (Lu), or eye. (**c**) Ears of control wild-type (WT) and TSLP$^{ep-/-}$ mice were topically treated with MC903 (2 nmol per ear) daily for 3 days, and sampled at day 4 (D4). Ear sections were stained with an antibody against TSLP (upper and middle panels), or with IgG from goat serum as negative (Neg) control (lower panels). Yellow corresponds to staining of TSLP antibody, whereas blue corresponds to DAPI staining of nuclei. White arrow points to one of the TSLP-stained cells in epidermis of WT + MC903 mice, and white arrowheads point to autofluorescent erythrocytes. White dashed lines indicate the dermal/epidermal junction. Scale bar, 50 μm. (**d**) Serum TSLP levels at D4 in WT and TSLP$^{ep-/-}$ mice.

Transgenic mice overexpressing TSLP in keratinocytes have been shown to develop a human AD-like syndrome (Li *et al.*, 2005; Yoo *et al.*, 2005), indicating that TSLP expression is sufficient to initiate AD-like skin inflammatory responses. We have also reported that topical application of either active vitamin D3 or the low-calcemic analogue MC903 (calcipotriol) triggers a mouse AD-like syndrome, characterized by a red, scaly, and lesioned skin, accompanied by an epidermal hyperplasia and a dermal infiltration of CD4$^+$ lymphocytes, eosinophils, dendritic cells, and mast cells, as well as by an increase of Th2 cytokine in skin, and an elevated serum IgE and blood eosinophilia (Li *et al.*, 2006). Importantly, we demonstrated that MC903 treatment induced TSLP expression in mouse keratinocytes and that this induction was mediated through keratinocytic vitamin D receptor, as upon MC903 treatment, VDR$^{ep-/-}$ mice in which vitamin D receptor was selectively ablated in keratinocytes neither expressed TSLP, nor developed an AD-like syndrome (Li *et al.*, 2006). However, it has not yet been demonstrated that TSLP expression in keratinocytes is necessary for the generation of an AD-like phenotype. It is indeed known that vitamin D3 has pleiotropic actions (Lin and White, 2004), and it has been shown that vitamin D3 can have a direct effect on naive CD4$^+$ T cells to enhance the development of Th2 cells (Boonstra *et al.*, 2001), and also act directly on antigen-presenting cells (such as macrophages and dendritic cells) (Lin and White, 2004).

With the aim of demonstrating the indispensability of keratinocytic TSLP in the generation of MC903-induced AD, a loxP-flanked (“floxed”) TSLP mouse line in which exons 2, 3, and 4 of both alleles of the TSLP gene are floxed (TSLP$^{L2/L2}$ mice) was produced (Figure 1a; Supplementary Methods), and crossed with K14-Cre transgenic mice (Li *et al.*, 2001) to obtain keratinocyte-selective TSLP mutant mice (TSLP$^{ep-/-}$), or with cytomegalovirus-Cre transgenic mice (Dupé *et al.*, 1997) to generate germline null mutant mice (TSLP$^{-/-}$). Quantitative PCR analyses of L$^-$ and L2 alleles (Supplementary Methods) of various tissues from 6-week-old TSLP$^{ep-/-}$ mice showed, as expected, that the excision of TSLP selectively occurred in the epidermis, as well as in salivary gland, tongue, and thymus (Figure 1b; data not shown). TSLP RNA level was severely diminished in TSLP$^{ep-/-}$ skin when compared to age- and sex-matched control wild-type (WT) littermate mice (Figure 2k). Accordingly, when 6-week-old female TSLP$^{ep-/-}$ and WT mice were daily topically treated with MC903 on both ears (2 nmol per ear) for 3 days, and

ears were sampled at day 4 (D4), TSLP was detected by immunohistochemistry in epidermal keratinocytes of MC903-treated WT ears, whereas no signal could be seen in MC903-treated TSLP$^{ep-/-}$ ears (Figure 1c). Consistently, MC903-treated WT mice exhibited a high TSLP serum level (>2500 pg/ml) at D4 (Li *et al.*, 2006), whereas in TSLP$^{ep-/-}$ mice, MC903 failed to induce serum TSLP (<16 pg/ml; Figure 1d).

TSLP$^{ep-/-}$ pups grew normally and did not exhibit any apparent abnormalities with time (3–50 weeks), and histological analyses in the skin did not reveal any obvious differences between WT and TSLP$^{ep-/-}$ mice (Figure 2b ; data not shown). MC903 (1 nmol per ear) was applied daily on 8-week-old WT or TSLP$^{ep-/-}$ ears for 15 days to generate the AD-like syndrome (Li *et al.*, 2006). At D16, ethanol (as vehicle control) treatment had no effect on WT and TSLP$^{ep-/-}$ ears (Figure 2a, upper panel), whereas MC903-treated WT ears were red, scaly, swollen, lesioned, and crusted (Figure 2a, lower

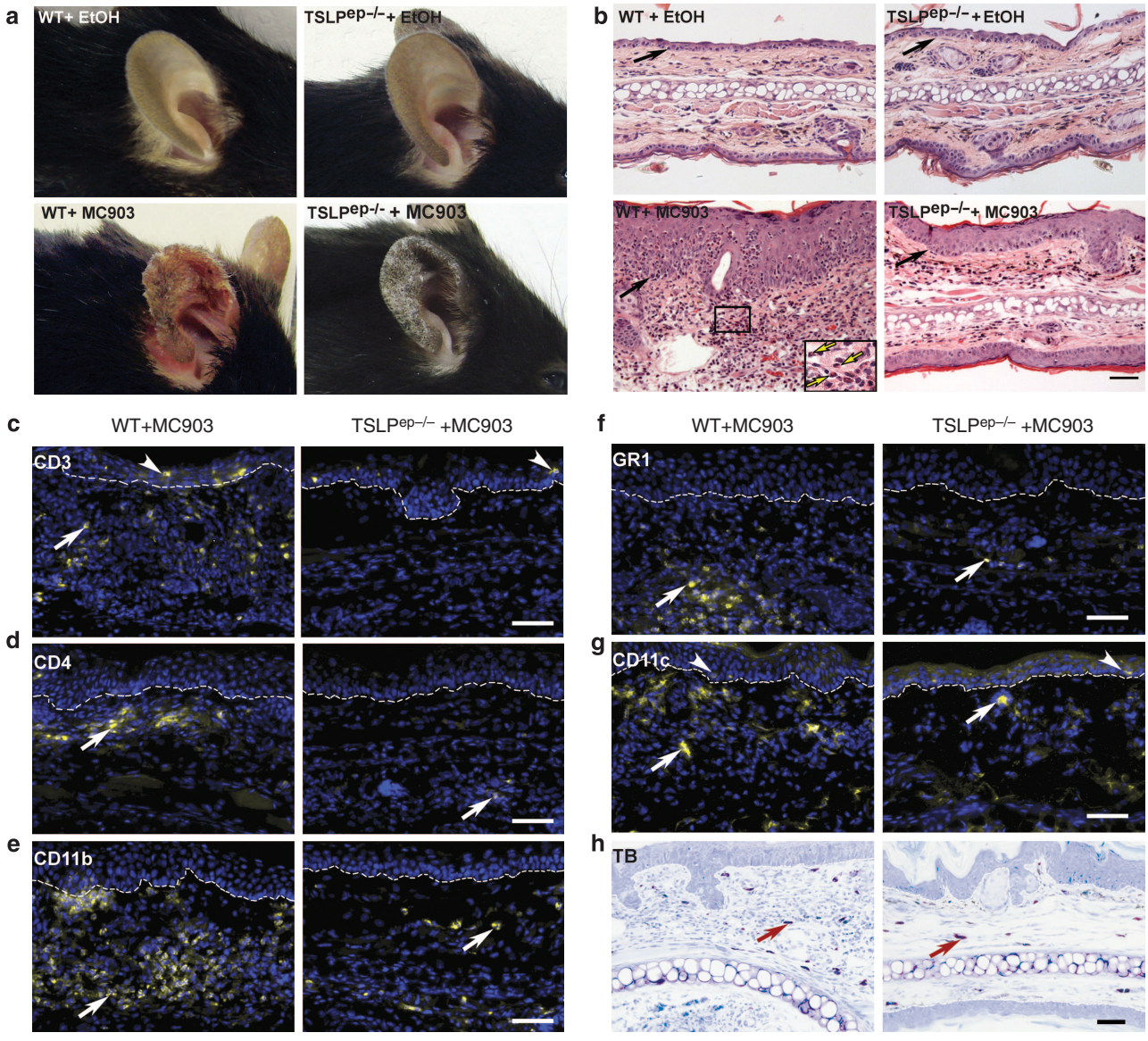

Figure 2. Induction of TSLP expression in keratinocytes is necessary for generating an AD-like syndrome upon application of the active vitamin D3 analogue MC903 on mouse skin. (**a**) Appearance and (**b**) hematoxylin/eosin-stained sections of ears sampled at day 16 (D16) from wild-type (WT) and TSLP$^{ep-/-}$ mice, topically ear-treated with ethanol (EtOH, as vehicle control) or MC903 (1 nmol per ear) daily for 15 days. Arrows point to dermal/epidermal junction. Scale bar, 50 μm. (**c**–**g**) Immunohistochemical (IHC) staining of CD3 (**c**), CD4 (**d**), CD11b (**e**), GR1 (**f**), and CD11c (**g**) on ear sections from MC903 topically treated WT (left panels) and TSLP$^{ep-/-}$ (right panels) mice at D16. White dashed lines indicate the dermal/epidermal junction. Yellow corresponds to staining of antibodies, whereas blue corresponds to DAPI staining of nuclei. White arrows point to one of the specific antibody-stained cells in the dermis, and white arrowheads to one of the specific antibody-stained cells in the epidermis. Scale bars, 50 μm. (**h**) Toluidine blue (TB)-stained sections. Red arrows point to one of the mast cells with intense blue in the dermis. Scale bar, 50 μm. (**i**) Serum IgE levels of MC903-treated WT and TSLP$^{ep-/-}$ mice at D0, D8, and D16. (**j**) Eosinophil counts in blood of MC903-treated WT and TSLP$^{ep-/-}$ mice at D0 and D16. (**k**, **l**) Cytokine and chemokine expression in ears (**k**) and ear-draining lymph nodes (**l**) of EtOH or MC903-treated WT and TSLP$^{ep-/-}$ mice at D16. *P<0.05. Error bars indicate s.d.

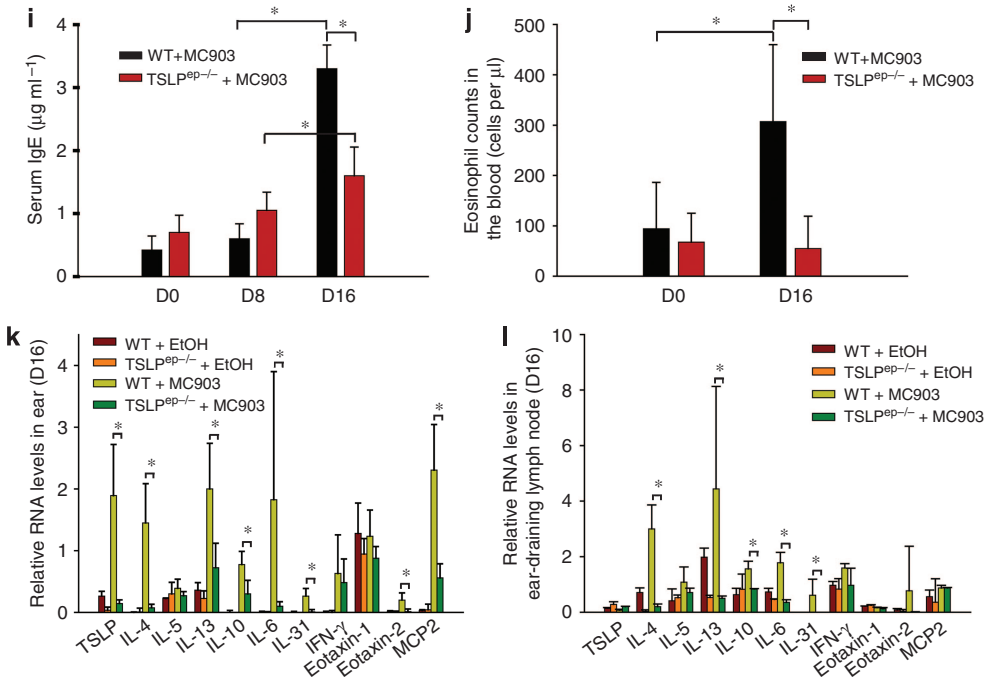

Figure 2. Continued.

left panel). In contrast, MC903-treated TSLP$^{ep-/-}$ ears appeared dry and scaly, but were not red or inflamed, and no lesion developed (Figure 2a, lower right panel). Histologically, at D16, MC903-treated WT skin exhibited an epidermal hyperplasia and a heavy dermal cell infiltrate (Figure 2b, lower left panel) that included numerous eosinophils (as shown by hematoxylin/eosin staining (Figure 2b, inset), and by CD11b or GR1 immunohistochemistry that stains granulocytes), CD3$^+$ T lymphocytes mainly comprising CD4$^+$ helper T cells, CD11c$^+$ dendritic cells, and mast cells (toluidine blue staining) (Figure 2c–h; Supplementary Methods), as previously reported (Li *et al.*, 2006). In contrast, dermal infiltration was largely abrogated in MC903-treated TSLP$^{ep-/-}$ ears, showing only few eosinophils, CD4$^+$ helper T cells, dendritic cells, and mast cells (Figure 2c–h). However, some epidermal hyperplasia was observed (Figure 2b, lower right panel), suggesting that MC903 application could induce some epidermal hyperplasia in a TSLP-independent manner. A systemic increase in serum IgE levels, which was lower in TSLP$^{ep-/-}$ than in WT mice at D16, was observed upon MC903 treatment (Figure 2i). Furthermore, an increase in eosinophil and lymphocyte counts was observed in WT but not in TSLP$^{ep-/-}$ blood (Figure 2j; data not shown). Taken together, these results indicated that selective ablation of TSLP in epidermal keratinocytes precludes the generation of an AD-like syndrome upon MC903 topical application. Not unexpectedly, similar observations were made with TSLP germline mutants (TSLP$^{-/-}$) and with mutants in which TSLP was selectively ablated in keratinocytes of adult mice by using the tamoxifen-inducible CreER^{T2} recombinase (Metzger *et al.*, 2003; data not shown).

To further characterize the involvement of TSLP-dependent signaling in AD generation, we next examined the pattern of skin cytokine expression upon MC903 treatment (Figure 2k; Supplementary Methods). TSLP expression was highly induced by MC903 treatment in WT, but not in TSLP$^{ep-/-}$ skin. However, a slight increase of TSLP in TSLP$^{ep-/-}$ skin was noted upon MC903 treatment, most probably reflecting an induction of TSLP by MC903 in nonkeratinocytic cells (for example, mast cells and basophils that also express TSLP; Soumelis and Liu, 2004; Sokol *et al.*, 2008), as this increase was not observed in TSLP$^{-/-}$ null mutant mice (Figure S1). Th2 cytokines (IL4, IL13, IL10, IL6, and IL31) and eosinophil-attractant chemokines (eotaxin-2 and monocyte chemotactic protein-2) were highly induced by MC903 in WT skin, whereas this induction was much weaker in MC903-treated TSLP$^{ep-/-}$ skin, although not abolished, when compared with vehicle (ethanol) treatment. To examine whether this weak induction could reflect a keratinocytic TSLP-independent regulation, cytokine expression was also analyzed in TSLP$^{-/-}$ null mutant skin (Figure S1). IL4, IL13, IL31, and eotaxin-2 were not induced in TSLP$^{-/-}$ skin upon MC903 treatment, indicating that the MC903-induced expression of these cytokines is fully dependent on TSLP. In contrast, some induction of IL10, IL6, and monocyte chemotactic protein-2 was observed in TSLP$^{-/-}$ skin upon MC903 treatment, suggesting that their overall induction may be contributed by both TSLP-dependent and -independent signaling. On the other hand, upregulation of the Th1 cytokine IFNγ by MC903 similarly occurred in WT and TSLP$^{ep-/-}$ skin, indicating that its induction was independent of TSLP.

Cytokine expression was also analyzed in skin-draining lymph nodes (LN; Figure 2l). Upon MC903 treatment, the induction of Th2 cytokines (IL4, IL13, IL10, IL6, and IL31) in WT LNs was not observed in $TSLP^{ep-/-}$ LNs, indicating that the MC903-triggered Th2 response is abolished in $TSLP^{ep-/-}$ mice. No change was seen for IFNγ transcript levels in WT or $TSLP^{ep-/-}$ LNs, from either MC903- or ethanol-treated mice, suggesting that MC903 application does not involve a Th1 response in LNs.

In conclusion, we demonstrate unequivocally here that TSLP produced by keratinocytes is absolutely required in pathogenesis of AD triggered by topical application of the vitamin D3 analogue MC903. We also show that in this AD model, induction of IL4, IL13, IL31, and eotaxin-2 is fully TSLP dependent, whereas that of IL6, IL10, and monocyte chemotactic protein-2 is only partially TSLP dependent, and that of IFNγ is TSLP independent. Finally, our floxed TSLP mice will be helpful for selective ablation of TSLP in other cell types (Soumelis and Liu, 2004; Ziegler and Liu, 2006; Holgate, 2007; Sokol *et al.*, 2008), and therefore to further elucidate the physiological and pathological function of this cytokine.

CONFLICT OF INTEREST

The authors state no conflict of interest.

ACKNOWLEDGMENTS

We thank the staff of the mouse knockout, histopathology, hematology, and animal facilities of the Institut de Génétique et de Biologie Moléculaire et Cellulaire (IGBMC) and Institut Clinique de la Souris for their kind help; Dr N Rochel-Guiberteau (IGBMC) and Dr D Moras (IGBMC) for vitamin D3 analogue MC903 from LEO Pharmaceutical Products (Denmark); and Dr SM Dymecki (Harvard Medical School, Boston) for FLP deleter (ACTB:FLPe) mice. This work was supported by funds from the Centre National de la Recherche Scientifique, the Institut National de la Santé et de la Recherche Médicale, the Collège de France, the Ministère de l'Enseignement supérieur et de la Recherche, the Association pour la Recherche à l'IGBMC (ARI), and l'Agence Nationale de la Recherche.

Mei Li, Pierre Hener, Zhikun Zhang, Krishna P. Ganti, Daniel Metzger and Pierre Chambon

Institut de Génétique et de Biologie Moléculaire et Cellulaire, Illkirch Cedex, France
E-mails: Mei.Li@igbmc.u-strasbg.fr; Pierre.CHAMBON@igbmc.u-strasbg.fr

SUPPLEMENTARY MATERIAL

Supplementary Methods
Figure S1. Comparison of cytokine and chemokine expression in ears of ethanol or MC903-treated wild-type (WT) and $TSLP^{-/-}$ null (germline mutation of TSLP) mice.

REFERENCES

Boonstra A, Barrat FJ, Crain C, Heath VL, Savelkoul HF, O'Garra A (2001) 1alpha,25-Dihydroxyvitamin d3 has a direct effect on naive CD4(+) T cells to enhance the development of Th2 cells. *J Immunol* 167:4974–80

Dupé V, Davenne M, Brocard J, Dollé P, Mark M, Dierich A *et al.* (1997) *In vivo* functional analysis of the Hoxa-1 3′ retinoic acid response element (3′RARE). *Development* 124:399–410

Holgate ST (2007) The epithelium takes centre stage in asthma and atopic dermatitis. *Trends Immunol* 28:248–51

Li M, Chiba H, Warot X, Messaddeq N, Gerard C, Chambon P *et al.* (2001) RXR-alpha ablation in skin keratinocytes results in alopecia and epidermal alterations. *Development* 128: 675–88

Li M, Hener P, Zhang Z, Kato S, Metzger D, Chambon P (2006) Topical vitamin D3 and low-calcemic analogs induce thymic stromal lymphopoietin in mouse keratinocytes and trigger an atopic dermatitis. *Proc Natl Acad Sci USA* 103:11736–41

Li M, Messaddeq N, Teletin M, Pasquali JL, Metzger D, Chambon P (2005) Retinoid X receptor ablation in adult mouse keratinocytes generates an atopic dermatitis triggered by thymic stromal lymphopoietin. *Proc Natl Acad Sci USA* 102:14795–800

Lin R, White JH (2004) The pleiotropic actions of vitamin D. *Bioessays* 26:21–8

Liu YJ (2006) Thymic stromal lymphopoietin: master switch for allergic inflammation. *J Exp Med* 203:269–73

Metzger D, Indra AK, Li M, Chapellier B, Calleja C, Ghyselinck NB *et al.* (2003) Targeted conditional somatic mutagenesis in the mouse: temporally-controlled knock out of retinoid receptors in epidermal keratinocytes. *Methods Enzymol* 364: 379–408

Sokol CL, Barton GM, Farr AG, Medzhitov R (2008) A mechanism for the initiation of allergen-induced T helper type 2 responses. *Nat Immunol* 9:310–8

Soumelis V, Liu YJ (2004) Human thymic stromal lymphopoietin: a novel epithelial cell-derived cytokine and a potential key player in the induction of allergic inflammation. *Springer Semin Immunopathol* 25:325–33

Soumelis V, Reche PA, Kanzler H, Yuan W, Edward G, Homey B *et al.* (2002) Human epithelial cells trigger dendritic cell mediated allergic inflammation by producing TSLP. *Nat Immunol* 3:673–80

Yoo J, Omori M, Gyarmati D, Zhou B, Aye T, Brewer A *et al.* (2005) Spontaneous atopic dermatitis in mice expressing an inducible thymic stromal lymphopoietin transgene specifically in the skin. *J Exp Med* 202:541–9

Ziegler SF, Liu YJ (2006) Thymic stromal lymphopoietin in normal and pathogenic T cell development and function. *Nat Immunol* 7:709–14